ELASTICITY OF SOLIDS AT HIGH PRESSURES AND TEMPERATURES: THEORY, MEASUREMENT AND GEOPHYSICAL APPLICATION

Thesis by

Geoffrey Frederick Davies

In Partial Fulfillment of the Requirements

for the Degree of

Doctor of Philosophy

California Institute of Technology

Pasadena, California

1973

(Submitted November 7, 1972)

"Little do they know how little
I know about the little they know.

If only I knew about the little
that they know, I'd know a little."

--The Goon Show,
"Tales of Old Dartmoor"
BBC, February 7, 1956

ACKNOWLEDGEMENTS

I am indebted to Dr. Leon Thomsen, the critical tone of this thesis notwithstanding, for his refusal to accept my half-baked ideas, which forced me to pursue the subject to much greater depth than I otherwise would have. Without his pioneering work, of course, I would never have become involved in this subject. Dr. Thomas J. Ahrens provided encouragement and critical discussion over a long period, and was especially helpful and generous in involving me in the shock-wave experiments reported here. Many discussions with Dr. Don L. Anderson have contributed to the ideas contained herein. "Coffee break" was always a stimulating forum, both directly and indirectly, thanks to all of my colleagues at the Caltech Seismological Lab.

I am grateful to Dr. Hartmut Spetzler for providing me with his original data, and to Dr. Hitoshi Mizutani for providing data in advance of publication.

The assistance of Mr. David Johnson, Mr. Harold Richeson and Mr. John Lower in performing the shock-wave experiments is gratefully acknowledged. Mr. Laszlo Lenches' assistance in preparing the figures is appreciated.

Special thanks go to my wife, Susie, for her patience and perseverance in typing this thesis and while I was working on its contents.

This work was supported by National Science Foundation Grants GA-12703 and GA-21396.

ABSTRACT

A theory for describing the elasticity of solids at simultaneous high pressures and high temperatures is developed by incorporating the fourth-order anharmonic theory of lattice dynamics into finite strain theory. The theory is applied to the analysis of a variety of data for MgO, SiO_2 and NaCl, and the results for MgO and SiO_2 used as the basis of a discussion of the constitution of the lower mantle. New results are reported of measurements of elastic properties of MgO shock-compressed to over 500 Kb.

The condition that finite strain equations be frame-indifferent is shown to require that only strain tensors belonging to a class of frame-indifferent strain tensors be used in finite strain expansions. It is shown that the generality of finite strain theory is not impaired by the inclusion of an explicit theory of thermal effects. Explicit equations for isotherms, isentropes and Hugoniots and for the effective elastic moduli of materials of cubic symmetry under hydrostatic stress are derived. The primary parameters of these equations are related to the elastic moduli and their pressure and temperature derivatives in an arbitrary reference state using thermodynamic identities, some of which are derived here.

Hugoniot data corresponding to different initial sample

densities of MgO, SiO_2 and NaCl and original ultrasonic data of NaCl are used to test both the compressional and thermal parts of the theory, and to refine the equations of state of these materials. The frame-indifferent analogue, $\underline{E}$, of the usual "Eulerian" strain tensor, $\underline{\epsilon}$, is found to usually give faster convergence of finite strain expansions than the "Lagrangian" strain tensor, η. The effect of using different strain measures on the values of parameters derived from data is demonstrated, and the adverse effects of using inappropriately derived parameters in extrapolation equations is demonstrated. Thermal effects in Hugoniot data are reasonably well described, but higher-order anharmonic effects appear to be required in the theory in order to describe the high temperature ultrasonic and thermal expansion data.

Measured velocities of rarefaction waves propogating into shocked MgO are in accord with a two-stage longitudinal (elastic)-hydrodynamic (plastic) decompression model, and constrain the high-pressure elastic moduli of MgO.

The effects on the determination of the lower mantle constitution of temperature, varying composition, the presence of phases denser than oxides mixtures, and the presence of iron in the "low-spin" electronic state are estimated, and a trade-off between many of these factors demonstrated. Iron content could range between 6% and 15% by weight of FeO. Silica content could range from 33% to 50% or more by weight.

Phases a few percent denser than oxides mixtures seem to be likely. The temperature is very indeterminate.

TABLE OF CONTENTS

TABLE OF CONTENTS (continued)

TABLE OF CONTENTS (continued)

TABLE OF CONTENTS (continued)

CHAPTER 1

INTRODUCTION

The application of the theory of equations of state of solids to the question of the internal constitution of the earth was pioneered and admirably demonstrated by the work of Birch (1938, 1939, 1947), based on the work of Murnaghan (1937), which culminated in Birch's important 1952 paper (Birch, 1952). The main objective, and achievement, of this work was, of course, to account for the effects of very large pressures upon the properties of solids so as to provide a basis for the comparison of the properties of the earth's interior with those of substances measured in the laboratory. Another result was the demonstration that temperature is a significant, though secondary, variable in the earth's interior. Birch estimated the temperature inside the earth to range up to several thousand degrees centigrade.

In order to pursue the question of the earth's internal constitution, it is thus necessary to be able to account for the effects of simultaneous high temperatures and pressures. Then, of course, the temperature becomes one of the factors of the earth's interior to be determined. Birch's (1952) approach was to make use of measurements of thermal effects in solids at atmospheric pressure, a number of thermodynamic

identities, and some calculations based on lattice models, to obtain estimates of the effect of pressure on thermal expansion. This led to the conclusion that thermal expansion of silicates tends to decrease with increasing pressure at roughly the same relative rate as the compressibility decreases, and to the general idea that pressure tends to reduce the effects of temperature on the density and elasticity of solids.

The state of the art remained more or less at this level until it was perceived by Thomsen (1970, 1972) that a well developed theory of thermal effects in solids, due to Leibfried and Ludwig (1961) could be extended into the domain of finite strain, thus providing the desired description of thermal effects at high pressures. In this theory the thermal effects and their pressure dependence are governed by a few parameters which can be evaluated from currently available laboratory measurements for many relevant substances.

In the meantime, a new technique, that of shock-waves in solids, was being applied to geophysically relevant materials (e.g., Al'tshuler et al., 1965; McQueen et al., 1967). The analysis of the results of these experiments, which involve, simultaneously, high pressures and temperatures, relied heavily on Grüneisen's (1912) theory of thermal effects in solids, and in particular, on the Grüneisen parameter, γ, which relates pressure and internal energy in this theory

(e.g., Rice et al., 1958). Again, the pressure dependence of γ was a problem, and various approximations were invoked to estimate this (Slater, 1939; Dugdale and MacDonald, 1953). Leibfried and Ludwig (1961) showed that their theory led to a Mie-Grüneisen type of equation under suitable approximations. Thus Thomsen's (1970) extension of their theory to finite strains allowed the Grüneisen parameter to be calculated as a function of pressure, and the analysis of shock-wave experiments was included in the same theoretical framework.

The purpose of this thesis is to re-derive, generalize and exploit Thomsen's (1970, 1972) theory. Thomsen (1970) claimed that the lattice dynamics theory, and hence his extension of it, could be written only in terms of a particular "Lagrangian" strain tensor, $\underset{\sim}{\eta}$. This claim is unreasonable since the role of lattice dynamics in his theory is to make <u>explicit</u> the temperature dependence of finite strain equations which can be given <u>implicit</u> temperature dependence by allowing parameters to depend on temperature. The generality of the finite strain equations should not be limited in this process. This expectation is verified in the re-derivation given here, as it is shown that the theory may be written in terms of any one of a whole class of "frame-indifferent" strain tensors, as is the case in finite strain theory. Equations in terms of two particular strain

tensors are developed as examples.

The wide applicability of the theory, mentioned above, is demonstrated and exploited here in a series of analyses of different kinds of data - shock-wave, ultrasonic, static compression, thermal expansion and calorimetric. These analyses yield new, and superior, determinations of the equations of state of MgO (periclase), SiO_2 (stishovite) and sodium chloride. They also present the opportunity for some general discussion of the problem of fitting and extrapolating data with particular analytic forms. Finally, the newly determined equations of state of periclase and stishovite are used as the basis for a discussion of the constitution of the earth's lower mantle.

Chapters 2 to 5 present the theoretical development.

In using the strain tensor $\underline{\eta}$, Thomsen (1970, 1972) followed the common practice of both lattice dynamics theory and continuum finite strain theory, in which $\underline{\eta}$ is usually invoked in order to assure the "rotational invariance" of the resulting equations. In Chapter 2, the requirement that finite strain equations be invariant under changes of frame of reference is reviewed, and the necessary and sufficient conditions for "frame-indifference" are obtained.

In Chapter 3, the approximations made in Leibfried and Ludwig's (1961) lattice dynamics theory are discussed, and

that theory is extended to the domain of finite strain in the special case of isotropic stresses and strains. Pressure-temperature-density equations of state are obtained in terms of three particular strain measures.

In Chapter 4, equations for isentropes and Hugoniots are obtained from the above equations, which have the form of isotherms. Chapters 3 and 4 correspond to Thomsen's first paper (Thomsen, 1970).

Chapter 5, corresponding to Thomsen's second (1972) paper, gives the generalization of the above theory necessary to calculate effective elastic moduli as functions of density and temperature for the special case of hydrostatic prestress, but allowing arbitrary material symmetry. The specialization to cubic symmetry is given.

Applications of the theory are given in Chapters 6 to 10.

In Chapter 6, an analysis of shock-wave data of MgO allows numerical evaluation of some of the differences between various equations, including Thomsen's (1970), a test of the thermal contribution to the pressure predicted by this theory, and a determination of the MgO equation of state.

In Chapter 7 a large body of shock-wave and other data of SiO_2 is analysed to provide equations of state of stishovite and a phase of about the density of coesite. The identification of this phase requires some calculation and dis-

cussion of the SiO_2 phase diagram to one megabar and several thousand degrees Kelvin.

Recent ultrasonic measurements of the elastic properties of sodium chloride at simultaneously high pressure and temperature are analysed in Chapter 8 in terms of the theory given in Chapter 5. This allows some discussion of the accuracy of the thermal part of the theory. Combined with calorimetric and thermal expansion data, these data are sufficient to predict the Hugoniot of sodium chloride. Comparison with Hugoniot data allows some discussion of the empirical merits of different strain measures and of the most advantageous methods of extrapolating such data to high pressures. Using the Hugoniot data as a constraint, the equation of state of sodium chloride is accurately determined to 300 kilobars.

Preliminary results are given in Chapter 9 of shock-wave experiments on MgO which use a technique to measure elastic properties of substances under shock-compression. The analysis of these results requires a theory of the type given here to calculate elastic properties at high pressures and temperatures.

Finally, in Chapter 10, the equations of state of MgO and SiO_2 determined in Chapters 6 and 7 are used as the basis of a discussion of the constitution of the earth's lower mantle.

References

AL'TSHULER L.V., and TRUNIN R. F., Bull. (Izv.) Acad. Sci. USSR, Earth Physics Series, No. 10 (1965).

BIRCH F., J. Appl. Phys. 9, 279 (1938).

BIRCH F., Bull. Seis. Soc. Am. 29, 463 (1939).

BIRCH F., Phys. Rev. 71, 809 (1947).

BIRCH F., J. Geophys. Res. 57, 227 (1952).

DUGDALE J. S., and MacDONALD D. K. C., Phys. Rev. 89, 832 (1953).

GRÜNEISEN E., Ann. Phys. Berlin 39, 257 (1912).

LEIBFRIED G. and LUDWIG W., Solid State Physics (Edited by Bradley) 12, 275, Academic Press, New York (1961).

McQUEEN R. G., MARSH S. P. and FRITZ J. N., J. Geophys. Res. 72, 4999 (1967).

MURNAGHAN F. D., Am. J. Math. 59, 235 (1937).

RICE M. H., McQUEEN R. G. and WALSH J. M., Solid State Physics 6 (Edited by F. Seitz and D. Turnbull), Academic Press, New York (1958).

SLATER J. C., Introduction to Chemical Physics, McGraw-Hill, New York (1939).

THOMSEN L., J. Phys. Chem. Solids 31, 2003 (1970).

THOMSEN L., J. Phys. Chem. Solids 33, 363 (1972).

CHAPTER 2

INVARIANT FINITE STRAIN MEASURES IN ELASTICITY AND LATTICE DYNAMICS

Summary

Some vagueness in the literature concerning the proper measures of strain which may be used in finite elastic strain theory and lattice dynamics is discussed. The requirements for strain-dependent quantities to be invariant under changes of frame of reference are briefly reviewed, and it is pointed out that the common practice of writing strain-dependent quantities explicitly in terms of the Lagrangian strain $\underline{\eta}$ is sufficient, but not necessary, for them to be invariant. Invariance is assured if any one of a class of invariant strain tensors is used for this purpose. The use of the non-invariant Eulerian strain tensor $\underline{\epsilon}$ in some applications has not usually led to difficulties because of the restricted situations which have been considered. Applications to more general situations would require the use of an invariant strain measure. An analogous invariant strain tensor can be defined which reduces to the Eulerian strain tensor in the case of isotropic strain.

2.1 Introduction

There seems to be some vagueness and ambiguity in the literature concerning the proper measures of finite strain which may be used in formulating theories of elasticity or lattice dynamics (Murnaghan, 1951; Toupin and Bernstein, 1960; Thurston and Brugger, 1964; Brugger, 1964; Thurston, 1965; Wallace, 1967; Born and Huang, 1954; Leibfried and Ludwig, 1961; Ludwig, 1965; Thomsen, 1970). The common practice is to write expressions in terms of the "Lagrangian" strain, $\underline{\eta}$ (defined below), with the comment that these expressions are thereby rendered "rotationally invariant", and without any discussion of the necessity of this condition. The result is that it is easy to gain the impression that $\underline{\eta}$ possesses some special property not possessed by any other strain measure. This is especially true, for instance, of Brugger's (1964) reference to the $\underline{\eta}$ derivatives of internal energy, U, or Helmholtz free energy, A, as "thermodynamic elastic coefficients", and of Wallace's (1967) statement that U and A depend on the position in the current configuration only through $\underline{\eta}$ and the position in the initial configuration. Wallace goes on to assert that "this dependence is necessary and sufficient to insure rotational invariance" of U and A. It is easy to misinterpret this statement as implying that U and A must depend on $\underline{\eta}$ <u>explicitly</u>, when in fact rotational invariance is still assured if U and A depend on some strain

measure which itself depends only on $\underline{\eta}$. This point is trivial so long as one is content to use $\underline{\eta}$ as a strain measure, but in some applications, such as geophysics, where large strains are considered, the differences between different strain measures are of practical importance (Thomsen, 1970; Murnaghan, 1937; Birch, 1947)

In the geophysical literature, on the other hand, the "Eulerian" strain, $\underline{\epsilon}$ (also defined below), has been popularly used, due largely to the work of Birch (1947, 1938, 1952). The "Birch-Murnaghan equation" is derived by writing the strain energy density as a third-order polynomial in $\underline{\epsilon}$, and has been established as an empirically successful equation (Birch, 1947, 1938, 1952). The use of $\underline{\epsilon}$ deserves comment in the present context, since it does not, in fact, assure rotational invariance in general. This fact seems to have received little notice since the earlier work of Murnaghan (1937), apparently because his theory was immediately specialized to situations in which the invariance requirement was trivially satisfied (Murnaghan, 1937; Birch, 1947, 1938). The question has recently been raised again by Thomsen (1970, 1972) however, in the context of his work on incorporating some general results of lattice-dynamics into the theory of finite strain.

It is thus appropriate to point out that there exist two classes of strain tensors (Truesdell and Toupin, 1960,

sects. 32, 33), one consisting of tensors which are invariant under changes of frame of reference, and the other consisting of tensors which are not. Further, to every tensor which is not invariant (or "frame-indifferent" (Truesdell and Noll, 1965)) there corresponds a tensor which is frame- indifferent and to which the tensor reduces in some special situations, notably the case of isotropic strain. The frame-indifference requirement has been fully discussed by Truesdell and Noll (1965, sects. 19, 26, 29) and a useful account is given by Malvern (1969, sect. 6.7). A particular pair of strain tensors has been discussed by Thomsen (1972). For the present discussion, some particular strain measures will be defined and the frame-indifference requirement briefly reviewed.

2.2 Strain Measures

A notation somewhat similar to that of Truesdell and Noll (1965) will be used. Attention will be confined to hyperelastic materials, i.e., those elastic materials for which a strain energy function exists. Rectangular Cartesian coordinates will be used, and initial and final configurations will both be referred to the same coordinate frame. Denote the position vector of the initial position of a particle by $\underline{X} = (X_1, X_2, X_3)$ and the position vector of the same particle after deformation by $\underline{x} = x_1, x_2, x_3)$. Define the deformation gradient, $\underline{F}$, by

$$\underline{F} = \mathrm{grad}_{\underline{X}}\, \underline{x} \quad ; \quad F_{ij} = x_{i,j} = \frac{\partial x_i}{\partial X_j} \,. \tag{1}$$

Indices i, j, etc., run from 1 to 3, and repeated indices are summed. $\underline{F}$ is assumed to have an inverse, which will be denoted by $\underline{G}$: $\underline{G} = \underline{F}^{-1}$.

By the polar decomposition theorem (Truesdell and Noll, 1965, sect. 23; Ericksen, 1960, sect. 43), $\underline{F}$ has two unique multiplicative decompositions:

$$\underline{F} = \underline{R}\,\underline{U} \,, \quad \underline{F} = \underline{V}\,\underline{R} \,, \tag{2}$$

in which $\underline{R}$ is orthogonal and $\underline{U}$ and $\underline{V}$ are symmetric and posi-definite. These are termed, by Truesdell and Noll, the rotation tensor, and the right and left stretch tensors, respectively. From these can be defined the right and left Cauchy-Green tensors (Truesdell and Noll, 1965, sect. 23).

$$\underline{C} = \underline{U}^2 = \underline{F}^T\underline{F} \,, \quad \underline{B} = \underline{V}^2 = \underline{F}\,\underline{F}^T = \underline{R}\,\underline{C}\,\underline{R}^T \,. \tag{3}$$

Some other stretch and strain tensors will now be defined, the analogous quantities defined, respectively, from $\underline{U}$ and $\underline{V}$ being carried in parallel. The inverses of $\underline{C}$ and $\underline{B}$ are

$$\underline{c} = \underline{C}^{-1} = \underline{F}^{-1}\underline{F}^{-1T} = \underline{G}\,\underline{G}^T \,, \quad \underline{b} = \underline{B}^{-1} = \underline{G}^T\underline{G} \,. \tag{4}$$

$\underline{b}$ is the Cauchy deformation tensor (Truesdell and Toupin, 1960, sect. 26). The Green-St. Venant strain tensor, $\underline{E}$

(Truesdell and Noll, 1965, sect. 63), and its analogue are

$$\underline{E} = \tfrac{1}{2}(\underline{C} - \underline{1}) = \underline{\eta} \quad , \qquad \underline{D} = \tfrac{1}{2}(\underline{\beta} - \underline{1}) . \tag{5}$$

$\underline{E}$ is the "Lagrangian" strain tensor, $\underline{\eta}$, discussed above. Corresponding to these, we have

$$\underline{e} = \tfrac{1}{2}(\underline{1} - \underline{c}) \quad , \qquad \underline{d} = \tfrac{1}{2}(\underline{1} - \underline{b}) = \underline{\epsilon} \quad . \tag{6}$$

$\underline{d}$ is the "Eulerian" strain tensor, $\underline{\epsilon}$, discussed above. It is also known as the Almansi-Hamel strain tensor. The analogous strain tensor $\underline{e}$ was defined by Thomsen (1972) (his $\underline{E}$).

2.3 Frame-Indifference

For a hyperelastic material, the Cauchy stress tensor, $\underline{T}$, is given by (Truesdell and Noll, 1965, sect. 82)

$$\underline{T} = \rho \underline{F}\, \sigma_{\underline{F}}^{T}(\underline{F}) = \rho \underline{F} \left(\frac{\partial \sigma}{\partial \underline{F}}\right)^{T} , \tag{7}$$

where ρ is the density in the deformed configuration and $\sigma(\underline{F})$ is the strain energy function. Thermodynamically, σ can be identified with either the internal energy or the Helmholtz free energy.

It is required that the constitutive relation (7) be invariant under changes of frame of reference. It has been shown that this can be achieved by requiring $\sigma(\underline{F})$ to be "frame-indifferent", i.e., invariant under changes of frame of reference (Truesdell and Noll, 1965, p. 308).

Under a general change of frame of reference, the position vector $\underline{x}$ is transformed into $\underline{x}^*$, where

$$\underline{x}^* = \underline{a} + \underline{Q}\underline{x} , \tag{8}$$

$\underline{a}$ is a constant vector and $\underline{Q}$ is a constant orthogonal tensor. Taking the gradient of (8) with respect to the initial position $\underline{X}$, and using the definition (1) of $\underline{F}$, it is seen that $\underline{F}$ transforms according to the relation

$$\underline{F}^* = \underline{Q}\,\underline{F} . \tag{9}$$

For $\sigma(\underline{F})$ to be frame-indifferent thus requires that

$$\sigma(\underline{F}^*) = \sigma(\underline{Q}\,\underline{F}) = \sigma(\underline{F}) . \tag{10}$$

Since $\underline{Q}$ is an arbitrary orthogonal tensor, we may take $\underline{Q} = \underline{R}^{-1} = \underline{R}^T$, where $\underline{R}$ is defined by (2), and obtain (Truesdell and Noll, 1965, p. 308)

$$\sigma(\underline{F}) = \sigma(\underline{U}) , \tag{11}$$

i.e., the strain energy depends upon $\underline{F}$ only through the right stretch tensor $\underline{U}$. Since the tensors $\underline{C}$, $\underline{c}$, $\underline{E}$, and $\underline{e}$ are themselves functions of $\underline{U}$, it follows that σ will be frame-indifferent if it is a function of any one of these, or of any other such tensor which is a function of $\underline{U}$.

It is easy to see that this frame-indifference of σ follows because the strain tensors $\underline{U}$, $\underline{C}$, etc. are themselves

frame-indifferent. Since $\underline{F}$ transforms according to (9), we see from the definition (3) that $\underline{C}$ transforms according to

$$\underline{C}^* = (\underline{F}^*)^T \underline{F}^* = \underline{F}^T \underline{Q}^T \underline{Q} \underline{F} = \underline{F}^T \underline{F} = \underline{C} , \tag{12}$$

so that $\underline{C}$ itself is frame-indifferent. It follows that the other tensors related to $\underline{C}$ are also frame-indifferent.

The above result may be contrasted with that for $\underline{V}$ and the tensors derived from it. For instance, $\underline{B}$ transforms according to

$$\underline{B}^* = \underline{F}^* (\underline{F}^*)^T = \underline{Q} \underline{F} \underline{F}^T \underline{Q}^T = \underline{Q} \underline{B} \underline{Q}^T , \tag{13}$$

so that $\underline{B}$ is not frame-indifferent. Defining $\bar{\sigma}(\underline{B}) = \sigma(\underline{F})$, the requirement that

$$\bar{\sigma}(\underline{Q} \underline{B} \underline{Q}^T) = \bar{\sigma}(\underline{B}) \tag{14}$$

for arbitrary $\underline{Q}$ is just the requirement that the material described by $\bar{\sigma}(\underline{B})$ be isotropic (Truesdell and Noll, 1965, sect. 85). On the other hand, the requirement that

$$\underline{Q} \underline{B} \underline{Q}^T = \underline{B} \tag{15}$$

is the requirement that the strain be isotropic (Truesdell and Noll, 1965, sect. 7).

If the strain is isotropic, $\underline{F}$ is a scalar multiple of the unit tensor. In that case, $\underline{F}^T = \underline{F}$, and all of the pairs of strain tensors defined in (2-6) are equal: $\underline{B} = \underline{C} = \underline{F}^2$,

etc.

2.4 Discussion

Some general comments can now be made on the basis of the foregoing. The strain energy will be frame-indifferent if its strain-dependence is expressed in terms of one of the class of frame-indifferent strain tensors. Truesdell and Toupin (1960, sect. 32) have discussed the equivalence of strain measures, and they go on (ibid., sect. 33) to give examples of strain measures which reduce the classical strain tensor of the linear theory of elasticity for infinitesimal deformations. Since, for many applications, strain-dependent quantities are expanded as a Taylor series in strain, this additional requirement is convenient in practice. The strain tensors $\underline{E}$ and $\underline{e}$ (5, 6) are examples of this class of strains. Some more specific comments will now be made.

The uniqueness of the pair of polar decompositions of $\underline{F}$ means that any one frame-indifferent tensor is a function of any other frame-indifferent tensor. This is the basis for the validity of Wallace's statement (1967), discussed earlier. In those cases where the Eulerian strain tensor, which is not frame-indifferent, has been used to describe isotropic strain, the correct generalization to general strain is through the tensor $\underline{e}$, defined by (6), as has been pointed out by Thomsen (1972).

Murnaghan (1937) derived an expression for stress in terms of $\underline{E}$ (his η) but immediately specialized this to an isotropic medium to discuss applications. At the end of that paper he gives the expression for $\underline{T}$ in terms of $\underline{E}$ as

$$\underline{T} = \rho \underline{F} \hat{\sigma}_{\underline{E}}(\underline{E}) \underline{F}^T \quad , \tag{16}$$

where $\hat{\sigma}(\underline{E}) = \sigma(\underline{F})$. He also gives what he calls "the corresponding Eulerian equations" in terms of $\underline{c}$ (his $\underline{j}$):

$$\underline{T} = -2\rho \underline{G}^T \tilde{\sigma}_{\underline{c}}(\underline{c}) \underline{G} \quad , \tag{17}$$

where $\tilde{\sigma}(\underline{c}) = \sigma(\underline{F})$. Thomsen (1972) uses, at one point, the closely related strain $\underline{e}$ (see equation 6) and the relation

$$\underline{T} = \rho \underline{G}^T \sigma'_{\underline{e}}(\underline{e}) \underline{G} \quad , \tag{18}$$

where $\sigma'(\underline{e}) = \sigma(\underline{F})$. However, Thomsen, correctly, calls this a Lagrangian equation. The confusion of terms here should be clarified. In the sense that the frame-indifferent tensors are functions of η, which is defined with reference to the <u>initial</u> configuration, they are all "Lagrangian". Conversely, all of the non-frame-indifferent tensors are "Eulerian". Murnaghan's (1937) incorrect description of equation (17) as Eulerian was presumably due to the close relation of $\underline{c}$ to $\underline{e}$, the frame-indifferent analogue of $\underline{\epsilon}$ (see equation 6). Actually, Truesdell (1952, sect. 12) has pointed out that the terms "Eulerian" and "Lagrangian" are historically in-

accurate, and has proposed, instead, the terms "spatial" and "material", respectively.

Semantics aside, it is clear that all of the forms (16), (17), and (18) are frame-indifferent, and also that the strain $\underline{e}$ is analogous to what is conventionally called the "Eulerian" strain, namely $\underline{d}$ (or $\underline{\epsilon}$).

Birch (1947) developed expressions for the effective elastic constants of a medium of cubic symmetry under hydrostatic stress. His results are written in terms of both $\underline{E}$ and $\underline{d}$ (his η and $\underline{\epsilon}$). That the expressions in terms of $\underline{d}$ are valid depends on the restricted situation which was considered and on the particular way in which they were derived. Firstly, Birch considered only strains which are a combination of an isotropic compression and a superposed arbitrary infinitesimal strain. These strains can be represented by a deformation gradient of the form

$$\underline{F} = F\underline{1} + \underline{f} \quad , \tag{19}$$

where F is a scalar, $\underline{1}$ is the unit tensor, and $\underline{f}$ is infinitesimal. From the definitions (3), we see that in this case

$$\underline{C} = F^2\underline{1} + F(\underline{f} + \underline{f}^T) + \underline{f}^T\underline{f} \quad , \tag{20}$$

while

$$\underline{B} = F^2 \underline{1} + F(\underline{f} + \underline{f}^T) + \underline{f}\,\underline{f}^T . \qquad (21)$$

To first order in $\underline{f}$, (20) and (21) are the same. Birch then evaluated equation (17) for $\underline{I}$ in terms of $\underline{d}$ to first order in $\underline{f}$. The coefficients of the infinitesimal strains then yielded the effective elastic constants. The success of this procedure depends on having to go only to first order in $\underline{f}$, since, to second order in $\underline{f}$, $\underline{d}$ is not frame-indifferent.

In conclusion, the common practice of writing the equations of finite elastic strain or of lattice dynamics explicitly in terms of the Lagrangian strain tensor $\underline{\eta}$ is sufficient, but not necessary, to assure the frame-indifference of those equations. Any frame-indifferent strain tensor can be used for this purpose. The use of the non-frame-indifferent Eulerian strain tensor $\underline{\epsilon}$ in some applications has not usually led to errors because of the restricted situations which have been considered, but the extension of these applications to more general situations would require the use of a frame-indifferent strain tensor.

2.5 References

BIRCH F., J. Appl. Phys. 9, 279 (1938).

BIRCH F., Phys. Rev. 71, 809 (1947).

BIRCH F., J. Geophys. Res. 57, 227 (1952).

BORN M. and HUANG K. H., Dynamical Theory of Crystal Lattices, Clarendon Press, Oxford (1954).

BRUGGER K., Phys. Rev. 133, A1611 (1964).

ERICKSEN J. L., Handb. Phys. Vol. III/1, 794, Springer-Verlag, Berlin (1960).

LEIBFRIED G. and LUDWIG W., Solid State Physics (Edited by Bradley), 12, 275, Academic Press, New York (1961).

LUDWIG W., Springer Tracts in Modern Physics (Edited by G. Hohler) 43, 1, Springer-Verlag, Berlin (1965).

MALVERN L. E., Introduction to the Mechanics of a Continuous Medium, Prentice-Hall, New Jersey (1969).

MURNAGHAN F. D., Am. J. Math. 59, 235 (1937).

MURNAGHAN F. D., Finite Deformation of an Elastic Solid, Wiley, New York (1951).

THOMSEN L., J. Phys. Chem. Solids 31, 2003 (1970).

THOMSEN L., J. Phys. Chem. Solids 33, 363 (1972).

THURSTON R. N., J. Acoust. Soc. Am. 37, 348 (1965); Erratum 37, 1148 (1965).

THURSTON R. N. and BRUGGER K., Phys. Rev. 133, A1604 (1964).

TOUPIN R. A. and BERNSTEIN B., J. Acoust. Soc. Am. 33, 216 (1960).

TRUESDELL C., J. Rat. Mech. Anal. 1, 125 (1952). Reprinted in The Mechanical Foundations of Elasticity and Fluid Dynamics (Edited by C. Truesdell) 1, Gordon and Breach, New York (1966).

TRUESDELL C. and NOLL W., Handb. Phys. Vol. III/3, Springer-Verlag, Berlin (1965). (Especially sects. 15-19, 43, 44, 68, 79-84).

TRUESDELL C. and TOUPIN R. A., Handb. Phys. Vol. III/1, 226, Springer-Verlag, Berlin (1960).

WALLACE D. C., Phys. Rev. 162, 776 (1967).

CHAPTER 3

QUASI-HARMONIC FINITE STRAIN EQUATIONS OF STATE OF SOLIDS

Summary

Thomsen's "fourth-order anharmonic" theory, which explicitly evaluates thermal effects in finite strain equations of elasticity according to the fourth-order approximation in lattice dynamics, is reconsidered for the special case of isotropic stresses and strains. It is shown that the approximations made in the finite strain theory are independent from those made in the lattice dynamics theory, with the result that strain dependence may be described in terms of any frame-indifferent strain tensor, not just the "Lagrangian" strain tensor, η, and that the finite strain expansions may be taken to any order, not just the fourth. This result is valid for general stresses and strains. Illustrative equations are derived in terms of three strain measures, including η and the frame-indifferent analogue, $\underline{E}$, of the "Eulerian" strain tensor, $\underline{\epsilon}$.

The reference state is here left arbitrary, rather than identifying it with the "rest" state, as was done by Thomsen. This results in greater convenience in applying the equations. Not being restricted to fourth

order, the present equations do not depend for their application on knowing the second pressure derivative of the bulk modulus.

3.1 Introduction

In an important pair of papers, Thomsen (1970, 1972) has given a theory extending lattice dynamics into the domain of finite strain. Such a theory allows thermal effects to be explicitly accounted for at large stresses and in terms of a small number of parameters. However, Thomsen claims that such a theory can be written only in terms of a particular "Lagrangian" strain tensor, $\underline{\eta}$, with the following reasoning. The "fourth-order" theory of lattice dynamics of Leibfried and Ludwig (1961) is based on a Taylor expansion of the lattice potential energy, ϕ, in terms of atomic displacements which is truncated after the fourth-order terms. Finite strain equations of elasticity are based on a truncated expansion of the Helmholtz free energy, A, in terms of a strain measure (of which there are an infinity of possibilities). Since both microscopic thermal motions and a macroscopic homogeneous strain involve displacements of atoms, it follows, Thomsen argued, that in a theory which purports to describe both thermal and large strain effects, the lattice dynamics and finite strain parts of the theory should both be based on expansions to the same order in terms of the same displacement measure, so that the same approximation is involved in each part of the theory. Thomsen (1970) concluded that $\underline{\eta}$ was the appropriate measure.

It is intended in this chapter to establish two main

points concerning this argument. The first point is that Thomsen employs a concept of consistency between the thermal and finite strain parts of the theory which is unnecessarily restrictive. Finite strain theory makes no assumptions about inter-atomic forces and no predictions about thermal effects. However, thermal effects can be incorporated implicitly into this theory by supposing the "constants" which occur in it to be temperature dependent. The role of the lattice dynamics theory is to make this temperature dependence explicit and specific. It is unreasonable that the generality of the finite strain part of the theory should be limited in this process, however approximate and limited the thermal part of the theory may be. In this chapter it will be pointed out that the approximations made in the two parts of the theory are in fact independent. If the approximations in the thermal part of the theory are poor, then the effect is to limit the range of temperatures over which the theory is useful. Within this temperature range, the finite strain equations are limited only by the approximation made in the truncation of the free energy expansion. A corollary of this is that the finite strain part of the equations need not be limited to being in terms of η.

The second main point is that even if Thomsen's more restrictive concept of consistency is adopted, η is not the appropriate strain measure with which to describe finite

strain effects. Thomsen (1970) transforms his expansion of ϕ in terms of atomic displacements (his equation 17) to one in terms of η (his equation 20) but fails to note that the latter expansion involves a different approximation than the former since η does not depend linearly on atomic displacements.

The appropriate strain measure would have been Thomsen's "$\underline{e}$", which is linear in displacements. However, the use of $\underline{e}$ raises special difficulties. The common practice (eg. Born and Huang, 1954; Leibfried and Ludwig, 1961), which Thomsen (1970) followed, is to transform the expansion of ϕ to be in terms of η, since η describes only pure strains, and, further, since this renders ϕ invariant under changes of frame of reference (Murnaghan, 1937; Truesdell and Noll, 1965; see also Chapter 2). If ϕ is left in terms of $\underline{e}$, these requirements are not automatically accounted for in general, and additional explicit restrictions on the equations must be imposed (Leibfried and Ludwig, 1961).

It has been pointed out in Chapter 2 that the use of η is sufficient to assure frame-indifference of ϕ, but that it is only necessary to use any strain measure which is a function of η only. This class of strain measures has been discussed in Chapter 2.

In this chapter, the incorporation of lattice dynamics into finite strain theory is reconsidered in the light of these points. It is necessary to go over the derivation of the equations in some detail in order to discuss these points. In this chapter, only isotropic stresses and strains will be considered, so that the rest of the treatment will be simplified and the essential points at issue will not be obscured.

Equations in terms of three strain measures will be derived here: η, $\underline{e}$, and $\underline{E}$, the invariant analogue of the Eulerian strain tensor $\underline{\epsilon}$ (Thomsen, 1972; Chapter 2). The choices of η and $\underline{E}$ serve to relate this to previous work and as examples of the infinity of possible invariant strain measures. The thermal contributions take a simpler form when expressed in terms of $\underline{e}$.

A further difference from Thomsen's equations is that the reference state will here be left arbitrary, rather than identifying it with the "rest" state as Thomsen (1970) did. The parameters of the equations will then be related to measured quantities, such as the bulk modulus and its pressure and temperature derivatives, in the reference state. Two inconvenient aspects of Thomsen's (1970) equations are thereby avoided. Thomsen's procedure requires the solution of six simultaneous non-linear algebraic equations (his equations 40) in order to determine the rest-state parameters from room temperature data. Further, Thomsen's insistence

on taking the finite strain equations to fourth-order means that the second pressure derivative of the bulk modulus is required, but this quantity has been measured for very few substances. Without this quantity, or some estimate of it, Thomsen's (1970) equations (40) cannot be evaluated nor his theory applied. In the present procedure, the reference state can be identified with that of the data, and the parameters evaluated with simple independent equations. The equations need only be taken to the order appropriate to the data.

3.2 Strain Energy and Lattice Energy

Consider, first, the point of view of finite strain theory. A hyperelastic material is defined (Truesdell and Noll, 1965, sect. 82) as an elastic material for which a strain energy function can be defined. This strain energy per unit mass, σ, is, of course, a function of strain. To specify strain, and, at the same time, satisfy the requirement of invariance under changes of frame of reference, we may use any of the "invariant" class of strain tensors discussed in Chapter 2. For instance, consider the strain tensor $\underline{e}$ defined by (6) of Chapter 2, which is the invariant analogue of the commonly used "Eulerian" strain $\underline{\epsilon}$. It is convenient, for the remainder of this discourse, to use the notations of the geophysical literature or of Thomsen (1970,

1972), since it will be mainly these sources which are referred to henceforth. Thus, instead of $\underline{e}$, define $\underline{E}$ as follows. If $\underline{X}$ is the position vector of a point in the medium in a reference configuration and $\underline{x}$ is the position of the same point in some other configuration, then the displacement gradient, $\underline{f}$, is defined through the relation

$$\underline{x} - \underline{X} = \underline{f}\,\underline{x} \; ; \qquad x_i - X_i = f_{ij} x_j \; . \tag{1}$$

The symmetric strain tensor $\underline{E}$ is then defined (Thomsen, 1972) as

$$\underline{E} = \tfrac{1}{2}(\underline{f} + \underline{f}^T - \underline{f}\,\underline{f}^T) \; ; \quad E_{ij} = \tfrac{1}{2}(f_{ij} + f_{ji} - f_{ik} f_{jk}) . \tag{2}$$

In equations (1) and (2), the indices i,j,k, denoting components with respect to rectangular Cartesian coordinates, run from 1 to 3, and repeated indices are summed.

The Cauchy stress tensor, $\underline{T}$, is given in terms of σ and $\underline{E}$ by (Murnaghan, 1937; Truesdell and Noll, 1965, sect. 84)

$$\underline{T} = \rho(\underline{1} - \underline{f})^T \left(\frac{\partial \sigma}{\partial \underline{E}}\right)(\underline{1} - \underline{f}) \; ; \quad T_{ij} = \rho(\delta_{ki} - f_{ki})\left(\frac{\partial \sigma}{\partial E_{km}}\right)(\delta_{mj} - f_{mj}) \; , \tag{3}$$

where ρ is the density of the material and $\underline{1}$ is the unit tensor. If σ is identified with the Helmholtz free energy per unit mass, A, then the derivative in (3) should be taken isothermally, and the stress along an isotherm results; if σ is identified as the internal energy per unit mass, U, then the derivatives in (3) should be taken isentropically,

and the stress along an isentrope results.

In order to apply (3), we require an explicit functional dependence of σ on $\underline{E}$. Since $\underline{E}$ is small when the "deformed" configuration is close to the reference configuration, we may expand $\sigma(\underline{E})$ as a Taylor series in $\underline{E}$:

$$\sigma(\underline{E}) = \sigma^{\circ} + \sigma^{\circ}_{ij} E_{ij} + \tfrac{1}{2} \sigma^{\circ}_{ijk\ell} E_{ij} E_{k\ell} \ , \qquad (4)$$

where $\sigma_{ij} = (\partial\sigma/\partial E_{ij})$, etc., and superscript "o" denotes evaluation at the reference configuration. Then σ^{o}_{ij}, σ^{o}_{ijkl}, etc., are parameters, to be determined empirically, which characterize a given material.

Now consider the point of view of lattice dynamics. The Helmholtz free energy per unit mass, A, of a vibrating atomic lattice is (Leibfried and Ludwig, 1961) the sum of the vibrational energy per unit mass, A_s, and the static potential energy per unit mass, $\bar{\phi}$, of the lattice when every atom is in its <u>mean</u> position:

$$A = \bar{\phi} + A_s \ . \qquad (5)$$

The bar will henceforth denote evaluation in the mean configuration. For the moment, consider just the form of ϕ.

To describe the dependence of ϕ on the instantaneous position of each atom, Thomsen (1970) generalized his displacement gradient $\underline{e}$, where (his equation 1)

$$x_i - X_i = e_{ij} X_j \tag{6}$$

as follows (his equation 18):

$$x^{\underline{m}}_{\mu i} - X^{\underline{m}}_{\mu i} = e^{\underline{m}\,\underline{m}}_{\mu i\,\mu j} X^{\underline{m}}_{\mu j} \quad . \tag{7}$$

Here $\underline{m} = (m_1, m_2, m_3)$ defines the unit cell, and μ specifies the atom in that cell (Leibfried and Ludwig, 1961; Thomsen, 1970). One could similarly generalize $\underline{f}$ and $\underline{E}$:

$$x^{\underline{m}}_{\mu i} - X^{\underline{m}}_{\mu i} = f^{\underline{m}\,\underline{m}}_{\mu i\,\mu j} x^{\underline{m}}_{\mu j} \quad , \tag{8}$$

$$E^{\underline{m}}_{\mu i} = \tfrac{1}{2}\left(f^{\underline{m}\,\underline{m}}_{\mu i\,\mu j} + f^{\underline{m}\,\underline{m}}_{\mu j\,\mu i} - f^{\underline{m}\,\underline{m}}_{\mu i\,\mu k} f^{\underline{m}\,\underline{m}}_{\mu j\,\mu k} \right) . \tag{9}$$

For convenience, this notation may be contracted by replacing $(\underline{m}, \mu, i)$ by α, $(\underline{m}, \mu, j)$ by β, etc. Since $f_{\alpha\beta}$ or $E_{\alpha\beta}$ serve as well as $e_{\alpha\beta}$ to describe the positions of atoms in the lattice, we could expand ϕ in terms of either of these; for example the generalized analogue of (4) would be

$$\phi = \phi^0 + \phi^0_{\alpha\beta} E_{\alpha\beta} + \tfrac{1}{2} \phi^0_{\alpha\beta\gamma\delta} E_{\alpha\beta} E_{\gamma\delta} + \cdots \quad , \tag{10}$$

where $\phi^0_{\alpha\beta}$, etc., are to be interpreted as the $E_{\alpha\beta}$ derivatives of ϕ in this context.

Although (10) is a valid representation of the dependence of ϕ on atomic positions, it does not give ϕ in a form suitable for solving the equation of motion of the lattice,

which is, of course, the subject of the theory of lattice dynamics. In this theory, ϕ is expanded in terms of atomic displacements, $u_\alpha = x_\alpha - X_\alpha$ (see Thomsen, 1970, equation 17):

$$\phi = \phi^\circ + \phi^\circ_\alpha u_\alpha + \tfrac{1}{2} \phi^\circ_{\alpha\beta} u_\alpha u_\beta + \cdots \quad . \tag{11}$$

If this expansion is truncated after the second order, the equation decouples into that for a system of independent harmonic oscillators - the modes of vibration of the lattice. If up to fourth-order terms are retained, then a perturbation scheme may be used to relinearize the equation of motion (Leibfried and Ludwig, 1961; Ludwig, 1967).

Now, from (7) we see that, since the reference position, X_α, is a constant, $e_{\alpha\beta}$ is linearly related to u_α. Thus, in (11), the u_α can be replaced by $X_\beta e_{\alpha\beta}$, etc., and an expansion of ϕ in terms of $e_{\alpha\beta}$ results (see Thomsen, 1970, equation 19), which is identical to (11). In particular, if (11) is truncated after the fourth order, say, then the expansion of ϕ in terms of $e_{\alpha\beta}$ truncated after the fourth order is exactly equivalent. This is not true if ϕ is expanded in terms of any displacement measure which is non-linearly related to u_α, such as $f_{\alpha\beta}$ or $E_{\alpha\beta}$. Thus, (10) truncated after the fourth order involves a different approximation than does (11) truncated after the fourth order. This point was neglected by Thomsen (1970) when he transformed (and specialized) from his expansion (19) of ϕ in terms of $e_{\alpha\beta}$ to his

expansion (20) in terms of the Lagrangian strain $\underline{\eta}$, which is related (non-linearly) to $\underline{e}$ through

$$\eta_{ij} = \tfrac{1}{2}\left(e_{ij} + e_{ji} + e_{ki}\, e_{kj}\right) . \qquad (12)$$

For the purpose of deriving strain-dependent quantities from the lattice theory which are invariant under changes of frame of reference ("frame-indifferent"), the equations are usually transformed from $\underline{e}$- (or $\underline{u}$-) dependence to $\underline{\eta}$-dependence in this manner (eg. Leibfried and Ludwig, 1961, sects. 8, 11; Born and Huang, 1954). Leibfried and Ludwig (1961, sect. 2) have considered the restrictions on the u_α derivatives of ϕ imposed by the frame-indifference requirement. According to the discussion of Chapter 2, restrictions will also apply in the case of a homogeneous strain, described by $\underline{e}$, and these will be satisfied only in such special cases as isotropic strain or an isotropic medium. Thus, in a limited sense, the expansion (11) can serve as the basis of both lattice dynamics and finite strain.

Another reason for using other than $\underline{u}$ or $\underline{e}$ as displacement measures, of course, is that the truncated expansions in terms of these may not be a suitable functional form. It has been established that expansions in terms of the Eulerian strain, $\underline{\epsilon}$, which is identical to $\underline{E}$ of (2) in the case of isotropic strain (see Chapter 2), are empirically preferable to expansions in terms of $\underline{\eta}$, for instance (Birch, 1947, 1952).

To conclude this section, the frame-indifference requirement, and possibly empirical preference also, requires that a strain measure other than $\underline{e}$ be used for describing strain dependence in general situations. The displacement gradient $\underline{e}$ can be used only for special applications. The consequences of such a transformation will be given below.

3.3 Vibrational Energy and the Mie-Grüneisen Equation

The pertinent parts of the theory of anharmonic lattice dynamics will be briefly reviewed here, so that the approximations involved can be made explicit for comparison in the next section with the approximations made in finite strain theory. The problem of anharmonic lattice dynamics has been reviewed at length by Leibfried and Ludwig (1961) and Ludwig (1967), who give a general treatment of the "fourth-order" case, i.e., the case when terms up to the fourth order are retained in the expansion (11) of ϕ in terms of $\underline{u}$ or the equivalent expansion in terms of $\underline{e}$. The Hamiltonian of the lattice in this case can be written

$$\begin{aligned} H &= E_k + \phi_0 + \phi_1 + \phi_2 + \phi_3 + \phi_4 \\ &= H_0 + \phi_1 + \phi_3 + \phi_4 \,, \end{aligned} \tag{13}$$

where E_k is the kinetic energy, $\phi_1 = \phi^0_{\alpha\beta} e_{\alpha\beta}$, etc., and $H_0 = E_k + \phi_0 + \phi_2$ is the Hamiltonian in the "harmonic approximation", i.e., when ϕ is truncated after the second order term.

The equation of motion derived from (13) is non-linear because of the terms ϕ_3 and ϕ_4. In order to re-linearize it, it is necessary to assume that ϕ_3 and ϕ_4 are small, so that a perturbation treatment can be used. The assumption made by Leibfried and Ludwig is, in effect, that

$$|\phi_3| \sim \delta |H_0| , \tag{14}$$

$$|\phi_4| \sim \delta^2 |H_0| , \tag{15}$$

where δ is small compared to unity. For a given material, for which ϕ is fixed, the $\phi^0_{\alpha\beta}$, etc., are fixed and (14) and (15) limit the magnitude of the $e_{\alpha\beta}$, i.e., (14) and (15) assume that the amplitudes of the thermal motions of the lattice are not too large.

Leibfried and Ludwig (1961) then show that the vibrational energy is given by

$$A_s = E_2(\phi_2) + E_3(\phi_3^2) + E_4(\phi_4) + E_1(\phi_1^2, \phi_1\phi_3) + O(\delta^3) , \tag{16}$$

where

$$\begin{aligned} E_3 &\sim \delta^2 E_2 , \\ E_4 &\sim \delta^2 E_2 , \\ E_1 &\sim \delta^2 E_2 . \end{aligned} \tag{17}$$

E_2 is the "quasi-harmonic" vibrational energy, i.e., the harmonic vibrational energy

$$E_2 = kT \sum_j \ln \left[2 \sinh \left(\tfrac{1}{2} \hbar \omega_j / kT \right) \right] , \qquad (18)$$

but with the eigenfrequencies ω_j dependent on strain. In (18), T is temperature, k is Boltzmann's constant, $\hbar$ is Planck's constant and ω_j is the frequency of the j^{th} mode of vibration of the lattice. The summation is over all modes of vibration, of which there are 3N, where N is the number of atoms in the lattice. The ω_j^2 are proportional to a linear combination of the second derivatives of ϕ with respect to displacement, evaluated at the <u>mean</u> positions of the atoms. Thus in the harmonic approximation, the ω_j are constants and E_2 depends only on T. In the fourth-order approximation, E_2 depends on both temperature and strain. Expressions for E_3, E_4 and E_1 are given by Leibfried and Ludwig (1961), but for the present we need only note that E_3 and E_4 are temperature dependent, while E_1 is not.

If we use equation (16) for the vibrational energy in equation (5) for the Helmholtz free energy, then we include, approximately, both the strain and the temperature dependence of A:

$$A(\text{strain}, T) = \bar{\phi}(\text{strain}) + A_s(\text{strain}, T) \; ; \qquad (19)$$

the particular strain measure is deliberately left unspecified at this stage. By taking successive strain derivatives of A, one obtains the stress (Cf. equation 3) and the elastic constants of second, third, etc., orders. By taking temperature derivatives of A and its strain derivative, one obtains the entropy, internal energy, specific heat, etc.

The concern of this paper is primarily to derive expressions for the pressure as a function of strain and temperature in the case of isotropic stresses and strains. Therefore, we will proceed directly from (19) to an expression for the pressure, before considering in detail the expansion of (19). This will show explicitly the Mie-Grüneisen form of the equations derived later (Thomsen, 1970).

In the case of isotropic stresses and strains, equation (3) reduces to

$$P = -\frac{\partial \sigma}{\partial V} \; , \qquad (20)$$

where P is pressure and V is (specific) volume. We will consider here just the isothermal pressure. Then we may identify σ in (20) as the free energy A given by (19), and the derivative in (20) is taken isothermally. From the expressions given by Leibfried and Ludwig, for E_3, E_4 and E_1, it can be shown (Leibfried and Ludwig, 1961, sects. 7, 10) that

$$\left(\frac{\partial E_3}{\partial V}\right)_T , \left(\frac{\partial E_4}{\partial V}\right)_T , \left(\frac{\partial E_1}{\partial V}\right)_T \sim O(\delta^3) , \tag{21}$$

i.e., that these derivatives are third order in δ. Thus they may be neglected, in accord with the perturbation expansion, and the fourth-order expansion of ϕ, which retained only terms out to second order in δ. Thus, using (16), (19) and (21) in (20), we obtain

$$P = -\frac{d\phi}{dV} - \left(\frac{\partial E_2}{\partial V}\right)_T + O(\delta^3) . \tag{22}$$

In this approximation, only the "quasi-harmonic" contribution, E_2, to the vibrational energy enters the pressure.

In order to rewrite (22), we note the following relations. The internal energy, U, is defined thermodynamically as

$$U = A + TS , \tag{23}$$

where

$$S = -\left(\frac{\partial A}{\partial T}\right)_V \tag{24}$$

is the entropy. Using equation (5), we may identify the vibrational contribution, U_s, to U as

$$U_s = U - \bar{\phi} = A_s - TS \ . \tag{25}$$

Defining U_q as

$$U_q = \sum_j u_j = \sum_j \left(\frac{\partial E_2}{\partial \ln \omega_j} \right)_T \ , \tag{26}$$

it can be shown (Leibfried and Ludwig, 1961) that U_q is the contribution to U_s (and hence to U) arising from E_2, i.e., it is the quasi-harmonic vibrational contribution to U.

Now, defining γ and γ_j as

$$\gamma = \frac{1}{U_q} \sum_j u_j \gamma_j = - \frac{1}{U_q} \sum_j u_j \frac{d \ln \omega_j}{d \ln V} \ , \tag{27}$$

we can write (22) as

$$\begin{aligned} P &= - \frac{d\phi}{dV} - \sum_j \frac{d \ln \omega_j}{dV} \left(\frac{dE_2}{d \ln \omega_j} \right) + O(\delta^3) \\ &= - \frac{d\phi}{dV} + \frac{1}{V} \sum_j \gamma_j u_j + O(\delta^3) \\ &= - \frac{d\phi}{dV} + \frac{\gamma}{V} U_q + O(\delta^3) \ . \end{aligned} \tag{28}$$

The last form of (28) has the form of the "Mie-Grüneisen equation", but we may note that it is only an approximation to the Mie-Grüneisen equation, which is

$$P = -\frac{d\phi}{dV} + \frac{\gamma}{V} U_s . \tag{29}$$

The Mie-Grüneisen equation is derived from the assumptions that U_s depends on V only through the ω_j, and that all of the ω_j have the same volume derivative. The quantity γ in (29) is the "Grüneisen parameter", defined, in accordance with this approximation, as

$$\gamma = -\frac{d \ln \omega}{d \ln V} , \tag{30}$$

where ω is any ω_j. Comparison with (27) shows that γ may be identified as a mean of the "mode Grüneisen parameters" γ_j.

The fourth-order approximation and the approximations made in (14) and (15) thus lead to a quasi-harmonic equation of state. The additional "Grüneisen" approximation yields a Mie-Grüneisen type of equation of state.

3.4 Finite Strain Equations of State

We now have, in (19) and (28), expressions for the free energy and the pressure which include both the static and vibrational contributions, and in which the vibrational contribution is evaluated to within the approximations described above. Further, the strain dependence of both the static

and vibrational contributions is implicit in these equations, the latter through the strain dependence of the ω_j's. The task of this section is to make this strain dependence explicit, keeping in mind the limitations imposed by the approximations already made.

Isotropic strain is specified in terms of V, the specific volume. In terms of V, the strain measures to be used here are

$$e_{ij} = e\,\delta_{ij}\,; \quad e = (V/V_o)^{1/3} - 1\,, \tag{31}$$

$$E_{ij} = E\,\delta_{ij}\,; \quad E = \tfrac{1}{2}\left[1 - (V/V_o)^{-2/3}\right], \tag{32}$$

$$\eta_{ij} = \eta\,\delta_{ij}\,; \quad \eta = \tfrac{1}{2}\left[(V/V_o)^{2/3} - 1\right], \tag{33}$$

where V_o is the specific volume in the reference configuration.

The strain dependence of the vibrational terms E_2 and U_q is through the ω_j, so it is made explicit by writing, for instance,

$$\omega_j^2 = (\omega_j^2)_o\left(1 + g_j e + \tfrac{1}{2} h_j e^2 + \ldots\right), \tag{34}$$

where g_j and h_j are constants. The <u>square</u> of ω_j is expanded here because a simple interpretation of g_j and h_j follows in this case. The ω_j^2 are linear combinations of the second derivatives of ϕ, with respect to displacements, evaluated at the mean configuration (Leibfried and Ludwig, 1961, p.304).

Since e is linear in displacements (see equation 6), it follows from the definitions of g_j and h_j in (34) that they are, respectively, linear combinations of the third and fourth derivatives of ϕ, with respect to displacements, evaluated at the mean configuration. Insertion of (34) into the definition (27) of γ_j leads to an expression for the strain dependence of γ_j:

$$\gamma_j = -\frac{(1+e)(g_j + h_j e + \dots)}{6(1 + g_j e + \tfrac{1}{2} h_j e^2 + \dots)} \quad . \tag{35}$$

If the Grüneisen approximation is extended, and it is assumed that all of the g_j and h_j are the same, the volume dependence of γ is

$$\gamma = -\frac{(1+e)(g + h e + \dots)}{6(1 + g e + \tfrac{1}{2} h e^2 + \dots)} \quad . \tag{36}$$

If analogous expansions in terms of η and E are made, analogous expressions are obtained:

$$\omega_j^2 = (\omega_j^2)_0 (1 + g'\eta + \tfrac{1}{2} h'\eta^2 + \dots) \tag{35a}$$

$$= (\omega_j^2)_0 (1 + g'' E + \tfrac{1}{2} h'' E^2 + \dots) \, , \tag{35b}$$

$$\gamma = -\frac{(1+2\eta)(g' + h'\eta + \dots)}{6(1 + g'\eta + \tfrac{1}{2} h'\eta^2 + \dots)} \tag{36a}$$

$$= -\frac{(1-2E)(g'' + h''E + \ldots)}{6(1 + g''E + \tfrac{1}{2}h''E^2 + \ldots)} \quad . \tag{36b}$$

It is easy to show that

$$\begin{aligned} g' &= g'' = g \ , \\ h' &= h - g \ , \\ h'' &= h + 3g \ . \end{aligned} \tag{37}$$

Following a procedure similar to that used in deriving equation(28), we can obtain (Leibfried and Ludwig, 1961)

$$\begin{aligned} \left(\frac{\partial u_q}{\partial \ln V}\right)_T &= \sum_j \frac{d \ln \omega_j}{d \ln V} \left(\frac{\partial u_q}{\partial \ln \omega_j}\right)_T \\ &= -\sum_j \gamma_j (u_j - T c_j) \\ &= -\gamma (u_q - T C_q) \ , \end{aligned} \tag{38}$$

where the last step also requires the Grüneisen approximation, and $C_q = \sum_j c_j = \sum_j (\partial u_j / \partial T)_V$ is the quasi-harmonic contribution to the specific heat at constant volume. Using these results, and equation (31), the expansion of E_2 in terms of e, for example, is

$$\begin{aligned} E_2(e,T) &= E_2(0,T) + \tfrac{1}{2} g u_{q0} e \\ &\quad + \tfrac{1}{8}\left[(2h - g^2)u_{q0} - g^2 T C_{q0}\right] e^2 + \ldots \ . \end{aligned} \tag{39}$$

We may now use equation (39) for E_2 and the expansion of ϕ in terms of $\underline{e}$ in equation (19) to obtain an expansion of A in terms of e. If this expansion is taken to fourth order and substituted into equation (20), we get, for the pressure, using equation (31),

$$P(e,T) = -\frac{(1+e)^{-2}}{3V_0}\left(\frac{\partial A}{\partial e}\right)_T$$
$$= -\frac{(1+e)^{-2}}{3V_0}\left(a_0 + a_1 e + a_2 e^2 + a_3 e^3 + \ldots\right), \tag{40}$$

where

$$a_0 = \left(\frac{d\phi}{de}\right)_0 + \tfrac{1}{2} g U_{q0}\,, \tag{40a}$$

$$a_1 = \left(\frac{d^2\phi}{de^2}\right)_0 + \tfrac{1}{4}(2h - g^2)U_{q0} - \tfrac{1}{4} g^2 T C_{q0}\,, \tag{40b}$$

$$a_3 = \tfrac{1}{2}\left(\frac{d^3\phi}{de^3}\right)_0 + \ldots\,, \tag{40c}$$

$$a_4 = \tfrac{1}{6}\left(\frac{d^4\phi}{de^4}\right)_0 + \ldots\,. \tag{40d}$$

Equations (40) give the equation of state in the desired form - namely, the pressure as a function of strain and temperature. Before analogous equation in terms of η and E are given, the truncation of the expansion in (40) will be discussed.

The relative smallness of the thermal contributions

means that they need not be carried for as many terms as the static contributions. Consider, for instance, equation (40b). At higher temperatures than the Debye temperature, U_{qn} is approximately linear in T, and C_{qn} is approximately constant. The temperature is the macroscopic expression of the mean thermal vibration amplitude (temperature is proportional to energy which is proportional to amplitude squared, classically). The presence of h, involving fourth derivatives of ϕ, and of g^2 (g involves third derivatives of ϕ) indicates that these thermal terms are $O(\delta^2)$ relative to $(d^2\bar{\phi}/de^2)$ - recall that δ specifies the magnitude of ϕ_3 and ϕ_4 relative to ϕ_2, in effect. Similar arguments establish that the thermal contributions to subsequent terms (a_2, a_3, ...) are $O(\delta^2)$ relative to the static contribution (the presence of an arbitrary factor in a_0 depending on the choice of the reference state complicates consideration of this term). Thus, for instance, terms to $O(e^3)$ are included in (40), so thermal terms to $O(e\delta^2)$ need only be retained. In general, the expansion of the thermal contribution can be truncated two terms earlier than the expansion of the static contribution.

Equation (40) can be viewed from two slightly different viewpoints. On the one hand, it gives the pressure in two parts - that arising from the static lattice potential, and that arising from the lattice vibrations (Cf. the Mie-Grüneisen form, equation 28). One would thus expect it to be a reasonable approximation between absolute zero and some finite temperature. (Note that because of "zero point" vibrations, some approximation is involved even at absolute zero.) On the other hand, equation (40) has exactly the form which would result from expanding the strain energy function, σ, to fourth order in e without considering ex-

plicitly any temperature dependence. If σ is interpreted as the free energy at a certain temperature, then equations (40a-d), in effect, give, approximately, the temperature dependence of the coefficients in the expansion of σ at that temperature. Equation (40) could thus be expected to be a reasonable approximation within some range of temperatures about that temperature. (It should be remarked that since the approximation is poorer at higher temperatures, this range of temperatures will be smaller at higher temperatures.) From either point of view, the effect of the approximations made in the solution of the lattice dynamics is to limit the range of temperatures over which equation (40) is a reasonable approximation. This is in accordance with the assumption, implicit in (14) and (15), that the amplitudes of the thermal motions are not too large. On the other hand, the truncation of the expansion of A in terms of strain implies the assumption that the strain-induced displacements are not too large. The truncation of the expansion of A in terms of e after the fourth order in the derivation of (40) is coincidental (it was done for empirical usefullness and for comparison with Thomsen's equations). If one wished to consider very large strains, then a different (or higher-order) form of A (or ϕ) might be required, but if, at the same time, only a limited range of temperature needed to be considered, then the "fourth-order" approximation to the vibrational

effects might be quite sufficient. Hence, within the restrictions imposed by the invariance requirement, any form may be assumed for A (or ϕ), and the fourth-order theory of lattice dynamics may be used to evaluate approximately the vibrational (or thermal) effects in the resulting finite strain equation.

A "Lagrangian" equation of state can now be derived from (40) by using equations (31) and (33) to relate derivatives with respect to η to derivatives with respect to e. Retaining up to fourth-order terms, the result is

$$P(\eta,T) = -\frac{(1+2\eta)^{-\frac{1}{2}}}{3V_0}\left(\frac{\partial A}{\partial \eta}\right)_T$$

$$= -\frac{(1+2\eta)^{-\frac{1}{2}}}{3V_0}\left(b_0 + b_1\eta + b_2\eta^2 + b_3\eta^3\right), \qquad (41)$$

where

$$b_0 = \left(\frac{d\phi}{d\eta}\right)_0 + \tfrac{1}{2} g U_{q0}\,, \qquad (41a)$$

$$b_1 = \left(\frac{d^2\phi}{d\eta^2}\right)_0 + \tfrac{1}{4}(2h'-g^2)U_{q0} - \tfrac{1}{4} g^2 T C_{q0}\,, \qquad (41b)$$

$$b_2 = \tfrac{1}{2}\left(\frac{d^3\phi}{d\eta^3}\right)_0 + \ldots\,, \qquad (41c)$$

$$b_3 = \tfrac{1}{6}\left(\frac{d^4\phi}{d\eta^4}\right)_0 + \ldots\,. \qquad (41d)$$

A similar procedure, using equations (31) and (32), yields the fourth-order "Eulerian" equation (recalling that, for isotropic strain, $E_{ij} = \epsilon_{ij} = E\delta_{ij}$):

$$P(E,T) = -\frac{(1-2E)^{5/2}}{3V_0}\left(\frac{\partial A}{\partial E}\right)_T$$

$$= -\frac{(1-2E)^{5/2}}{3V_0}\left(c_0 + c_1 E + c_2 E^2 + c_3 E^3\right), \quad (42)$$

where

$$c_0 = \left(\frac{d\phi}{dE}\right)_0 + \tfrac{1}{2} g U_{q0} , \quad (42a)$$

$$c_1 = \left(\frac{d^2\phi}{dE^2}\right) + \tfrac{1}{4}(2h'' - g^2)U_{q0} - \tfrac{1}{4} g^2 T C_{q0} \quad (42b)$$

$$c_2 = \tfrac{1}{2}\left(\frac{d^3\phi}{dE^3}\right)_0 + \cdots , \quad (42c)$$

$$c_3 = \tfrac{1}{6}\left(\frac{d^4\phi}{dE^4}\right)_0 + \cdots . \quad (42d)$$

Before some further remarks about these equations are made, in the next section, the parameters entering these

equations will be related to quantities which are commonly (or potentially) determined experimentally. By successive differentiation of equation (40), the isothermal bulk modulus $K_T = -V(\partial P/\partial V)_T$, and its isothermal pressure derivatives, $K_T' = (\partial K_T/\partial P)_T$, etc., can be obtained in terms of the a's. Evaluating these and equation (40) at e = 0, we can solve for the a's in terms of P_0, K_0, etc., where the subscript "0" denotes evaluation at e = 0 and the subscript "T" is dropped for now, obtaining

$$a_0 = -3V_0 P_0 , \tag{43a}$$

$$a_1 = -3V_0 (-3K_0 + 2P_0) , \tag{43b}$$

$$a_2 = -3V_0 \left(\tfrac{9}{2} K_0 K_0' - \tfrac{9}{2} K_0 + P_0\right) , \tag{43c}$$

$$a_3 = -3V_0 \left[-\tfrac{9}{2} K_0^2 K_0'' - \tfrac{9}{2} K_0 K_0' (K_0' - 1) - K_0\right] . \tag{43d}$$

Similarly, from equations (32) and (33),

$$b_0 = -3V_0 P_0 , \tag{43e}$$

$$b_1 = -3V_0 (-3K_0 + 3P_0) , \tag{43f}$$

$$b_2 = -3V_0 \left(\tfrac{9}{2} K_0 K_0' - \tfrac{7}{2} P_0\right) , \tag{43g}$$

$$b_3 = -3V_0 \left[-\tfrac{9}{2} K_0^2 K_0'' - \tfrac{9}{2} K_0 K_0' (K_0' + 1) + \tfrac{1}{2} K_0 + \tfrac{19}{2} P_0\right] , \tag{43h}$$

$$c_0 = -3V_0 P_0 , \tag{43k}$$

$$c_1 = -3V_0(-3K_0 + 5P_0), \tag{43m}$$

$$c_2 = -3V_0\left(\tfrac{9}{2}K_0K_0' - 18K_0 + \tfrac{35}{2}P_0\right), \tag{43n}$$

$$c_3 = -3V_0\left[-\tfrac{9}{2}K_0^2K_0'' - \tfrac{9}{2}K_0K_0'(K_0'-7) - \tfrac{143}{2}K_0 + \tfrac{105}{2}P_0\right]. \tag{43p}$$

To obtain g and h, we first differentiate equation (37) for and solve for g and h, obtaining

$$g = -6\gamma_0 , \tag{44}$$

$$h = g\left[3\left(\frac{\partial \ln \gamma}{\partial \ln V}\right)_{0T} + g - 1\right]. \tag{45}$$

γ_0 can be obtained from the thermodynamic identity

$$\gamma = \frac{V \alpha K_T}{C_V} , \tag{46}$$

and the volume derivative of γ is given by the identity (Bassett et al., 1968)

$$\left(\frac{\partial \ln \gamma}{\partial \ln V}\right)_T = 1 + \delta_T - K_T' - \left(\frac{\partial \ln C_V}{\partial \ln V}\right)_T , \tag{47}$$

where

$$\delta_T = -\frac{1}{\alpha K_T}\left(\frac{\partial K_T}{\partial T}\right)_P . \tag{48}$$

In these equations, C_V is the specific heat at constant volume and $\alpha = (\partial V/\partial T)_P/V$ is the volume coefficient of thermal expansion.

Equations (43) to (48) determine the six equation of state parameters V_0, a_1, a_2, a_3, g and h in terms of the six laboratory quantities V_0, K_0, K_0', K_0'', α and $(\partial K/\partial T)_P$. P_0 and a_0 are determined by V_0 and g through (40a) and (43a).

The procedure for determining the parameters is as follows. Assuming that V_0, K_0, K_0', K_0'', α and $(\partial K/\partial T)_P$ are known at some temperature T_0 and zero pressure, then g and h (which are temperature independent) and a_1, a_2 and a_3 can be evaluated, using (43-48), at T_0. This serves to define the

reference state as P = 0, T = T_0, V = V_0. Then $P_0(T_0) = 0 = a_0(T_0)$. Finally, a_0 and a_1, which specify the temperature dependence of the equations of state (40), (41) or (42), can be evaluated at any temperature T using (40a) and (40b):

$$a_0(T) = a_0(T_0) + \tfrac{1}{2} g \left[U_{q0}(T) - U_{q0}(T_0) \right], \tag{49a}$$

$$a_1(T) = a_1(T_0) + \tfrac{1}{4}(2h - g^2)\left[U_{q0}(T) - U_{q0}(T_0) \right] - \tfrac{1}{4} g^2 \left[T C_{q0}(T) - T_0 C_{q0}(T_0) \right]. \tag{49b}$$

Of course, in this procedure, U_{q0} and C_{q0} must be known or estimated as functions of temperature. For many applications, the Debye or Einstein models can be used to estimate these. These require the empirical input of the characteristic temperature of the solid. If more extensive empirical input of U_{q0} and C_{q0} is desired, the specifically anharmonic contribution to the U and C_v must be subtracted before such data are used (Leibfried and Ludwig, 1961). This point is discussed further in the next section.

Illustrative numerical applications of the equations derived in this section are given in Chapters 6 and 7.

3.5 Discussion

Firstly, some further comments on the approximations used in the derivation of these equations will be made.

Equations (40), (41) and (42) are all derived from

fourth-order expansions (in terms of the appropriate strain) of the free energy. According to the discussion of the previous section, however, these expansions can, in general, be taken to any order. For example, if the "Eulerian" equation is truncated after the third-order term, and P_0 is assumed to be zero, the well known "Birch-Murnaghan" equation (Murnaghan, 1937; Birch, 1938) results. The contribution of the present theory is to give, approximately, the explicit temperature dependence of such finite strain equations.

The "Mie-Grüneisen approximation" was invoked at several points in this derivation. Strictly, such a strong assumption is not necessary. If we were to follow the procedure used in deriving the Mie-Grüneisen form (28) of the equation of state, then we would define, in (38), another mean of the derivatives of the ω_j, and the corresponding summations could thus be replaced. In general, however, these means bear no simple relation to each other. In the Mie-Grüneisen approximation, all of the quantities being averaged are identical, and this difficulty is removed. An alternative, weaker assumption, discussed by Leibfried and Ludwig (1961), is to replace the means of these derivatives with the derivatives of the mean of the ω_j^2, which can be fairly easily calculated from lattice models. Evidently, this approximation may be reasonable at very low or very high temperatures (relative to the Debye temperature), but will be poorer at intermediate

temperatures. We see, for instance, that this approximation leaves γ independent of temperature. At high temperatures, γ is observed to be fairly constant, but below the Debye temperature it usually becomes temperature dependent.

The vibrational terms given here contain only the quasi-harmonic contributions to the internal energy and the specific heat, but in the fourth-order theory of lattice dynamics there are additional contributions to these quantities from the terms E_3 and E_4 (see equations 16 and 23). To apply these equations in a manner fully consistent with the fourth-order approximation, while making maximum use of available data, one should therefore evaluate the contributions from E_3 and E_4 and subtract them from measured values of the internal energy and specific heat to obtain the quasi-harmonic contributions. However, the contributions from E_3 and E_4 are difficult to evaluate (Leibfried and Ludwig, 1961), so in practice it is much simpler to assume that the quasi-harmonic contributions approximate the measured values. This is an approximation in the vibrational terms in addition to the fourth-order approximation, so it seems preferable, if the equations are applied in this way, to refer to them as "quasi-harmonic equations of state".

The relation of Thomsen's (1970) equations to those given here should be clarified. Thomsen's equation (40) is analogous to the present equation (41), in terms of η,

truncated after the fourth-order term. The only substantial difference is that the reference state has not been specified here, whereas Thomsen identified it with the stress-free rest state of the lattice. From the point of view of lattice dynamics, the latter is the natural reference state, but if the present equations are viewed as finite strain equations in which thermal effects are (approximately) explicitly included, then the reference state is arbitrary (with the qualification that the approximation is poorer, further from the rest state). Considerable convenience accrues in some applications from identifying the reference state as that at which experimental data are available, since Thomsen's (1970) set of six simultaneous non-linear equations, relating his parameters to experimental quantities, is thereby avoided.

The expressions (36), (36a) and (36b) for γ given here have a certain arbitrariness. It would be possible, for instance, to expand them to appropriate order in strain, or to do as Thomsen (1970) did, i.e., by analogy with the pressure equation, to retain the factor arising from the volume differentiation and expand the remaining quotient. Thomsen's expression (43) for γ, apart from the reference state, is

$$\gamma = (V/V_0)^{2/3} (\gamma_0 + 3\lambda\eta), \qquad (50)$$

where $\lambda = -(h' - g^2)/18$, which could be obtained from (36a). In principle, there is no reason to prefer any of these forms over the others, but some trial calculations indicate that equations (36),(36a) or (36b) are less likely to give negative values of γ at large compressions than (50) or its analogues.

Finally, some comments on the capabilities of the present theory. Thomsen (1972, p. 367) pointed out that although this theory predicts that the elastic moduli (in the present case, K) are linear in T at high temperature and at constant volume, this does not imply linearity at constant pressure. Thus, measured non-linearity with T of elastic moduli, taken at zero pressure, does not imply that a higher order thermal theory is required. However, Thomsen (1970, p. 2009, 2010; 1972, p. 370) goes on to claim that non-zero values of $(\partial^2 c_{\alpha\beta}/\partial P \partial T)$, where $c_{\alpha\beta}$ is an elastic modulus, do require a higher order theory for their description. It has been argued here that the Mie-Grüneisen equation is valid at arbitrary volumes; therefore, an arbitrary number of derivatives may be taken, and the thermal contribution will be included in these, although it will be $O(\delta^2)$. Thus, thermal contribution to all pressure derivatives will result from this theory. Of course, the predicted value of the temperature coefficient may not agree with the measured values, but the mere existence of a non-zero

temperature coefficient is not sufficient grounds for requiring a higher order thermal theory.

Similarly, a non-zero value of K_0'' does not necessarily require a fourth-order expansion in strain. For instance, a third-order expansion in e, so that $a_3 = 0$, implies, from (43d),

$$K_0 K_0'' = -K_0'(K_0' - 1) - \frac{2}{9}, \tag{51}$$

which is not zero, in general. Of course, this may not give a suitable value of K_0'', in which case a fourth-order expansion in strain, or a third-order one in terms of a more suitable strain measure, is required.

3.6 References

BASSETT W. A., TAKAHASHI T., MAO H. K. and WEAVER J. S., J. Appl. Phys. 39, 319 (1968).

BIRCH F., J. Appl. Phys. 9, 279 (1938).

BIRCH F., Phys. Rev. 71, 809 (1947).

BIRCH F., J. Geophys. Res. 57, 227 (1952).

BORN M. and HUANG K. H., Dynamical Theory of Crystal Lattices, Clarendon Press, Oxford (1954).

LEIBFRIED G. and LUDWIG W., Solid State Physics (Edited by Bradley) 12, 275, Academic Press, New York (1961).

LUDWIG W., Springer Tracts in Modern Physics 43, Springer-Verlag, Berlin (1967).

MURNAGHAN F. D., Am. J. Math. 59, 235 (1937).

THOMSEN L., J. Phys. Chem. Solids 31, 2003 (1970).

THOMSEN L., J. Phys. Chem. Solids 33, 363 (1972).

TRUESDELL C. and NOLL W., Handb. Phys. Vol. III/3, Springer-Verlag, Berlin (1965).

CHAPTER 4

ISENTROPES AND HUGONIOTS

Summary

Expressions are obtained for isentropes and Hugoniots in terms of the same parameters as entered the isothermal equations of state of the last chapter. The isothermal and isentropic bulk moduli and their first and second pressure derivatives are also related in accordance with the fourth-order approximation of lattice dynamics.

4.1 Introduction

Since expressions were obtained in Chapter 3 for the Helmholtz free energy and the pressure as functions of both specific volume and temperature, it is possible to derive expressions for any other (P, V, T) locus from these. No new parameters or approximations need be introduced in this procedure. Expressions will be derived here for isentropes and Hugoniots.

4.2 Isentropes

The Mie-Grüneisen equation (Chapter 3, equation 28)

$$P = -\frac{d\phi}{dV} + \frac{\gamma}{V} U_q \qquad (1)$$

can be regarded as giving the pressure either as a function of strain and temperature, or as a function of strain and entropy. Thus an expression for the pressure along an isentrope can be obtained by expanding (1) in terms of strain at constant entropy. The temperature, or entropy, dependence of (1) is through U_q. From the result (Leibfried and Ludwig, 1961; compare equation 38, Chapter 3) that

$$\left(\frac{\partial U_q}{\partial V}\right)_s = -\frac{\gamma}{V} U_q \quad , \qquad (2)$$

one can obtain the expansion of U_q in terms of e at constant

entropy, for instance:

$$U_q(e,S) = U_{q0} + \tfrac{1}{2} g U_{q0} e + \tfrac{1}{8}(2h-g^2) U_{q0} e^2 + \ldots . \qquad (3)$$

The result of substituting (3) into (1) is an equation of exactly the same form as (40) of Chapter 3:

$$P(e,S) = -\frac{(1+e)^{-2}}{3V_0}(a_{0S} + a_{1S} e + a_{2S} e^2 + a_{3S} e^3 + \ldots , \qquad (4)$$

where the new coefficients are

$$a_{0S}(S) = \phi_0' + \tfrac{1}{2} g U_{q0} , \qquad (4a)$$

$$a_{1S}(S) = \phi_0'' + \tfrac{1}{4}(2h-g^2) U_{q0} , \qquad (4b)$$

$$a_{2S} = \tfrac{1}{2} \phi_0''' + \ldots , \qquad (4c)$$

$$a_{3S} = \tfrac{1}{6} \phi_0^{IV} + \ldots . \qquad (4d)$$

Equations (4) thus give the pressure along an isentrope in terms of the same parameters (namely g, h, and the derivatives of ϕ) as (40) of Chapter 3 for an isotherm.

Comparison with (40a-d) of Chapter 3 shows that only a_{1S} differs from its isothermal counterpart. As in the isothermal case, the a_{NS} can be written in terms of the isentropic bulk modulus, K_S, and its isentropic pressure derivatives. The results are of exactly the same form as (43a-d) of Chapter 3, but with isentropic quantities. These results

can be used to obtain expressions for the difference between the isothermal and isentropic bulk moduli and their respective derivatives. From the analogues of (43a-d) of Chapter 3 we obtain, omitting "S" subscripts,

$$P_0 = -\frac{1}{3V_0} a_0 , \tag{5a}$$

$$K_0 = \frac{1}{9V_0}(a_1 - 2a_0) , \tag{5b}$$

$$K_0 K_0' = -\frac{1}{27V_0}(2a_2 - 3a_1 + 4a_0) , \tag{5c}$$

$$K_0^2 K_0'' = \frac{1}{81V_0}\left[6a_3 + (3K_0' - 1)(2a_2 - a_1)\right] , \tag{5d}$$

which are the analogues of (53a-d) of Chapter 3. Comparing (4a-d) with (40a-d) of Chapter 3, it can be seen that the only contribution to the differences $(K_{0S}-K_{0T})$, etc., is from the differences $(a_{1S}-a_{1T})$. From (4b) and (40b) of Chapter 3 we get

$$a_{1S} - a_{1T} = \tfrac{1}{4} g^2 T C_{q0} = q\gamma^2 T C_{q0} ,$$

and substituting this into (5b-d),

$$K_{0S} - K_{0T} = \frac{\gamma^2 T C_{q0}}{V_0} , \tag{6a}$$

$$K_{0S} K_{0S}' - K_{0T} K_{0T}' = K_{0S} - K_{0T} , \tag{6b}$$

$$K_{0S}(K_{0S} K_{0S}')' - K_{0T}(K_{0T} K_{0T}')' = \frac{\gamma}{q}(K_{0S} - K_{0T}) . \tag{6c}$$

Using the identity

$$\gamma C_V = V \alpha K_T \ , \tag{7}$$

where C_V is the specific heat at constant volume and α is the volume coefficient of thermal expansion, (6a) becomes

$$K_{OS} - K_{OT} \approx \alpha_o \gamma_o T K_{OT} \ ,$$

(assuming $C_q \approx C_V$) which can be recognized as a special case of the identity

$$K_S - K_T = \alpha \gamma T K_T \ . \tag{8}$$

Equations (6a-c) are, of course, approximations to the exact relations according to the approximations made in the lattice dynamics theory, and discussed in Chapter 3.

4.3 Hugoniots

In principle, it is possible to relate derivatives along a Hugoniot to isothermal derivatives in a manner similar to that of the previous section, but since these relations are more complicated, it is easier to obtain the Hugoniot pressure from the energy difference between it and some reference curve. Expressions for Hugoniots have been given, for instance, by Thomsen (1970), who related the Hugoniot to the static pressure $-(d\phi/dV)$, and, for example, Ahrens et al. (1969) and McQueen et al. (1967), who relate the Hugoniot to an

isentrope. Since the latter method does not require the intermediate calculation of the derivatives of ϕ, and since the results of the last section can be used, it will be used here.

The Hugoniot equation derived here will be generalized to take account of possible initial porosity of the material or a phase change during the shock process. The term "high pressure phase" will be taken here to include the compacted, non-porous material in the case of initial porosity.

Take the initial state of the material to be $P = 0$, $V = V_0'$, $T = T_0$, the ($P = 0$, $T = T_0$) volume of the high pressure phase to be V_0, and the final shocked state to be (P_h, V, T_h). The Rankine-Hugoniot equations give, in this case,

$$U(V,T) - U(V_0', T_0) = \tfrac{1}{2} P(V_0' - V), \tag{9}$$

where U is the total internal energy, which, in the quasi-harmonic approximation, is $U = \overline{\phi} + U_q$. Define the transition energy E_t as

$$E_t = U(V_0, T_0) - U(V_0', T_0). \tag{10}$$

E_t can be obtained from the enthalpy of phase change, if it is known. If there is no phase transition, i.e., if there is only a reduction of porosity, then this can be taken as zero (the surface energy of the pores can be neglected;

Brace and Walsh, 1962).

If the pressure and temperature on the isentrope centered at P = 0, V = V_0 are P_s and T_s, respectively, at V, then, from (1),

$$P_h - P_s = \frac{\gamma}{V}\left[U_q(V,T_h) - U_q(V,T_s)\right]. \tag{11}$$

P_s can be calculated according to the previous section. From the identity

$$P = -\left(\frac{\partial U}{\partial V}\right)_S , \tag{12}$$

we see that

$$\Delta U \equiv U(V,T_s) - U(V_0,T_0) = -\int_{V_0}^{V} P_s\, dV . \tag{13}$$

Thus, for instance, if P_s is given in terms of e,

$$\Delta U = a_{0s}\, e + \tfrac{1}{2} a_{1s} e^2 + \tfrac{1}{3} a_{2s} e^3 + \tfrac{1}{4} a_{3s} e^4 . \tag{14}$$

Eliminating $U_q(V, T_h)$ between (9) and (11), using (10) and noting that $\phi(V_0) = 0$, the final expression for the Hugoniot is

$$P_h\left[1 - \frac{\gamma}{2}\left(\frac{V_0'}{V} - 1\right)\right] = P_s - \frac{\gamma}{V}(\Delta U + E_t) . \tag{15}$$

4.4 References

AHRENS T. J., ANDERSON DON L. and RINGWOOD A. E., Rev. Geophys. 7, 667 (1969).

BRACE W. F. and WALSH J. B., Am. Mineral. 46, 1111 (1962).

LEIBFRIED G. and LUDWIG W., Solid State Physics (Edited by Bradley) 12, 275, Academic Press, New York (1961).

McQUEEN R. G., MARSH S. P. and FRITZ J. N., J. Geophys. Res. 72, 4999 (1967).

THOMSEN L., J. Phys. Chem. Solids 31, 2003 (1970).

CHAPTER 5

EFFECTIVE ELASTIC MODULI UNDER HYDROSTATIC STRESS IN THE QUASI-HARMONIC APPROXIMATION

Summary

Fourth-order finite strain expressions for the effective elastic moduli of a solid under hydrostatic stress are derived from a general expression for effective elastic moduli. Expressions in terms of the strains η, $\underline{E}$ and $\underline{e}$ are given. The expressions are then written in terms of the moduli and their pressure derivatives evaluated at the reference state. The temperature dependence of these expressions is derived from the fourth-order quasi-harmonic expression for the lattice vibration energy. Some thermodynamic relations are derived which relate the parameters which specify the thermal effects to the pressure and temperature derivatives of the elastic moduli at the reference state. General relations between isothermal and isentropic elastic moduli and their pressure and temperature derivatives are also given. Much of the development is valid for materials of arbitrary symmetry, but the complete development is given only for materials of cubic symmetry.

5.1 Introduction

The equations developed in Chapter 3 can be generalized in two ways - by including the effects of non-hydrostatic stress and by considering anisotropic materials. A number of authors have discussed the various ways in which general second- and higher-order elastic constants (which arise when arbitrary large stresses are considered) may be defined, and their relationship with the "effective" elastic moduli (which arise when infinitesimal stresses are added to prevailing large stresses) (e.g., Thurston, 1964, 1965; Thurston and Brugger, 1964; Wallace, 1965, 1967; Thomsen, 1970; Sammis, 1971). In general, materials cannot sustain very large non-hydrostatic stresses and, especially in geophysics, the case of most interest is that of an infinitesimal non-hydrostatic stress superimposed on an arbitrarily large hydrostatic stress. Accordingly, equations will be developed directly for this special case, without reference to the more general treatments. Although much of this chapter is valid for materials of arbitrary symmetry, parts of the treatment are greatly simplified by considering only isotropic materials or materials of cubic symmetry, for which the response to a hydrostatic stress is an isotropic strain, which can be specified with a single scalar strain parameter.

The treatment separates into three parts. First, the appropriate finite strain expressions for the effective

elastic moduli are derived and written in terms of the moduli and their pressure derivatives at zero pressure. Second, the temperature dependence of these expressions is derived from lattice dynamics. Third, some general thermodynamic relations are derived which relate the equation of state parameters to the elastic moduli and their pressure and temperature derivatives, and which relate isothermal and isentropic elastic moduli and their pressure and temperature derivatives. Some of these thermodynamic relations generalize those used in Chapter 3, and many of them have not been given before, to the author's knowledge.

As in Chapter 3, it is convenient here to first derive expressions for thermal contributions in terms of $\underline{e}$, and then to derive others in terms of $\underline{\eta}$ and $\underline{E}$. In the special case of hydrostatic prestress, frame-indifferent expressions in terms of $\underline{e}$ can still be derived, although some care is required.

This chapter corrects and generalizes the results of Thomsen (1972). The relation between these is the same as that between Chapter 3 and Thomsen (1970). The reference state is again left arbitrary.

5.2 Effective Elastic Moduli Under Hydrostatic Stress

The effective elastic moduli can be defined either in terms of the response of a prestressed material to a further infinitesimal stress, or in terms of the equation of motion of small amplitude waves. In this section, exact general expressions for the effective elastic moduli under arbitrary prestress (e.g., Thurston, 1965; Wallace, 1967) are specialized to the case of hydrostatic prestress, and further, to the case of a material of cubic symmetry. They are also written explicitly in terms of the particular strain measures to be used here, and the parameters in these expressions are related to the pressure derivatives of the moduli.

In order to obtain expressions in terms of $\underline{e}$ which are frame-indifferent, it is necessary to define some additional deformation measures. Consider a point in the material which, in the "natural", i.e., unstressed, state has position vector (referred to Cartesian axes) $\underline{a} = (a_1, a_2, a_3)$. Denote its position vector after the material is subject to a hydrostatic stress as $\underline{X}$ and its position vector after a further infinitesimal arbitrary stress has been imposed as $\underline{x}$. Then the displacement gradients $\underline{e}$, $\underline{f}$ and $\underline{u}$ may be defined by

$$x_i - a_i = e_{ij} a_j = f_{ij} x_j \quad , \tag{1}$$

$$x_i - X_i = u_{ij} X_j \quad , \tag{2}$$

where u_{ij} is infinitesimal, all quantities are referred to the same Cartesian axes, and the summation convention is assumed. If u_{ij} is decomposed into symmetric and antisymmetric parts, s_{ij} and w_{ij}, respectively, then (Wallace, 1967)

$$u_{ij} = s_{ij} + w_{ij}$$

$$= \tfrac{1}{2}\left(s_{ij} + s_{ji} + w_{ij} - w_{ji} \right) , \tag{3}$$

where

$$s_{ij} = \tfrac{1}{2}\left(u_{ij} + u_{ji} \right) , \quad w_{ij} = \tfrac{1}{2}\left(u_{ij} - u_{ji} \right) . \tag{4}$$

From (3), we get that

$$\frac{\partial u_{ij}}{\partial s_{kl}} = \tfrac{1}{2}\left(\delta_{ik}\delta_{jl} + \delta_{jk}\delta_{il} \right) , \tag{5}$$

$$\frac{\partial}{\partial s_{kl}} = \frac{\partial u_{ij}}{\partial s_{kl}} \frac{\partial}{\partial u_{ij}} = \tfrac{1}{2}\left(\frac{\partial}{\partial u_{kl}} + \frac{\partial}{\partial u_{lk}} \right) . \tag{6}$$

For general strains, the Cauchy stress is given by (Truesdell and Noll, 1965, sect. 82)

$$T_{ij} = \rho \left(\frac{\partial A}{\partial u_{ij}} \right)_T = \rho F_{jp} \left(\frac{\partial A}{\partial e_{ip}} \right)_T , \tag{7}$$

where ρ is the density and A is the Helmholtz free energy. The effective elastic moduli are (Thurston, 1965)

$$C_{ijkl} = \frac{\partial T_{ij}}{\partial u_{kl}} = F_{kp} \frac{\partial T_{ij}}{\partial e_{lp}} \quad . \tag{8}$$

The moduli in (8) are isothermal or isentropic according to whether the derivative is taken isothermally or isentropically. In (7) and (8),

$$F_{ij} = \delta_{ij} + e_{ij} = \frac{\partial x_i}{\partial a_j} \quad . \tag{9}$$

The requirement that (7) be frame-indifferent has been shown (Noll, 1955; Truesdell and Noll, 1965) to be equivalent to the requirement that T_{ij} be symmetric. If $T_{ij} = T_{ji}$, then

$$\tau_{ij} \equiv \tfrac{1}{2}\left(T_{ij} + T_{ji} \right) = T_{ij} \, . \tag{10}$$

It has been shown by Thurston (1965) that in the special case of hydrostatic prestress,

$$c_{ijkl} \equiv \frac{\partial T_{ij}}{\partial s_{kl}} = C_{ijkl} \, . \tag{11}$$

Using (6), (10) and (11), the effective elastic constants under hydrostatic stress are

$$c_{ijkl} = \tfrac{1}{4}\left(\frac{\partial T_{ij}}{\partial u_{kl}} + \frac{\partial T_{ij}}{\partial u_{lk}} + \frac{\partial T_{ji}}{\partial u_{kl}} + \frac{\partial T_{ji}}{\partial u_{lk}} \right) . \tag{12}$$

Substituting (7) into (8) and using the relations (Thomsen, 1972)

$$\frac{\partial \rho}{\partial u_{k\ell}} = -\rho\,\delta_{k\ell}\,, \qquad \frac{\partial}{\partial u_{k\ell}} = F_{\ell p}\,\frac{\partial}{\partial e_{kp}}\,, \tag{13}$$

we get

$$C_{ijk\ell} = \rho\,F_{ip}\,F_{\ell n}\,\frac{\partial^2 A}{\partial e_{jp}\,\partial e_{kn}} - T_{ij}\,\delta_{k\ell} + T_{\ell j}\,\delta_{ik}\,. \tag{14}$$

Taking $T_{ij} = -P\,\delta_{ij}$, i.e., assuming hydrostatic pressure, this becomes

$$C_{ijk\ell} = \rho\,F_{ip}\,F_{\ell n}\,\frac{\partial^2 A}{\partial e_{jp}\,\partial e_{kn}} - P(\delta_{ik}\,\delta_{j\ell} - \delta_{ij}\,\delta_{k\ell})\,. \tag{15}$$

Substituting (15) into (12),

$$c_{ijk\ell} = \frac{\rho}{4}\left[F_{ip}\,F_{\ell n}\,\frac{\partial^2 A}{\partial e_{jp}\,\partial e_{kn}} + F_{jp}\,F_{\ell n}\,\frac{\partial^2 A}{\partial e_{ip}\,\partial e_{kn}} + F_{ip}\,F_{kn}\,\frac{\partial^2 A}{\partial e_{jp}\,\partial e_{\ell n}} + F_{jp}\,F_{kn}\,\frac{\partial^2 A}{\partial e_{ip}\,\partial e_{\ell n}}\right] - P\,\nabla_{ij}^{k\ell}\,, \tag{16}$$

where

$$\nabla_{ij}^{k\ell} = \tfrac{1}{2}(\delta_{ik}\,\delta_{j\ell} + \delta_{jk}\,\delta_{i\ell}) - \delta_{ij}\,\delta_{k\ell}\,. \tag{17}$$

Expressions for the stress, $\underline{I}$, and the elastic moduli, c_{ijkl}, will now be given in terms of the strain tensors η

and $\underline{E}$, where

$$\eta_{ij} = \tfrac{1}{2}\left(e_{ij} + e_{ji} + e_{ki}\, e_{kj} \right) , \tag{18}$$

$$E_{ij} = \tfrac{1}{2}\left(f_{ij} + f_{ji} - f_{ik}\, f_{jk} \right) . \tag{19}$$

It is emphasized again that η and $\underline{E}$ are but two examples of an infinity of possible frame-indifferent strain tensors. The expressions analogous to (7) and (16) are (Thomsen, 1972)

$$T_{ij} = \rho\, F_{im} \frac{\partial A}{\partial \eta_{mn}} F_{jn} , \tag{20}$$

$$c_{ijkl} = \rho\, F_{im} F_{kp} \frac{\partial^2 A}{\partial \eta_{mn} \partial \eta_{pq}} F_{jn} F_{lq} - P\, \delta_{ij}^{kl} , \tag{21}$$

where

$$\delta_{ij}^{kl} = \delta_{ik}\delta_{jl} + \delta_{il}\delta_{jk} - \delta_{ij}\delta_{kl} , \tag{22}$$

and

$$T_{ij} = \rho\, G_{mi} \frac{\partial A}{\partial E_{mn}} G_{nj} , \tag{23}$$

$$c_{ijkl} = \rho\, G_{mi} G_{pk} \frac{\partial^2 A}{\partial E_{mn} \partial E_{pq}} G_{nj} G_{ql} - P\, \Delta_{ij}^{kl} , \tag{24}$$

where

$$\Delta_{ij}^{kl} = -\delta_{ik}\delta_{jl} - \delta_{il}\delta_{jk} - \delta_{ij}\delta_{kl} , \tag{25}$$

and

$$G_{ij} = \delta_{ij} - f_{ij} = \frac{\partial a_i}{\partial x_j} = (F^{-1})_{ij} . \tag{26}$$

The derivation of equations (16-18) is aided by the relation

$$\frac{\partial}{\partial u_{kl}} = G_{pk} \frac{\partial}{\partial f_{pl}} . \tag{27}$$

The expressions (16), (21) and (24) for the effective elastic moduli and (7), (20) and (23) for the stress are exact in general. For them to be useful, however, explicit forms for the free energy A are required, and a customary procedure is to expand A in terms of some strain measure. Expansions of A will therefore be taken in terms of $\underline{e}$, $\underline{\eta}$ and $\underline{E}$, and these expansions will here be taken to fourth order. Since the truncations of the various expansions involve different approximations, the expressions in terms of the different strain tensors are no longer identical. This has some interesting consequences, as will be seen later, and it is the reason why the different expressions are developed in parallel here.

At this stage the development is simplified by specializing to the case where the material has cubic symmetry. In this case the response to hydrostatic stress is isotropic strain, so that the strain tensors reduce to scalar multiples

of the unit tensor. These scalar strains are (Thomsen, 1970, 1972; Chapter 3)

$$e = (\rho/\rho_0)^{-1/3} - 1 , \tag{28}$$

$$\eta = \tfrac{1}{2}\left[(\rho/\rho_0)^{-2/3} - 1\right] , \tag{29}$$

$$E = \tfrac{1}{2}\left[1 - (\rho/\rho_0)^{2/3}\right] , \tag{30}$$

where ρ_0 is the density at zero pressure.

In accordance with these assumptions, we may now write, for instance,

$$\frac{\partial^2 A}{\partial e_{ij}\,\partial e_{kl}} = s^0_{ijkl} + s^1_{ijkl}\,e + \tfrac{1}{2}\,s^2_{ijkl}\,e^2 , \tag{31}$$

where the s^n_{ijkl} are constants. Since the strain dependences of all of the elastic moduli are given by expressions of the same form, the indices can be temporarily supressed. By substituting (31) into (16), differentiating, and evaluating at e = 0, the s_n can be written in terms of the zero-pressure derivatives of the elastic constants (the implied s^0_{ijkl} in the following equations should be understood as linear combinations of those in (31), such as occur in (12)):

$$s_0 = V_0\,(c_0 + P_0\,\nabla) , \tag{32}$$

$$s_1 = -3\,V_0\,K_0\,(c_0' + \nabla) + s_0 , \tag{33}$$

$$s_2 = 9 V_0 K_0^2 c_0'' - (3K_0' - 1)(s_1 - s_0), \tag{34}$$

where a prime denotes a pressure derivative, $V = 1/\rho$ is the specific volume, $K = -V(\partial P/\partial V)$ is the bulk modulus, and subscript "o" denotes evaluation at zero pressure. With these assumptions and notations, equation (16) for the c's (still suppressing indices) reduces to the form

$$c = \rho_0 (1+e)^{-1} \left(s_0 + s_1 e + \tfrac{1}{2} s_2 e^2 \right) - P\nabla \tag{35}$$

Equations (32-35) thus give the effective elastic moduli in terms of e and the pressure derivatives of the elastic moduli evaluated at zero pressure.

Analogous expressions in terms of η are:

$$c = \rho_0 (1+2\eta)^{\frac{1}{2}} \left(t_0 + t_1 \eta + \tfrac{1}{2} t_2 \eta^2 \right) - P\delta, \tag{36}$$

with

$$t_0 = V_0 (c_0 + P_0 \delta), \tag{37}$$

$$t_1 = -3 V_0 K_0 (c_0' + \delta) - t_0, \tag{38}$$

$$t_2 = 9 V_0 K_0^2 c_0'' - 3K_0' (t_0 + t_1) - 4t_1 - t_0. \tag{39}$$

Analogous expressions in terms of E are:

$$c = \rho_0 (1-2E)^{7/2} (r_0 + r_1 E + \tfrac{1}{2} r_2 E^2) - P\Delta \,, \tag{40}$$

$$r_0 = V_0 (c_0 + P_0 \Delta) \,, \tag{41}$$

$$r_1 = -3 V_0 K_0 (c_0' + \Delta) + 7 r_0 \,, \tag{42}$$

$$r_2 = 9 V_0 K_0^2 c_0'' - 3K_0' (r_1 - 7 r_0) + 16 r_1 - 49 r_0 \,. \tag{43}$$

Finally, note that, in particular,

$$\nabla_{11}'' = 0 \quad , \quad \nabla_{11}^{22} = -1 \,, \quad \nabla_{23}^{23} = \tfrac{1}{2} \,, \tag{44}$$

$$\delta_{11}'' = 1 \,, \quad \delta_{11}^{22} = -1 \,, \quad \delta_{23}^{23} = 1 \,, \tag{45}$$

$$\Delta_{11}'' = -3 \,, \quad \Delta_{11}^{22} = -1 \,, \quad \Delta_{23}^{23} = -1 \,. \tag{46}$$

5.3 Thermal Effects in the Quasi-harmonic Approximation

In this section, the theory of anharmonic lattice dynamics is used to obtain an expansion of the vibrational contribution to the free energy in terms of general strains, and thence to evaluate the vibrational contributions to the effective elastic moduli. This treatment is a straightforward generalization of that given in Chapter 3 for the case of isotropic strain.

Expressions will first be developed in terms of $\underline{e}$ without regard to the frame-indifference requirement. This will then be accounted for by a redefinition of parameters. Also,

the derivation will initially be for the isothermal moduli. Expressions for the isentropic moduli will then be noted.

The squares of the lattice eigenfrequencies ω_ν are proportional to linear combinations of the second derivatives of ϕ with respect to displacements (Leibfried and Ludwig, 1961). Generalizing the expansion (34) of Chapter 3, we may write

$$\omega_\nu^2 = (\omega_\nu^2)_o \left(1 + G_{ij}^\nu e_{ij} + \tfrac{1}{2} H_{ijkl}^\nu e_{ij} e_{kl}\right), \tag{47}$$

where the G_{ij}^ν and H_{ijkl}^ν are constants (G_{ij}^ν should not be confused with the deformation gradient defined by (26)). Since the "quasi-harmonic" vibrational energy, A_2, depends on the strain only through the ω_ν, the strain dependence of A_2 is controlled by the G_{ij}^ν and the H_{ijkl}^ν. As was done in the case of isotropic strain (Chapter 3), A_2 may be expanded in terms of $\underline{e}$. The result, using the Mie-Grüneisen approximation, in which the G_{ij}^ν and H_{ijkl}^ν are assumed to be independent of ν, is

$$A_2(\underline{e},T) = A_2^o(T) + \tfrac{1}{2} G_{ij} U_{qo} e_{ij} + \tfrac{1}{8}\left[(2H_{ijkl} - G_{ij}G_{kl})U_{qo} - G_{ij}G_{kl}TC_{qo}\right] e_{ij} e_{kl}, \tag{48}$$

where

$$U_q = A_2 - T\left(\frac{\partial A_2}{\partial T}\right)_V \tag{49}$$

is the vibrational contribution to the internal energy in this approximation, and

$$C_q = \left(\frac{\partial U_q}{\partial T}\right)_V \tag{50}$$

is the vibrational contribution to the specific heat at constant volume in this approximation. The expansions (47) and (48) terminate two terms earlier than the expansion of ϕ, as in Chapter 3. From equation (48) we see that

$$\left(\frac{\partial A}{\partial e_{ij}}\right)_0 = \left(\frac{d\phi}{de_{ij}}\right)_0 + \tfrac{1}{2} G_{ij} U_{q0}, \tag{51}$$

$$\left(\frac{\partial^2 A}{\partial e_{ij}\partial e_{kl}}\right)_0 = \left(\frac{d^2\phi}{de_{ij}de_{kl}}\right)_0 + \tfrac{1}{4}(2H_{ijkl} - G_{ij}G_{kl})U_{q0} - \tfrac{1}{4} G_{ij}G_{kl} T C_{q0}, \tag{52}$$

$$\left(\frac{\partial^3 A}{\partial e_{ij}\partial e_{kl}\partial e_{mn}}\right)_0 = \left(\frac{d^3\phi}{de_{ij}de_{kl}de_{mn}}\right)_0 + \cdots, \tag{53}$$

etc. The third and fourth derivatives of A with respect to e have no vibrational contributions in this approximation.

Comparing with equation (31), we see that this is also true of s^1_{ijkl} and s^2_{ijkl}. The vibrational contributions to the effective elastic moduli come from s^0_{ijkl} and from the pressure term in equation (35). Equations (51) and (52) thus specify the temperature dependence of the pressure (Chapter 3) and the effective elastic moduli through U_{qo} and TC_{qo}.

The constants G_{ij} and H_{ijkl} can be related to a generalized Grüneisen parameter and its strain derivative. A generalized Grüneisen parameter can be defined thermodynamically as

$$\gamma_{ij} = -V\left(\frac{\partial T_{ij}}{\partial U}\right)_{\underline{e}} . \tag{54}$$

The correct microscopic definition of the Grüneisen parameter must be found so as to be consistent with this definition. From (19) of Chapter 3 and (7),

$$T_{ij} = \rho \frac{d\phi}{du_{ij}} + \rho \sum_{\nu} \frac{d \ln \omega_\nu}{du_{ij}} \left(\frac{\partial A_z}{\partial \ln \omega_\nu}\right)_T . \tag{55}$$

By defining

$$\gamma^\nu_{ij} = -\tfrac{1}{2} \frac{d \ln \omega_\nu^2}{du_{ij}} , \tag{56}$$

and substituting into equation (55), we can get, using the Mie-Grüneisen approximation (Leibfried and Ludwig, 1961;

Chapter 3),

$$\left(\frac{\partial T_{ij}}{\partial U_q}\right)_{\underline{e}} = -\rho\,\gamma_{ij} \quad , \tag{57}$$

to which (54) reduces in the present approximation.

Now, substituting the expansion (47) into the definition (56), and suppressing the index ν (i.e., using the Mie-Grüneisen approximation), the Grüneisen parameter becomes

$$\gamma_{ij} = -\tfrac{1}{2}\left(\delta_{ik} + e_{ik}\right)\frac{\omega_o^2}{\omega^2}\left(G_{jk} + H_{jkmn}\,e_{mn}\right) . \tag{58}$$

Evaluating this and its derivative at $\underline{e} = 0$, one can derive that

$$G_{ij} = -2\,\gamma^o_{ij} \quad , \tag{59}$$

$$H_{ijk\ell} = -2\left(\frac{\partial \gamma_{ij}}{\partial e_{k\ell}}\right)_o + G_{ij}\,G_{k\ell} - G_{i\ell}\,\delta_{jk} . \tag{60}$$

Now, as with (6), frame-indifference requires that $\gamma_{ij} = \gamma_{ji}$. Thus, by analogy with (10), (59) should actually be replaced by

$$g_{ij} = -2\,\gamma^o_{ij} , \tag{61}$$

where

$$g_{ij} = \tfrac{1}{2}\left(G_{ij} + G_{ji}\right). \tag{62}$$

Similarly, by analogy with (12), define

$$h_{ijkl} = \tfrac{1}{4}\left(H_{ijkl} + H_{ijlk} + H_{jikl} + H_{jilk}\right), \tag{63}$$

so that, using (6),

$$h_{ijkl} = -2\left(\frac{\partial \gamma_{ij}}{\partial s_{kl}}\right)_0 + g_{ij}\, g_{kl}$$

$$-\tfrac{1}{4}\left(g_{il}\,\delta_{jk} + g_{ik}\,\delta_{jl} + g_{jl}\,\delta_{ik} + g_{jk}\,\delta_{il}\right). \tag{64}$$

From the symmetry properties of g_{ij} and h_{ijkl}, it can be seen that the frame-indifference requirement has reduced the number of independent constants. Apart from the obvious symmetry of (64), it may easily be shown, from (47) and (63), that $h_{ijkl} = h_{klij}$.

If the medium has cubic symmetry, then the number of independent components is further reduced. γ_{ij}, in analogy to the stress tensor (Cf. 54), reduces to a scalar multiple of the unit tensor (Leibfried and Ludwig, 1961):

$$\gamma_{ij} = \gamma\,\delta_{ij}\ . \tag{65}$$

h_{ijkl}, in analogy to the second-order elastic constants, has three independent components, which, in the Voigt notation, may be called h_{11}, h_{12} and h_{44}. From (47), (62) and (63) it

can be seen that the "bulk" parameters g and h (Chapter 3) are related to g_{ij} and h_{ijkl} by

$$g = g_{ii}\,, \qquad g_{ij} = \tfrac{1}{3} g\, \delta_{ij}\,, \tag{66}$$

$$h = h_{iikk} = 3(h_{11} + 2h_{12})\,. \tag{67}$$

Then (64) gives

$$h_{11} = -2\left(\frac{\partial \gamma_{11}}{\partial s_{11}}\right)_0 + \frac{g^2}{q} - \frac{g}{3}\,, \tag{68}$$

$$h_{12} = -2\left(\frac{\partial \gamma_{11}}{\partial s_{22}}\right)_0 + \frac{g^2}{q}\,, \tag{69}$$

$$h_{44} = -2\left(\frac{\partial \gamma_{23}}{\partial s_{23}}\right)_0 - \frac{g}{6}\,. \tag{70}$$

Also, (52), (61) and (64) give, using the Voigt notation,

$$s^0_{11} = \phi^0_{11} + \tfrac{1}{4}(2h_{11} - g^2/q)U_{q0} - \tfrac{1}{4}(g^2/q)\,T\,C_{q0}\,, \tag{71}$$

$$s^0_{12} = \phi^0_{12} + \tfrac{1}{4}(2h_{12} - g^2/q)U_{q0} - \tfrac{1}{4}(g^2/q)\,T\,C_{q0}\,, \tag{72}$$

$$s^0_{44} = \phi^0_{44} + \tfrac{1}{2} h_{44} U_{q0}\,, \tag{73}$$

where $\phi_{\alpha\beta}$ is the appropriate combination of derivatives of ϕ.

The vibrational contributions to the expressions (36) and (40), in terms of η and E, for the effective elastic moduli enter through the $t^n_{\alpha\beta}$ of (37-39) and the $r^n_{\alpha\beta}$ of (41-43). These are given by expressions analogous to (71-73) for the $s^n_{\alpha\beta}$, with $h'_{\alpha\beta}$ and $h''_{\alpha\beta}$ replacing $h_{\alpha\beta}$, where

$$h'_{ijkl} = h_{ijkl} - \tfrac{1}{2}\left(g_{il}\delta_{jk} + g_{jl}\delta_{ik}\right), \tag{74}$$

$$h''_{ijkl} = h_{ijkl} + \tfrac{3}{2}\left(g_{il}\delta_{jk} + g_{jl}\delta_{ik}\right), \tag{75}$$

(compare with equations (37) of Chapter 3).

Note that the parameters a_i, defined in (40) of Chapter 3, are related to the $s^n_{\alpha\beta}$ (Voigt notation) by

$$a_1 = 3\left(s^0_{11} + 2s^0_{12}\right), \tag{80}$$

$$a_2 = \tfrac{3}{2}\left(s^1_{11} + 2s^1_{12}\right), \tag{81}$$

$$a_3 = \tfrac{1}{2}\left(s^2_{11} + 2s^2_{12}\right). \tag{82}$$

Identical relations hold between the b_i and the $t^n_{\alpha\beta}$, and between the c_i and the $r^n_{\alpha\beta}$.

Equations (48), (52) and (71-73) all involve isothermal derivatives. To derive the corresponding isentropic derivatives, note the following result, due to Leibfried and Ludwig (1961; equation 2 of Chapter 4):

$$\left(\frac{\partial U_q}{\partial e_{ij}}\right)_S = \tfrac{1}{2} G_{ij} U_q \ . \tag{83}$$

Then the analogues of (52) and (71-73) are

$$\left(\frac{\partial^2 U_q}{\partial e_{ij}\,\partial e_{kl}}\right)_{S,0} = \tfrac{1}{4} U_{q0} \left(2 H_{ijkl} - G_{ij} G_{kl}\right), \tag{84}$$

$$s^{OS}_{11} = \phi^0_{11} + \tfrac{1}{4}\left(2 h_{11} - g^2/q\right) U_{q0}, \tag{71a}$$

$$s^{OS}_{12} = \phi^0_{12} + \tfrac{1}{4}\left(2 h_{12} - g^2/q\right) U_{q0}, \tag{72a}$$

$$s^{OS}_{44} = \phi^0_{44} + \tfrac{1}{2} h_{44} U_{q0} \ . \tag{73a}$$

Note that there is no difference between s^{OS}_{44} and its isothermal counterpart, and thus no difference between c^S_{44} and c^T_{44}. This is a well known result.

5.4 Thermodynamic Relations

In the "isotropic strain" theory of Chapter 3, the Grüneisen parameter and its volume derivative were related

to the bulk modulus and its pressure and temperature derivatives through thermodynamic identities. These identities must be generalized for the present treatment. Also, although the relations between isothermal and isentropic quantities can be obtained from the previous section according to the quasi-harmonic approximation, the general exact relations will be derived here for comparison. The initial part of the treatment given here is similar to that given by Mason (1950).

The infinitesimal symmetric strain s_{ij} defined by (4) will be used in this section. The temperature and entropy will be denoted by θ and σ, respectively, to avoid confusion with stress and strain.

It is convenient to consider first the relation between isothermal and isentropic elastic moduli. From the first and second laws of thermodynamics, the change of internal energy per unit volume of a system in a reversible process is given by

$$dU = T_i\, ds_i + \theta\, d\sigma , \tag{85}$$

where the stress and strain are written in the Voigt notation. The Helmholtz free energy A is defined by

$$A = U - \theta\sigma , \tag{86}$$

whence

$$dA = T_i\, ds_i - \sigma\, d\theta \,, \tag{87}$$

and

$$T_i = \left(\frac{\partial A}{\partial s_i}\right)_\theta \,, \qquad \sigma = -\left(\frac{\partial A}{\partial \theta}\right)_{\underline{s}} \,. \tag{88}$$

With s_i and θ as independent variables, we may write

$$d\sigma = \lambda_i\, ds_i + \left(\frac{\partial \sigma}{\partial \theta}\right)_{\underline{s}} d\theta \,, \tag{89}$$

where

$$\lambda_i = \left(\frac{\partial \sigma}{\partial s_i}\right)_\theta = -\left(\frac{\partial T_i}{\partial \theta}\right)_{\underline{s}} \,, \tag{90}$$

using equation (88). In a reversible process, the quantity of heat absorbed by the system is

$$dQ = \theta\, d\sigma = \theta\lambda_i\, ds_i + \theta\left(\frac{\partial \sigma}{\partial \theta}\right)_{\underline{s}} d\theta \,, \tag{91}$$

from which we can make the identification

$$\left(\frac{\partial \sigma}{\partial \theta}\right)_{\underline{s}} = \frac{\rho C_s}{\theta} \,, \tag{92}$$

where ρ is density and C_s is the specific heat at constant strain. In an isentropic process, i.e., $d\sigma = 0$, the change

in temperature is, from (89),

$$d\theta = - \frac{\theta \lambda_i}{\rho C_s} ds_i \ . \tag{93}$$

Now, again in terms of s_i and θ, the change in stress is

$$dT_i = c^{\theta}_{ij} ds_j - \lambda_i d\theta \tag{94}$$

where

$$c^{\theta}_{ij} = \left(\frac{\partial T_i}{\partial s_j} \right)_{\theta} \tag{95}$$

is the isothermal elastic modulus. Thus, using (93), the isentropic change in stress is

$$dT_i = c^{\theta}_{ij} + \frac{\theta \lambda_i \lambda_j}{\rho C_s} ds_j \ , \tag{96}$$

from which the isentropic elastic modulus is

$$c^{\sigma}_{ij} = c^{\theta}_{ij} + \frac{\theta \lambda_i \lambda_j}{\rho C_s} \ . \tag{97}$$

Using the chain rule of differentiation, we see that

$$\lambda_i = \left(\frac{\partial s_j}{\partial \theta} \right)_{\underline{T}} \left(\frac{\partial T_i}{\partial s_j} \right)_{\theta} = \alpha_j c^{\theta}_{ij} \ , \tag{98}$$

where α_i is the thermal expansion tensor.

Next, consider the Grüneisen parameter and its strain derivatives. From the thermodynamic definition (54) of the generalized Grüneisen parameter (using the Voigt notation, and recalling that U is now energy per unit volume),

$$\gamma_i = -\left(\frac{\partial T_i}{\partial \theta}\right)_{\underline{s}} \left(\frac{\partial \theta}{\partial U}\right)_{\underline{s}}$$

$$= V\lambda_i / C_s = V \alpha_j c^{o}_{ij} / C_s \,, \qquad (99)$$

which generalizes the usual Grüneisen relation.

Equation (99) can be differentiated with respect to s_k, and, using the relations

$$\left(\frac{\partial V}{\partial s_k}\right)_{\theta} = V \delta_k \,, \qquad (100)$$

where

$$\delta_k = 1 \quad \text{if} \quad k = 1, 2, 3 \,,$$
$$\delta_k = 0 \quad \text{if} \quad k = 4, 5, 6 \,, \qquad (101)$$

and

$$\left(\frac{\partial \lambda_i}{\partial s_k}\right)_{\theta} = -\left(\frac{\partial c^{o}_{ik}}{\partial \theta}\right)_{\underline{s}} \,, \qquad (102)$$

(using equation 90), the result is

$$\left(\frac{\partial \gamma_i}{\partial s_k}\right)_\theta = \gamma_i Q_k + D^\theta_{ik} + \gamma_j \left(\frac{\partial c^\theta_{ik}}{\partial T_j}\right)_\theta , \tag{103}$$

where

$$Q_k = \delta_k - \left(\frac{\partial \ln C_s}{\partial s_k}\right)_\theta , \tag{104}$$

$$D^\theta_{ik} = -\frac{V}{C_s}\left(\frac{\partial c^\theta_{ik}}{\partial \theta}\right)_{\underline{T}} . \tag{105}$$

The following identity was also used in deriving (103):

$$\left(\frac{\partial}{\partial \theta}\right)_{\underline{s}} = \left(\frac{\partial}{\partial \theta}\right)_{\underline{T}} - \lambda_i \left(\frac{\partial}{\partial T_i}\right)_\theta . \tag{106}$$

Relations between the derivatives of the isothermal and isentropic elastic moduli can be derived as follows. Define

$$\mu_{ij} = c^\sigma_{ij} - c^\theta_{ij} = \theta \lambda_i \lambda_j / \rho C_s = \theta \rho C_s \gamma_i \gamma_j . \tag{107}$$

Differentiating (107), and using (103),

$$\left(\frac{\partial \mu_{ij}}{\partial T_k}\right)_\theta = S^\theta_{nk}\left(R_{ijn} - \mu_{ij} Q_n\right), \tag{108}$$

where

$$S^{\theta}_{ij} = \left(\frac{\partial \varepsilon_i}{\partial T_j}\right)_{\theta} = (\underline{c}^{\theta})^{-1}_{ij} , \tag{109}$$

i.e., S^{θ}_{ij} are the isothermal elastic compliances, and

$$R_{ijk} = \theta \rho C_s \left[\frac{\partial(\gamma_i \gamma_j)}{\partial \varepsilon_k}\right]_{\theta} \tag{110}$$

$$= 2\mu_{ij} Q_k + \theta\rho\lambda_i D^{\theta}_{jk} + \theta\rho\lambda_j D^{\theta}_{ik} + \mu_{\ell i} c^{\theta}_{jk,\ell} + \mu_{\ell j} c^{\theta}_{ik,\ell} , \tag{111}$$

where a comma preceeding a subscript denotes differentiation with respect to the corresponding stress component.

Similarly, differentiating (107) with respect to θ, and using (106),

$$\left(\frac{\partial \mu_{ij}}{\partial \ln \theta}\right)_{\underline{T}} = \mu_{ij}\left[1 + \left(\frac{\partial \ln C_s}{\partial \ln \theta}\right)_{\underline{\varepsilon}}\right] + \theta\rho C_s \left[\frac{\partial(\gamma_i\gamma_j)}{\partial \ln \theta}\right]_{\underline{\varepsilon}} + \theta\lambda_k\left(\frac{\partial \mu_{ij}}{\partial T_k}\right)_{\theta} . \tag{112}$$

The relations developed so far in this section, i.e., equations (97), (99), (103), (108) and (112), are completely general in that they refer to a material of arbitrary symmetry under an arbitrary stress. They will now be specialized to the case of a material of cubic symmetry under a hydrostatic stress. As was pointed out in section 2, only one strain parameter is required in this case, so that the application of these relations is simplified. Of course,

the resulting relations can also be further specialized to the case of an isotropic material.

Under cubic symmetry, the thermal expansion tensor becomes

$$\alpha_i = \tfrac{1}{3}\alpha\delta_i \ , \qquad \alpha = \alpha_i\delta_i = \left(\frac{\partial \ln V}{\partial\theta}\right)_{\underline{T}} . \tag{113}$$

Thus,

$$\lambda_i = \frac{\alpha}{3} c^{\circ}_{ij}\delta_j = \frac{\alpha}{3}(c^{\circ}_{11} + 2c^{\circ}_{12})\delta_i = \alpha K_\theta \delta_i = \lambda\delta_i \ , \tag{114}$$

where K_θ is the isothermal bulk modulus, and

$$\gamma_i = \frac{\alpha K_\theta}{\rho C_s}\delta_i = \gamma\delta_i \ , \tag{115}$$

$$\mu_{ij} = \alpha\gamma\theta K_\theta \delta_i\delta_j = \mu\delta_i\delta_j \ . \tag{116}$$

Note, in particular, that $\mu_{11} = \mu_{12} = \mu$, and $\mu_{44} = 0$.

Under hydrostatic stress, $T_i = -P\delta_i$, where P is the pressure, and the strain of a material of cubic symmetry can be specified by the specific volume V. Thus

$$Q_i = \left[1 - \left(\frac{\partial \ln C_V}{\partial \ln V}\right)_\theta\right]\delta_i = Q\delta_i \ , \tag{117}$$

$$D^{\circ}_{ij} = -\frac{\gamma}{\alpha K_\theta}\left(\frac{\partial c^{\circ}_{ij}}{\partial\theta}\right)_P = \gamma\delta^{\circ}_{ij} \ , \tag{118}$$

where δ^{θ}_{ij} is the generalized isothermal analogue of the Anderson-Grüneisen parameter (Grüneisen, 1912; Anderson, 1967). With these results, equation (103) becomes

$$\left(\frac{\partial \gamma_i}{\partial s_j}\right)_{\theta} = \gamma\left[Q\delta_i\delta_j + \delta^{\theta}_{ij} - \left(\frac{\partial c^{\theta}_{ij}}{\partial P}\right)_{\theta}\right]. \qquad (119)$$

There are three independent derivatives of γ_i in this case, just as there are three independent components each of c^{θ}_{ij} and δ^{θ}_{ij}. Note that Q does not contribute to $(\partial\gamma_4/\partial s_4)$. It may also be noted that this derivative is non-zero, even though under cubic symmetry γ_4 is zero. This is because the strain s_4 destroys cubic symmetry, thus allowing γ_4 to vary from zero as s_4 varies from zero. From (119)

$$\left(\frac{\partial \gamma}{\partial \ln V}\right)_{\theta} = \gamma\left[Q + \delta^{\theta} - \left(\frac{\partial K_{\theta}}{\partial P}\right)_{\theta}\right], \qquad (120)$$

where $\delta^{\theta} = (\delta^{\theta}_{11} + 2\delta^{\theta}_{12})/3$.

To specialize equations (108) and (112), note first that

$$\left(\frac{\partial \mu_{ij}}{\partial P}\right)_{\theta} = -\left(\frac{\partial \mu_{ij}}{\partial T_k}\right)_{\theta}\delta_k$$

and that $s_{nk}\delta_k = \delta_n/3K_{\theta}$. Then

$$R_{ijk}\,\delta_k = R\,\delta_i\delta_j = 6\mu\left(\frac{\partial \ln\gamma}{\partial \ln V}\right)_\theta \delta_i\delta_j\,, \tag{121}$$

and

$$\left(\frac{\partial \mu_{ij}}{\partial P}\right)_\theta = \left(\frac{\partial \mu}{\partial P}\right)_\theta \delta_i\delta_j = -(R - 3\mu Q)/3K_\theta\,\delta_i\delta_j$$

$$= -\frac{\mu}{K_\theta}\left[2\left(\frac{\partial \ln\gamma}{\partial \ln V}\right)_\theta - Q\right]\delta_i\delta_j\,. \tag{122}$$

The specialization of equation (112) is

$$\left(\frac{\partial \mu}{\partial \theta}\right)_P = \frac{\mu}{\theta}\left[1 + \left(\frac{\partial \ln C_V}{\partial \ln\theta}\right)_V + 2\left(\frac{\partial \ln\gamma}{\partial \ln\theta}\right)_V\right] - \lambda\left(\frac{\partial \mu}{\partial P}\right). \tag{123}$$

Finally, note that equation (120) involves the derivatives of the isothermal elastic modulus, whereas it is usually the derivatives of the isentropic modulus which are measured experimentally. The conversion from the temperature derivative of one to the other involves $(\partial\mu/\partial\theta)_P$, which involves $(\partial\mu/\partial P)_\theta$, which in turn involves δ^θ. Equations (118), (120), (122) and (123) can be solved for $(\partial\mu/\partial P)_\theta$ in terms of just derivatives of isentropic quantities:

$$\left(\frac{\partial \mu}{\partial P}\right)_\theta = \frac{\mu}{K_\theta}\left\{2\left(\frac{\partial K_\sigma}{\partial P}\right)_\theta - Q + \frac{2}{\lambda}\left(\frac{\partial K_\sigma}{\partial \theta}\right)_P - 2\gamma\left[1 + \left(\frac{\partial \ln C_V}{\partial \ln\theta}\right)_V + 2\left(\frac{\partial \ln\gamma}{\partial \ln\theta}\right)_V\right]\right\} \tag{124}$$

5.5 Discussion

The comments made at the end of Chapter 3 concerning the independence of the approximations made in the thermal and finite strain parts of the theory, the Mie-Grüneisen approximation, the evaluation of U_q and C_q, the relationship of this work to that of Thomsen (1970, 1972) and the capabilities of this theory all apply here in the more general case. In particular, note that this theory predicts that the $c_{\alpha\beta}$ are non-linear in temperature at high temperature and constant pressure (Thomsen, 1972), and that the $(\partial^2 c_{\alpha\beta}/\partial p \partial T)$ are non-zero, in general.

The more general theory given here contains the special theory of Chapter 3, which can be obtained through the relations (66), (67) and (80-82). It is thus a theory of great utility which is capable of describing the effects of shock compression and hydrostatic compression, as well as giving the elastic constants as functions of pressure and temperature. The application given in Chapter 8 demonstrates this utility.

The primary parameters which enter these equations are the $s^n_{\alpha\beta}$ (or $t^n_{\alpha\beta}$, or $r^n_{\alpha\beta}$) of (35), the g_α and $h_{\alpha\beta}$ of (62) and (63), in (51), (61) and (64) and the density, ρ_0, in the reference state. These are related to a similar number of secondary parameters: to $c_{\alpha\beta}$, $c'_{\alpha\beta}$ etc., through (32-34), to the thermal expansion tensor, α_β, through (61) and (99)

and to the temperature derivatives of the elastic moduli through (64) and (103). In the case of cubic symmetry and hydrostatic stress, the volume coefficient of thermal expansion, α, enters through (115), and the temperature derivatives of $c_{\alpha\beta}$ through (68-70) and (119). The evaluation of these parameters follows a scheme analogous to that outlined at the end of Chapter 3.

5.6 References

ANDERSON O.L., J. Geophys. Res. 72, 3661 (1967).

GRÜNEISEN E., Ann. Phys. Berlin 39, 257 (1912).

LEIBFRIED G. and LUDWIG W., Solid State Physics (Edited by Bradley) 12, 275, Academic Press, New York (1961).

MASON W. P., Piezoelectric Crystals and Their Application To Ultrasonics, Van Nostrand, Princeton, New Jersey (1950).

NOLL W., J. Rat. Mech. Anal. 4, 3 (1955). Reprinted in Rational Mechanics of Materials, Intl. Sci. Rev. Ser., Gordon and Breach, New York (1965).

SAMMIS C. G., Ph.D. Thesis, California Institute of Technology, Pasadena, California (1971).

THOMSEN L., J. Phys. Chem. Solids 31, 2003 (1970).

THOMSEN L., J. Phys. Chem. Solids 33, 363 (1972).

THURSTON R. N., Physical Acoustics 1A (Edited by W. P. Mason), Academic Press, New York (1964).

THURSTON R. N., J. Acoust. Soc. Am. 37, 348 (1965).

THURSTON R. N. and BRUGGER K., Phys. Rev. 133, A1604 (1964).

TRUESDELL C. and NOLL W., Handb. Phys. Vol. III/3, Springer-Verlag, Berlin (1965).

WALLACE D. C., Rev. Mod. Phys. 37, 57 (1965).

WALLACE D. C., Phys. Rev. 162, 776 (1967).

CHAPTER 6

EQUATION OF STATE OF MgO

Summary

Ultrasonic, thermal expansion and calorimetric data for MgO are used to evaluate the parameters of third-order equations of state of MgO.

The equations of state are tested and refined with Hugoniot data. The third-order "E" Hugoniot is much closer to the data than the third-order "η" Hugoniot. Inclusion of fourth-order terms allows both "E" and "η" Hugoniots to fit the data within their scatter. The separation of Hugoniots corresponding to different initial densities is predicted within the accuracy of the data by the thermal part of this theory.

6.1 Introduction

In this and the next chapters, the theory developed in Chapter 3 for isotropic stresses and strains is applied to particular materials. Ultrasonic, thermal expansion and calorimetric data for MgO are sufficient to evaluate the equation of state parameters of MgO. The equations of state thus determined are sufficient to predict Hugoniots of MgO. Shock-wave data can then be used to test and refine these equations of state. Comparisons will be given of the thermal and finite strain parts of the equations of state resulting from the use of different strain measures, and of the theory of Chapter 3 with that of Thomsen (1970).

6.2 Determination of Equations of State

The elastic moduli of single-crystal MgO have been measured as a function of pressure and temperature by Spetzler (1970). The bulk modulus and its first pressure and temperature derivatives can be determined from such measurements. The parameters determined by Spetzler (1970) are listed in Table 6.1, along with the density, thermal expansion coefficient and specific heat of MgO, from the indicated sources.

These parameters were used in (43-48) of Chapter 3 to determine the parameters of the equations of state (41) and (42), in terms of η and E, respectively. Since the second

pressure derivative of the bulk modulus, K", is not given, only the third-order versions of these equations are determined in this way.

Using the 300°K isotherms given by (41) and (42) of Chapter 3, the corresponding isentropes and Hugoniots were calculated according to Chapter 4.

6.3 Comparison and Discussion of Equations of State

The fact that both the finite strain and the thermal parts of the equation of state are determined, so that Hugoniots can be calculated with reasonable accuracy, means, in effect, that extrapolations of the lower pressure data (specifically, the ultrasonic data) can be tested against Hugoniot data.

Carter et al. (1971) have given data for a series of MgO Hugoniots, corresponding to different initial densities of the MgO samples. The lower initial density Hugoniots obtained by them are offset to higher pressures, and hence higher temperatures, than the single-crystal Hugoniot at the same density. These data thus provide a test of both the finite strain and the thermal parts of the present theory.

First, consider the finite strain part of the theory. In Fig. 6.1 are shown the single-crystal Hugoniot data of Carter et al. (1971), along with the corresponding third-order Hugoniots calculated in terms of both the η and E

strain measures. It can be seen that the "E" Hugoniot is considerably closer to the data than the "η" Hugoniot. This is an example of the empirical superiority of the "E" equations which was, of course, pointed out by Birch (1947, 1952), and is the reason for the subsequent popularity of the "Birch-Murnaghan" equation (Birch, 1938).

Also shown in Fig. 6.1 are fourth-order η and E Hugoniots in which K_0'' was determined by requiring a least-squares fit of the calculated curve to the data. The resulting values of (K_0K_0'') are given in Table 6.2. Clearly, the fourth-order η and E Hugoniots fit equally well within the scatter of the data.

Comments on two important points can be made here. Firstly, it is clearly desirable to use an equation of state which involves the least number of disposable parameters, while still giving an acceptable representation of data. The greater success of the third-order E equation indicates faster convergence of the expansion in terms of E than that in terms of η. While there is no guarantee that this rapid convergence will continue to higher orders, it is certainly more reasonable to assume this about the E expansion than the η expansion, and E therefore appears to be a more useful strain measure than η.

The second point is that the value of K_0K_0'' obtained depends on the equation used to fit the data (Table 6.2).

It is, of course, a general property of truncated series expansions that the higher-order coefficients are less well determined empirically, but it is one that seems to have received little notice in the context of finite strain expansions. This point will be considered more fully in Chapter 8.

The thermal part of the equation of state will now be discussed. The volume dependence of γ resulting from equations (36, 36a, 36b, and 50) of Chapter 3 is shown in Fig. 6.2. For the range of compressions shown, the differences are not large. At larger compressions, γ given by (50) will be the first to become negative.

The isentropic parameters were calculated from the isothermal ones according to the relations (6a-c) of Chapter 4. The values are given in Table 6.3. Note that we are <u>not</u> considering the "mixed" quantities, such as $(\partial K_S/\partial P)_T$, but only the purely isothermal or isentropic ones, such as $(\partial K_S/\partial P)_S$. Evidently, the difference between isothermal and isentropic quantities is not very significant for the higher order quantities.

In Fig. 6.3, the MgO isentrope calculated according to these parameters is given relative to the isotherm. The Hugoniot corresponding to the single-crystal initial density is included for comparison.

As mentioned previously, the Hugoniot data for different initial densities provide a test of the thermal part of the theory. The fourth-order E equations, with K_0'' evaluated from the single-crystal Hugoniot data (Table 6.2), were used to calculate the corresponding family of Hugoniots. These are compared with the data in Fig. 6.4. There is considerable scatter in the data, but the separation of the various Hugoniots is quite apparent. The calculated Hugoniots reproduce this separation within the scatter of the data. The fourth-order η equations would have yielded slightly smaller separations, as shown by the extrapolations of γ in Fig. 6.2, and would thus appear to be slightly less successful in explaining the data, but the evidence is marginal.

In conclusion, the finite strain extrapolations of the Mie-Grüneisen equation developed here appear to explain the available MgO Hugoniot data quite successfully. The strain parameter E appears to be more empirically successful than η.

6.4 References

BIRCH F., J. Appl. Phys. 9, 279 (1938).

BIRCH F., Phys. Rev. 71, 809 (1947).

BIRCH F., J. Geophys. Res. 57, 227 (1952).

CARTER W. J., MARSH S. P., FRITZ J. N. and McQUEEN R. G., in Accurate Characterization of the High Pressure Environment (Edited by E. Lloyd), National Bureau of Standards Spec. Publ. 326, Washington (1971).

SKINNER B. J., Amer. Mineral. 42, 39 (1957).

SPETZLER H., J. Geophys. Res. 75, 2073 (1970).

THOMSEN L., J. Phys. Chem. Solids 31, 2003 (1970).

VICTOR A. C. and DOUGLAS T. B., J. Res. N.B.S. (U.S.) 67A, 325 (1963).

TABLE 6.1

Zero pressure elastic and thermodynamic data of magnesium oxide at $300^{o}K$.

$\rho_o (g/cm^3)^{a,b}$	3.584
$K_{OT} (Mb)^{b}$	1.605
$K'_{OT}{}^{b}$	3.89
$(\partial K_{OT}/\partial T)_p$ $(Kb/^{o}K)^{b}$	-0.272
$\alpha_o (10^{-6}\ ^{o}K^{-1})^{a,b}$	31.5
$C_V (10^{6}$ erg $g^{-1}\ ^{o}K^{-1})^{c}$	9.25

a. Skinner (1957)

b. Spetzler (1970)

c. Victor & Douglas (1963)

Table 6.2

Values of K_0K_0'' of MgO Determined from Hugoniot Data

Strain measure	K_0K_0''
η	10.53
E	-1.08

Table 6.3

Isothermal and Isentropic MgO Parameters

	K_0 (Mb)	K_0'	K_0K_0''
Isothermal	1.605	3.89	-1.08
Isentropic	1.628	3.85	-1.05

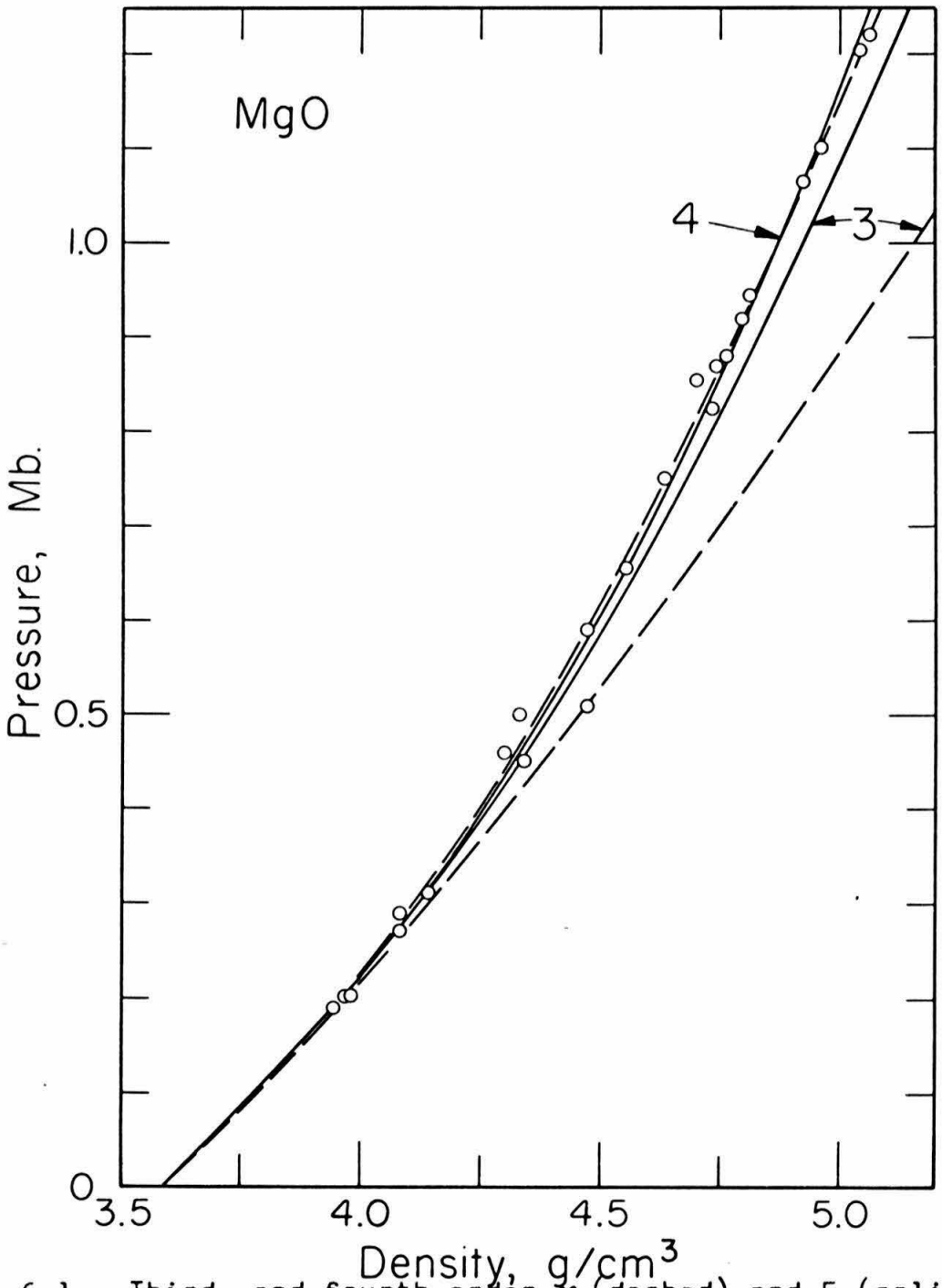

Fig. 6.1. Third- and fourth-order η (dashed) and E (solid) calculated MgO Hugoniots compared with single-crystal Hugoniot data of Carter et al. (1971).

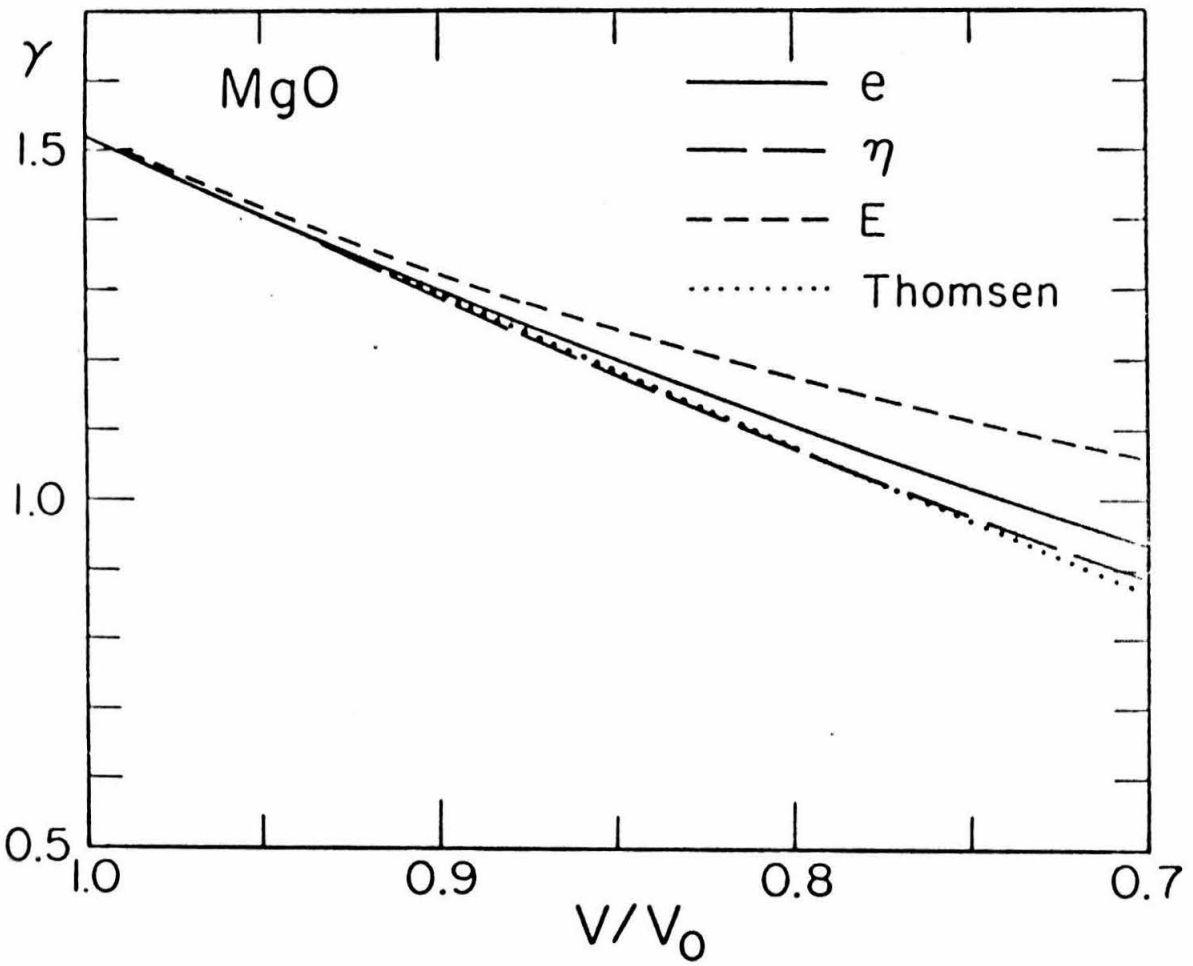

Fig. 6.2. Comparison of γ from equations (36), (36a), (36b) and (50) of Chapter 3, in terms of e, η, and E, respectively. Equation (50) was given by Thomsen (1970).

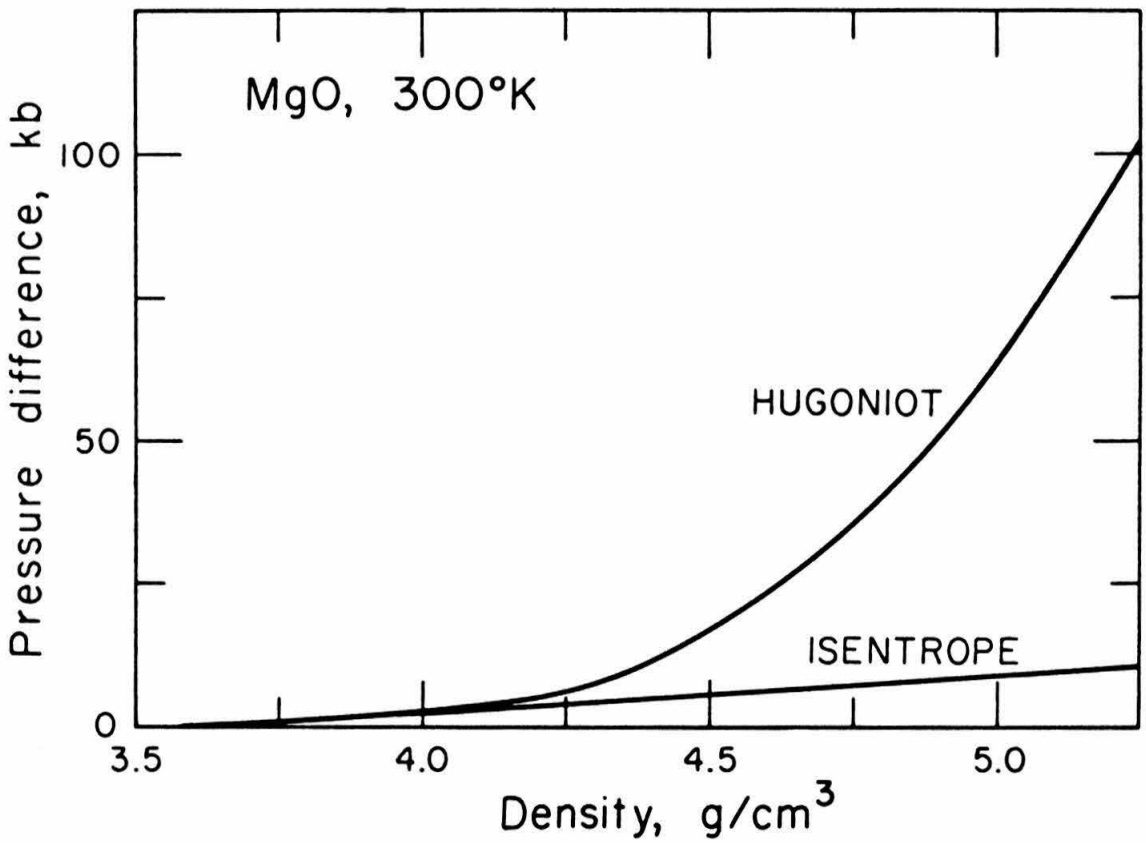

Fig. 6.3. Pressure offsets of MgO isentrope and Hugoniot from 300°K isotherm.

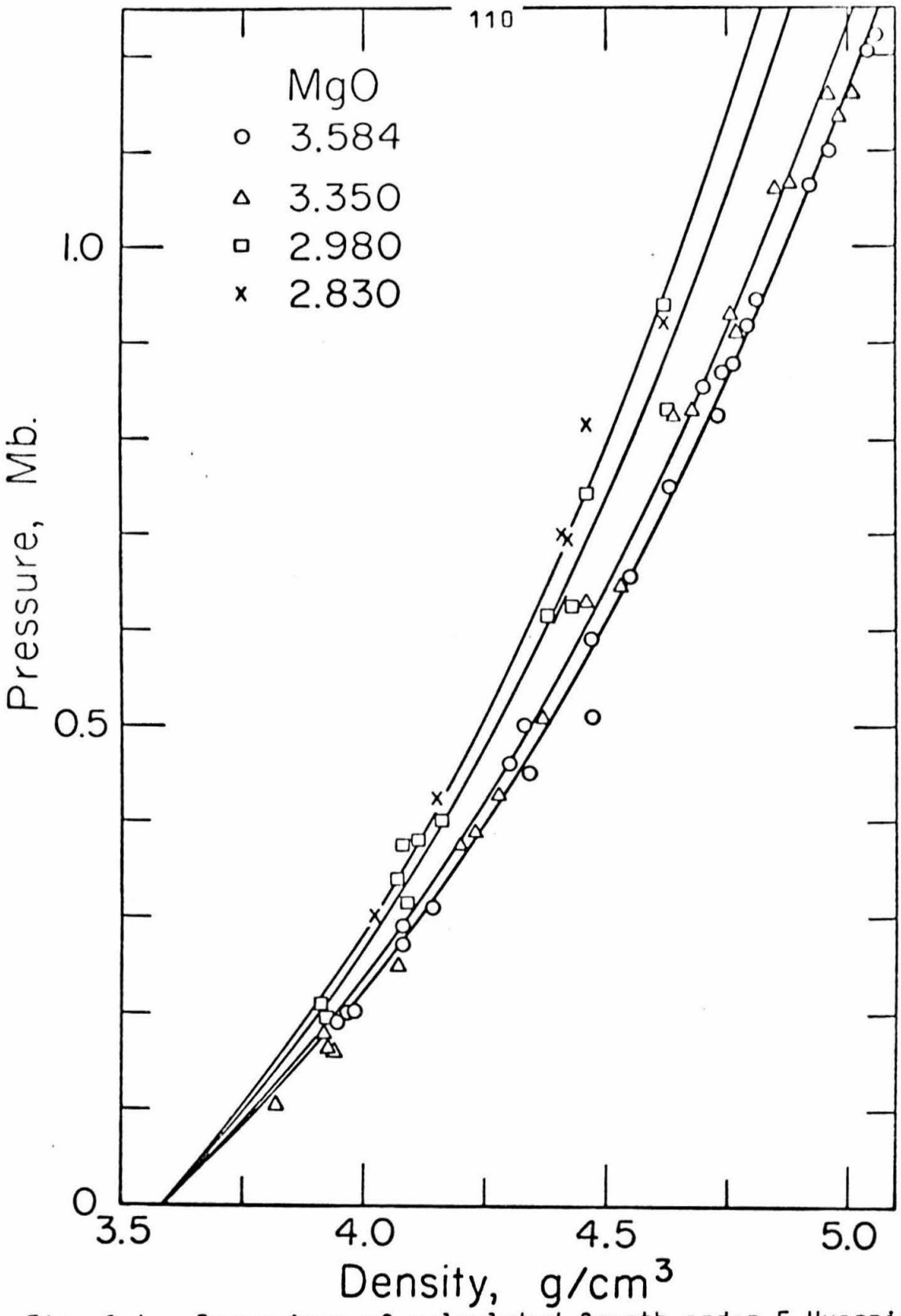

Fig. 6.4. Comparison of calculated fourth-order E Hugoniots of MgO with Hugoniot data of Carter et al. (1971).

CHAPTER 7

EQUATIONS OF STATE AND PHASE EQUILIBRIA OF STISHOVITE AND A COESITE-LIKE SiO_2 PHASE FROM SHOCK-WAVE AND OTHER DATA

Summary

Shock-wave, static compression (X-ray), ultrasonic, thermal expansion and thermodynamic data are simultaneously inverted to determine the equations of state of stishovite and a coesite-like SiO_2 phase. All of the stishovite data except the thermal expansion data are found to be satisfied by a Mie-Grüneisen type equation of state with a zero pressure bulk modulus, K, of about (3.50 ± 0.1) megabar, a pressure derivative dK/dP of 3.3 ± 1 and a Grüneisen parameter, initially 1.25 ± 0.1, which decreases slowly with compression. The volume coefficient of thermal expansion at ambient conditions is found to be (13 ± 1) x $10^{-6}/^{o}K$, compared to (16.4 ± 1.3) measured by Weaver. Some Hugoniot data of Trunin et al. for very porous quartz have densities very close to that of coesite. However, a calculation of the coesite-stishovite phase line shows that the coesite-like phase persists to about twice the predicted transition pressure at 10,000°K. It is suggested that the discrepancy can be explained if this phase is interpreted as a liquid of about coesite density.

7.1 Introduction

Since the discovery of the dense high-pressure silica polymorph stishovite (Stishov and Popova, 1961), and its subsequent identification in natural silica from a meteor crater (Chao et al., 1962) and as the dense phase obtained in the shock-wave experiments of Wackerle (1962) by McQueen et al. (1963), a variety of experiments have yielded a considerable amount of data on stishovite. To date, these include more shock-wave, static compression (X-ray), thermodynamic, thermal expansion and, very recently, ultrasonic data. These data, with their sources and other relevant information, are summarized in Table 7.1. A succession of analyses of these data has accompanied their accumulation (Anderson and Kanamori, 1968; Ahrens et al., 1969; Ahrens et al., 1970). This paper is another in this succession.

The Grüneisen parameter, γ, is an important quantity which characterizes thermal effects in the equation of state. Ahrens et al. (1970), returning to the method used by McQueen et al. (1963), determined the values of γ at large compression from the difference in pressure between Hugoniots corresponding to different initial densities. This method is preferable to that used by Anderson and Kanamori (1968) and Ahrens et al. (1969), who used the "Slater" or "Dugdale-MacDonald" formulae for the volume dependence of γ (Slater, 1939; Dugdale and MacDonald, 1953). These formulae have been severely

criticized because they fail to take account of the frequently large pressure dependence of the shear modes of vibration (Knopoff and Shapiro, 1969). Fitting these results with the functional form

$$\gamma = \gamma_o (V/V_o)^A , \qquad (1)$$

where V is specific volume, A is a constant and subscript "o" denotes zero pressure, Ahrens et al. (1970) adjusted γ_o until the volume coefficient of thermal expansion, α, obtained from the identity

$$\alpha = \frac{\gamma \rho C_p}{K_s} , \qquad (2)$$

and using K_s determined from the shock-wave analysis, agreed with the measured value. (The value used was the preliminary value $\alpha = 15 \times 10^{-6}/^{o}K$ obtained from Weaver by personal communication. Cf. Table 7.1.) In equation 2, K_s is the isentropic bulk modulus, ρ is the density and C_p is the specific heat at constant pressure.

Since that analysis, several new sets of data have been published. The data of Trunin et al. (1971a) greatly extend the pressure range of the Hugoniot data, and those of Trunin et al. (1971b) extend the range of initial porosities. The resultant wide spread of the Hugoniots provides stronger constraints on γ. Also, Mizutani et al. (1972) have measured ultrasonically the compressional and shear wave velocities of

stishovite, providing another constraint on K_S.

In addition to benefiting from the newly available data, and using a different form of the equation of state, the present analysis determines simultaneously the "compressional" and "thermal" parts of the equation of state by adjusting simultaneously all free parameters to give a "least-squares" fit to all of the data. This procedure accomplishes implicitly the two sequential stages of the analysis of Ahrens et al. (1970).

Trunin et al. (1971b) noted that the Hugoniots of their most porous quartz samples achieved densities significantly less than that of stishovite, and that these Hugoniots extrapolated approximately to the zero pressure density of coesite. On this basis they identified these Hugoniots as representing the coesite phase. Although, at room temperature coesite is stable in the approximate pressure range 30 to 70 kb, between the stability fields of quartz and stishovite, it has not previously been observed in shock-wave experiments, the transformation usually being directly from quartz to stishovite. There is sufficient other coesite data (Table 7.2) that, combined with these Hugoniot data, and assuming that they do indeed represent coesite, the equation of state can be approximately determined. The success of this procedure seems to support the coesite identification, but other calculations suggest otherwise, as will be seen.

Trunin et al. (1971b) also calculated approximate Hugoniot temperatures and suggested that the boundary separating the coesite and stishovite fields in a pressure-temperature plot represented the coesite-stishovite phase transition line. Hugoniot temperatures have been recalculated here, and in addition, the coesite-stishovite phase line has been independently calculated from the equations of state of the two phases (again, assuming the coesite identification). There is a large discrepancy between the two approaches. It is suggested that the new phase may in fact be a liquid of approximately the density of coesite, rather than coesite itself. Since some of the properties of this liquid are unknown, it is necessary to proceed as if the phase were solid coesite, and to examine the plausibility of the results.

7.2 Equations of State - General Discussion

The procedure used here to determine the equation of state was to calculate, according to chapters 3 and 4, all relevant quantities, such as Hugoniots, isotherms, bulk modulus, etc., and to adjust the equation of state parameters so as to obtain a weighted least-squares fit to the data. The weighting basically was according to the estimated standard error of the data, but was also adjusted in some cases, as will be seen, to preferentially fit some of the data.

The specific heat at constant volume, required in these

equations, has been approximated here by the Debye model. A discussion of the inadequacy of the Debye model for a number of minerals is given by Kieffer and Kamb (1972). Their results indicate that the Debye model is fairly good for stishovite, but less good for coesite. In view of the other uncertainties in the equations of state, particularly that of coesite, the errors arising from the use of the Debye model are considered acceptable.

Hugoniot temperatures are calculated according to a method given, for example, by Ahrens et al. (1969). For this calculation, the volume dependence of the Debye temperature θ_D is required. Since θ_D is defined in terms of a characteristic frequency of lattice vibration, it must have the same volume dependence as the lattice frequencies. Thus, for consistency with equation 34 of chapter 3,

$$\theta_D(V) = \theta_D(V_0)\left(1 + g e + \tfrac{1}{2} h e^2\right)^{\frac{1}{2}}. \qquad (3)$$

Some general features of the silica Hugoniot data and a representative set of calculated Hugoniots and isotherms are illustrated in Fig. 7.1. Most of the Hugoniot data radiate from either of two points - the coesite and stishovite zero-pressure densities, respectively. This is the basis of the identification by Trunin et al. (1971b) of the Hugoniots of the two most porous silica samples as being in the coesite phase. This identification will be discussed subsequently;

in the meantime, the phase will be referred to as "coesite".

The Hugoniots of successively more porous silica, starting at zero porosity, become successively steeper up to the initial density, ρ_0', of 1.77 g/cm^3, whose Hugoniot is nearly vertical on this plot. The 1.55 g/cm^3 initial density Hugoniot data are at densities lower than, but fairly close to, the zero-pressure, 300°K stishovite density, while the 1.35 and 1.15 g/cm^3 initial density Hugoniots are less steep and centered about the coesite density. The ρ_0' = 1.55 g/cm^3 Hugoniot may represent a mixture of "coesite" and stishovite (Trunin et al., 1971b). This point will be discussed further below.

The calculated Hugoniots shown in Fig. 7.1 (stishovite, case 2 and "coesite" case 1, discussed below) reproduce these features fairly well. However, the coesite-stishovite transition is not predicted by these calculations. Thus, "stishovite" Hugoniots corresponding to all seven initial porosities are shown. The three "most porous" Hugoniots are notable for having negative slopes - there is a critical initial density for which the Hugoniot is vertical. The two "most porous" Hugoniots are shown dashed, since they clearly fail to represent the corresponding data. The ρ_0' = 1.55 g/cm^3 Hugoniot data approach, but do not agree very well with, the corresponding calculated stishovite curve shown in Fig. 7.1. Only the two "most porous" "coesite" Hugoniots are shown in

Fig. 7.1. The others will lie between these and the 300°K isotherm (shown short-dashed) and clearly will not coincide with the corresponding data.

The details of the analyses will now be discussed individually for stishovite and "coesite", and the effects of various assumptions made in the analyses will be noted. However, it will be seen that the above general picture is not greatly perturbed.

7.3 Equations of State - Stishovite

The results of three different analyses of the stishovite data will now be given. In the first case, standard errors of the pressure of each set of compression data (shock and static) were estimated and the data weighted accordingly. (The quantity minimized was $\sum(p_i^c - p_i)^2/\sigma_i^2$, where p_i^c is the calculated pressure, p_i the observed pressure, σ_i the estimated standard error and the summation is over all data points (see, for example, Mathews and Walker, 1965).) Although K_o is known approximately from the ultrasonic measurements of Mizutani et al. (1972), it was preferred to determine it independently from the compression data. Thus the quantities K_o, K_o', K_o'' and $(\partial K/\partial T)_p$ were determined from the compression data, V_o and α were taken from Table 1, and C_v was calculated from the Debye model. For the calculation of C_v, the Debye temperature given by Kieffer and Kamb (1972) as

the high temperature limit of the data of Holm et al. (1967) was used. The estimated standard errors are listed in Table 7.3, the resulting values of the parameters and their calculated standard errors are in Table 7.4 (case 1), and the calculated Hugoniots and the 300°K isotherms are compared to the Hugoniot data in Fig. 7.2. It can be seen that this solution does not fit the Hugoniots of the more porous samples very well at all. This is partly because of the greater density of data points on the lower porosity Hugoniots and partly because the value of γ_0 is constrained to a high value by the value of α used and the value of K_0 required to fit the lower porosity Hugoniots.

As a first step to improving the fit of the higher porosity Hugoniots, α was allowed to be determined by the compression data along with the other parameters previously determined. The results are given in Table 7.4 (case 2) and illustrated in Fig. 7.1, the stishovite curves used in that figure being those corresponding to the present case. Lowering the value of α to $13 \times 10^{-6}/°K$ has lowered γ_0 to 1.3 and significantly improved the fit to the higher porosity Hugoniots. However, the full range of the Hugoniot data is not shown in Figs. 7.1 and 7.2. The data of Trunin et al. (1971a) and Trunin et al. (1971b) extending up to 6.5 Mb for the initial densities 1.77 and 2.65 g/cm^3 are shown in Fig. 7.3. The corresponding calculated Hugoniots and 300°K

isotherm of the present case are also shown (case 2). The 1.77 g/cm^3 Hugoniot curve does not fit the corresponding datum at 2.3 Mb very well.

To further improve the fit to the higher porosity Hugoniots, the Hugoniot data were assigned new standard errors so as to weight the "porous" data more heavily relative to the other data. The new set of standard errors are given in Table 7.3. The results are given in Table 7.4 (case 3) and illustrated in Figs. 7.3 and 7.4. Fig. 7.3, in particular, shows that the fit to the 1.77 g/cm^3 Hugoniot data has improved. The value of α has decreased further to 12 x $10^{-6}/^{o}K$.

The values of the zero pressure bulk modulus, K_o, range from 3.42 to 3.55 Mb for the three cases considered. These fall within the range 3.46 $\pm$ .24 Mb given by Mizutani et al. (1972) for the isentropic bulk modulus determined from elastic wave velocity measurements. The 300^{o}K isotherms for these cases also agree well with the static compression data of Liu et al. (1971). These are shown in Fig. 7.5, together with the three calculated isotherms. Also shown in Fig. 7.5 are the static compression data of Bassett and Barnett (1970). These have been discussed by Liu et al. (1971), who suggest that the five highest pressure data points are systematically low because the anvils of the tetrahedral press used by Bassett and Barnett (1970) may have come into contact at about this pressure. These points

were not used in the present analysis. The calculated isotherms agree with the remaining data within the scatter of the data.

For the record, the last two cases were rerun with K_0 given the fixed value 3.45 Mb, which gives an isentropic bulk modulus very close to that given by Mizutani et al. (1972). (In all of the cases given here, the isentropic bulk modulus is about 0.02 Mb greater than the isothermal bulk modulus.) The results are given in Table 7.4 as cases 4 and 5. The changes from the previous solutions are small. The standard errors given in Table 7.4 are calculated using the error 0.24 Mb given by Mizutani et al. for the bulk modulus.

In view of the current discussion of the relative merits of the "Lagrangian" and the "Eulerian" formulations of finite strain (Thomsen, 1970, 1972; Ahrens and Thomsen, 1972; Chapters 2 and 3), the dependence of the above results on the form of the equation of state should be tested. This was done using a Lagrangian <u>isotherm</u> (Thomsen, 1970; Chapter 3), but keeping equation 36 of chapter 3 for γ. This does <u>not</u> correspond to the Lagrangian equation used by Thomsen (1970) and Ahrens and Thomsen (1972), who used a different expression for γ (Thomsen, 1970). This has been discussed previously (Chapters 3 and 6). In any case, using a different equation for γ should yield a significantly different value only for $(\partial K/\partial T)_p$, for which we have no other control. Cases 2 and 3

were repeated using the Lagrangian isotherm. The results are given in Table 7.4 as cases 2a and 3a. The values of K_0 are comparable, K_0' somewhat lower, K_0K_0'' much higher and the other parameters comparable to the corresponding values in cases 2 and 3. In particular, the value of α is very little changed -- it is still much lower than the value given by Weaver (1971).

Ahrens et al. (1970) interpreted the $\rho_0' = 1.98$ g/cm^3 data as indicating a reversal in the slope of the Hugoniot at about 1.2 Mb (see Fig. 7.1). A criterion was given which relates the density at which the slope of the Hugoniot becomes infinite to the value of γ at that point: $\gamma = 2/(\rho/\rho_0' - 1)$. However, it can be seen from an equation for the Hugoniot (e.g., Chapter 4) that the Hugoniot pressure also becomes infinite at this density; in other words, the Hugoniot pressure assymptotes to infinity rather than "bending over". This interpretation biased the high pressure values of γ to lower values, since it favored an interpretation in which the Hugoniots were crowded together at these compressions. The discrepancy between the results of Ahrens et al. (1970) and those of this study is due partly to the last effect, partly to the fewer data available at the time and partly to the higher value of α used. Case 1 given here is closer to the solution of Ahrens et al., and shows similar effects.

The main limitation of the present analysis is probably

the use of an equation based on the Mie-Grüneisen approximation, which allows no temperature dependence of γ. At temperatures below the Debye temperature, γ is probably temperature dependent because of mode under-saturation, and at very high temperatures (greater than several thousand degrees K, say), it is possible that we are dealing with a fluid phase (see later) which has a different value of γ. In the former connection, it is interesting to note that Nicol and Fong (1971), measuring Raman spectra, have observed a negative mode γ for a mode of rutile, which is isostructural with stishovite.

The temperature dependence of α is dominated by the temperature dependence of C_p and possibly of γ (see equation 46, Chapter 3). Weaver (1971) notes that his value of $\epsilon = (\partial\alpha/\partial T)_p/\alpha^2 = 33 \pm 17$ seems too small - it implies $(\partial\gamma/\partial T)_v = -5 \times 10^{-3}/^oK$, a value which is sufficient to reduce γ to zero within 300^oK. With $(\partial\gamma/\partial T)_v = 0$, Weaver estimates $\epsilon = 190 \pm 20$. If we take Weaver's <u>mean</u> value of α in the range $300\text{-}900^oK$, i.e., $\alpha = 18.6 \times 10^{-6}/^oK$, to apply to 600^oK, and combine it with the 300^oK value of $13 \times 10^{-6}/^oK$ found here, we get $\epsilon = 100$, approximately. This is an intermediate value, implying a moderate value of $(\partial\gamma/\partial T)_v$. Of course, it has not been determined whether this would be allowed by Weaver's data.

To conclude this section, it appears that most of the relevant stishovite data, with the exception of α, can be

incorporated with reasonable accuracy into the Mie-Grüneisen type of equation of state used here. Although case 3 gives the best fit to the Hugoniot data, the Mie-Grüneisen equation is probably a poor approximation over the range of temperatures involved in these data. Thus case 2, which is based on data at more moderate temperatures, is probably the preferable solution.

An analysis by E. K. Graham (unpublished manuscript, 1972) of some of the stishovite Hugoniot data analyzed here yielded the values K_0 = 3.35 Mb, K_0' = 5.5 and γ_0 = 1.64. A high value of K_0' was also obtained by Ahrens et al. (1970) (K_0 = 3.0, K_0' = 6.9, γ_0 = 1.58). Although some differences between these analyses and the present one are due to the different equations used, a critical difference is that cases 2 and 3 of the present analysis rely on the Hugoniot data of the more porous samples to constrain γ, whereas the others rely on Weaver's (1971) coefficient of thermal expansion. The effect of these different approaches can be seen by comparing case 1 with cases 2 and 3, above. Case 1 also relies on Weaver's data. The preference for case 2 rests on the critical assumption that the Grüneisen parameter does not vary greatly with temperature at very high temperatures.

7.4 Equations of State - "Coesite"

This section will proceed on the assumption that the Hugoniots of the most porous quartz samples represent coesite. The difficulties raised by this assumption, and an alternative interpretation, will be discussed in the next section.

Because of the smaller range and quantity of "coesite" data, it is not possible to determine as many parameters of the equation of state as it was for stishovite. Since the data extend to only about 15 per cent volume compression, it is not necessary to use the full "fourth-order" finite strain equation (Equation 42, Chapter 3), so the "ϵ^3" term is here assumed to be zero. Since there is not a large range in the initial porosities of the Hugoniot data, the volume dependence of γ, and hence $(\partial K/\partial T)_p$, cannot be well determined. Conversely, the value of $(\partial K/\partial T)_p$ does not strongly affect the equation of state in this range. A value of -0.05 Kb/°K was therefore assumed. This value of $(\partial K/\partial T)_p$ gives values of δ_T in the range 5 to 10, a range which seems reasonable on the basis of a few other examples, including stishovite (see, for example, Anderson et al., 1968; Roberts and Ruppin, 1971). V_0 and α were taken from Table 2 and C_v was calculated from the Debye model.

It can be seen from Fig. 7.1 that the $\rho_0' = 1.35$ g/cm^3 Hugoniot data are considerably scattered and that they do not trend towards the coesite density of 2.91 g/cm^3. This

may be because there has been a partial conversion to the stishovite phase. When compared to the $\rho_0' = 1.15$ g/cm^3 Hugoniot data, the lower three points in particular are seen to deviate towards higher densities. Two cases were therefore treated, one including these three points and the other excluding them.

Initially, both K_0 and K_0' were allowed to be determined by the Hugoniot and static compression data. The results are given as cases 1 and 2, Table 6, case 1 excluding the three doubtful Hugoniot points and case 2 including them. The "standard errors" used to weight the compression data are given in Table 5. Case 1 is illustrated in Fig. 1, and case 2 in Fig. 6. The bulk moduli in these two cases are significantly above the value of 0.97 Mb measured ultrasonically by Mizutani et al. (H. Mizutani, private communication, 1972), so a third case was run with K_0 fixed at this value and allowing only K_0' to be determined by the compression data (Table 6, Fig. 6). From Fig. 6 it can be seen that case 3 does not fit the static compression data of Bassett and Barnett (1970) very well, and it falls below most of the corresponding Hugoniot data.

The scatter in the Hugoniot data, and the uncertainty in their interpretation, are such that they cannot definitely be said to be discordant with case 3, but the discrepancy between case 3 and the static compression data seems to be

significant. Because of this, the equation of state of coesite must remain somewhat uncertain at this stage.

7.5 SiO_2 Phase Equilibria

Using the equations of state just given, the Gibbs free energies of "coesite" and stishovite can now be calculated, and the "coesite"-stishovite transition pressure calculated as a function of temperature using the condition that the Gibbs free energies of the two phases are equal at the phase transition.

For detailed comparison, the Hugoniot temperatures, which were calculated approximately by Trunin et al. (1971b), have been calculated according to the method described earlier. The results, plotted versus Hugoniot pressure, are shown in Figs. 7.7 and 7.8. It is notable that the 5.5 Mb point is over 40,000°K, and the $\rho_0' = 1.77$ point at 2.3 Mb is over 30,000°K. The temperatures are only changed by a few percent by using the different equations of state given in the previous sections. A greater uncertainty in the points is due to the scatter in Hugoniot pressures, but this would only cause the points to move along the Hugoniot locus, which, in a P-T plot, is approximately radial from the initial point.

In Fig. 7.8, the boundary between the "coesite" and stishovite fields, shown by the dashed curve, is closely defined by the $\rho_0' = 1.77$ and 1.55 g/cm^3 Hugoniot points,

which, as was discussed earlier, both show signs of involving a mixture of the two phases.

The Gibbs free energy is defined by

$$G = H - TS = U + PV - TS , \qquad (4)$$

where H is the enthalpy and S the entropy. G has the property (see, e.g., Slater, 1939)

$$\left(\frac{\partial G}{\partial P}\right)_T = V . \qquad (5)$$

We wish to evaluate G at the state (P,V,T) starting from the state $(0,V_0,T_0)$. (Atmospheric pressure can be ignored here.) This will be done via the state (P_0,V_0,T) where $P_0(T) = P(V_0,T)$. I.e., by first raising the temperature at constant volume and then compressing isothermally. From equation 4,

$$G(V_0,T) = G(V_0,T_0) + [U(V_0,T) - U(V_0,T_0)] + P_0(T)V_0 - [TS(V_0,T) - T_0 S(V_0,T_0)] , \qquad (6)$$

and from equation 5, upon integration,

$$G(V,T) = G(V_0,T) + \int_{P_0(T)}^{P(T)} V(P',T)\, dP' . \qquad (7)$$

Denoting the difference between the stishovite and coesite Gibbs free energies at the state (V_0,T_0) by ΔG_0, i.e.,

$$\Delta G_o = G^s(V_o^s, T_o) - G^c(V_o^c, T_o),$$

where superscripts "s" and "c" denote stishovite and coesite, respectively, and defining ΔH_o and ΔS_o similarly, equation 4 gives

$$\Delta G_o = \Delta H_o - T_o \Delta S_o \quad . \tag{8}$$

ΔH_o and ΔS_o can be found from the results of Holm et al. (1967). At 298°K, they give ΔH_o = 10.58 Kcal/mole = 7.36×10^9 erg/g and ΔS_o = 13.01 cal/mole °K = -2.09×10^6 erg/g °K.

Now from equation 6, using equation 8, we obtain

$$G^s(V_o^s,T) - G^c(V_o^c,T) = P_o(T)(V_o^s - V_o^c) + U^s(V_o^s,T) - U^c(V_o^c,T) - T[S^s(V_o^s,T) - S^c(V_o^c,T)]. \tag{9}$$

To evaluate this, we need U and S as functions of T for both stishovite and coesite. These are known accurately (Holm et al., 1967) only up to 350°K. However, the difference $U^s(V_o^s,T) - U^c(V_o^c,T)$, and the analogous difference for S, can be approximated as being constant above about 350°K, for the following reasons. The specific heats, C_p, of stishovite and coesite given by Holm et al. (1967) converge towards each other above about 150°K. Also, at 300°K, C_p differs

from C_v by about 0.6 per cent for stishovite and about 0.1 per cent for coesite. Thus the C_v will also converge at higher temperatures. Since U and S are integrals of C_v, $U^s - U^c$ will approach a constant value at higher temperatures, as will $S^s - S^c$. Thus, the differences in U and S in equation 9 can be replaced by their values at 298°K. Noting, finally, that $\Delta U_o \approx \Delta H_o$, equation 9 becomes

$$G^s(V_o^s,T) - G^c(V_o^c,T) = P_o(V_o^s - V_o^c) + \Delta H_o - T\Delta S_o . \qquad (10)$$

Returning to equation 7, the integral is more easily evaluated here by noting that

$$\int_{P_o}^{P} V\,dP' = \int_{V}^{V_o} P(V',T)\,dV' + VP - V_o P_o . \qquad (11)$$

Equations 7, 10 and 11, and equation 3 for an isotherm, allow the Gibbs free energies of "coesite" and stishovite to be compared.

The phase line resulting from these calculations is shown in Fig. 8. The error bars shown represent the variations due to the use of the alternative equations of state given in the previous sections. The uncertainty due to the approximations used for $U^s - U^c$ and $S^s - S^c$ is difficult to estimate, but should not be greater than a few percent. Errors of 5 percent in $U^s - U^c$ and $S^s - S^c$ would cause errors of about 1 percent and 3 percent, respectively, in the

calculated transition pressure at 10,000°K.

As can be seen in Fig. 8, the calculated phase line deviates considerably from the line separating the "coesite" and stishovite Hugoniot fields. The difference is about a factor of two in temperature, which would seem to be well outside the range of uncertainties of the calculations. If this is correct, it means that the "coesite" phase obtained in the shock-wave experiments is metastable. This is a surprising result, as it might have been expected that the high temperatures involved would have promoted the transition to stishovite.

An alternative interpretation of the data is suggested by re-examining Fig. 8, where the lower pressure, quartz-liquid-gas region of the phase diagram is also shown (Levin et al., 1969; JANAF Tables, 1965). The "coesite"-stishovite Hugoniot boundary intersects the calculated phase line at about 2,500°K, which is comparable to the melting temperature of quartz. Is it possible that the "coesite" is the liquid phase?

The plausibility of this hypothesis can be tested using the "Clausius-Clapeyron" relation for the slope of a phase line:

$$\frac{dP}{dT} = \frac{\Delta S}{\Delta V}, \qquad (12)$$

where "Δ" denotes the change through the phase transition. Let us apply this at the hypothetical coesite-stishovite-liquid triple point at 125 Kb, 2,500°K. We know that the volumes of coesite and the liquid must be very similar at this pressure because of the agreement between the coesite static compression data and the "coesite" Hugoniot data (see Fig. 6). If the difference in their volumes is zero, equation 12 shows that the coesite-liquid phase line is horizontal in Fig. 8 - also shown by the line labelled "1" in Fig. 9, which illustrates the relevant region of the phase diagram in more detail. If the difference in volumes is not zero, the slope of the phase line can be estimated as follows. The coesite-stishovite phase line is still fairly well determined below the triple point. The coesite-stishovite volume difference is about 0.09 cm^3/g. The entropy difference is then, from either the slope of the phase line (0.02 Kb/°K) and equation 12 or the approximation made in the previous section, about 2×10^6 erg/g °K. Assuming the liquid-stishovite volume difference to be also about 0.09 cm^3/g, the slope of the liquid-stishovite phase line (0.06 Kb/°K) and equation 12 give the liquid-stishovite entropy difference as about 5×10^6 erg/g °K. Combining these results, the liquid-coesite entropy difference is about 3×10^6 erg/g °K. From Fig. 6 we can estimate a reasonable maximum volume difference between coesite and the liquid to be about 0.01

cm^3/g. Equation 12 then gives a slope of about 0.3 $Kb/^oK$ - line "2" in Fig. 9. Line "3", having the same slope as the stishovite-liquid phase line, would imply that coesite would have a volume similar to that of stishovite, which is clearly unreasonable.

Lines "1" and "2" both extrapolate to the range of melting temperatures of quartz. There is a difficulty, though, since a similar set of relationships would hold at the quartz-coesite-liquid triple point, which would lead us to predict a slope of the quartz-liquid phase line which is rather different from the one shown. However, we may observe that the liquid would have to vary continuously from a density of about 2.2 g/cm^3 at zero pressure (the density of fused quartz) to about 3.1 g/cm^3 at 100 Kb. This would cause the phase lines to be concave downwards (in Fig. 9) in this range, and might allow these relationships to hold without contradiction.

The preceeding discussion is intended as a plausibility argument. It is concluded that it must be considered a serious possibility that a coesite-like liquid phase was produced in the shock-wave experiments.

Returning, finally, to the coesite-stishovite phase line below the hypothetical triple point, the calculated transition pressure at 300^oK is 78 Kb. This is in reasonable agreement with the value 69 Kb estimated from their experi-

mental results by Akimoto and Syono (1969). It may also be compared with their values 85 to 95 Kb calculated using a rough estimate of the coesite compressibility.

The average slope of the phase line is about 0.023 Kb/^{o}K, which compares very well with the value 0.024 Kb/^{o}K found by Akimoto and Syono (1969).

7.6 Discussion

The determinations of the equations of state of stishovite and "coesite" accomplished here depend a lot for their success on the ability to incorporate a variety of data, which constrain different aspects of the equation of state, into a single consistent equation of state. In this respect there is nothing unique about the particular equations used here. For instance, a combination of the Birch-Murnaghan equation and equation (1) for γ would have served just as well. (The comments in Chapters 6 and 8 concerning the dependence of derived parameters on the form of the equations used should be born in mind, though.) The present contribution in this regard is merely to point out and demonstrate an approach which could, and should, have been used much more widely. A further, more thorough, demonstration and discussion of this approach is given in Chapter 8.

7.7 References

AHRENS T. J., ANDERSON DON L. and RINGWOOD A. E., Rev. Geophys. 7, 667 (1969).

AHRENS T. J., TAKAHASHI T. and DAVIES G. F., J. Geophys. Res. 75, 310 (1970).

AHRENS T. J. and THOMSEN L., Earth Planet. Sci. Lett. Submitted for publication (1972).

AKIMOTO S. and SYONO Y., J. Geophys. Res. 74, 1653 (1969).

AL'TSHULER L. V., TRUNIN R. F. and SIMAKOV G. V., Izv. Akad. Sci. USSR, Phys. Solid Earth, 10, Engl. Transl., 657 (1965).

ANDERSON DON L. and KANAMORI H., J. Geophys. Res. 73, 6477 (1968).

ANDERSON O. L., SCHREIBER E., LIEBERMANN R. C. and SOGA N., Rev. Geophys. 6, 491 (1968).

BASSETT W. A. and BARNETT J. D., Phys. Earth Planet. Interiors 3, 54 (1970).

BASSETT W. A., TAKAHASHI T., MAO H. K. and WEAVER J. S., J. Appl. Phys. 39, 319 (1968).

BIRCH F., J. Geophys. Res. 57, 227 (1952).

CHAO E. C. T., FAHEY J. J., LITTLER J. and MILTON D. J., Amer. Mineral. 46, 807 (1962).

DUGDALE J. S. and MacDONALD D. K. C., Phys. Rev. 89, 832 (1953).

HOLM J. L., KLEPPA O. J. and WESTRUM E. F., Geochim. Cosmochim. Acta 31, 2289 (1967).

JANAF Thermochemical Tables, Clearinghouse for Federal Scientific and Technical Information (1965).

JONES A. A., ISBELL W. M., SHIPMAN F. H., PERKINS R. D., GREEN S. J. and MAIDEN C. J., General Motors Materials and Structures Laboratory Report NAS2-3427 (1968).

KIEFFER SUSAN W. and KAMB B., Rev. Geophys. in press (1972).

KNOPOFF L. and SHAPIRO J. N., J. Geophys. Res. 74, 1439 (1969).

LEIBFRIED G. and LUDWIG W., Solid State Physics 12, 275, Academic Press, New York (1961).

LEVIN E. M., ROBBINS C. R. and McMURDIE H. F., Phase Diagrams for Ceramicists, The American Ceramics Society, Columbus, Ohio, 2nd edition (1969).

LIU L., BASSETT W. A. and TAKAHASHI T., J. Geophys. Res. in press (1971).

MATHEWS J. and WALKER R. L., Mathematical Methods of Physics, Benjamin, New York (1965).

McQUEEN R. G., Seismic Coupling (Edited by G. Simmons), 53, VESIAC Report, Geophysics Laboratory, University of Michigan (1968).

McQUEEN R. G., FRITZ J. N. and MARSH S. P., J. Geophys. Res. 68, 2319 (1963).

MIZUTANI H., HAMANO Y. and AKIMOTO S., in preparation (1972).

NICOL M. and FONG N. Y., J. Chem. Phys. 54, 3167 (1971).

ROBERTS R. W. and RUPPIN R., Phys. Rev. B 4, 2041 (1971).

ROBIE R. A., BETHKE P. M., TOULMIN M. S. and EDWARDS J. L., Handbook of Physical Constants (Edited by S. P. Clark Jr.), Mem. 97, Geol. Soc. Am. (1966).

SHIPMAN H., private communication (1969). (See Ahrens et al., 1970).

SKINNER B. J., Handbook of Physical Constants (Edited by S. P. Clark Jr.), Mem. 97, Geol. Soc. Am. (1966).

SLATER J. C., Introduction to Chemical Physics, McGraw-Hill, New York (1939).

STISHOV S. M. and POPOVA S. V., Geokhimiya, No. 10, 923 (1961).

THOMSEN L., J. Phys. Chem. Solids 31, 2003 (1970).

THOMSEN L., J. Phys. Chem. Solids 33, 363 (1972).

TRUNIN R. F., SIMAKOV G. V., PODURETS M. A., MOISEYEV B. N. and POPOV L. V., Izv. Earth Physics No. 1, 13 (1971a).

TRUNIN R. F., SIMAKOV G. V. and PODURETS M. A., Izv. Earth Physics No. 2, 33 (1971b).

WACKERLE J., J. Appl. Phys. 33, 922 (1962).

WEAVER J. S., Ph.D. Thesis, University of Rochester, Rochester, New York (1971).

TABLE 7.1

Stishovite data

Shock-wave data

Code	Source	Number of points	Initial density (g/cm^3)	Pressure range (Mb)
S1	Wackerle (1962)	12	2.65	0.4-0.7
S2	Al'tshuler et al. (1965)	3	2.65	0.6-2.0
S3	Trunin et al. (1971a)	12	2.65	0.4-6.5
S4	Wackerle (1962)	3	2.20	0.5-0.6
S5	Shipman (1969)	5	2.20	0.6-1.6
S6	McQueen et al. (1968)	34	2.20	0.4-0.8
S7	Trunin et al. (1971b)	2	2.20	0.5-1.6
S8	Jones et al. (1968)	6	1.98	0.4-1.4
S9	Trunin et al. (1971b)	6	1.77	0.2-2.3
S10	Trunin et al. (1971b)	(3)*	1.55	0.3-0.6

* May be interpreted as coesite-stishovite mixture (see text).

TABLE 7.1 (continued)

Static compression data

Code	Source	Number of points	Pressure range (Kb)
X1	Liu et al. (1969)	9	0-223
X2	Bassett and Barnett (1970)	14	0-85

Other data

Source	Quantity	Value
Mizutani et al. (1972)	Compression wave velocity	$V_p = 11.0$ Km/s
	Shear wave velocity	$V_s = 5.50$ Km/s
	Isentropic bulk modulus	$K_s = 3.46 \pm .24$ Mb
Weaver (1971)	Volume coeeficient of thermal expansion (300^oK)	$\alpha = (16.4 \pm 1.3)/^oK$
Holm et al. (1967)	Specific heat at constant pressure (300^oK)	$C_p = 7.15 \times 10^6$ erg/g. ^oK
Kieffer and Kamb (1972)	High temperature limit of Debye temperature	$\theta_D \approx 1120^oK$
Robie et al. (1966)	Density, zero pressure, 298^oK	$\rho_o = 4.287$ g/cm^3

TABLE 7.2

Coesite data

Shock-wave data

Code	Source	Number of points	Initial density (g/cm^3)	Pressure range (Kb)
S11	Trunin et al. (1971b)	3	1.35	119-322
S12	Trunin et al. (1971b)	2	1.35	454-552
S13	Trunin et al. (1971b)	5	1.15	65-477

Static compression data

X3	Bassett and Barnett (1970)	11		0-80

Other data

Source	Quantity	Value
Skinner (1966)	Volume coefficient of thermal expansion ($293^{o}K$)	$\alpha = 8.0 \times 10^{-6}/^{o}K$
Holm et al. (1967)	Specific heat at constant pressure ($300^{o}K$)	$C_p = 7.46 \times 10^{6}$ erg/^{o}K
Kieffer and Kamb (1972)	High temperature limit of Debye temperature	$\theta_D \approx 1170^{o}K$

TABLE 7.2 (continued)

Other coesite data (continued)

Source	Quantity	Value
Robie et al. (1966)	Density, zero pressure, 298°K	$\rho_o = 2.91$ g/cm^3
Mizutani et al. (1972)	Compression wave velocity	$V_p = 7.53$ Km/s
	Shear wave velocity	$V_s = 4.19$ Km/s
	Isentropic bulk modulus	$K_s = 0.97$ Mb

TABLE 7.3

Standard errors (Mb) assumed for the stishovite compression data.

Data	Cases 1, 2 and 4	Cases 3 and 5
S1	0.3	0.5
S2	0.2	0.2
S3	0.2	0.1
S4	0.3	0.5
S5	0.3	0.5
S6	0.6	1.0
S7	0.3	0.3
S8	1.0	0.5
S9	1.0	0.1
S10	1.0	1.0
X1	0.015	0.015
X2	0.015	0.015

TABLE 7.4

Stishovite parameters found in various cases
(standard errors due to the scatter in the data are given in parentheses).

Case	K_0 (Mb)	K_0'	(K_0K_0'')	$(\partial K_0/\partial T)_p$ (Kb/°K)	α (10^{-6}/°K)	γ_0	$\frac{d \ln \gamma}{d \ln V}$	δ_T
1	3.42	4.9	-2	-0.61	16.4*	1.61	5.7	10.9
	(.09)	(.7)	(5)	(.07)	- *	(.1)	(1.6)	(1.6)
2	3.50	3.5	-2	-0.30	12.9	1.30	3.1	6.7
	(.15)	(1.0)	(3)	(.10)	(1.3)	(.15)	(3)	(3)
3	3.55	2.8	-2	-0.20	12.0	1.22	1.9	4.7
	(.13)	(.4)	(1)	(.03)	(.5)	(.07)	(.7)	(.7)
4	3.45*	3.8	-3	-0.32	13.3	1.32	3.3	7.1
	- *	(.8)	(3)	(.10)	(1.1)	(.15)	(3)	(3)
5	3.45*	3.0	-2	-0.20	12.2	1.22	1.7	4.7
	- *	(.2)	(1)	(.02)	(.2)	(.09)	(.7)	(.7)
2a	3.57	2.1	27	-0.23	12.6	1.30	2.9	5.0
	(.19)	(1.8)	(20)	(.10)	(1.1)	(.14)	(2.5)	(2)
3a	3.50	2.2	14	-0.17	12.1	1.22	1.8	4.0
	(.16)	(1.0)	(10)	(.05)	(.6)	(.08)	(1)	(1)

* Fixed value (from Table 1).

TABLE 7.5

Standard errors (Mb) assumed for the "coesite" compression data.

Data	Error
S11	0.20
S12	0.10
S13	0.10
X3	0.02

TABLE 7.6

"Coesite" parameters for various cases.

Case	K_0 (Mb)	K_0'	$\left(\frac{\partial K_0}{\partial T}\right)_p$ *	γ	$\frac{d \ln \gamma}{d \ln V}$	δ_T
1	1.27	5.6	-0.05	0.43	-0.04	4.9
2	1.36	4.1	-0.05	0.46	1.2	4.6
3	0.97**	7.3	-0.05	0.33	-0.15	6.4

* Assumed values, see text.

** Fixed value (Table 2).

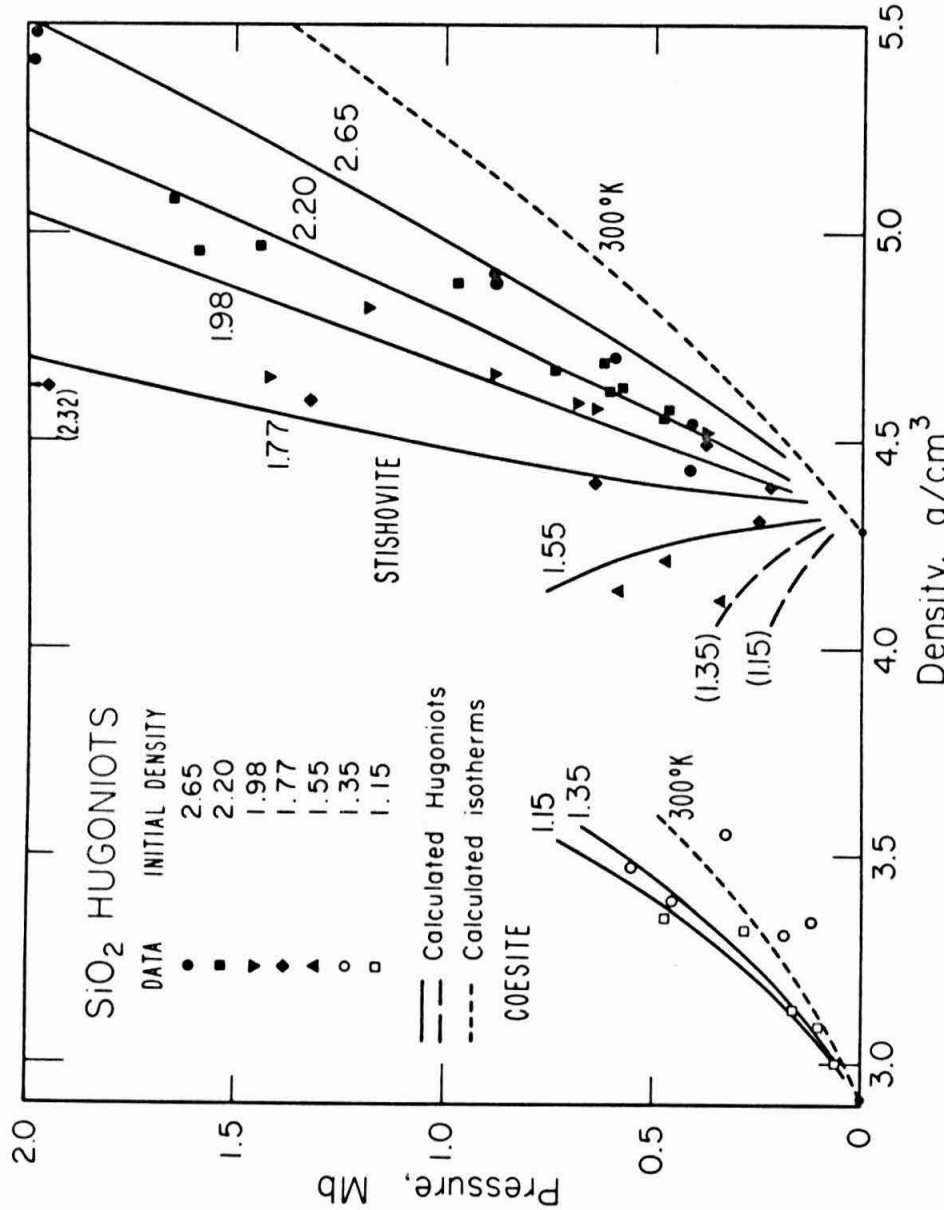

Fig. 7.1. Hugoniot data of quartz and porous quartz and calculated Hugoniots and 300°K isotherms (short-dashed) of "coesite" and stishovite. Data sources are given in Tables 7.1 and 7.2. Calculated curves are from stishovite case 2 (Table 7.4) and "coesite" case 1 (Table 7.6). Numbers labelling curves indicate the initial density of the shocked sample.

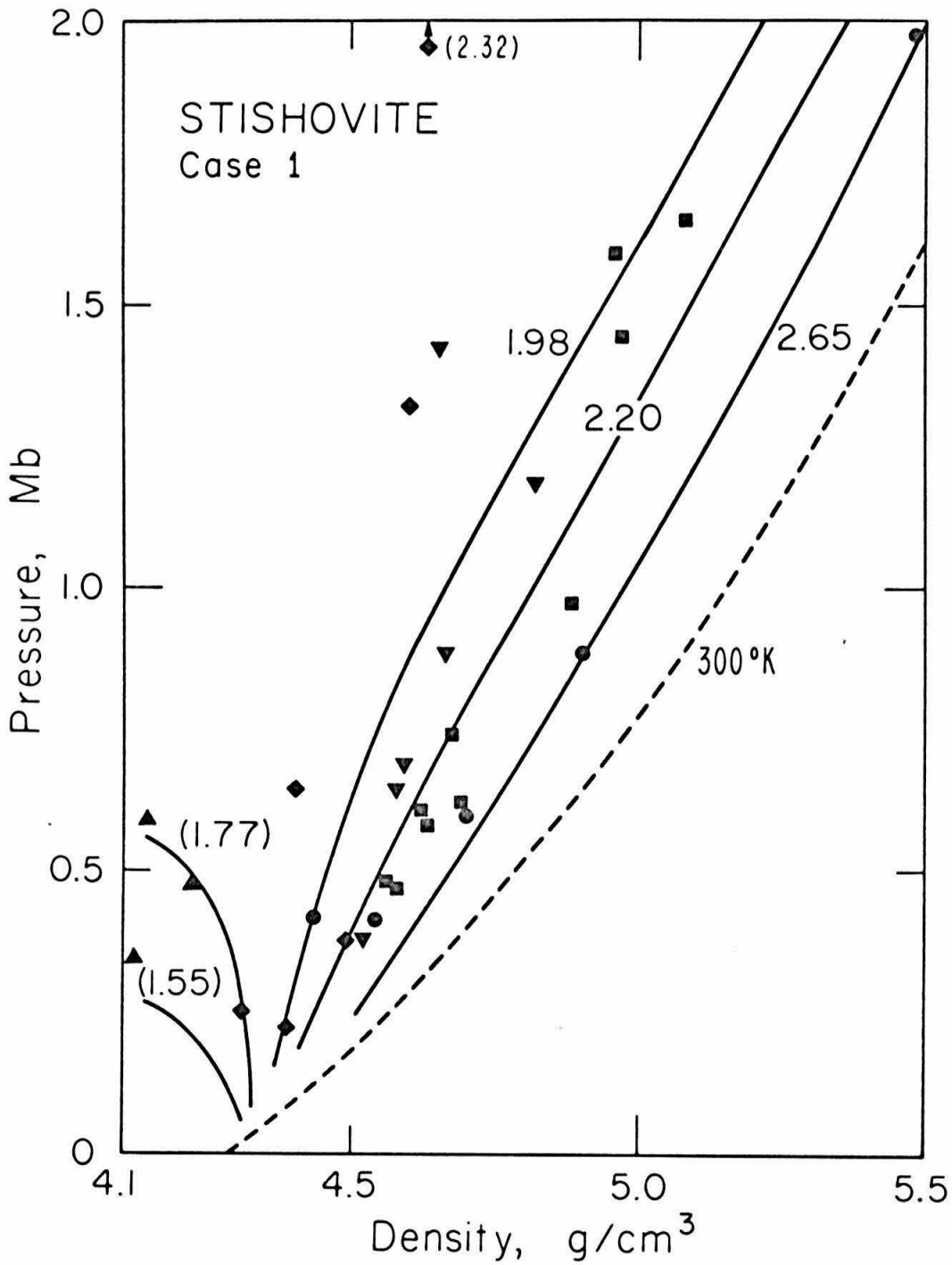

Fig. 7.2. Stishovite Hugoniot data and calculated Hugoniots and 300°K isotherm from case 1 (Table 7.4). Symbols as in Fig. 7.1.

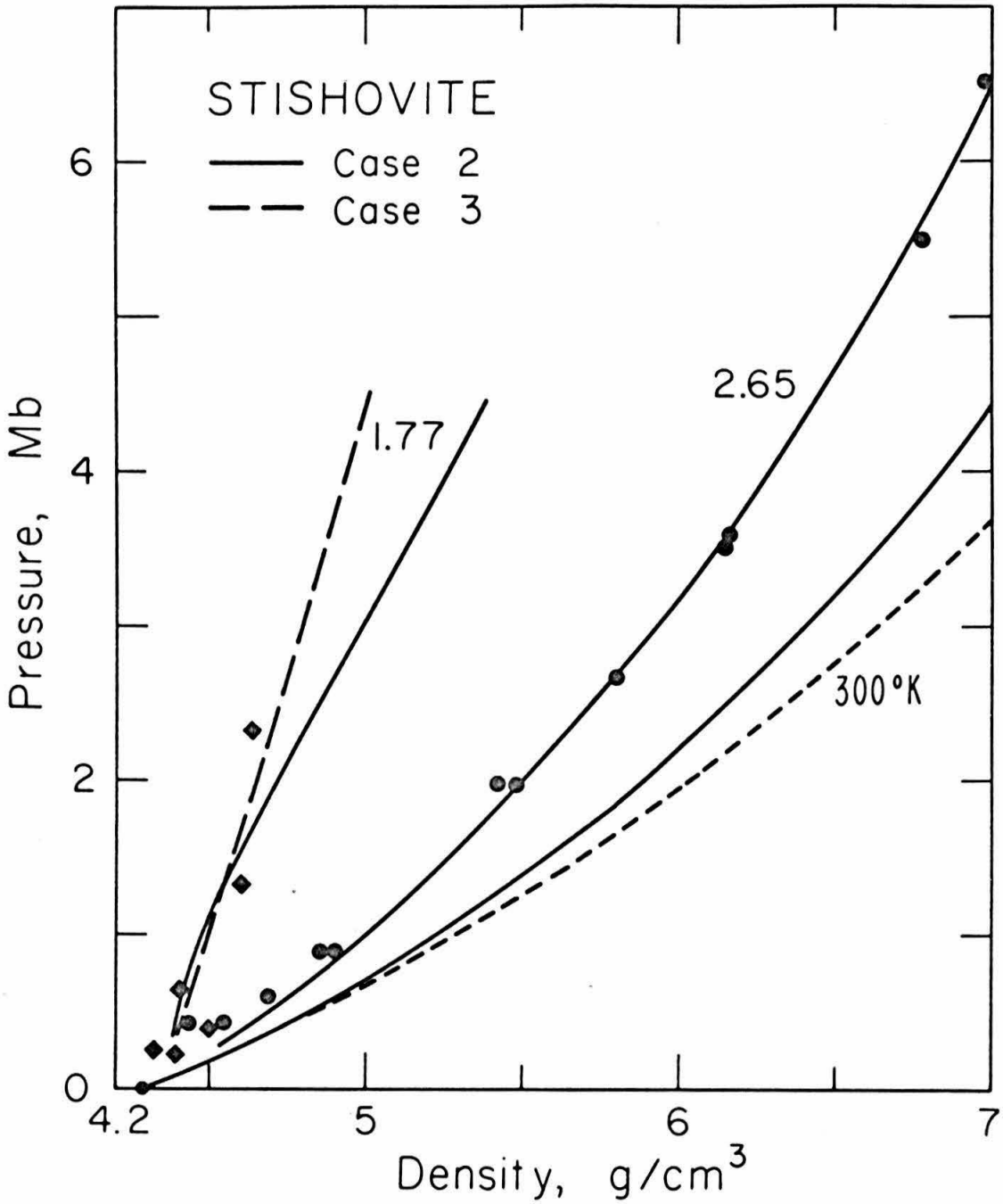

Fig. 7.3. Stishovite very high pressure Hugoniot data and calculated Hugoniots and isotherms from case 2 (solid) and case 3 (dashed). Only the Hugoniots corresponding to initial densities 2.65 and 1.77 g/cm^3 are shown. Symbols as in Fig. 7.1.

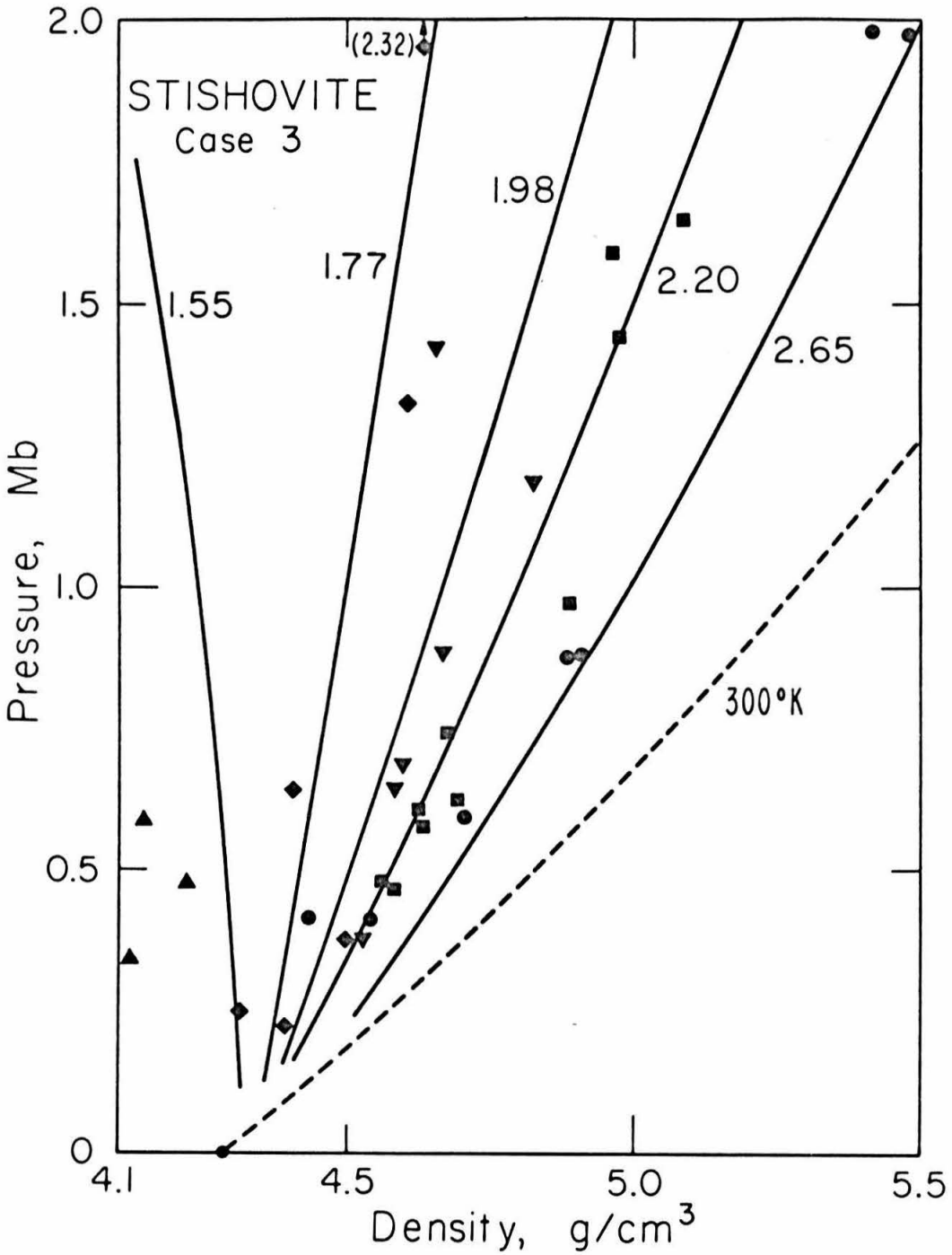

Fig. 7.4. Stishovite Hugoniot data and calculated Hugoniots and 300°K isotherm from case 3 (Table 7.4). Symbols as in Fig. 7.1.

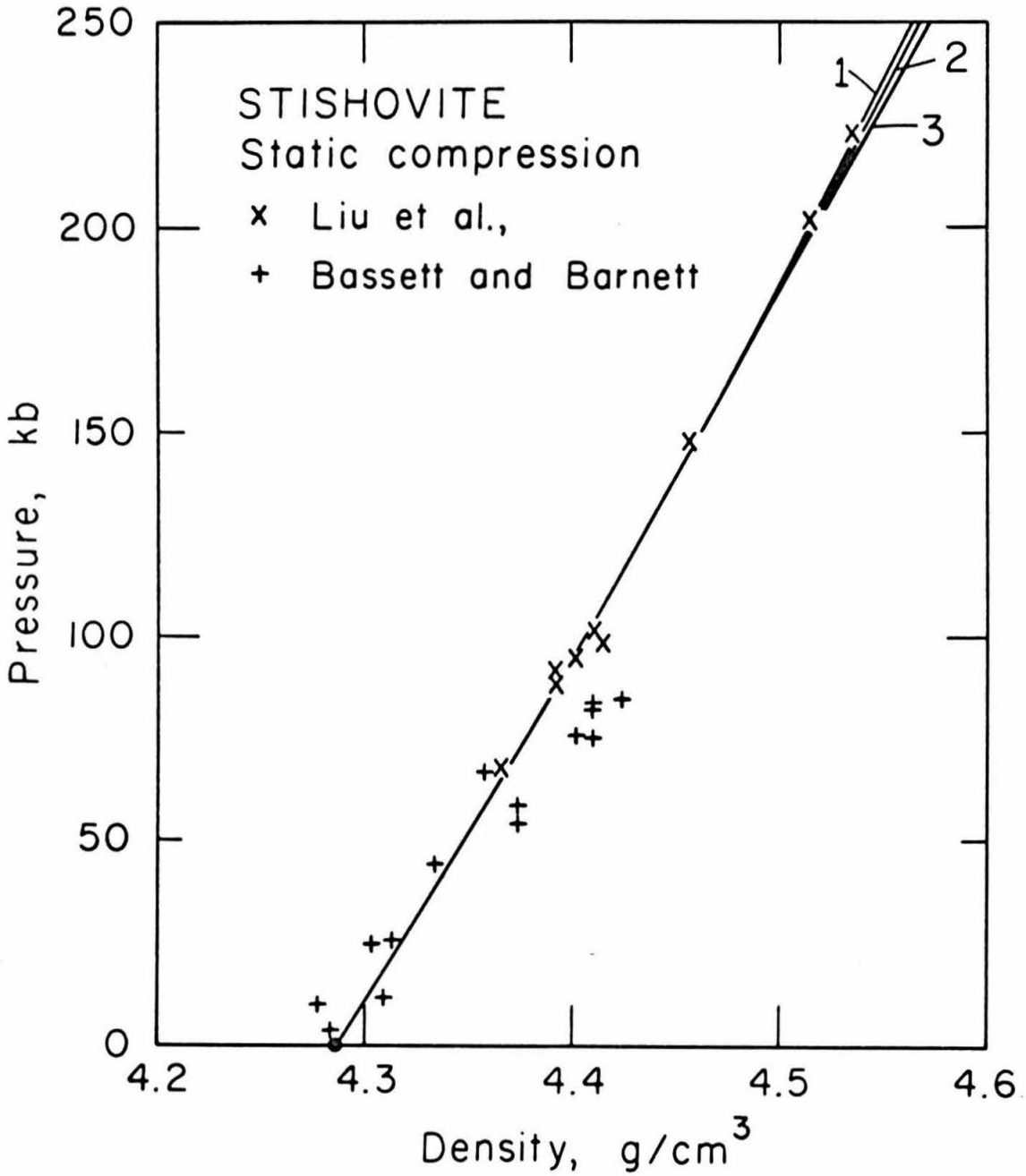

Fig. 7.5. Stishovite static compression data compared to 300°K isotherms calculated from cases 1, 2 and 3.

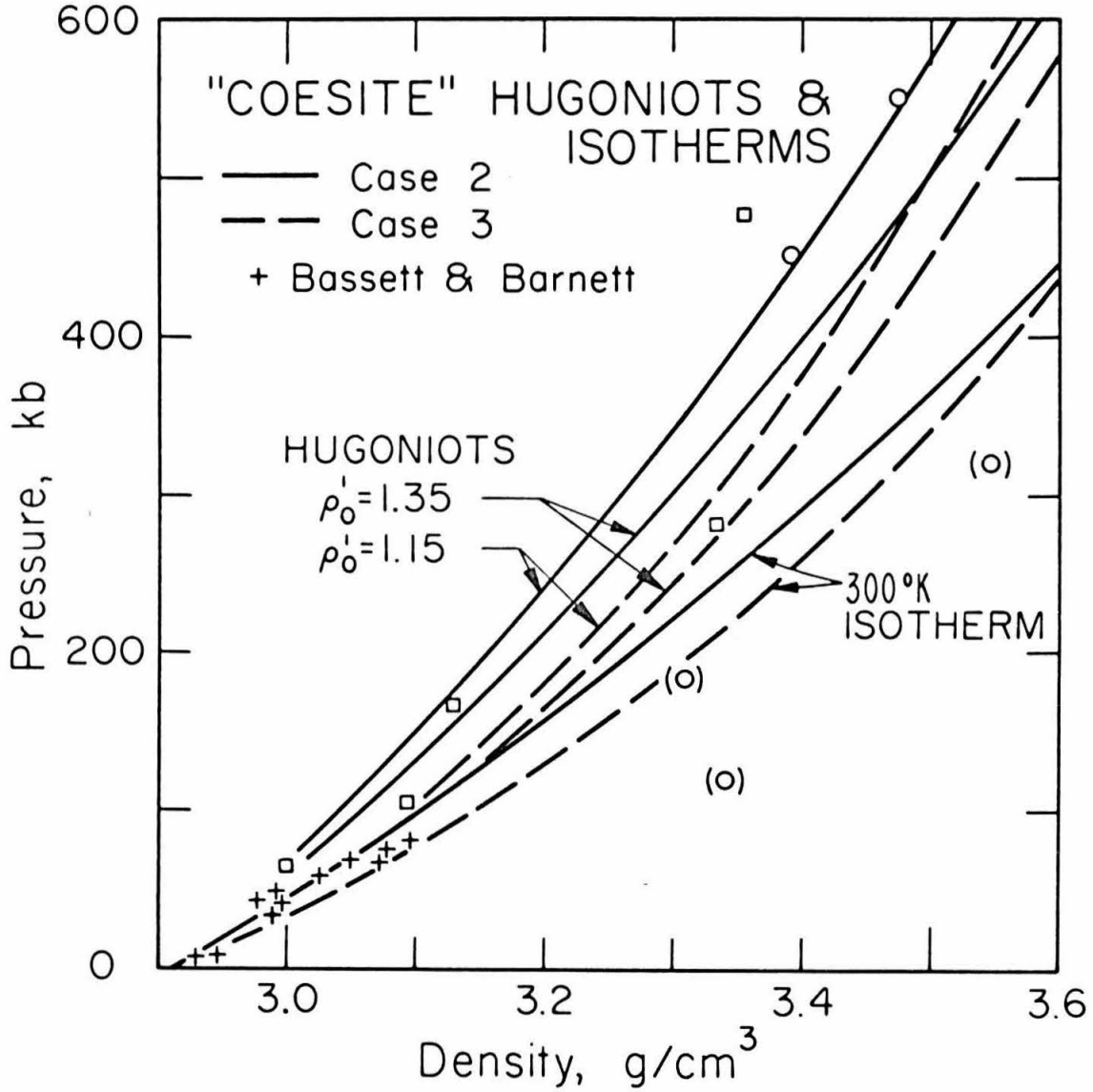

Fig. 7.6. "Coesite" Hugoniot data and calculated Hugoniots and 300°K isotherm from cases 2 and 3 (Table 7.6). Symbols as in Figs. 7.1 and 7.5.

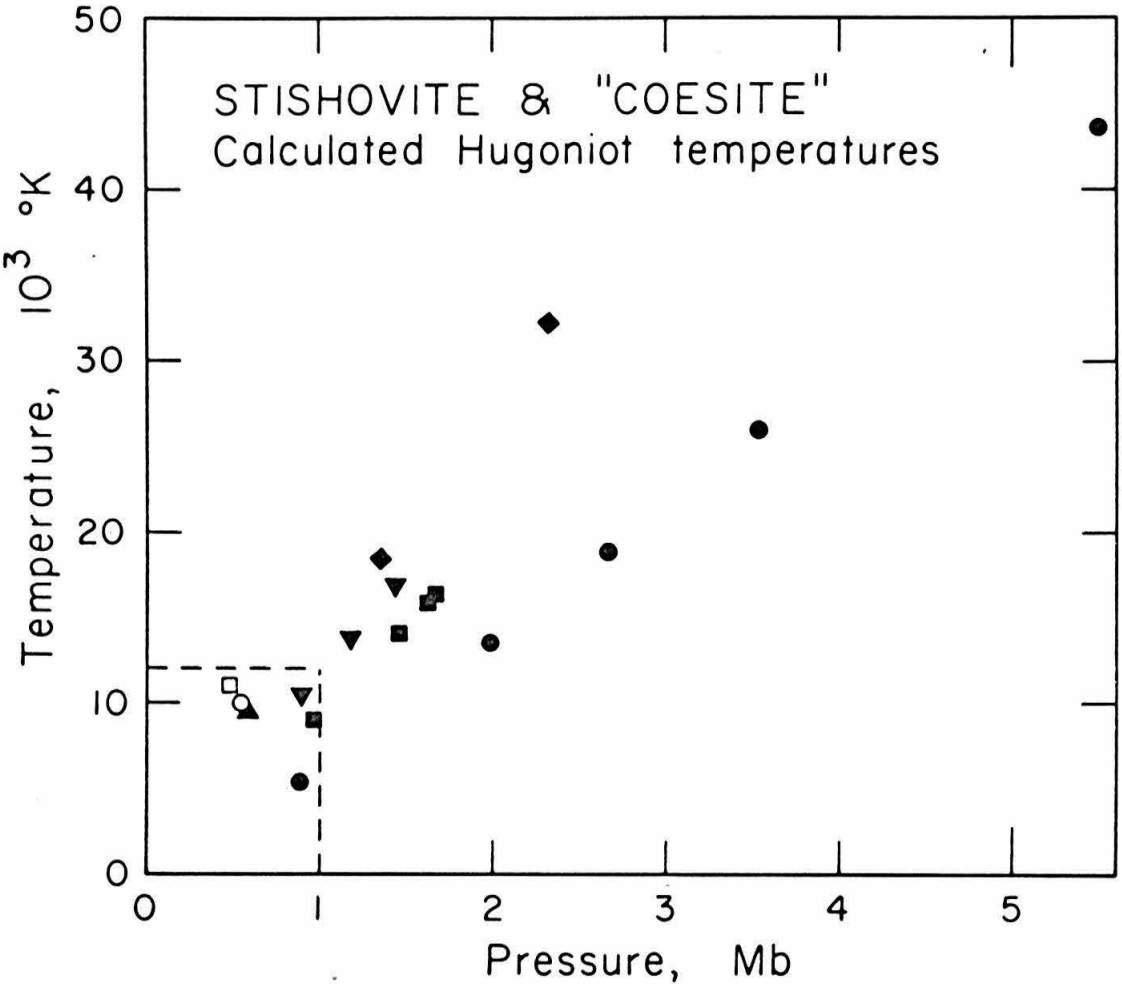

Fig. 7.7. Stishovite and "coesite" calculated Hugoniot temperatures vs Hugoniot pressure. Box is shown enlarged in Fig. 7.8. Symbols as in Fig. 7.1.

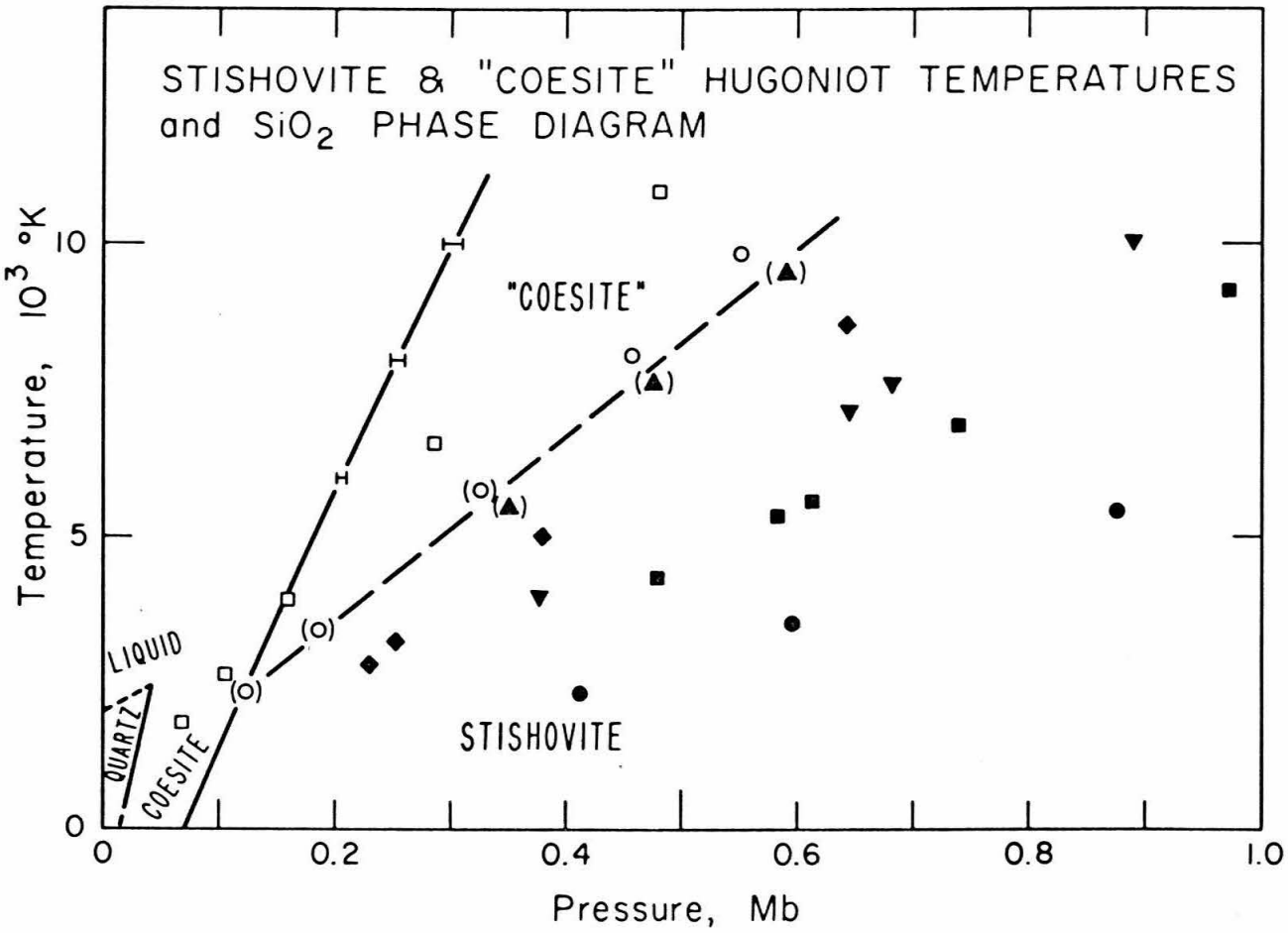

Fig. 7.8. Stishovite and "coesite" calculated Hugoniot temperatures vs Hugoniot pressure, compared with observed and calculated phase lines (solid and short-dashed). Long-dashed line separates stishovite and "coesite" fields. Symbols as in Fig. 7.1.

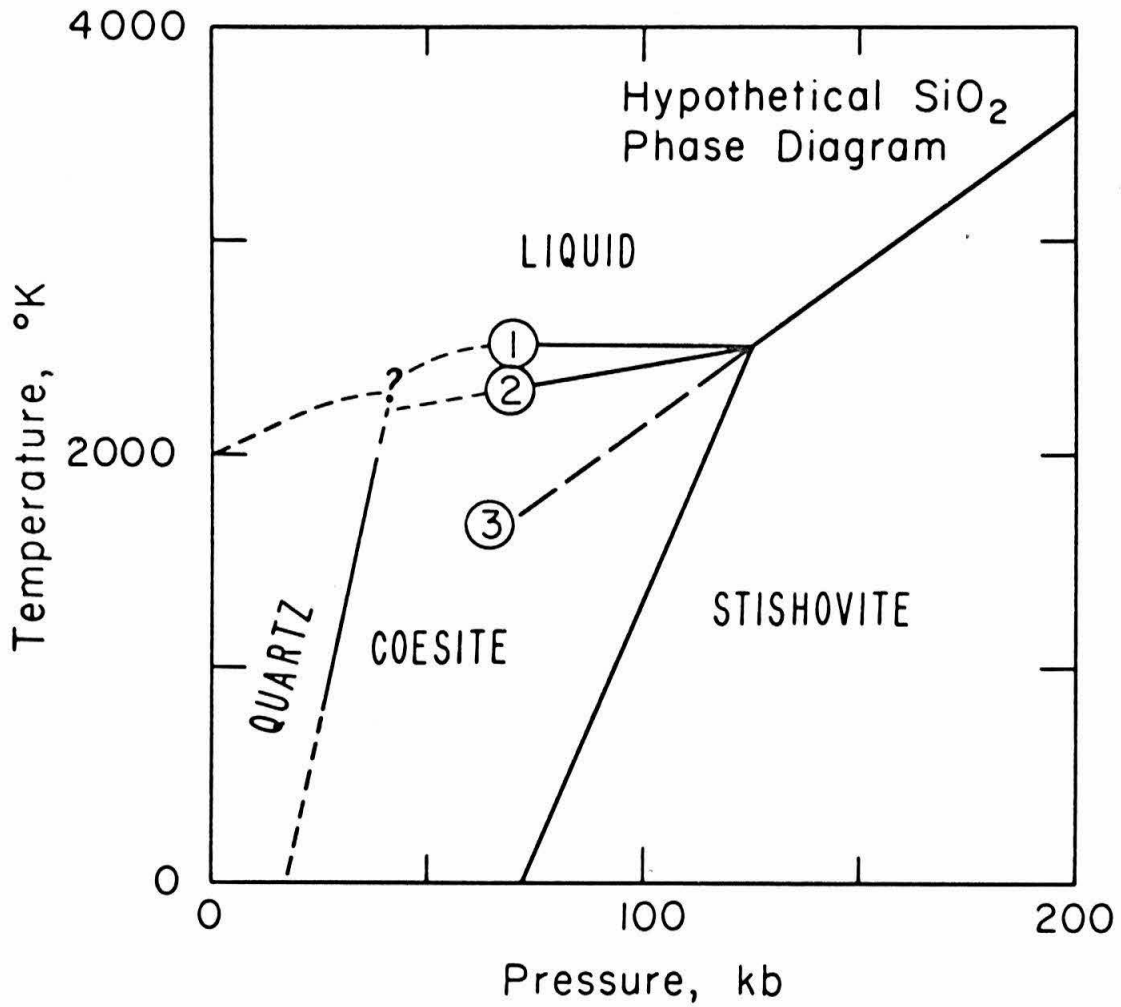

Fig. 7.9. Hypothetical silica phase diagram. Lines labelled 1, 2 and 3 correspond to different assumptions about the relative densities of coesite and the liquid (see text).

CHAPTER 8

HIGH PRESSURE AND TEMPERATURE ELASTICITY OF NaCl

Summary

The quasi-harmonic finite-strain equations for the effective elastic moduli at high pressures and temperatures are applied to the analysis of sodium chloride ultrasonic data in the pressure range 0-8 Kb and the temperature range 300°K-800°K, zero pressure thermal expansion data and Hugoniot data up to 260 Kb. The theory can give a reasonable representation of the high-temperature ultrasonic data, but systematic discrepancies, especially in the thermal expansion at high temperatures, are attributed to anharmonic effects of order higher than those included in the theory. The effect of using different strain measures on the values of derived STP parameters is demonstrated. The Hugoniot data are used to test extrapolations of the ultrasonic data. The adverse effects of using inappropriate parameters in extrapolation equations are demonstrated. Finite strain expansions in terms of the frame-indifferent analogue, $\underline{E}$, of the Eulerian strain tensor $\underline{\epsilon}$ are found to be empirically superior to expansions in terms of the Lagrangian strain, η, in this application. The Hugoniot data are used, finally, to constrain the equation of state of sodium chloride at high pressures. A 300°K

isotherm derived in this way agrees closely with some recent determinations from the same Hugoniot data and from static-compression X-ray data, but deviates slightly from others calculated from atomic force models. The accuracy of the present isotherm is estimated as 1.5% to 200 Kb, 3% at 300 Kb, with the pressure under-estimated by perhaps a few kilobars at higher pressures because of the limitations of the present thermal theory.

8.1 Introduction

The abundant high quality data which is available for sodium chloride allows a demonstration of the application of the theory developed here, a test of the approximations made in this theory, a discussion of methods of analysis of equation of state and elastic data, and an accurate determination of the sodium chloride equation of state.

The elastic properties of sodium chloride have recently been measured throughout the pressure-temperature region 0 to 8 Kb and 300 to 800°K using an ultrasonic interferometric technique (Spetzler et al., 1972). These measurements are of sufficient accuracy to determine the second pressure derivative of the elastic moduli. The elastic moduli had previously been measured at 195°K and 295°K as functions of pressure (Bartels and Schuele, 1965), and at zero pressure between 300 and 1100°K (Slagle and McKinstry, 1967). Static compression measurements using a piston displacement method have been made to 100 Kb by Bridgeman (1940, 1945) and to 45 Kb by Vaidya and Kennedy (1971). Static compression measurements using X-rays have been made by Perez-Albuerne and Drickamer (1965) to over 200 Kb. Shock compression measurements have been made by Fritz et al. (1971). The specific heat of sodium chloride has been measured by Kelley (1934) and the thermal expansion by Enck and Dommell (1965).

Sodium chloride is commonly used as a high pressure standard, so an accurate determination of its pressure-density relation is desirable. Decker (1965, 1971) and Weaver et al. (1971) have investigated the accuracy with which this can be determined. Their determinations depend critically on the values of the equation of state parameters, especially the elastic moduli and their derivatives, as well as on the functional forms assumed.

Beyond the determination of the equation of state of sodium chloride in particular, the determination of equations of state in general, and of equations of state parameters, deserves some critical comment. Ideally, a particular form of equation of state would be assumed which was capable of describing all thermo-elastic and calorimetric properties of a substance, and then all available relevant data would be used to determine any disposable parameters in this form. The resulting equation of state could then be used with maximum confidence for interpolation and extrapolation, provided that the functional form assumed was appropriate enough so that all data could be fit to within experimental error. Since the accurate calculation of equations of state of solids from fundamental quantum mechanical theory is beyond present capabilities, the functional forms to be used in the above empirical approach are not known, and appropriate forms have themselves to be determined empirically. This flexibility

in the choice of functional forms has two important practical consequences. Firstly, extrapolations based on different functional forms diverge from each other. Secondly, the values of parameters determined by the above method depend on the functional form assumed.

Common practice departs in several important respects from this ideal procedure. Firstly, data are separately analyzed and reduced to parameters as they are accumulated. Secondly, these parameters are used indiscriminately in the reduction of other, independent, data, and in various extrapolation formulae. The effect of using different functional forms on extrapolations has often been discussed (e.g., Weaver et al., 1971), but the effect of using different functional forms on the values of parameters is usually not considered. Also, the possibility of inconsistencies between the various functional forms assumed in different parts of the complete equation of state are obscured in this piecemeal approach.

Two kinds of functional forms are used in equations of state. The first kind includes those forms which have some physical basis, such as the Coulomb electrostatic potential. These, by definition, have the potential of giving insight into the physical processes involved but the disadvantage of being too inflexible if not all relevant physical processes have been considered. In this case, unrealistic values of

parameters would be obtained. The second kind includes those forms based on some kind of series expansion. These have greater flexibility and can give an accurate representation of data, but they have the disadvantage of involving, potentially, a large number of parameters and of giving no physical insight.

In the particular case of sodium chloride, Slagle and McKinstry (1967) represented their data as a polynomial of elastic moduli versus temperature. Spetzler et al. (1972) represented their data as a polynomial of frequency versus pressure and temperature, and Bartels and Schuele (1965) use a polynomial of frequency versus pressure. Vaidya and Kennedy (1971) used a polynomial of volume versus pressure, while Perez-Albuerne and Drickamer (1965) assumed a particular interatomic force model and a particular approximation to the thermal pressure. Fritz et al. (1972) used a polynomial in shock velocity versus particle velocity to represent the sodium chloride Hugoniot, and made very specific (though reasonable) assumptions, through the Grüneisen parameter, concerning the thermal pressure, to obtain an isotherm. Enck and Dommell (1965) used a polynomial of the coefficient of thermal expansion versus temperature to represent their data. In their calculations of sodium chloride isotherms, Decker (1965, 1971) and Weaver et al. (1971) assumed particular interatomic force models, various approximations for

the thermal pressure and took parameters from a variety of sources.

The theory of equations of state developed in this thesis is capable of representing all of the data discussed above. It is neither unique nor the most complete that could be used. The strain dependence is based on a polynomial of the Helmholtz free energy in terms of strain. It thus has the flexibility and lack of physical assumptions of the series expansions, discussed above, in this respect. Further, there is great flexibility in the choice of strain measures, as was discussed in previous chapters. The temperature dependence is based on a theory which, while very general in a certain sense, makes specific approximations which limit both its flexibility and the number of parameters involved. It may also give some physical insight, i.e., some indication of the validity of the approximations made.

The present application is, to the author's knowledge, the first time in which such a quantity and variety of data have been considered in terms of a single equation of state. An analysis of the ultrasonic data of Spetzler et al. (1972) is the basis of the discussion. These data determine the pressure and temperature dependence of the elastic moduli of sodium chloride. Combined with the zero pressure, room temperature value of the thermal expansion coefficient, all of the equation of state parameters are thereby determined.

The effect on the values of the parameters of using different functional forms will be illustrated by using both the "E" and "η" strain measures. Extrapolations to high pressure using these two examples will be compared and tested with Hugoniot data. These extrapolations will also be compared with those obtained by substituting the parameters of Spetzler et al. (1972) directly into the E and η equations. Calculation of the room temperature isotherm will also allow comparison with static compression data in these cases. The adequacy of the thermal part of the theory will be discussed in terms of the fit to the ultrasonic versus temperature data of both Spetzler et al. (1972) and Slagle and McKinstry (1967) and to the thermal expansion data of Enck and Dommell (1965).

8.2 Method of Analysis of Ultrasonic Data

The ultrasonic measurements of sodium chloride by Spetzler et al. (1972) consist of frequencies measured along a series of isotherms as a function of pressure up to about 8 Kb, and at zero pressure as a function of temperature. Four modes of propagation were measured. These are identified in Table 8.1. Since the four mode frequencies depend on only the three elastic moduli of sodium chloride, the three elastic moduli are overdetermined by these data.

As supplied to the author, the basic frequency data for

each mode consisted of frequency versus temperature at zero pressure normalized to the 300°K value, and frequencies versus pressure along various isotherms, the latter frequencies being arbitrary multiples of the fundamental frequency of the particular path being measured (Spetzler et al., 1972). These were normalized in the present analysis to the zero pressure, 300°K value as described below. The absolute values of the elastic moduli are fixed by the zero pressure, room temperature values of the mode sound velocities given by Spetzler et al. (1972). These, and the derived values of the elastic moduli, are given in Table 8.1.

The sound velocity, V_i, in a particular mode of propagation is related to the appropriate combination, C_i, of elastic moduli by

$$V_i = (C_i/\rho)^{1/2} , \qquad (1)$$

where ρ is density, and the resonant frequency, F_i, over a path of length L is

$$F_i = n V_i / L , \qquad (2)$$

where n is an integer. Denoting values in a reference state by subscript "o", and noting that in a crystal of cubic symmetry under hydrostatic pressure

$$L/L_o = (\rho/\rho_o)^{-1/3} , \qquad (3)$$

(1) and (2) give

$$(F/F_o)_i = (C/C_o)_i^{\frac{1}{2}} \cdot (\rho/\rho_o)^{-1/6}. \qquad (4)$$

Equation (4) thus relates the normalized frequencies to the elastic moduli and density.

The elastic moduli can be calculated according to the theory given in Chapter 5. Since, in this theory, strain (or density) and temperature are the independent variables, rather than pressure and temperature, the normalized frequencies must be calculated as follows. First the density at which the calculated pressure equals the observed pressure is determined. The elastic moduli can then be calculated at this density. The zero pressure density and elastic moduli can also be calculated as a function of temperature in this way.

Once the normalized frequencies were determined for a given isotherm, the observed frequencies were scaled so as to obtain a least-squares fit with the calculated values. Thus only the pressure derivatives of the moduli were determined at this stage.

The thermal expansion data were not included in their original density versus temperature form, but through the volume coefficient of thermal expansion given by Enck and Dommell (1965). This departs from the ideal procedure discussed in the previous section, but, on the one hand, the

data are not published in their original form, and on the other, the thermal part of the present theory is apparently not sufficient to describe them completely anyway, as will be seen. The specification of the thermal part of the theory is completed by fitting of the theory to the frequency versus temperature data, at both zero and higher pressures.

The equations were fitted to the data in a maximum likelihood sense, i.e., in a weighted least-squares sense with the weighting according to the variance of the data. Initially, all of the ultrasonic data were weighted equally, but the weighting is useful for preferentially fitting parts of the data, and for including other types of data, such as Hugoniot data, in the fitting procedure. The parameters which gave the best fit to the data were determined iteratively using an automatic computation algorithm.

8.3 Results of Analyses

It was found that not all of the ultrasonic data could be fitted within the experimental error by the present equations. Figs. 8.1 to 8.3 show the result of fitting the fourth-order "E" equations to the ultrasonic data. Fig. 8.1 shows the normalized frequency versus pressure data and the corresponding calculated curves for modes 1, 2 and 4 (Table 8.1). Fig. 8.2 shows the same for mode 3 and the normalized zero pressure frequency versus temperature data and curves.

In Fig. 8.3, the Hugoniot extrapolated from this fit is compared to the data of Fritz et al. (1972). The specification of this case is summarized in Table 8.3 as Case 1, and its parameters are given in Table 8.4. Close inspection of Figs. 8.1 and 8.2 shows that the curvature of the frequency-pressure data has not been exactly matched.

The reason for this became evident when only the low-pressure ultrasonic data in the temperature range 300°K to 500°K were allowed to constrain the temperature dependence and only the room-temperature isotherm data were allowed to constrain the pressure dependence. This case is given in Tables 8.3 and 8.4 (Case 2) and illustrated in Figs. 8.4 to 8.6. The room-temperature isotherm data are now more closely fitted, but at the expense of all of the higher temperature data. The Hugoniot extrapolated from this case is very close to the data (Fig. 8.6).

The thermal part of this theory is evidently insufficient to accurately describe the data. This can also be seen from other data. In Fig. 8.7, the elastic modulus versus temperature data of Slagle and McKinstry (1967, calculated from their polynomial fits to their data) are compared to the corresponding curves calculated from Case 2 (solid lines). The same divergence at high temperatures is evident. Also shown in Fig. 8.7 are the (dashed) curves obtained by requiring the present equations to fit all of

Spetzler et al.'s (1972) zero-pressure data. This fit is illustrated in Fig. 8.8, for the zero-pressure and mode 3 ultrasonic data, and given as Case 3 in Tables 8.3 and 8.4. It is notable that the high-pressure, high-temperature ultrasonic data are still not fit very well, but the close match between Case 3 and the data of Slagle and McKinstry (1967) demonstrates the consistency between the two data sets at zero pressure.

These cases also illustrate Thomsen's (1972) point that the elastic moduli at constant pressure are not necessarily linear in temperature, and they show the significant extent to which the temperature dependence at zero pressure depends on the pressure derivatives of the elastic moduli (Cf. Table 8.4).

The thermal expansion predicted by Case 2 was calculated, and is compared in Fig. 8.9 with the data of Enck and Dommell (1965). Since these authors gave a polynomial for the linear relative expansion coefficient, $(\partial L/\partial T)_p L_o$, where L is a dimension of the sample and L_o is its value at 298^oK, it was necessary first to integrate this to obtain $L(T)/L_o$, and then to calculate the usual linear coefficient $(\partial L/\partial T)/L$, from which the volume coefficient, $\alpha = (\partial V/\partial T)/V$, and volume expansion could be obtained. The values of α and density obtained from Case 2 deviate significantly from the data at high temperatures. Note that this error does not have very

much effect on the elastic moduli derived from the ultrasonic data, since the density enters equation (4) only in the 1/6th power. Decker (1971) also found that the thermal expansion data and the high-temperature elastic moduli data could not be simultaneously fit.

Turning now from the thermal to the "compressional" part of the theory, note that for Hugoniot extrapolations it is more important to have a good fit to the frequency-pressure data than to the frequency-temperature data, since the thermal contribution to the Hugoniot pressure at 300 Kb is found to be only about 40 Kb. Thus Case 2 is more appropriate than Cases 1 and 3 for the Hugoniot extrapolation. It has already been remarked that Case 2 gives a Hugoniot which closely approaches the data (Fig. 8.6).

In Figs. 8.10 and 8.11 and Tables 8.3 and 8.4 (Case 4), the corresponding analysis in terms of the fourth-order "η" equations is presented (only the high-pressure ultrasonic frequencies for mode 3 are illustrated since they are quite representative). The same comments apply to the thermal part of the η-equations in Case 4 as apply to Case 2 for the E-equations. The Hugoniot extrapolation is not quite so successful in this case, however (Fig. 8.11).

A stronger test of the relative empirical merits of the E and η strain measures is to use only the "third-order" form of the finite strain equations. These are given as

Cases 5 and 6, respectively in Tables 8.3 and 8.4 and Figs. 8.12 and 8.13. The third-order "E" Hugoniot, Fig. 8.12, is clearly superior to the third-order "η" Hugoniot, Fig. 8.13. The fit to the high-temperature ultrasonic data for Case 5 is similar to that for Case 2, but Case 6 fits worse than Case 4.

The isothermal extrapolations to high pressure of the effective elastic moduli are illustrated in Fig. 8.14 for Cases 2, 4, 5 and 6. The fourth-order extrapolations are reasonably close, but, curiously, the third-order E extrapolation of c_{44} deviates the most from the others, while the third-order η extrapolations of c_{11} and c_{12} deviate the most from the most from the others. E may not be superior in all situations.

The price paid for using values of parameters which are not appropriate to the equations used for extrapolation is illustrated by Cases 7 and 8, in which the parameters given by Spetzler et al. (1972) were used in the fourth-order E and η equations, respectively. The extrapolations of the effective elastic moduli are compared in Fig. 8.15. The η-extrapolations have not changed much, but the E-extrapolations have been drastically affected. Case 7 is further illustrated in Figs. 8.16 and 8.17. The Hugoniot extrapolation has also been considerably altered (Fig. 8.17), and even the high temperature data are poorly fit (Fig. 8.16).

The sharp curvature in the elastic moduli curves (Fig. 8.15) is due to the pressure varying more slowly with density at 200 Kb (Fig. 8.17).

By using the Hugoniot data as an additional constraint, rather than as a test, the equation of state of sodium chloride can be more accurately determined at high pressure. Because of the evident superiority of E as a strain measure, this was done with the fourth-order E equations, using the same set of ultrasonic data as in Case 2. The result is given as Case 9 in Tables 8.3 and 8.4. The fit to the Hugoniot data is shown in Fig. 8.18. A fuller tabulation of derived reference state quantities is given in Table 8.5 for this case, and the $300^{o}K$ isotherm is briefly tabulated in Table 8.6.

As a check on the accuracy of the thermal part of the equation of state, and hence of the derived isotherm, the Hugoniot data were combined with all of the ultrasonic data (Cf. Case 1) to determine the equation of state. This is given as Case 10 in Tables 8.3 and 8.4. The deviation of the derived isotherm from that of Case 9 is shown in Fig. 8.19. They are within about 1 Kb to pressures up to about 220 Kb. The Hugoniot data, which extend up to 264 Kb, constrain the isotherm to about 230 Kb. The Hugoniot data are fitted in Case 9 with a standard deviation of 2.5 Kb, and, in Case 10, of 2.8 Kb. Thus the error in the thermal correc-

tion from the Hugoniot to the 300°K isotherm is probably less than the error due to the scatter of the Hugoniot data. Assuming the Hugoniot data have no systematic errors, the accuracy of the isotherms given here should be about 3 Kb at 200 Kb, or about 1.5%.

8.4 Discussion

The data used here have been sufficient to test both the thermal and compressional parts of the present theory. These aspects of the theory will now be discussed.

The thermal part of the theory, i.e., the "fourth-order" anharmonic theory of Leibfried and Ludwig (1961), seems to over-estimate the anharmonic effects, as witnessed by the temperature-dependence of the elastic moduli (Fig. 8.7), and the coefficient of thermal expansion (Fig. 8.9). This is surprising, since it might be expected that the Grüneisen approximation, which may well be inaccurate below the Debye temperature, would be reasonably accurate at temperatures substantially above the Debye temperature (Leibfried and Ludwig, 1961). It is even more surprising in view of Spetzler et al.'s (1972) calculation showing the Grüneisen parameter, γ, to be almost independent of temperature at constant volume and high temperatures, as predicted by the fourth-order theory - this calculation, however, appears to be in error because they used incorrect values for the specific heat.

Their tabulated zero-pressure values of the specific heats at constant pressure and at constant volume, C_p and C_V, respectively, are plotted in Fig. 8.20, along with the data for C_p of Kelley (1934). At high temperatures, their values of C_V decrease, rather than approaching the Dulong-Petit value of 0.854 J/g ^{o}K. Also shown in Fig. 8.20 are the values of C_V obtained from the Debye model (used in this study) and from the C_p data. These are in quite close agreement.

When the specific heats of Kelley (1934) are used to calculate γ as a function of temperature, it is found that γ is almost constant at zero pressure (Fig. 8.21). This contrasts with the conclusion of Spetzler et al. (1972) that there is an increase in γ at zero pressure because of the decrease in density (Fig. 8.21). It also implies that γ decreases substantially as temperature increases at constant volume, contrary to the prediction of the fourth-order theory, the assumption of the Mie-Grüneisen equation, and the volume-only dependence of γ derived here (Fig. 8.21).

The most likely explanation of this behaviour may be that anharmonic effects of order higher than the fourth are large, and partly cancel the lower-order effects. Thus a higher-order, and substantially more difficult, theory may be required. Another possibility, that thermally induced lattice defects may be affecting the results, seems unlikely. This possibility was invoked by Enck and Dommell (1965) to

explain what appeared to them to be a too rapid increase of the thermal expansion coefficient. Thermally induced Schottky defects have been invoked to explain the conductivity of sodium chloride (Eitzel and Maurer, 1950), but it was shown by Fischmeister (1956) that there was no detectable difference between the macroscopic and microscopic thermal expansion coefficients, and in any case, the effect would be in the wrong direction to explain the present discrepancies (i.e., defects would increase the thermal expansion).

The ultrasonic data of Spetzler et al. (1972) yield non-zero values of $(\partial^2 c_{\alpha\beta}/\partial P \partial T)$, as can be seen directly from the data, e.g., in Figs. 8.1 and 8.2. As discussed in Chapters 3 and 5, this does not necessarily imply that a higher-order theory is required. This claim was made by Thomsen (1970, 1972), and repeated by Spetzler et al. (1972). The only strong evidence that a higher-order theory is required is the temperature-dependence of γ discussed above.

Compressional effects in sodium chloride seem to be described better in terms of E than in terms of η, as was found for MgO in Chapter 6. The extrapolation of c_{44} seems to be an exception to this. The empirical tests of E and η in this Chapter are superior to those of Chapter 6, since the ultrasonic data were extrapolated directly, rather than by using parameters derived by other methods. The faster convergence of expansions in terms of E can be seen by com-

paring the primary equation of state coefficients, $r^n_{\alpha\beta}$ and $t^n_{\alpha\beta}$, which are tabulated in Table 8.5 ($r^n_{\alpha\beta}$, Case 9) and Table 8.7 ($t^n_{\alpha\beta}$, Case 4). The $t^n_{\alpha\beta}$ increase much more rapidly with n than do the $r^n_{\alpha\beta}$.

The perils of using inappropriate parameters in extrapolation equations are most graphically demonstrated by Case 7, in which the parameters of Spetzler et al. (1972) were used in the fourth-order E equations (Figs. 8.15, 8.17). This is not meant to imply that the parameters of Spetzler et al. (1972) are wrong, or inaccurate. In fact, they are probably more accurate at STP than those derived here, since a more flexible equation was used to derive them. However, a less flexible equation would tend to average over the range of the data, so that a median value (say at 4 Kb) rather than an extremal value (zero pressure) would be more appropriate.

The fourth-order extrapolations of the effective elastic moduli (Fig. 8.14) do not predict the vanishing of c_{44} near the pressure at which sodium chloride transforms to the cesium chloride structure (300 Kb, Bassett et al., 1968). The finite strain extrapolation by Thomsen (1972) and the lattice models of Sammis (1971; Spetzler et al., 1972) both predict that c_{44} vanishes in the range 300 to 500 Kb. The present extrapolations differ from that of Thomsen (1972) in the terms retained in the expansion of the pressure enter-

ing the expressions for the effective elastic moduli (Chapter 5, equations 35, 36 and 40). Here, the pressure term was truncated after the second-order strain terms (in the "fourth-order" case), to match the truncation of the first term in these equations. Thomsen (1972), on the other hand, included third-order strain terms in the pressure, thus taking the two terms in the effective elastic moduli to different orders in strain. The highest-order strain term is thus incomplete, and the extrapolation may be less accurate as a result.

The most preferable of the present analyses, Case 9, summarized in Table 8.5, is most deficient in the thermal part of the theory, as discussed above. (Note that the elastic moduli, Tables 8.2 and 8.5, were determined as the least-squares fit to the four mode velocities given in Table 8.1. These values differ slightly from those of Spetzler et al., 1972.)

Several other recent determinations of the room temperature isotherm of sodium chloride are compared with that of Cases 9 and 10 in Fig. 8.19. Those of Decker (1971) and Weaver et al. (1971) are significantly below the Case 9 isotherm, while those of Perez-Albuerne and Drickamer (1965) and Fritz et al. (1971) agree within 1 Kb to over 200 Kb. Case 9 was derived from the Hugoniot data of Fritz et al. (1971), and those authors assumed a volume dependence of

very similar to that obtained here (Fig. 8.21) to derive their isotherm, so the agreement is to be expected. Although it was shown by Weaver (1971) that the equations of state of Weaver et al. (1971) and Decker (1971) give reasonable agreement with the combined Hugoniot data of several authors, the data of Fritz et al. (1971) have the least scatter of any set, and they are not fit very well by their equations. The possibility of systematic error in the lowest Hugoniot points of Fritz et al. (1971), suggested by Weaver (1971), due to shear strength effects, would probably have very little effect on the present results. It can be seen in Fig. 8.18 that these data are slightly above the fitted Hugoniot curve, and that they are not fit any better than in Case 2 (Fig. 8.6), for instance. The differences between the Case 9 isotherm and those of Weaver et al. (1971) and Decker (1971) is probably due to the functional forms assumed by them for the inter-atomic potentials. Those forms would appear to be slightly less successful, empirically, than the expansion in terms of E.

At lower pressures, the Case 9 isotherm fits the static compression data of Bridgeman (1945) better than the data of Vaidya and Kennedy (1971). The "fixed points" corresponding to the Bi I-II, Ba I-II and Bi III-IV phase transitions are fit within the error of their determination (Jeffery et al., 1966).

Finally, the apparent temperature dependence of the Grüneisen parameter indicated by the data may mean that γ has been over-estimated here. The isothermal pressure would then have been underestimated, especially at higher pressures, where greater thermal corrections from the Hugoniot are involved. This error would be of the order of a few kilobars.

8.5 References

BARRON T. H. K., LEADBETTER A. J. and MORRISON J. A., Proc. Roy. Soc. A279, 62 (1964).

BARTELS R. A. and SCHUELE D. E. , J. Phys. Chem. Solids 26, 537 (1965).

BASSETT W. A., TAKAHASHI T., MAO H. and WEAVER J. S., J. Appl. Phys. 39, 319 (1968).

BRIDGEMAN P. W., Proc. Am. Acad. Arts Sci. 74, 21 (1940).

BRIDGEMAN P. W., Proc. Am. Acad. Arts Sci. 76, 1 (1945).

DECKER D. L., J. Appl. Phys. 36, 157 (1965); 37, 5012 (1966).

DECKER D. L., J. Appl. Phys. 42, 3239 (1971).

EITZEL H. W. and MAURER R. J., J. Chem. Phys. 18, 1003 (1950).

ENCK F. D. and DOMMELL J. G., J. Appl. Phys. 36, 839 (1965).

FISCHMEISTER H. F., Acta Cryst. 9, 416 (1956).

FRITZ J. N., MARSH S. P., CARTER W. J. and McQUEEN R. G., in Accurate Characterization of the High Pressure Environment (Edited by E. C. Lloyd), N.B.S. Special Publication 326, U. S. Dept. of Commerce (1971).

JEFFERY R. N., BARNETT J. D., VANFLEET H. B. and HALL H. T., J. Appl. Phys. 37, 3172 (1966).

KELLEY K. K., Bull. U. S. Bur. Mines No. 371 (1934).

LEIBFRIED G. and LUDWIG W., Solid State Physics 12, 275, Academic Press, New York (1961).

PEREZ-ALBUERNE E. A. and DRICKAMER H. G., J. Chem. Phys. 43, 1381 (1965).

POWELL D. G. and FLETCHER G. C., Aust. J. Phys. 18, 205 (1965).

SAMMIS C. G., Ph. D. Thesis, California Institute of Technology, Pasadena (1971).

SLAGLE O. D. and McKINSTRY H. A., J. Appl. Phys. 38, 437 (1967).

SPETZLER H., J. Geophys. Res. 75, 2073 (1970).

SPETZLER H., SAMMIS C. G. and O'CONNELL R. J., J. Phys. Chem. Solids 33, 1727 (1972).

THOMSEN L., J. Phys. Chem. Solids 31, 2003 (1970).

THOMSEN L., J. Phys. Chem. Solids 33, 363 (1972).

VAIDYA S. N. and KENNEDY G. C., J. Phys. Chem. Solids 32, 951 (1971).

WEAVER J. S., in Accurate Characterization of the High-Pressure Environment (Edited by E. C. Lloyd), N.B.S. Special Publication 326, U. S. Dept. of Commerce (1971).

WEAVER J. S., TAKAHASHI T. and BASSETT W. A., in Accurate Characterization of the High-Pressure Environment (Edited by E. C. Lloyd), N.B.S. Special Publication 326, U. S. Dept. of Commerce (1971).

TABLE 8.1

Mode of propagation specifications and velocities and elastic moduli at room temperature and atmospheric pressure.

Mode	Velocity formula	Direction of propagation	Direction of particle motion	V_i^o (Km/sec)	$C_i^o = \rho_o (V_i^o)^2$ (Mb)
1	$V_1 = (c_{11}/\rho)^{\frac{1}{2}}$	(100)	(100)	4.786	0.4957
2	$V_2 = (c_{44}/\rho)^{\frac{1}{2}}$	(100)	(011)	2.434	0.1282
3	$V_3 = [(c_{11} - c_{12})/2\rho]^{\frac{1}{2}}$	(011)	$(0\bar{1}1)$	2.906	0.1827
4	$V_4 = [(c_{11} + c_{12} + 2c_{44})/2\rho]^{\frac{1}{2}}$	(011)	(011)	4.503	0.4388

TABLE 8.2

Fixed sodium chloride equation of state parameters at room temperature, atmospheric pressure.

Density[a]	$\rho_0 = 2.164$ g/cm^3
Volume coefficient of thermal expansion[b]	$\alpha = 119.5 \times 10^{-6}/^oK$
Debye temperature[c]	$\theta_D = 280^oK$
Mean atomic weight	$\bar{M} = 29.22$
Elastic moduli[d] (isentropic)	$c_{11} = 0.4951$ Mb
	$c_{12} = 0.1285$ Mb
	$c_{44} = 0.1276$ Mb
	$K = 0.2507$ Mb
Specific heat at constant pressure[e]	$C_p = 8.63 \times 10^6$ erg/g^oK

a) Rubin et al. (1961).
b) Enck and Dommell (1965).
c) from C_p.
d) Spetzler et al. (1972) (see text).
e) Barron et al. (1964); Kelley (1934).

TABLE 8.3

Specifications of different analyses of sodium chloride data. Data fitted in each case are denoted by "X".

Case	Data Set					Strain Measure
	Ultrasonic				Hugoniot	
	$P = 0$ $T<500^{\circ}K$	$P = 0$ $T>500^{\circ}K$	$P \geq 0$ $T\approx300^{\circ}K$	$P > 0$ $T>300^{\circ}K$		
1	X	X	X	X	-	E
2, 5	X	-	X	-	-	E
3	X	X	X	-	-	E
4, 6	X	-	X	-	-	η
7*	-	-	-	-	-	E
8*	-	-	-	-	-	η
9	X	-	X	-	X	E
10	X	X	X	X	X	E

* Parameters of Spetzler et al. (1972) used.

TABLE 8.4

Sodium chloride parameters evaluated in various cases (at 300°K, zero pressure). Moduli are isentropic unless denoted isothermal.

	Case 1	2	3	4	5	6	7, 8	9	10
c'_{11}*	10.90	11.32	10.49	11.29	11.22	12.09	11.65	11.46	10.78
c'_{12}*	2.10	2.02	2.23	2.00	1.97	2.11	2.05	2.13	1.91
c'_{44}*	0.37	0.37	0.38	0.39	0.42	0.39	0.37	0.36	0.38
K'_s*	5.04	5.12	4.98	5.09	5.05	5.44	5.25	5.24	4.87
$K_T c''_{11}$	25.5	-22.6	32.0	-20.0	(-13.0)+	(-90.4)+	-37.2	-25.2	22.5
$K_T c''_{12}$	-12.8	-4.8	-21.2	-4.8	(-3.2)	(-8.1)	-10.2	-3.2	-21.7
$K_T c''_{44}$	-3.0	-2.5	-3.0	-3.6	(-3.9)	(-9.7)	-2.1	-2.1	-2.3
$K_T K''_T$	0.0	-10.7	-3.4	-9.9	(-6.5)	(-35.5)	-19.2	-10.5	-6.9
$(\partial c_{11}/\partial T)_p$**	-.363	-.360	-.366	-.360	-.361	-.346	-.381	-.364	-.360
$(\partial c_{12}/\partial T)_p$**	.011	.016	.018	.016	.016	.019	.024	.014	.018
$(\partial c_{44}/\partial T)_p$**	-.033	-.033	-.032	-.033	-.032	-.033	-.030	-.033	-.033
$(\partial K_s/\partial T)_p$**	-.114	-.110	-.110	-.110	-.110	-.103	-.111	-.112	-.108

* megabars. ** kilobars/°K. + Determined from 3rd-order equations.

TABLE 8.5

Derived sodium chloride parameters[+] at 300°K, zero pressure, from Case 9.

$\gamma_0 = 1.608$ $\quad g = -9.65$ $\quad \lambda = \alpha K_T = 2.84 \times 10^{-2}$ Kb/°K

	(α,β) 11	12	44	Bulk
$c^S_{\alpha\beta}$ (Mb)	.495	.128	.128	.251
$c^T_{\alpha\beta}$ (Mb)	.481	.115	.128	.237
$(\partial c^S_{\alpha\beta}/\partial P)_T$	11.46	2.13	0.36	5.24
$(\partial c^T_{\alpha\beta}/\partial P)_T$	11.56	2.23	0.36	5.34
$(\partial c^S_{\alpha\beta}/\partial T)_P$ (Kb/°K)	-.364	.014	-.033	-.112
$(\partial c^T_{\alpha\beta}/\partial T)_P$ (Kb/°K)	-.417	-.039	-.033	-.165
$K_T(\partial^2 c^T_{\alpha\beta}/\partial P^2)_T$*	-25.2	-3.2	-2.1	-10.5
$\delta^T_{\alpha\beta}$	14.65	1.37	1.16	5.80
$d \ln \gamma_{\alpha\beta} / d \ln V$	3.95	0	0.81	1.32
$h_{\alpha\beta}$	0.86	10.34	-0.99	64.6
$r^0_{\alpha\beta}$ (Mb)**	.223	.053	.059	.986
$r^1_{\alpha\beta}$ (Mb)	-1.26	-0.03	0.62	-1.98
$r^2_{\alpha\beta}$ (Mb)	-10.75	0.17	1.65	-5.20

+ All quantities are defined in Chapters 3 and 5.

* This was assumed equal to the derivative of $c^S_{\alpha\beta}$.

** See Chapter 5, equations (80-82) for definitions of bulk quantities.

TABLE 8.6

300^{0}K sodium chloride isotherm and the Grüneisen parameter from Case 9.

ρ (g/cm^3)	γ	P (Kb)
2.163	1.651	0
2.3	1.516	17
2.4	1.428	32
2.5	1.348	50
2.6	1.277	70
2.7	1.214	92
2.8	1.157	117
2.9	1.105	144
3.0	1.059	174
3.1	1.017	206
3.2	0.978	240
3.3	0.943	277
3.4	0.911	316

TABLE 8.7

Primary equation of state parameters from Case 4 (η).

	(α,β) 11	12	44	Bulk
$t^0_{\alpha\beta}$ (Mb)	.222	.053	.059	.985
$t^1_{\alpha\beta}$ (Mb)	-4.29	-0.42	-0.51	-7.70
$t^2_{\alpha\beta}$ (Mb)	60.90	2.63	5.61	33.08

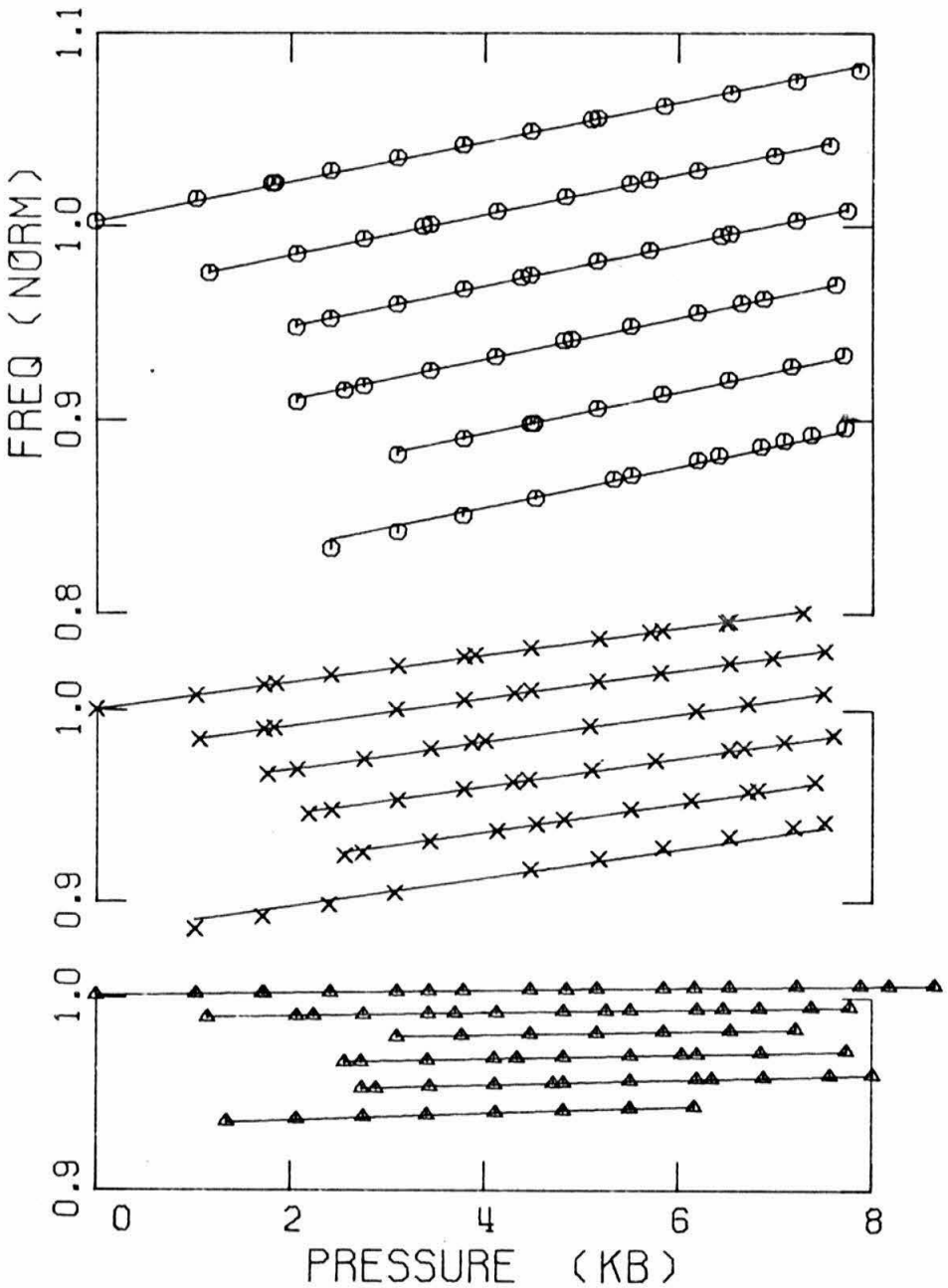

Fig. 8.1. Normalized sodium chloride ultrasonic frequency-pressure data of Spetzler et al. (1972) (symbols) compared with fitted theoretical curves from Case 1. Modes 1, 4 and 2 (top to bottom) and room-temperature to 800°K isotherms, at 100°K intervals (upper to lower) are shown.

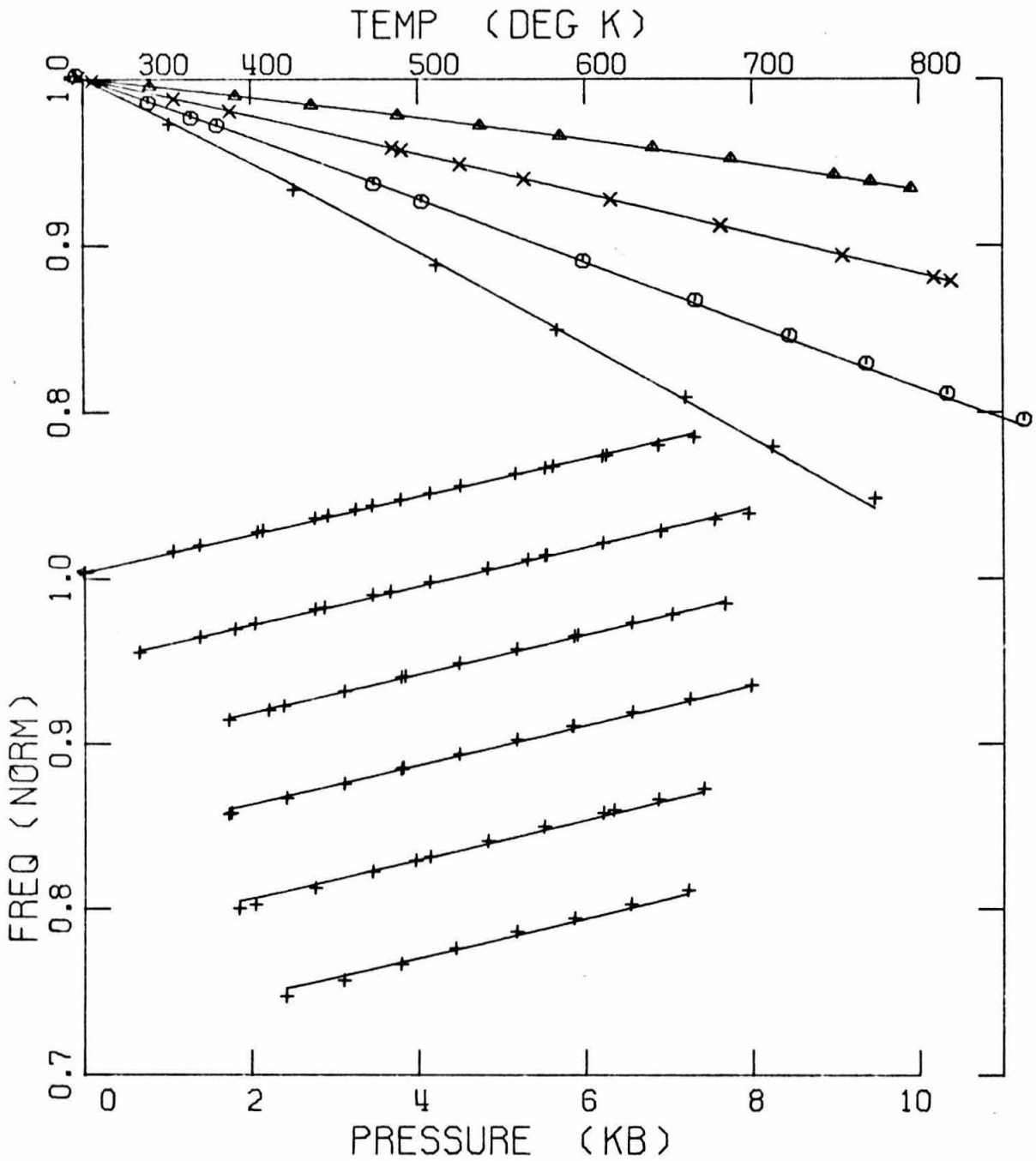

Fig. 8.2. Normalized ultrasonic data (symbols) and fitted curves from Case 1. Frequency-pressure data are for mode 3. Symbols in zero-pressure frequency-temperature data denote different modes and correspond to those for frequency-pressure data (Cf. Fig. 8.1).

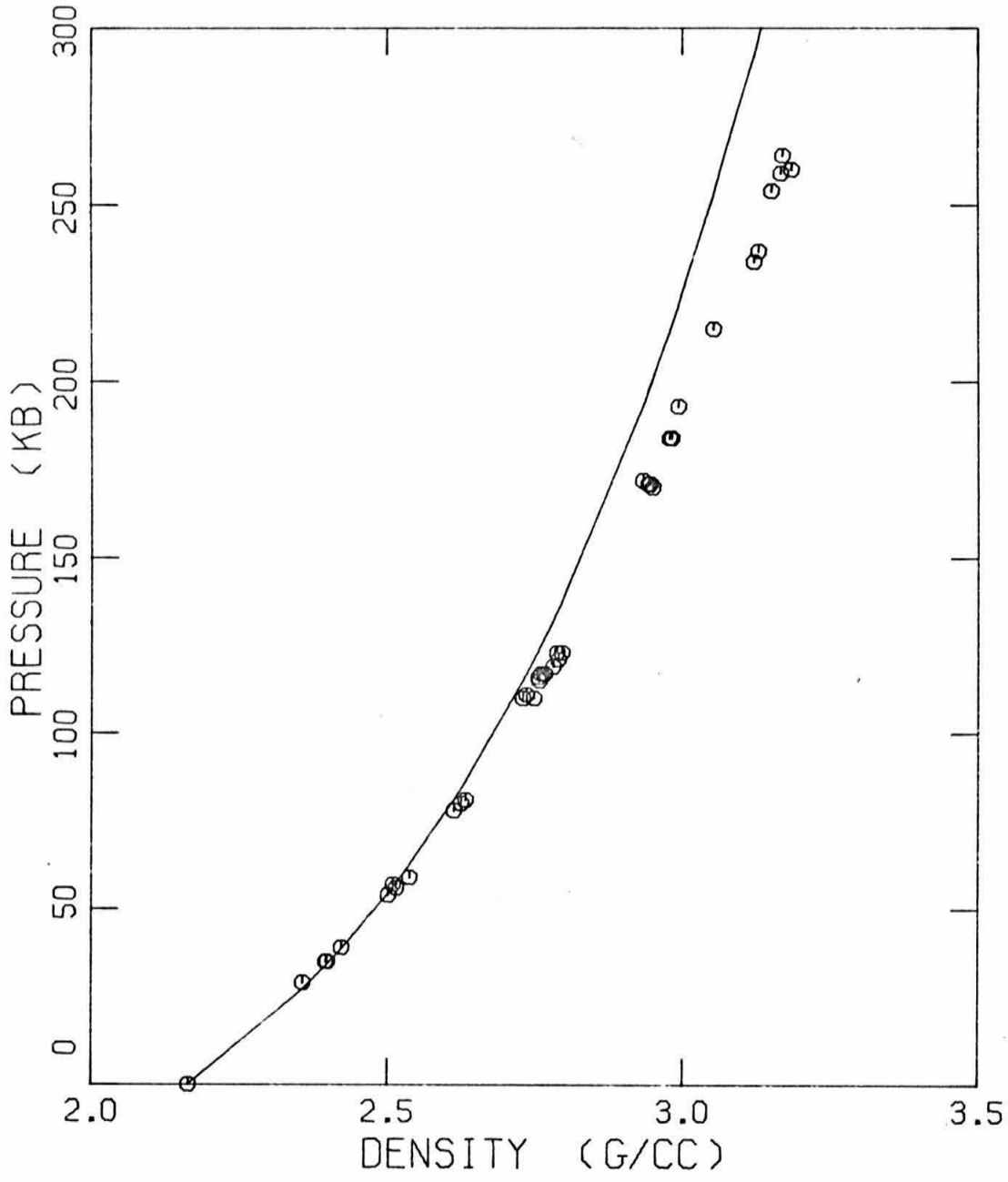

Fig. 8.3. Sodium chloride Hugoniot data of Fritz et al. (1971) (circles) compared with theoretical Hugoniot curve extrapolated from Case 1.

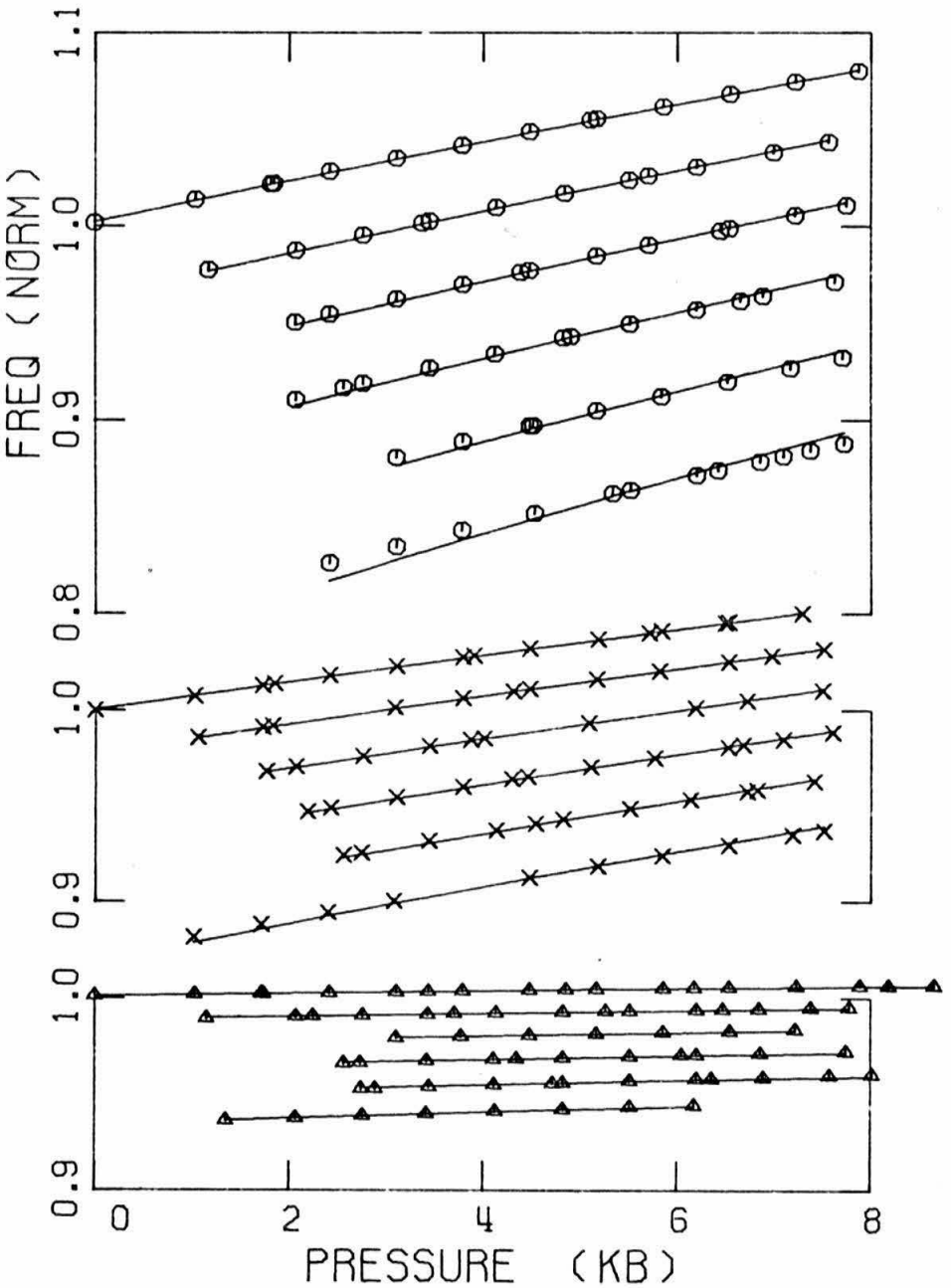

Fig. 8.4. Sodium chloride ultrasonic data for modes 1, 2 and 4 compared with curves from Case 2. Symbols and format as in Fig. 8.1.

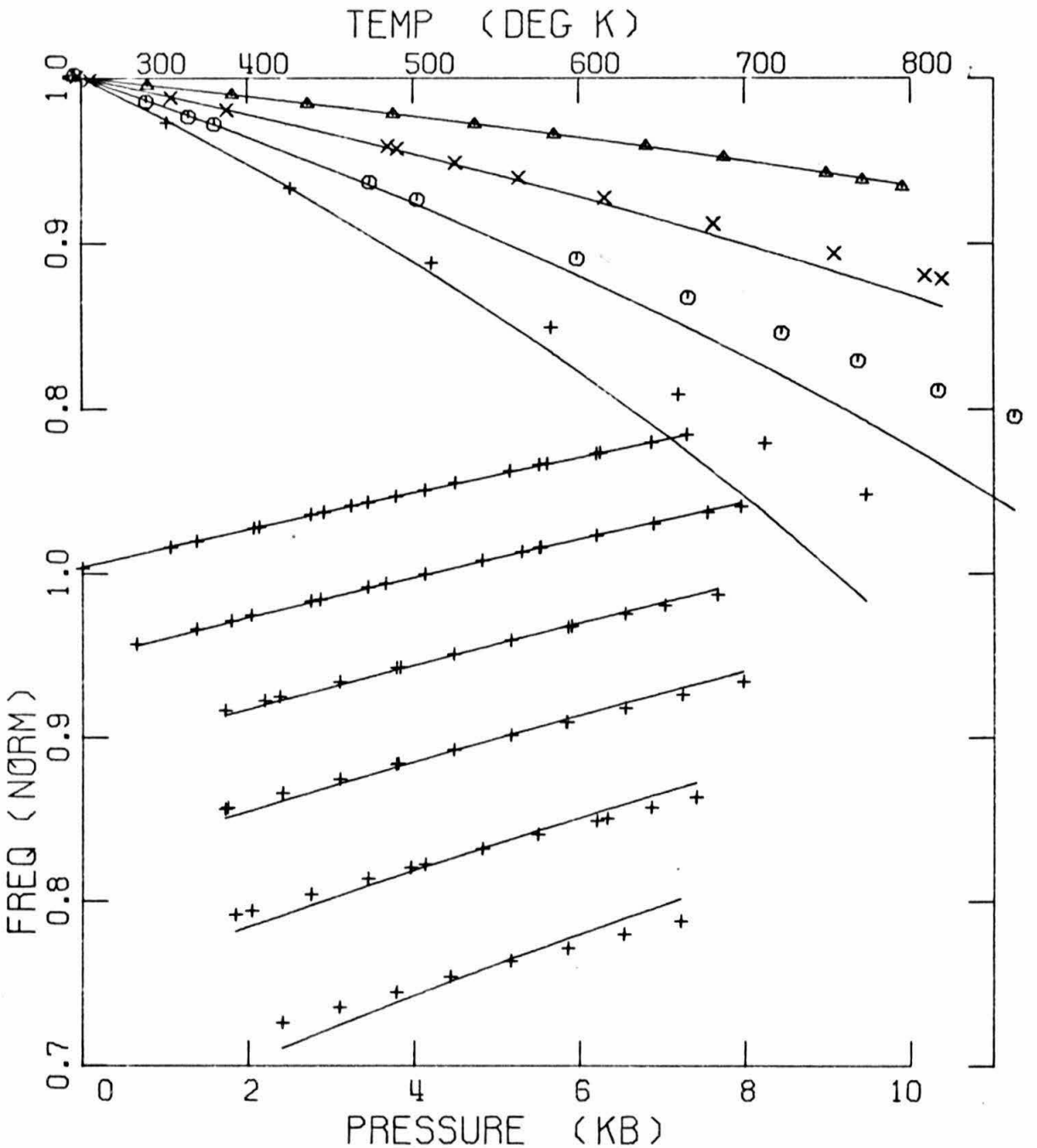

Fig. 8.5. Ultrasonic zero pressure frequency-temperature and mode 3 frequency-pressure data compared with curves from Case 2. Symbols as in Figs. 8.1 and 8.2.

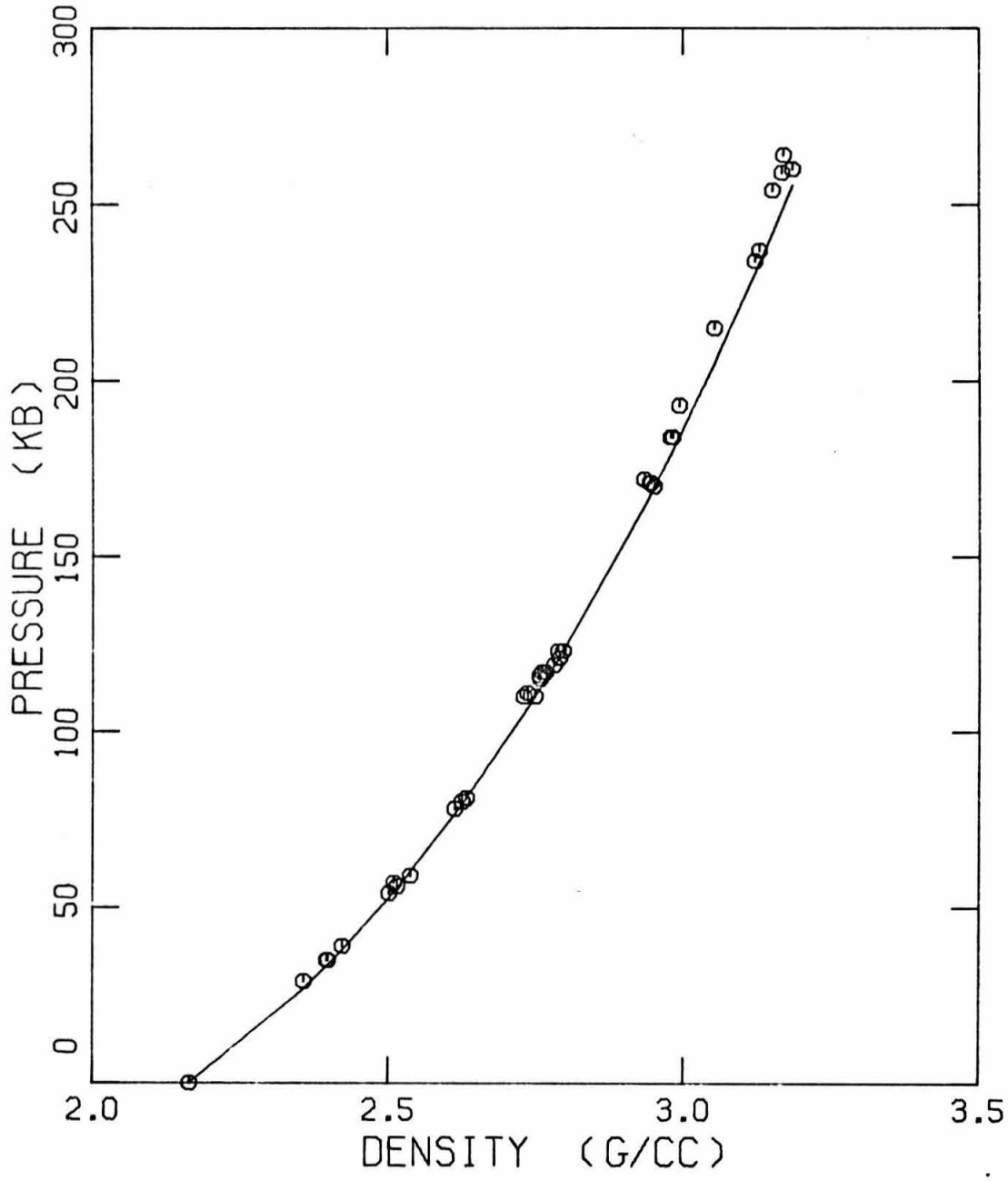

Fig. 8.6. Hugoniot data and Case 2 extrapolated Hugoniot curve.

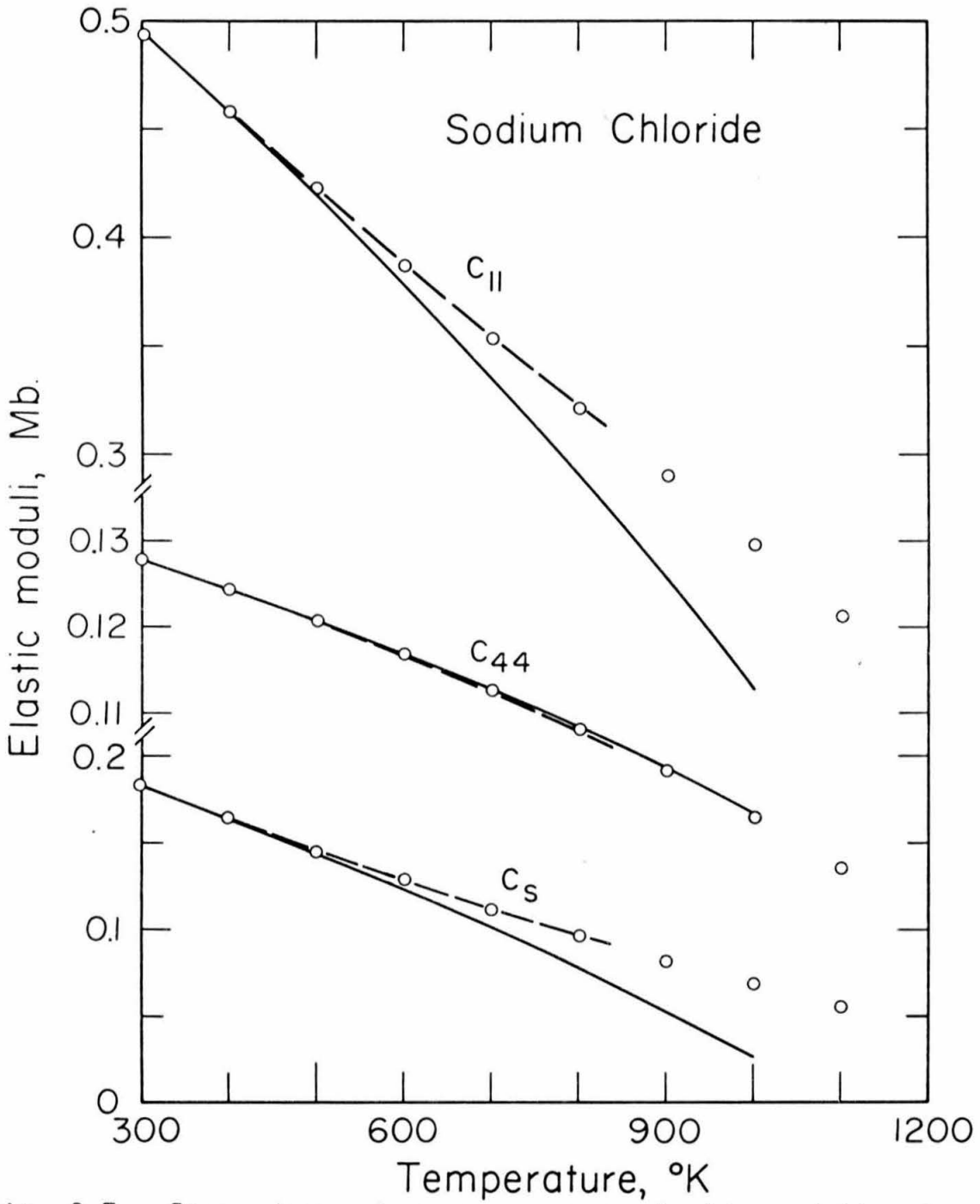

Fig. 8.7. Comparison of zero-pressure elastic moduli calculated from Cases 2 (solid lines) and 3 (dashed) with data of Slagle and McKinstry (1967).

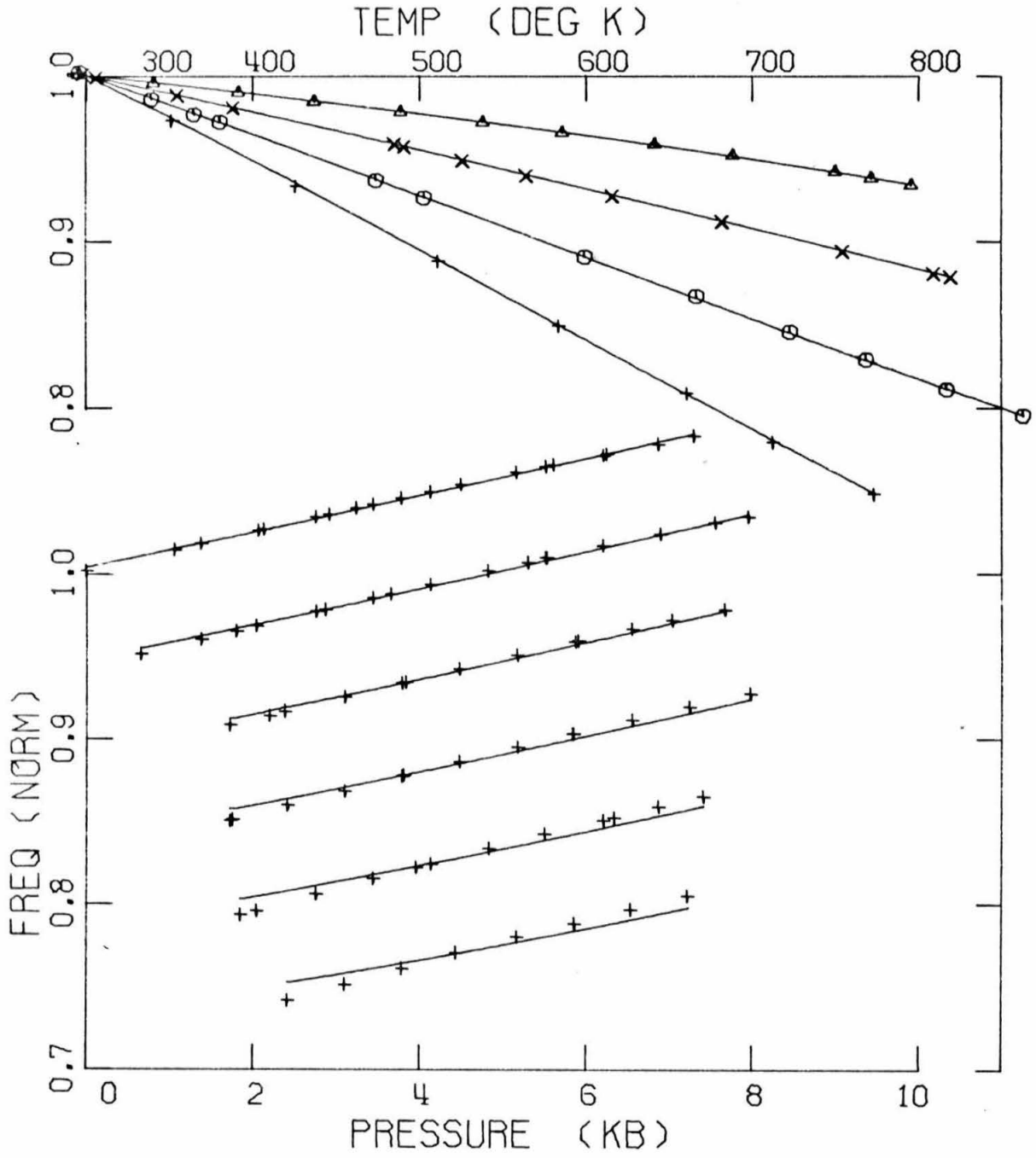

Fig. 8.8. Zero-pressure frequency-temperature and mode 3 frequency pressure ultrasonic data compared with curves from Case 3.

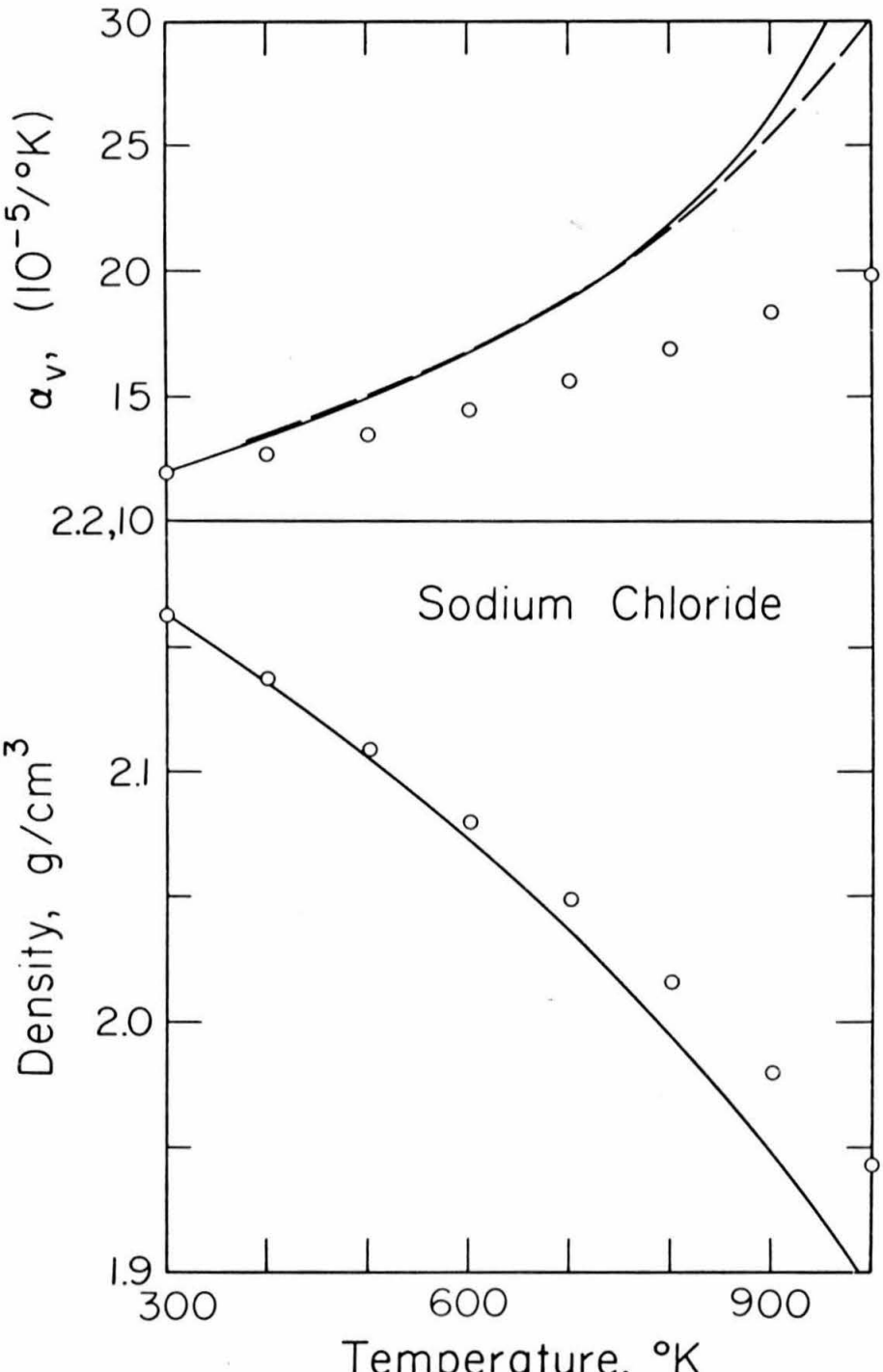

Fig. 8.9. Thermal expansion calculated from Cases 2 (solid lines) and 3 (dashed) compared with data of Enck and Dommell (1965).

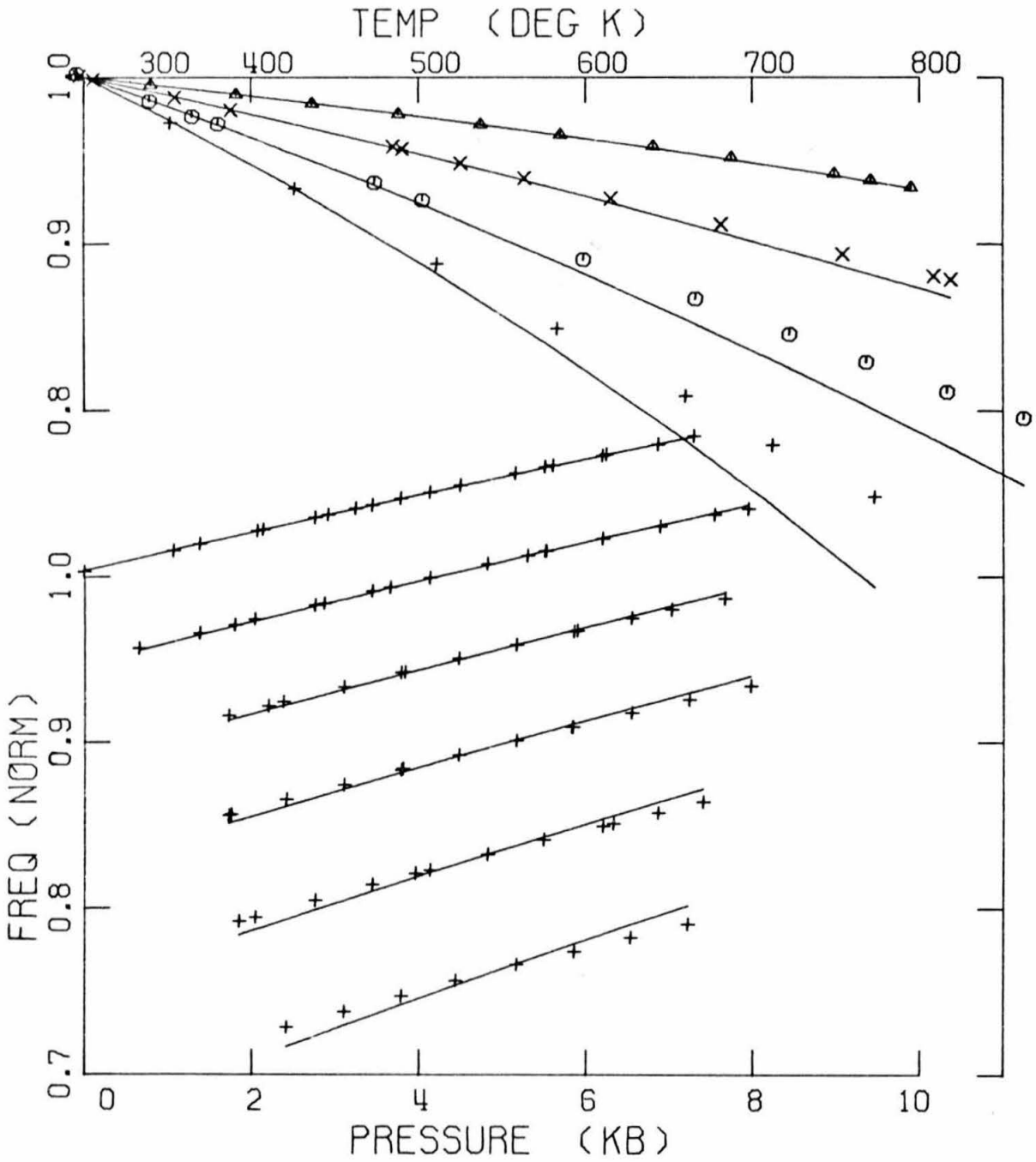

Fig. 8.10. Zero-pressure frequency-temperature and mode 3 frequency-pressure ultrasonic data compared with curves from Case 4.

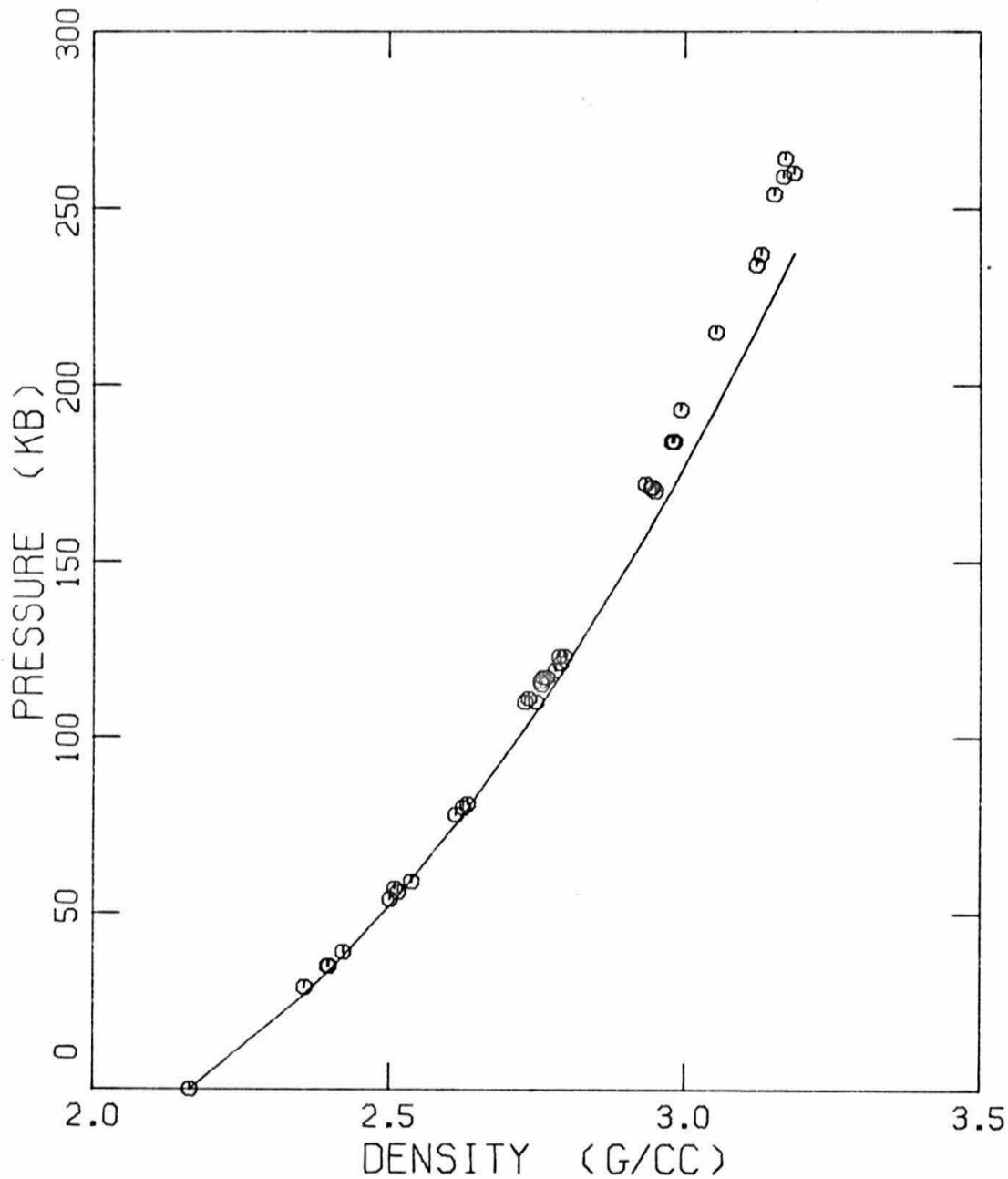

Fig. 8.11. Hugoniot data and Case 4 extrapolated Hugoniot curve.

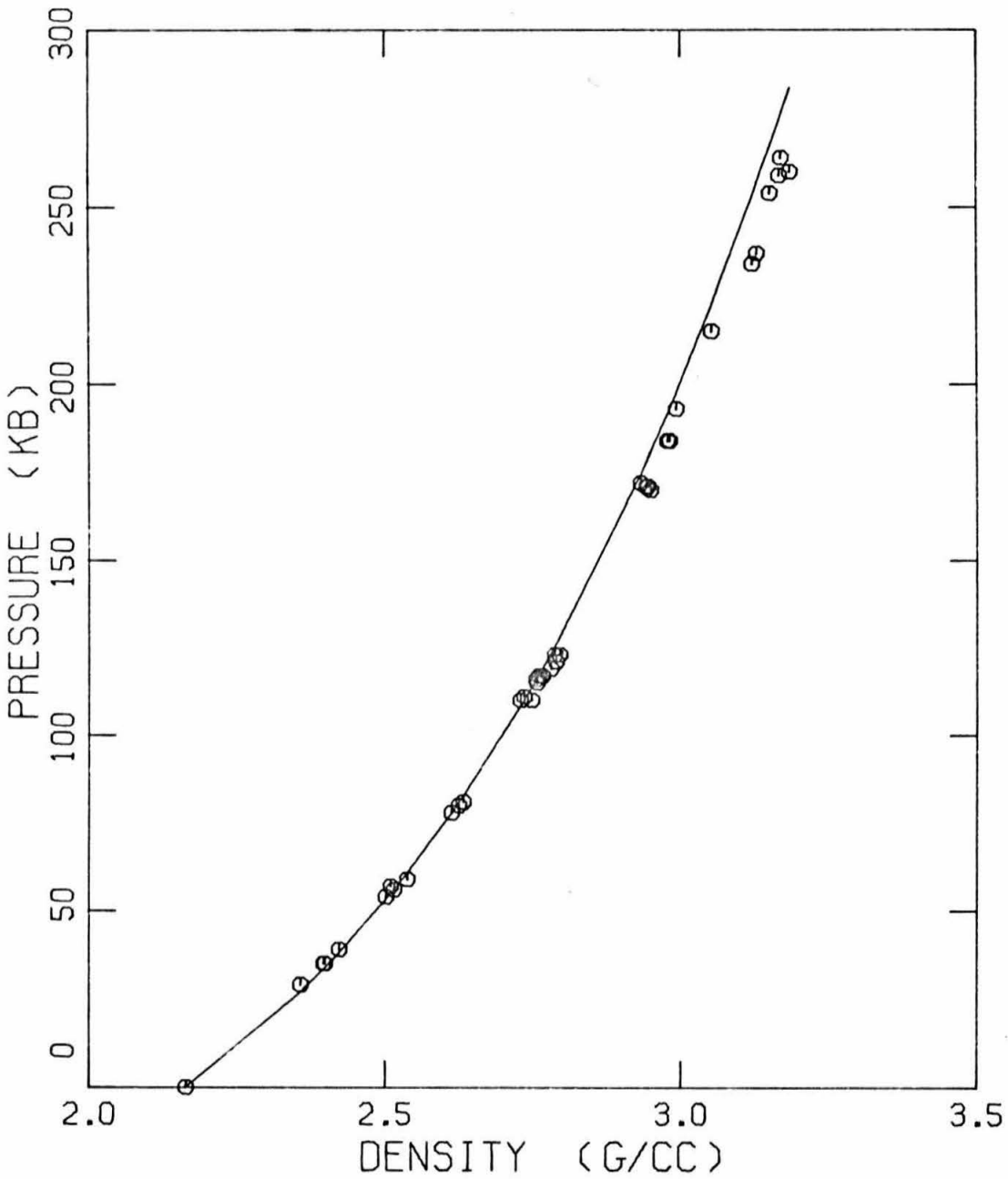

Fig. 8.12. Hugoniot data and Case 5 extrapolated Hugoniot curve.

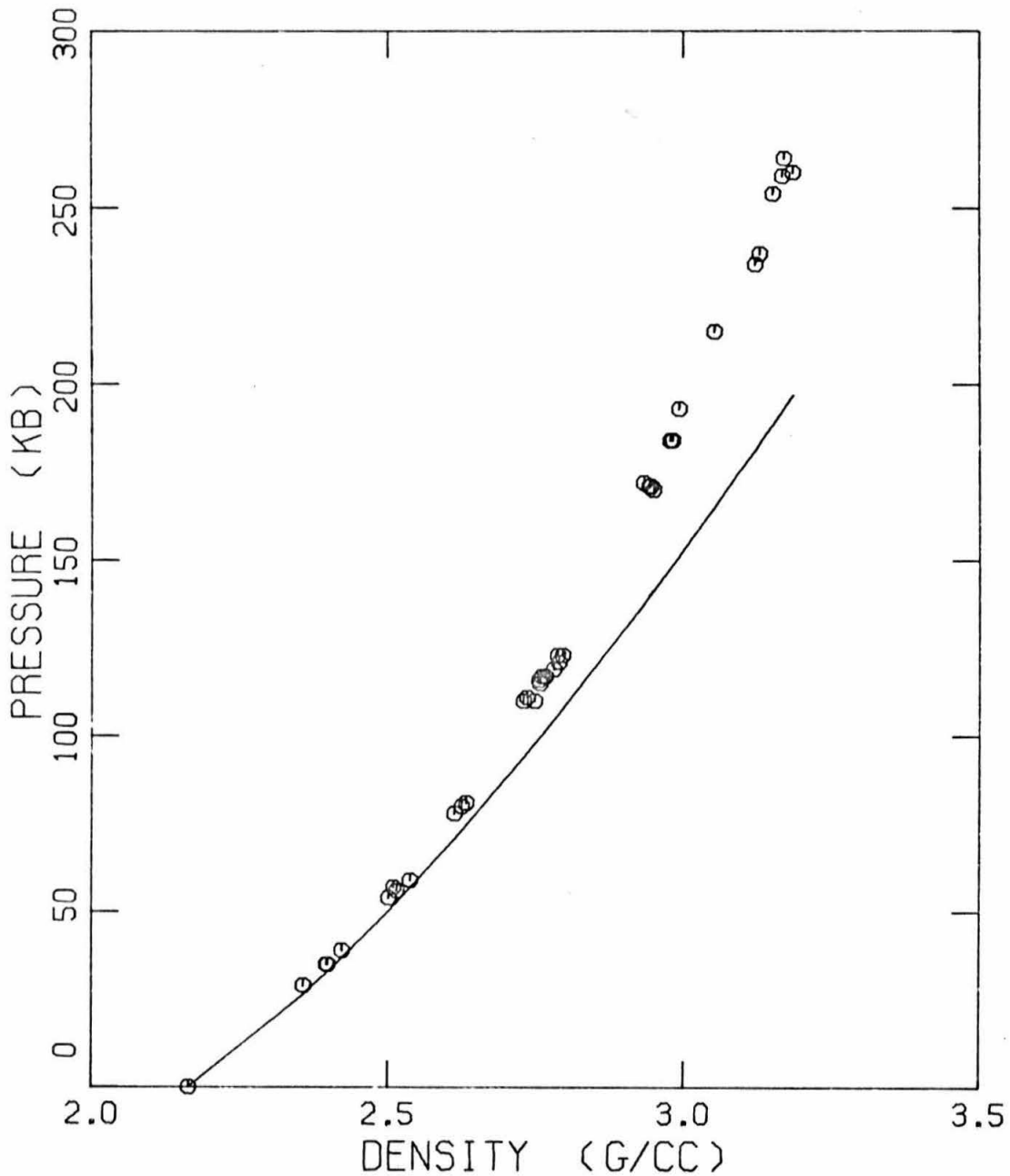

Fig. 8.13. Hugoniot data and Case 6 extrapolated Hugoniot curve.

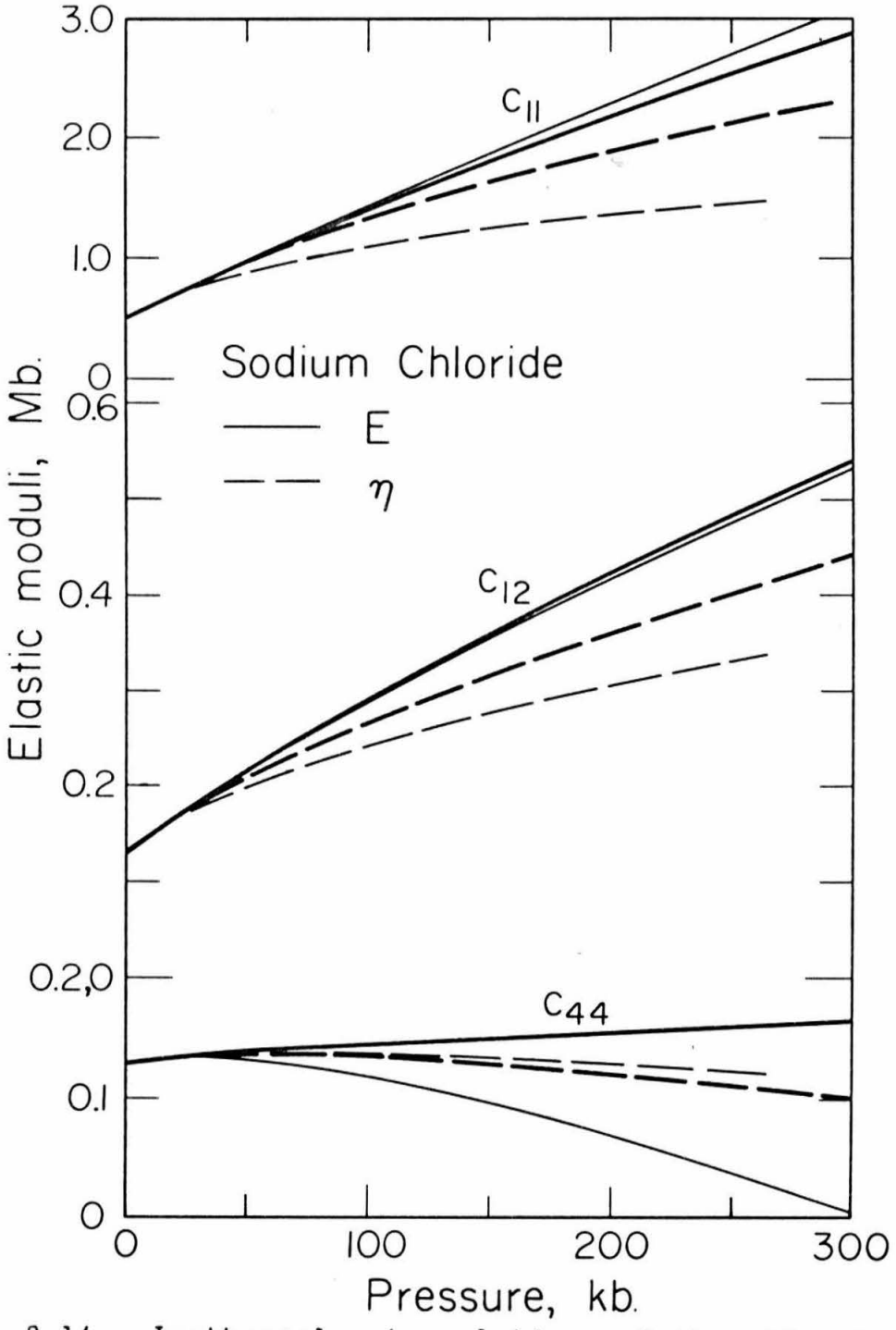

Fig. 8.14. Isothermal extrapolations of the effective elastic moduli from Cases 2 and 4 (heavy) and Cases 5 and 6 (light).

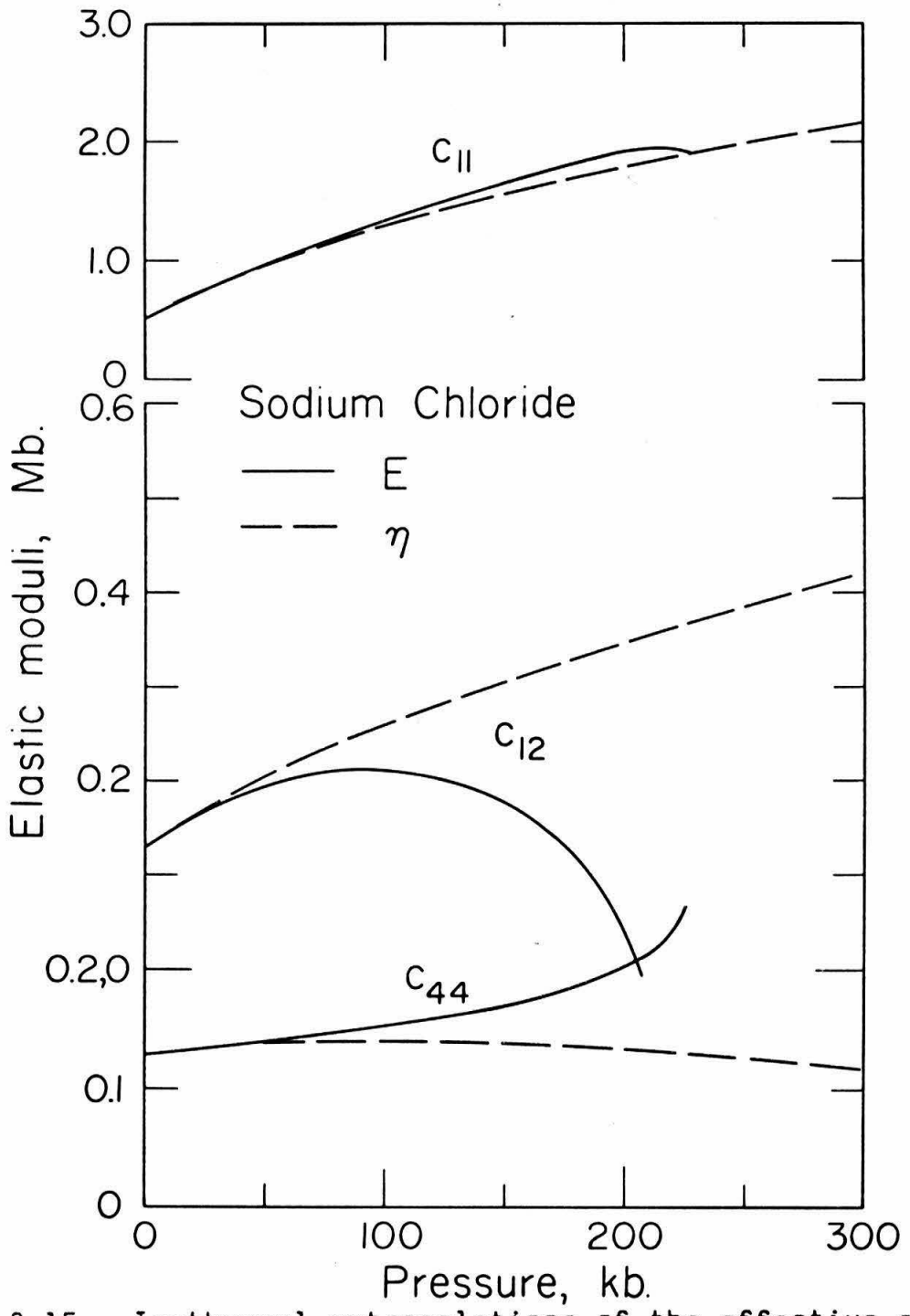

Fig. 8.15. Isothermal extrapolations of the effective elastic moduli from Cases 7 and 8.

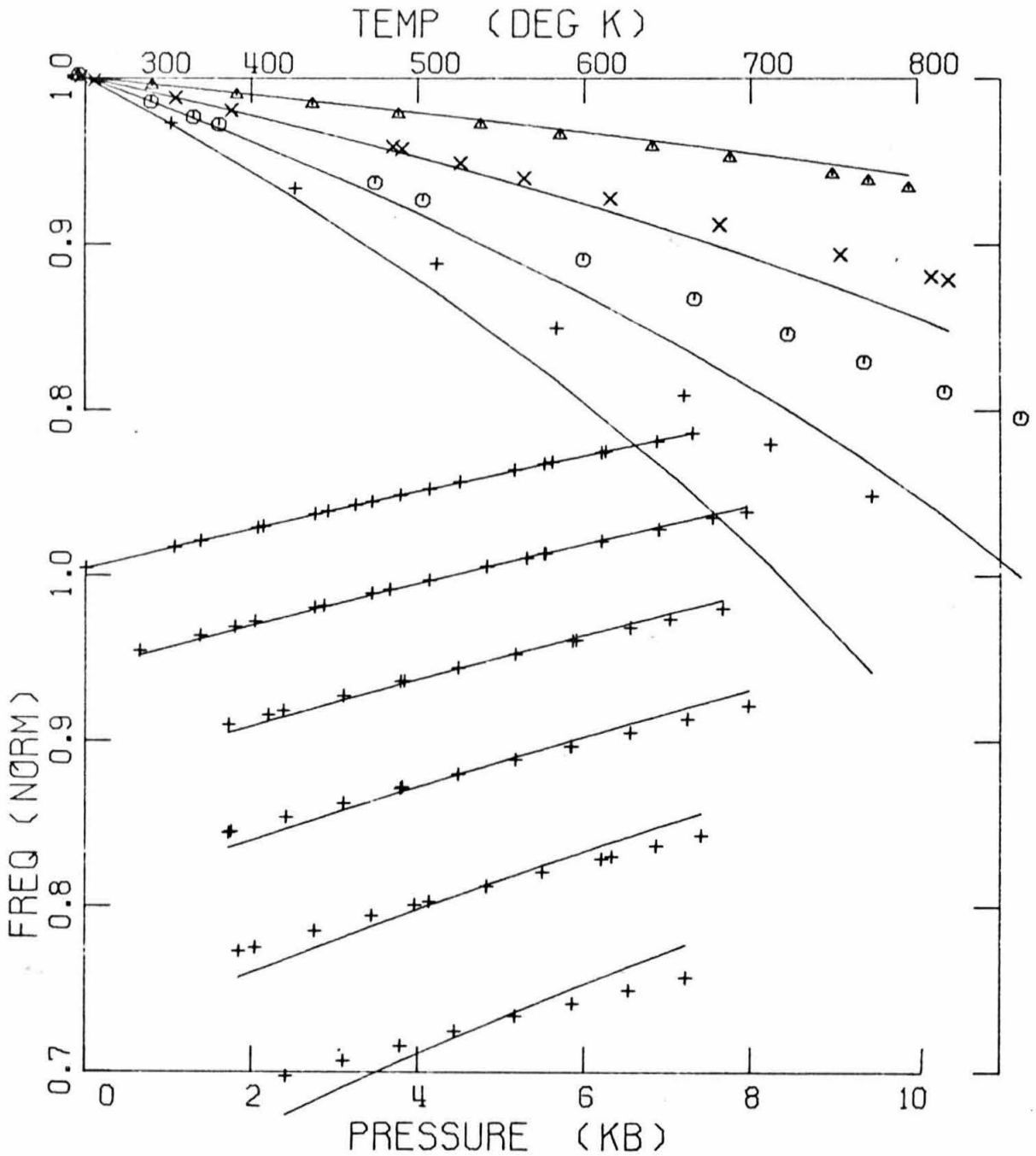

Fig. 8.16. Zero-pressure frequency-temperature and mode 3 frequency-pressure ultrasonic data compared with curves from Case 7.

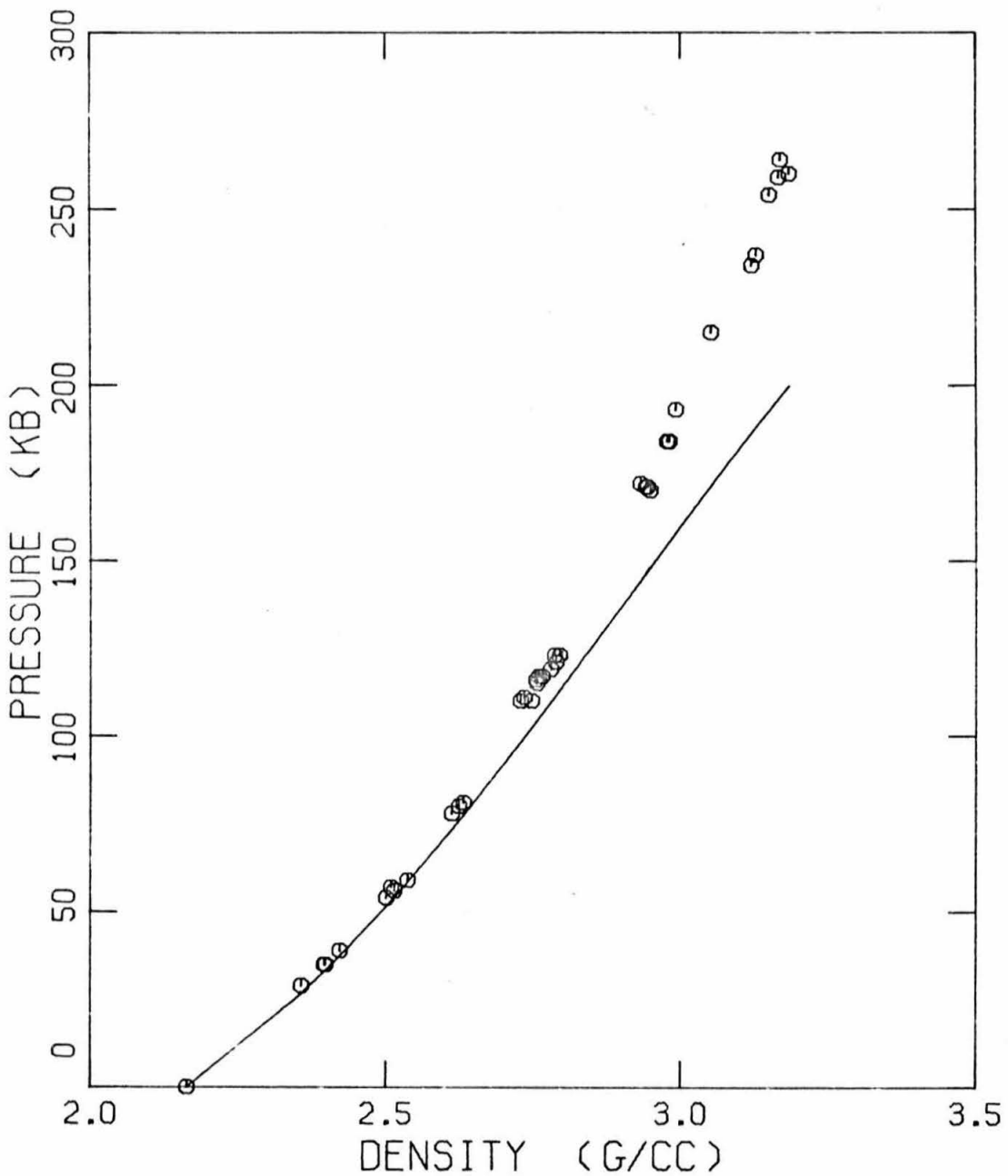

Fig. 8.17. Hugoniot data and Case 7 extrapolated Hugoniot curve.

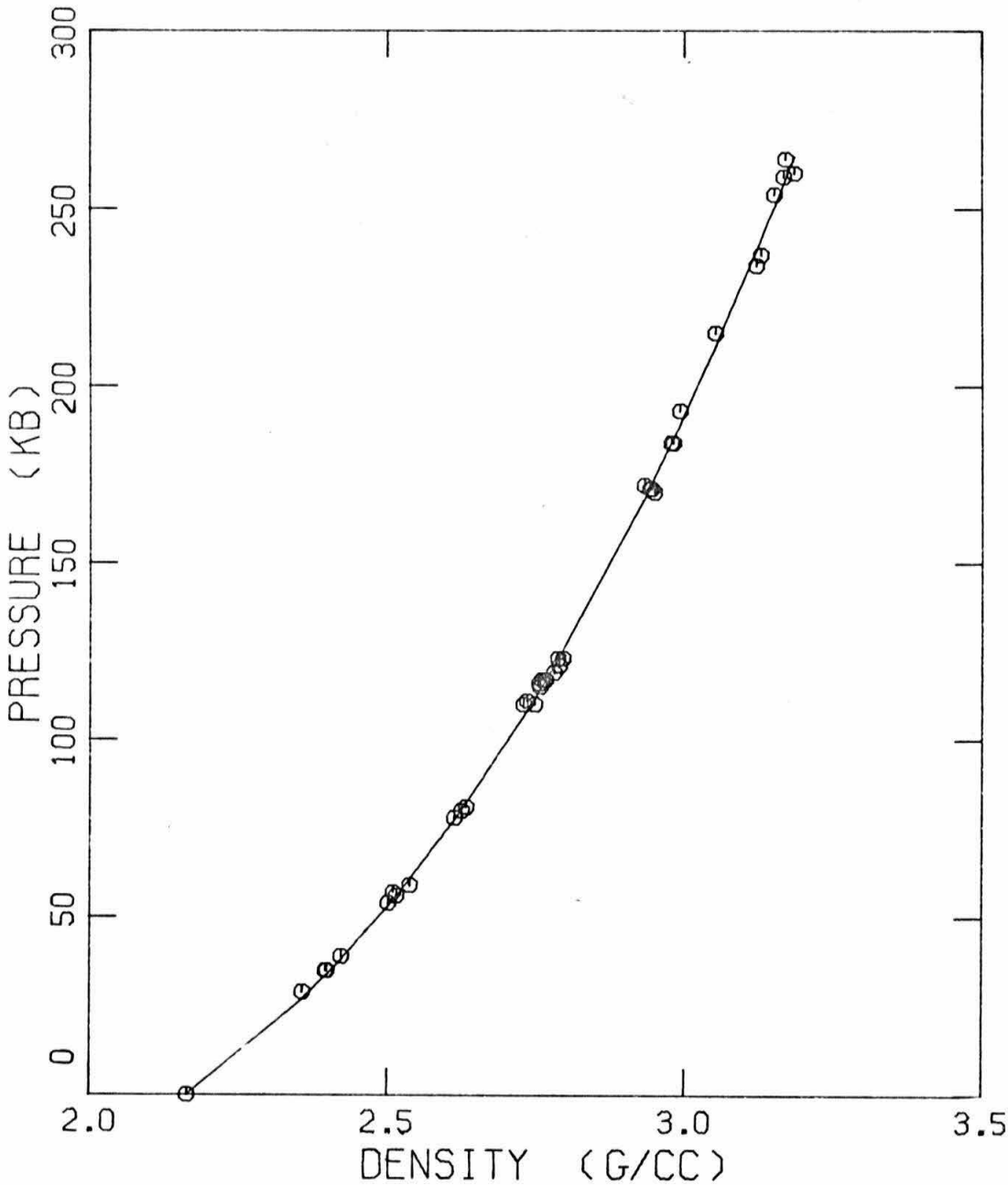

Fig. 8.18. Hugoniot data and Case 9 Hugoniot curve, which was fitted to the data.

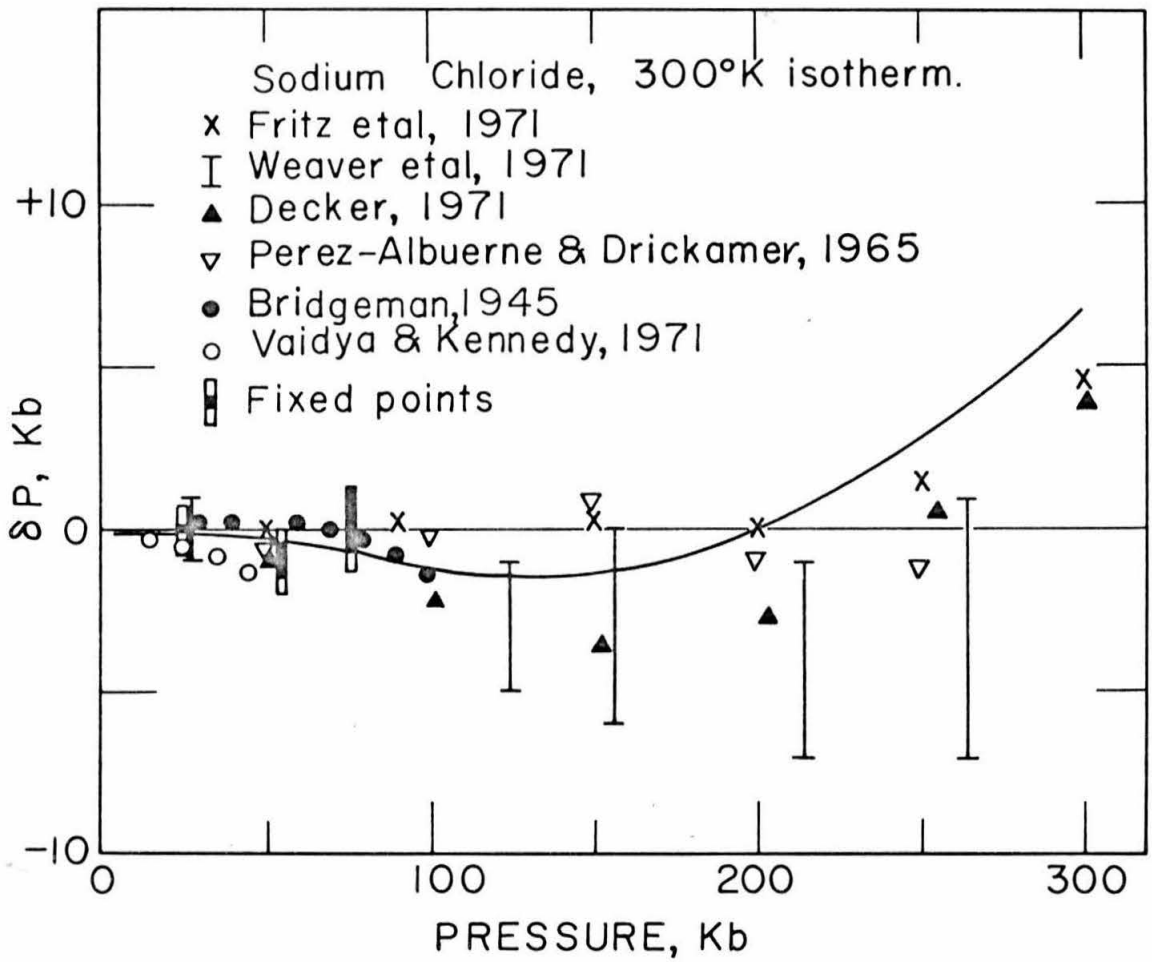

Fig. 8.19. Deviation of other determinations of the NaCl room temperature isotherm from that of Case 9. Solid curve is the isotherm of Case 10. Other data are discussed in the text.

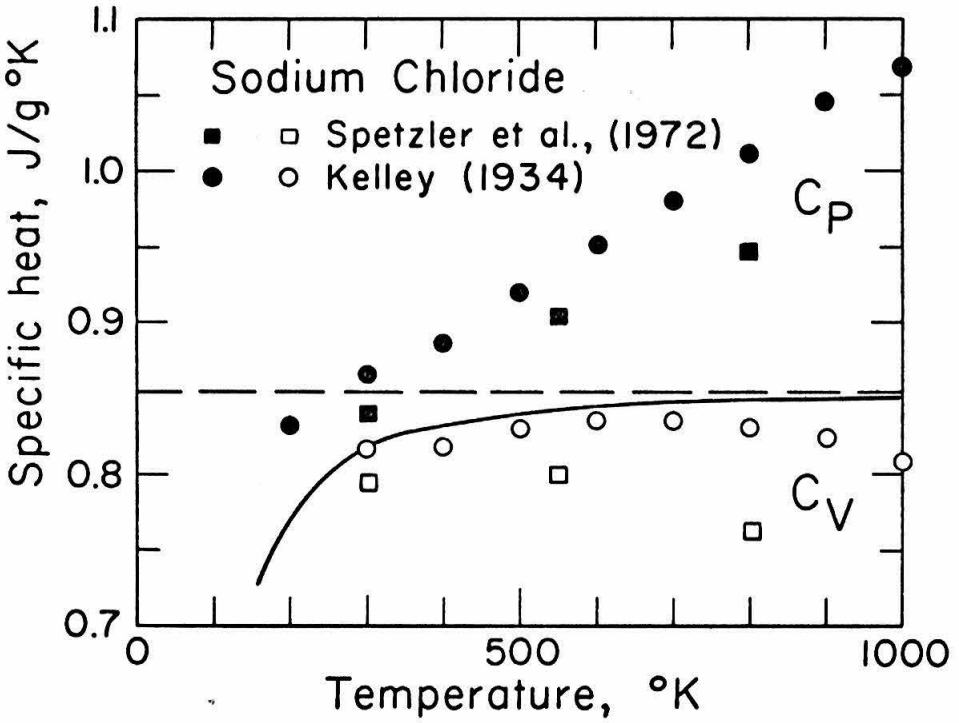

Fig. 8.20. Comparison of specific heats given by Spetzler et al. (1972) with the data of Kelley (1934) for the specific heat at constant pressure, C_p, the values for the specific heat at constant volume, C_v, derived from them in this study, the values of C_v predicted by the Debye model (solid curve), and the Dulong-Petit value for C_v (horizontal dashed line).

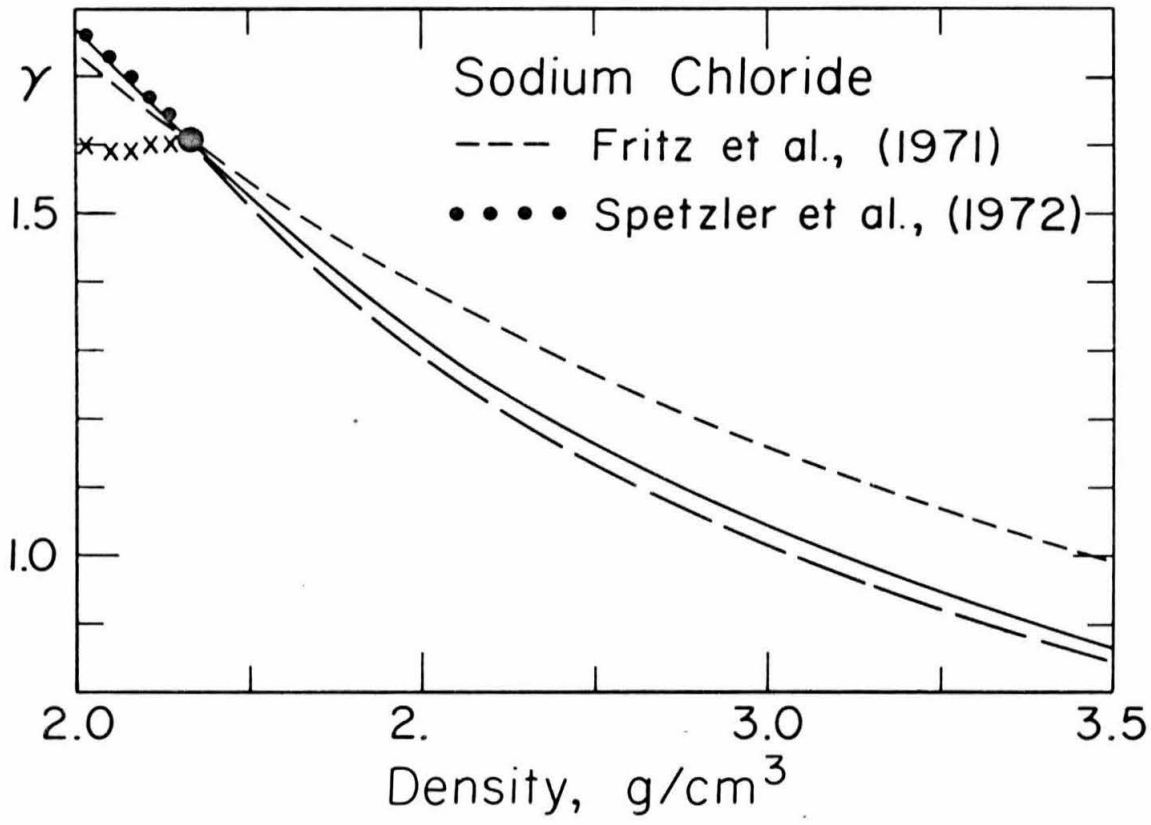

Fig. 8.21. Comparison of different sodium chloride Grüneisen parameters. Those of Case 9 (solid curve) and Case 10 (long-dashed) and Fritz et al. (short-dashed) are assumed to depend only on density. The dots (Spetzler et al.) and crosses (this study) are the density dependence at zero pressure (i.e., varying temperature) calculated from other data.

CHAPTER 9

MEASUREMENT OF ELASTIC PROPERTIES OF MgO UNDER SHOCK COMPRESSION TO 500 Kb

Summary

The velocities of rarefaction waves in shock compressed MgO were measured by observing the reduction of the shock-front velocity near the sample edges due to the rarefaction waves propogating from the edges. The extent of this "edge-effect" is difficult to determine accurately because of its emergent nature. Arrangements more sensitive to changes in shock-front velocity yielded rarefaction wave velocities close to predicted longitudinal velocities in the shocked state. Velocities reduced towards the hydrodynamic sound speed in the shocked state were obtained from less sensitive arrangements. These results support a two-stage longitudinal-hydrodynamic model of the decompression. The measured longitudinal velocities are consistent with second pressure derivatives of the elastic moduli, c''_{ij}, given by $K_o c''_{ij} = -1 \pm 15$, where K is the bulk modulus.

9.1 Introduction

Direct measurement of elastic properties of solids using ultrasonic techniques have so far only been made up to about 10 kilobars pressure. At higher pressures, information about elasticity is usually only obtained indirectly by differentiating pressure-density relations obtained from static compression X-ray measurements or derived from shock-wave Hugoniot data. The Hugoniot data require thermal corrections at high pressures, as illustrated in Chapters 6 and 7, and, in either method, only the bulk modulus is obtained. Considerable accuracy is also lost because the derivative of the data has to be taken. It is desirable, therefore, to have a method of obtaining more direct measurements of elasticity at high pressure. The development and initial results of such a method are described in this Chapter.

9.2 Experimental Arrangement

The method consists of measuring the speed of a rarefaction wave which propogates from the sides of a sample into the region behind a shock wave. Such a method has been applied by Al'tshuler et al. (1960) to the measurement of elastic properties of metals. The configuration of the sample and waves are illustrated in Fig. 9.1. A shock wave is generated at the lower surface of the sample (in the present case, by impacting a projectile). As the shock front pro-

gresses upwards, a lateral rarefaction propogates into the shocked region from the sides of the sample, which are unconstrained. This rarefaction reduces the pressure at the shock front, and hence slows the shock front. The result is an "edge-effect" on the shock front, which lags behind near the sides of the sample, as shown.

The object of the experiment is to measure the furthest lateral distance to which this edge effect has propogated when the shock front reaches the top surface of the sample. At any interior point, the first rarefaction signal to arrive is that propogating from the lower corner of the sample. At later times, rarefactions from higher up the sides of the sample will arrive. The locus of points of intersection of this first rarefaction wave with the shock front is a straight line, which makes an angle, α, with the sides of the sample. Simple geometrical relations, illustrated in Fig. 9.1, relate the rarefaction velocity, V, the shock-front velocity, U_s, and the particle velocity, u_p, behind the shock front:

$$V = U_s \left[\tan^2 \alpha + \left(\frac{U_s - u_p}{U_s} \right)^2 \right]^{\frac{1}{2}}. \qquad (1)$$

The angle α is determined from the extent of the edge effect at the top surface of the sample. The measurement of this quantity is now described.

A mirror is placed a small distance from the top sur-

face of the sample, as shown in Fig. 9.2, with the silvered surface facing the sample. The mirror is illuminated and viewed through a slit oriented across the sample, as shown. The image of this slit is recorded by a streak camera, which streaks the image of the slit transversely across a photographic plate (Ahrens et al., 1971). As the shock front reaches the top surface of the sample, the free surface moves upward at approximately twice the particle velocity behind the shock front (e.g., Rice et al., 1958). The free surface preserves the shock-front profile, since the material near the edges begins moving at a later time. As the free surface subsequently impacts the mirror, the reflectivity of the mirror is destroyed and the recorded streak image of the slit is progressively cut off. The process is illustrated in Fig. 9.3. Typical streak records are shown in Figs. 9.4a-c. The profile of the shock front is thus recorded by the streak record, and the extent of the edge effect can be measured.

The sample is mounted on a tungsten "driver plate" (Fig. 9.2), which is impacted by a tungsten "flyer plate" mounted in the tip of the projectile. The projectile velocity is measured just prior to impact (Ahrens et al., 1971), and the pressure, P, and particle velocity in the sample is calculated by the impedance matching method (Walsh and Christian, 1955) using pressure-particle velocity curves of tung-

sten (McQueen et al., 1970) and MgO (Carter et al., 1971). The shock velocity can then be obtained from the Rankine-Hugoniot relation

$$U_s = \frac{P}{\rho_o u_p} , \qquad (2)$$

where ρ_o is the zero pressure density of the sample.

9.3 Samples

Results are reported here for five polycrystalline and three single-crystal samples of MgO. The polycrystalline samples were generously supplied by Dr. T. Vasilos of Avco Corporation. The samples described and measured by Spetzler (1970) and Schreiber and Anderson (1968) were obtained from the same source. The MgO single-crystals were purchased from Norton Research Corporation. All faces of the crystals were (100) cleavage planes.

9.4 Results

A basic difficulty of this method is the emergent nature of the edge effect - its exact beginning is difficult to pick (Figs. 9.4a-c). Some variations in the target arrangement were therefore explored in an effort to maximize the accuracy of the measurement.

The amplitude of the "wings" on the streak record can be increased by increasing the separation of mirror and sample. The streak record measures the transit time of the

shock through the sample, t_s, plus the time for the free surface to reach the mirror, t_f. If the sample thickness is h and the mirror-sample separation is z, then the total time is

$$t = t_s + t_f = \frac{h}{U_s} + \frac{z}{2u_p} . \qquad (3)$$

In solids, U_s is approximately linearly related to u_p (e.g., Rice et al., 1958):

$$U_s = C_o + s u_p , \qquad (4)$$

where $C_o = (\partial P/\partial \rho)_s$ is the "bulk sound speed" and s is a constant. Using (4) in (3),

$$t = \frac{h}{U_s} + \frac{s z}{2(U_s - C_o)} , \qquad (5)$$

and

$$\frac{\partial t}{\partial U_s} = -\frac{h}{U_s^2} - \frac{s z}{2(U_s - C_o)^2} . \qquad (6)$$

For MgO, C_o = 6.74 mm./μsec., s $\approx$ 1.3, and in these experiments, $U_s \approx$ 8.7 mm./μsec., typically. Thus, in these units,

$$\frac{\partial t}{\partial U_s} \approx -0.013 h - 0.16 z . \qquad (7)$$

Thus a small increase in z can significantly increase the sensitivity of the transit time to changes in the shock velo-

city.

Typical sample thicknesses in these experiments are h = 4-5mm. Four of the shots reported here had z = 0.76mm., sufficient for the "free-surface effect" to be significant. Fig. 9.4a shows the streak record for one of these (A257). A central linear portion of the streak cutoff, corresponding to a central planar section of the shock front, is not clearly discernible, and a slight curvature persists across the cutoff. For the planar section to be obliterated by the edge effect would have required a rarefaction velocity of at least 14.7Km/sec., which is very unlikely (Cf. later results). It was therefore thought that this might be due to the free surface deforming before it hit the mirror. The free-surface transit time was about 0.25 μsec. In this time a compressional wave in MgO could travel the order of 2.5 mm. and a shear wave the order of 1.0 mm., so there may have been sufficient time for effects to propogate into the central region from the sample edges. A shot (A258) was therefore fired with z = 0.13 mm., giving a free-surface transit time of about .04 μsec. The resulting streak record is shown in Fig. 9.4b. (z was not reduced to zero because of the presence of an elastic precursor to the main shock front. This causes the free surface to move about .05 mm. before the main shock reaches it. With z = 0.13 mm., only the effect of the main shock was recorded.) The central region is no-

ticeably more linear in this case.

The relevant specifications and the results for the shots reported here are given in Table 9.1. The rarefaction velocities obtained are plotted against pressure in Fig. 9.5. It can be seen that the shots with z = 0.76 mm. (solid circles) gave fairly consistent velocities near 12 Km./sec., while shot A258 (z = 0.13 mm., open circle) gave a much lower velocity. This will be discussed below.

All of the above shots were on the polycrystalline samples. The remaining shots (A263, 266, 267) were on the single crystal samples and with intermediate values of z. A typical record (A266) is shown in Fig. 9.4c and the specifications and results are given in Table 9.1 and Fig. 9.5 (triangles). These shots gave intermediate velocities. The accuracy of the results is impared somewhat by the presence of low-angle irregularities in the cutoff (Fig. 9.4c) the origin of which is not clear.

The "half error bars" in Fig. 9.5 have the following significance. The velocities given in Table 9.1, and the points in Fig. 9.5, result from the best estimate of the beginning of the emergent edge effect. Bounds on these values were obtained by picking points at which an edge effect definitely existed. The points picked are indicated in Figs. 9.4a-c. The error bars were extended down to the resulting lower bounds on the velocities. Upper bounds to the velo-

cities obviously cannot be estimated.

9.5 Discussion

This method of measuring the rarefaction velocities requires a compromise between the low sensitivities obtained with small mirror-sample separations and the larger uncertainties, apparently caused by free-surface deformation, obtained with larger mirror-sample separations. The more sensitive experiments yielded very reasonable, though not very accurate, results, as will be discussed below. Some earlier experiments were performed with an aluminum foil (.015 mm. thick) stretched over the sample. This foil was spalled off the sample by the emerging shock wave and subsequently impacted the mirror. However, these experiments were evidently also affected by deformations of the foil during transit, since the resulting velocities were not very consistent and in the low range of 10.5 to 11.5 Km./sec., despite the larger (0.76 mm.) mirror-foil separation used. A superior method would be to use a material of low or zero rigidity to receive the momentum of the free surface. A layer of liquid, as described by Al'tshuler et al. (1960), or a powder would probably serve this purpose.

The velocities measured here are consistent with the decompressional behaviour of solids inferred by Al'tshuler et al. (1960) and observed directly by Kusubov and van Thiel

(1969). In this picture, the decompression occurs in two stages - first a longitudinal elastic decompression to a critical deviatoric stress, followed by a hydrodynamic or "plastic" decompression. Al'tshuler et al. (1960) observed rarefaction velocities in liquids which corresponded closely to the hydrodynamic sound speed of the compressed liquid, while in solids the observed rarefaction velocities were considerably faster than the estimated hydrodynamic sound speeds. Kusubov and van Thiel (1969) observed the compression and decompression of aluminum using piezoresistive manganin gauges. The decompression was observed to proceed in two stages, one travelling at approximately the longitudinal elastic velocity, and the other, identified by an increase in the rate of decompression, travelling at about the bulk sound speed. As discussed by Al'tshuler et al. (1960) and Kusubov and van Thiel (1969), this two-stage decompression corresponds closely to the observed behaviour of solids under compression, in which a longitudinal elastic wave preceeds the main "plastic" shock wave (see also, for example, Ahrens et al., 1968).

Al'tshuler et al. (1960) observed that in liquids the onset of the edge effect due to lateral rarefactions was quite sharp, while in solids it was more emergent, as observed in this study. Combined with the observation of Kusubov and van Thiel (1969) that the elastic rarefaction

accounts for only 30% of the decompression, this suggests that in the less sensitive arrangement (smaller z, shot A258) it was mainly the effects of the plastic decompression which were observed, while the more sensitive experiments were able to detect the onset of the elastic decompression.

Comparison with predicted values of the elastic and hydrodynamic velocities in the shocked states supports this interpretation. These quantities were predicted by taking the ultrasonically measured elastic moduli of MgO and their pressure and temperature derivatives (Spetzler, 1970) and extrapolating them to high pressures and temperatures using the theory given in Chapter 5. The required data are given in Table 9.2. Third-order extrapolations in terms of both the "E" and "η" strain measures of Chapter 5 were used. In addition, since $\zeta = K_0 K_0'' \approx -1$ (Chapter 6), where K_0 is the zero-pressure bulk modulus and a prime denotes a pressure derivative, a fourth-order "E" extrapolation was made with $\zeta_{ij} = K_0 c_{ij}'' = -1$, where c_{ij} are the elastic moduli. These isothermal extrapolations of the effective elastic moduli are shown in Fig. 9.6. Since considerable heating accompanies shock-compression, a thermal correction has to be included to obtain the moduli in the shocked state. The thermal corrections in a typical case are shown in Fig. 9.7. The average longitudinal velocity, V_L, (appropriate to the polycrystalline samples) resulting from the fourth-order "E"

extrapolation is shown in Fig. 9.5 (solid lines; the third-order "E" extrapolation is very similar - Fig. 9.6). For the single crystals, since the sample faces were (100) crystal planes and $\tan\alpha \approx 1$, the appropriate longitudinal velocity is that for the [110] crystal direction, which is $V_{110} = \left[(c_{11} + c_{12} + 2c_{44})/2\rho\right]^{\frac{1}{2}}$. This velocity is shown for the fourth-order "E" extrapolation in Fig. 9.5 (long-dashed; see also Fig. 9.7). For the accuracies of the present measurements, the distinction between these velocities, and the anisotropy of the velocity in the single crystals, is unimportant. The [110] velocity from the third-order "η" extrapolation is also shown in Fig. 9.5 (short-dashed).

In Fig. 9.5 it can be seen that the velocities obtained using the greatest mirror-sample separation (z = 0.76 mm.) correspond closely to the longitudinal velocities of the fourth-order "E" extrapolation, while that obtained using the smallest separation (z = 0.13 mm.) is only slightly above the bulk sound speed. Those with intermediate separation are intermediate between these. Evidently the initial effects of the longitudinal decompression were not observed in the less sensitive (smaller z) experiments, as surmised earlier.

The faster velocities obtained are much more consistent with the third-order "E" extrapolation than the third-order "η" extrapolation (Figs. 9.5, 9.6). Assuming that they do

represent the longitudinal velocity, these data can be used to put constraints on the second pressure derivatives of the elastic moduli. In Fig. 9.5, the velocity for $\zeta_{110} = \frac{1}{2}(\zeta_{11} + \zeta_{12} + 2\zeta_{44}) = -10$ is shown (dash-dot). A bound of $\zeta_{110} \gtrsim -15$ is estimated from the data.

Finally, some observations by Hauver and Melani (1970) deserve comment here. These authors observed an emergent edge effect in optical measurements of shocked sodium chloride. They calculated a rarefaction velocity close to the bulk sound speed of NaCl. Since they observed directly the change in reflectivity of the free surface of the samples, this is in accord with the present observations. They also noted that in the range of the phase transition from the B1 to the B2 phase the edge effect had a much sharper onset, and the calculated rarefaction velocity was considerably reduced. This is in accord with the observations by Al'tshuler et al. (1960) of fluids, and suggests that a loss of rigidity accompanied the phase change. Also, as pointed out by Hauver and Melani (1970), the edge effect is a much more sensitive indicator of phase changes in shock compression than is provided by the accompanying Hugoniot offsets.

9.6 Conclusions

It can be concluded from these results that

a) MgO remains in the solid state under shock compression to

500 Kb.

b) a two stage decompression from the shocked state, involving an initial longitudinal decompression to a critical deviatoric stress, followed by a hydrodynamic decompression to zero stress, is consistent with the observations reported here.

c) values of $\zeta_{ij} \approx -1$ are consistent with the best estimates obtained here for the longitudinal velocities of MgO between 300 and 500 Kb. A bound of $\frac{1}{2}(\zeta_{11} + \zeta_{12} + 2\zeta_{44}) \gtrsim -15$ is estimated from the data.

d) extrapolations in terms of the "E" strain measure are empirically more successful than those in terms of "η".

The present results largely confirm previous observations of the decompression of shocked solids. Refinement of the technique should allow more accurate determinations of the elastic properties of shocked solids, and promises to be a useful tool with which to detect high-pressure phase changes.

9.7 References

AHRENS T. J., GUST W. H. and ROYCE E. B., J. Appl. Phys. 39, 4610 (1968).

AHRENS T. J., LOWER J. H. and LAGUS P. L., J. Geophys. Res. 76, 518 (1971).

AL'TSHULER L. V., KORMER S. B., BRAZHNIK M. I., VLADIMIROV M. P., SPERANSKAYA M. P. and FUNTIKOV A. I., J. Exptl. Theoret. Phys. (USSR) 38, 1061 (1960). English translation Soviet Physics JETP 11, 766 (1960).

CARTER W. J., MARSH S. P., FRITZ J. N. and McQUEEN R. G., in Accurate Characterization of the High-Pressure Environment (Edited by E. C. Lloyd), N.B.S. Special Publication 326, U. S. Dept. of Commerce (1971).

HAUVER G. E. and MELANI A., Ballistics Research Laboratories Memorandum Report No. 2061, 23pp., Aberdeen, Maryland (1970).

KUSUBOV A. S. and van THIEL M., J. Appl. Phys. 40, 3776 (1969).

McQUEEN R. G., MARSH S. P., TAYLOR J. W., FRITZ J. N. and CARTER W. J., in High Velocity Impact Phenomena (Edited by R. Kinslow), Academic Press, New York (1970).

RICE M. H., McQUEEN R. G. and WALSH J. M., Solid State Phys. 6, 59 (1958).

SCHREIBER E. and ANDERSON O. L., J. Geophys. Res. 73, 2837 (1968).

SPETZLER H., J. Geophys. Res. 75, 2073 (1970).

WALSH J. M. and CHRISTIAN R. H., Phys. Rev. 97, 1544 (1955).

TABLE 9.1

MgO rarefaction velocity data.

Shot No.	Mirror separation z (mm.)	Edge effect x (mm.)	Sample dimensions y (mm.)	h (mm.)	tan α	U_s (Km/sec)	V (Km/sec)	P (Kb)
A250	0.76	4.29	11.43	3.81	1.13	8.57	12.0	446
A252	0.76	4.37	11.40	3.81	1.14	8.85	12.4	528
A257	0.76	4.42	11.46	3.86	1.14	8.15	11.7	326
A261	0.76	2.92	11.43	2.49	1.18	8.25	12.0	353
A258	0.13	2.46	11.43	3.83	0.64	8.20	8.8	340
A263	0.25	5.18	19.80	5.28	0.98	8.64	11.1	465
A266	0.25	3.94	19.20	4.62	0.85	8.85	10.4	528
A267	0.25	4.72	18.82	4.54	1.04	8.80	11.6	514

TABLE 9.2

Equations of state parameters of MgO.

ρ_0 $(g/cm^3)^a$	3.584
α_0 $(10^{-6}/^oK)^a$	31.5
C_V $(10^6$ erg/g $^oK)^b$	9.25

Elastic moduli and derivatives[c]:

	(i, j) 11	12	44
c_{ij} (Mb)	2.974	0.956	1.562
$\left(\frac{\partial c_{ij}}{\partial P}\right)_T$	8.70	1.42	1.09
$\left(\frac{\partial c_{ij}}{\partial T}\right)_P$ (Kb/^oK)	-0.606	0.074	-0.103

a) Skinner (1957).

b) Victor and Douglas (1963).

c) Spetzler (1970).

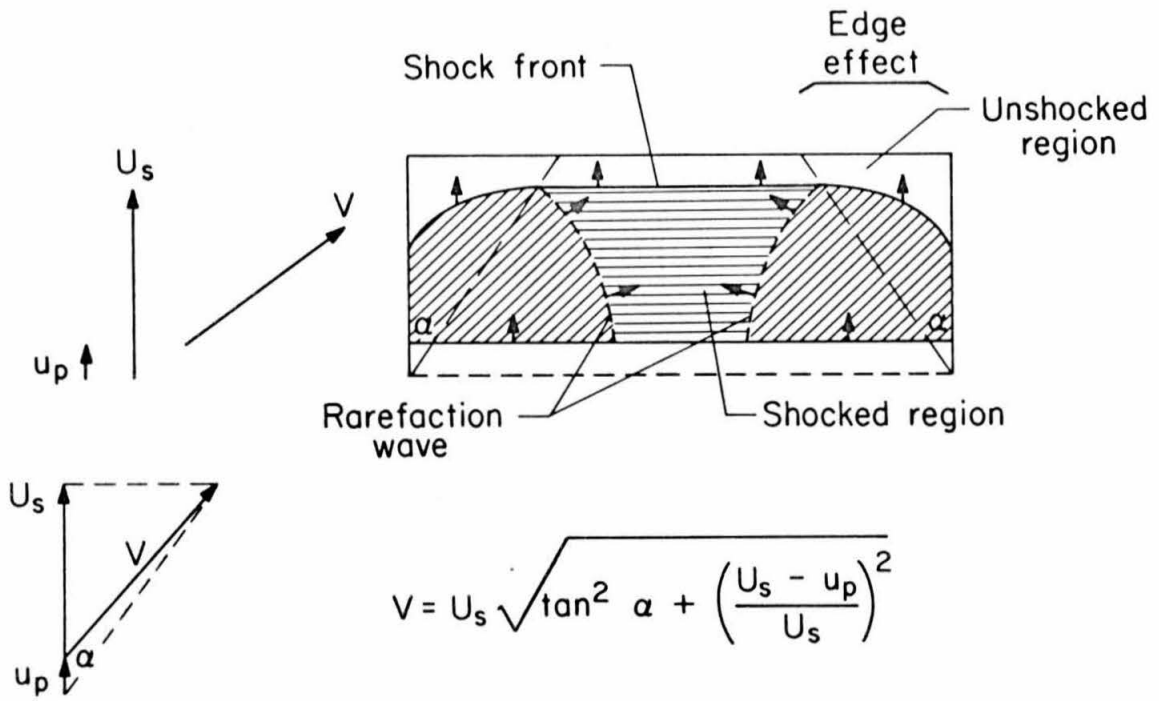

Fig. 9.1. Configuration of shock and rarefaction waves produced by passage of shock wave from lower surface of sample, and geometrical relationship of wave and particle velocities.

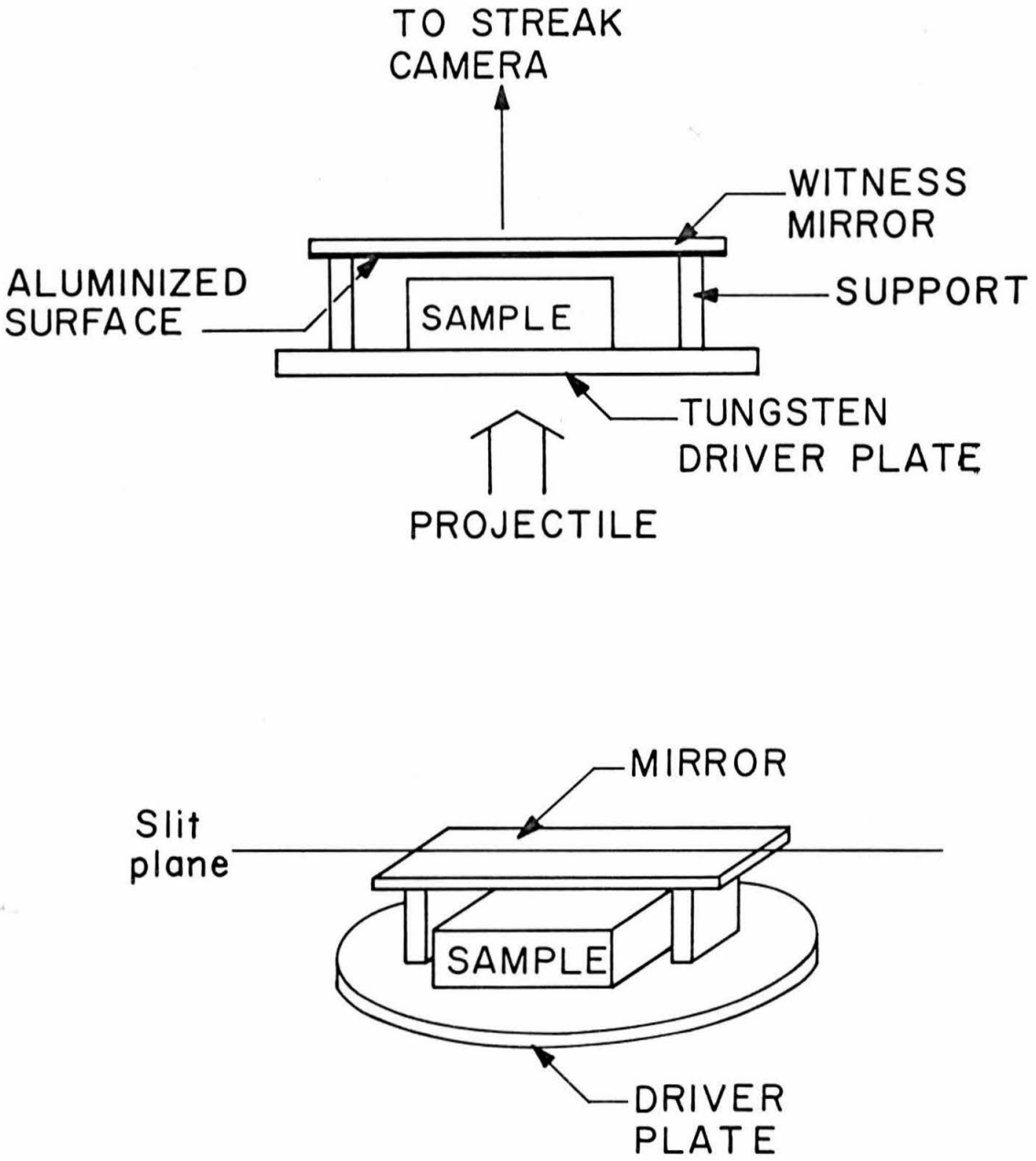

Fig. 9.2. Target arrangement for detection of lateral rarefaction waves.

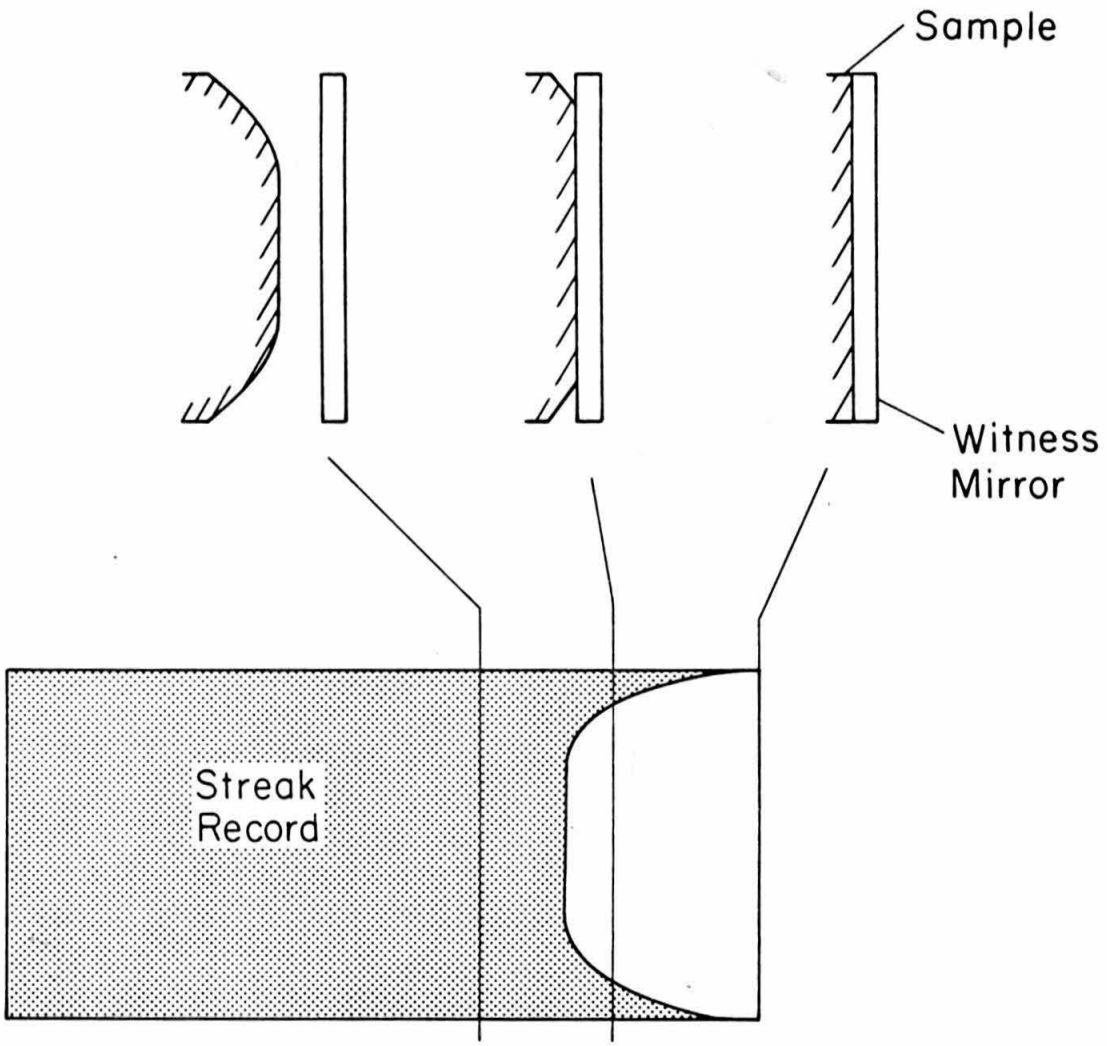

Fig. 9.3. Schematic illustration of the recording by a streak camera of the progressive cutoff of the image of the slit through which witness mirror is viewed.

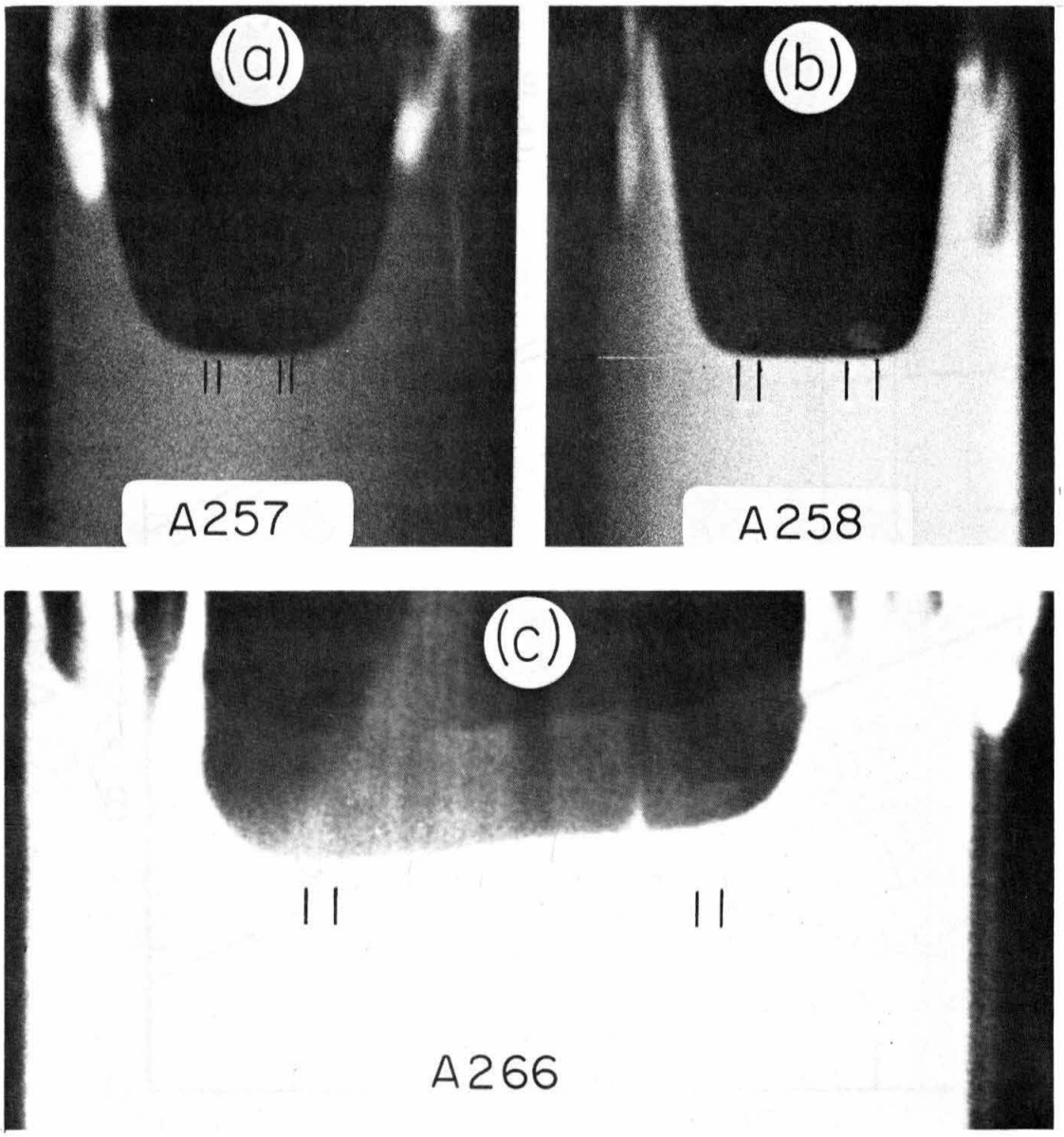

Fig. 9.4. Streak records obtained with different mirror-sample separations: (a) 0.76 mm., (b) 0.13 mm., (c) 0.25 mm. Samples (a) and (b) were polycrystalline, sample (c) single-crystal (see Table 9.1).

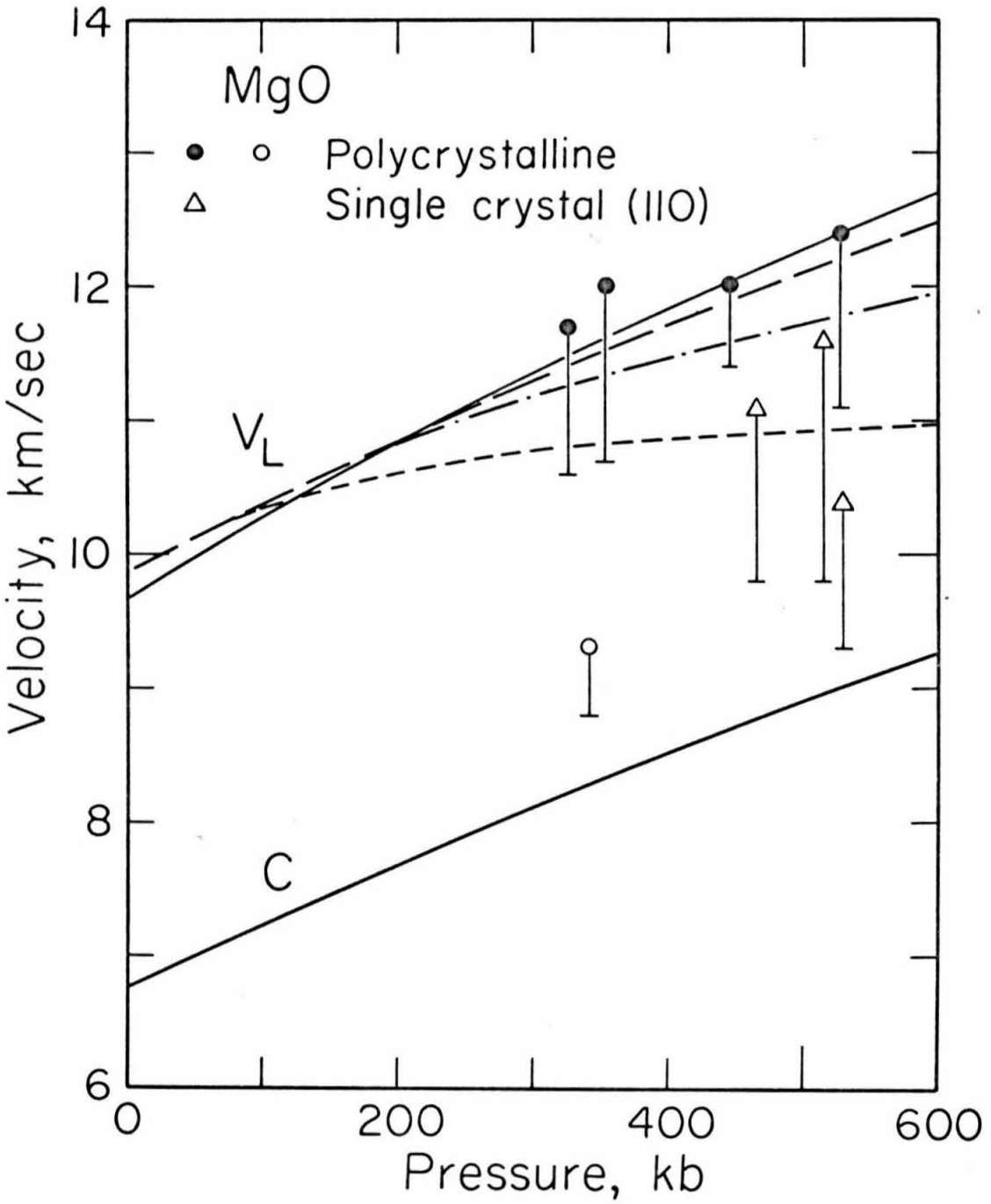

Fig. 9.5. Measured and extrapolated rarefaction velocities. Solid circles: polycrystal, z = 0.76mm. Open circle: polycrystal, z = 0.13mm. Triangles: single crystal, z = 0.25mm. Solid curves: fourth-order "E" extrapolations of C and V_L (poly.). Long-dashed: V_L in [110] direction. Short-dashed: third-order "η" V_L. Dash-dot: fourth-order "E" with $\zeta_{110} = -10$.

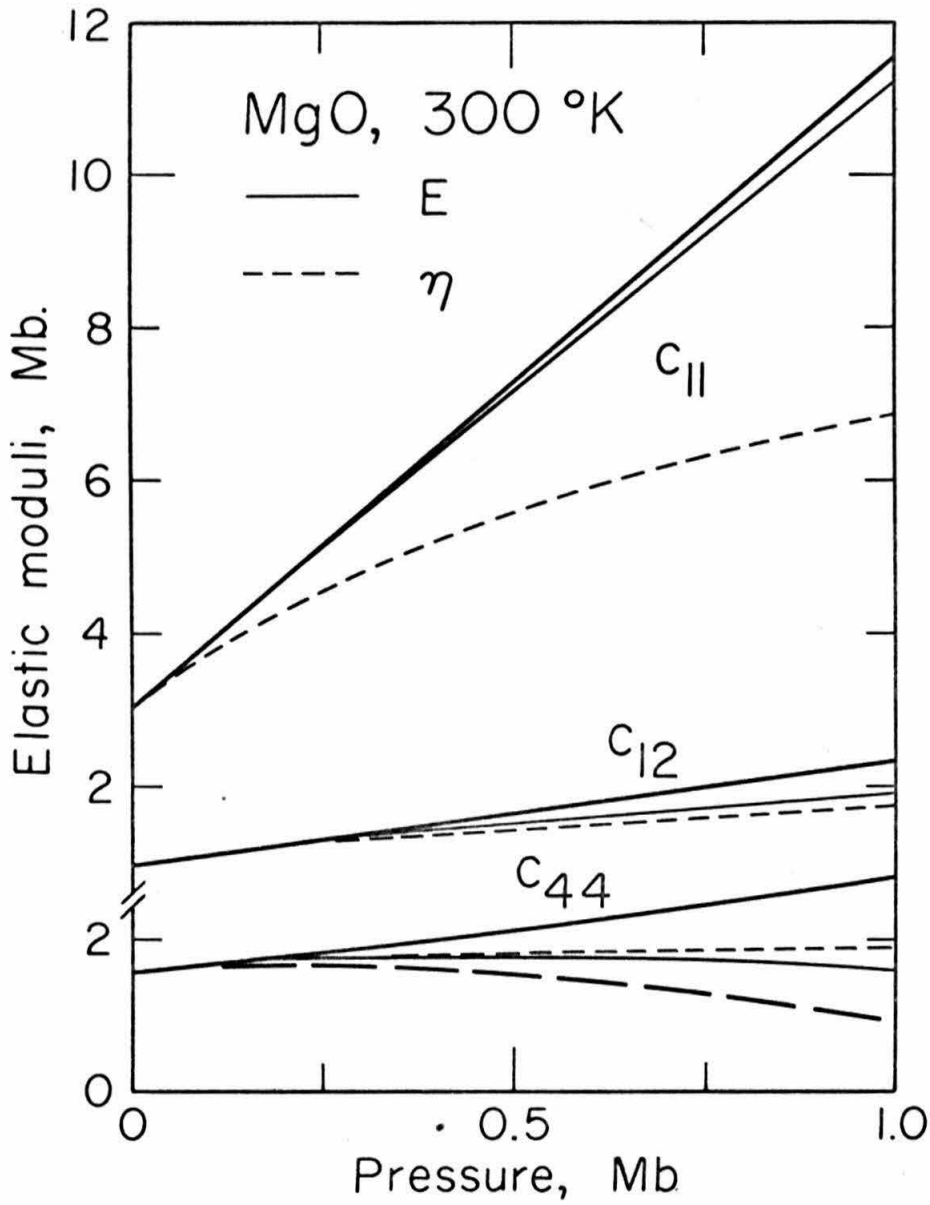

Fig. 9.6. Isothermal extrapolations of effective elastic moduli of MgO. Heavy solid curve: fourth-order "E"; light solid: third-order "E"; light dashed: third-order "η".

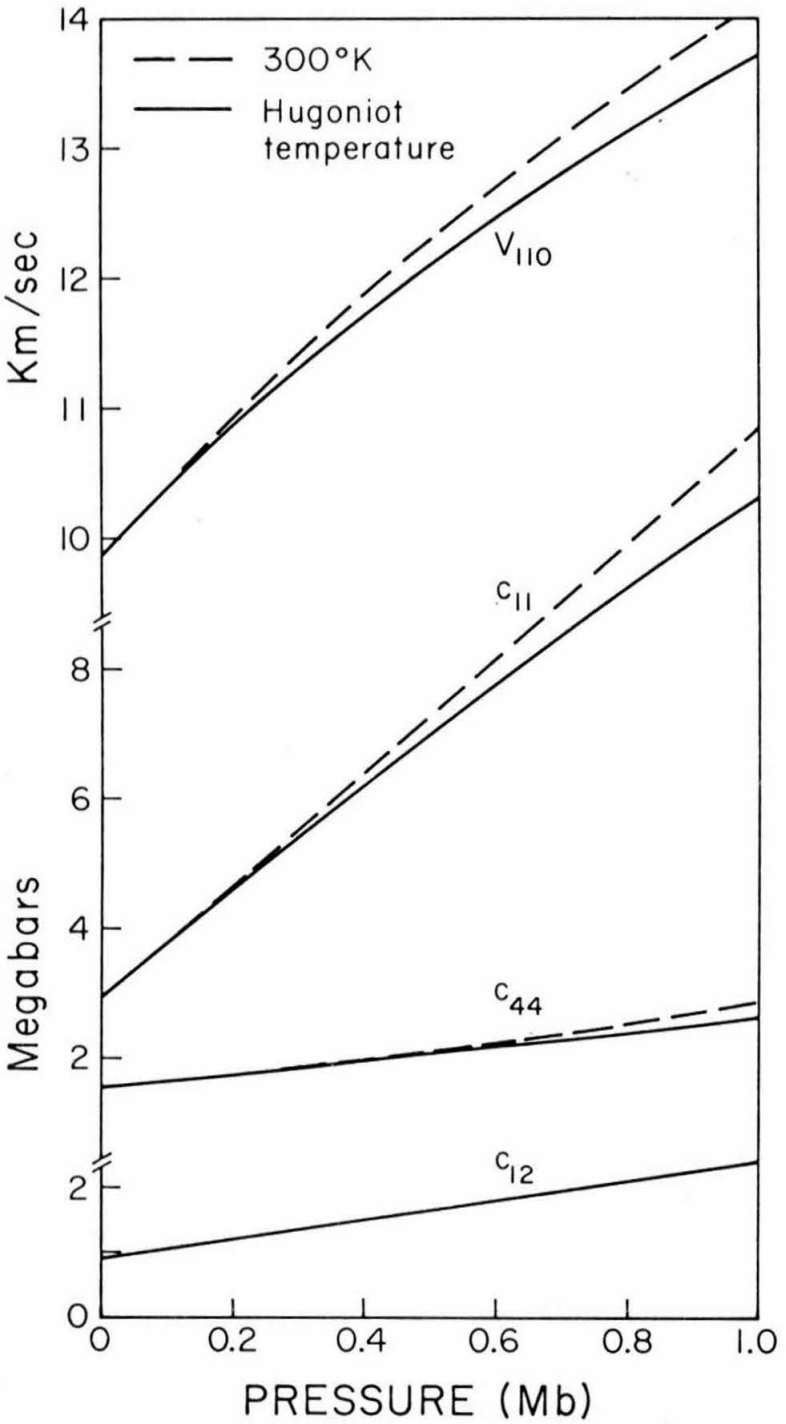

Fig. 9.7. Effect of temperature correction on elastic moduli and longitudinal [110] velocity.

CHAPTER 10

CONSTITUTION OF THE LOWER MANTLE

Summary

Equations of state of MgO (periclase) and SiO_2 (stishovite) and estimates of the equation of state of FeO (wüstite) are used to calculate the density, ρ, and seismic parameter, ϕ, at high pressures and temperatures of model mineral assemblages of the lower mantle. These are compared to the ρ and ϕ of the lower mantle, deduced from seismic observations, to determine the required composition of the models. The effects of temperature and phase changes are estimated. It is found that there is a trade-off between temperature, phase and Mg/Si molar ratio. These quantities are also uncertain because of uncertainty of ϕ of stishovite at high pressures. With wide limits placed on temperature, the most likely models are found to be a mixture of oxides, or equivalent single phase, of about pyroxene stoichiometry, or phases a few percent denser than the oxides mixtures with stoichiometries ranging between olivine and pyroxene. The iron content of the models depends somewhat on the assumed phase assemblage. The uncertainty in lower mantle densities also contributes to its uncertainty. The oxides mixtures require 12-14% by weight of FeO. The denser phases require 7-12% by weight.

The latter, especially, are comparable to the iron content of pyrolite and that deduced for the upper mantle. If iron is present in the low-spin electronic state, these estimates could be reduced by one third to one half. On the other hand, Hugoniot data of dunites would imply about 5% by weight more FeO and somewhat more SiO_2 than the above inferences.

10.1 Introduction

The determinations, in Chapters 6 and 7, of the equations of state of MgO (periclase) and SiO_2 (stishovite) are of particular significance to the study of the earth's lower mantle. In his important discussion of the constitution of the earth, Birch (1952) concluded that the density and elasticity of the lower mantle could be approximated by the properties of a mixture of the dense oxides of magnesium, silicon and iron. Since then a number of attempts have been made to refine this interpretation, more recently by Ringwood (1969, 1970), Wang (1970, 1972), Anderson and Jordan (1970) and Al'tshuler et al. (1972b). A chief concern of these studies was to determine the amount of iron in the lower mantle. Each, however, involved assumptions about other aspects of the constitution of the lower mantle. For instance, Ringwood, Wang and Al'tshuler et al. all assume particular values for the ratio (Mg + Fe)/Si, only Ringwood seriously considers the possibility of phases denser than the oxides, and only Wang attempts to avoid making specific assumptions about the temperature of the lower mantle.

In this chapter the starting point of the discussion is the assumption that the lower mantle can be represented as a mixture of MgO (periclase), SiO_2 (stishovite) and FeO (wüstite), but estimates are made of the effects of the assumed temperature and phase assemblage of the lower mantle.

Direct comparison of the density and elasticity of models of the mantle with the observed properties of the lower mantle at the appropriate high pressures and temperatures allow the determination of the relative proportions of the oxide components - i.e., of the molar ratios Fe/(Mg + Fe) and (Fe + Mg)/Si. An estimate of the dependence of the inferred composition on assumed temperature and phase assemblage is obtained. The effects of uncertainties in the equations of state of the components and in the lower mantle properties are also estimated.

10.2 Equations of State of Dense Oxides, Mixtures and Silicates

The equations of state of periclase and stishovite determined in Chapters 6 and 7 were used to calculate a set of isotherms for each. The seismic parameter, ϕ, where

$$\phi = K_s/\rho = V_p^2 - \tfrac{4}{3} V_s^2 , \qquad (1)$$

and K_s is the isentropic bulk modulus, ρ the density, V_p the compressional elastic velocity and V_s the elastic shear velocity, was calculated along these isotherms. The second equality in (1) means that ϕ can be calculated for the earth, for comparison (e.g., Birch, 1952). The calculated density and ϕ of periclase along the 300°K, 2,000°K and 3,000°K isotherms are shown in Fig. 10.1. For comparison, the 2,000°K

quantities of Al'tshuler et al. (1972a, b) (estimated from their geotherm using their estimates of the effects of temperature) are also shown. In Fig. 10.2, the same quantities are shown for stishovite calculated from the equation of state denoted as Case 2 in Chapter 7. For comparison, the 2,000°K quantities calculated from Cases 1,3 and by Al'tshuler et al. (1972a, b) are also shown (Al'tshuler et al.'s 2,000°K density is nearly identical to that of Case 2, and is therefore not shown in Fig. 10.2). Estimates of the 2,000°K quantities for wüstite, based on the density and bulk modulus measured by Mizutani (ρ = 5.84 and K = 1.74 for $Fe_{.98}O$; Mizutani et al., 1972) and two estimates of dK/dP, are shown in Fig. 10.3, with the values given by Al'tshuler et al. (1972a, b).

The uncertainty in the equation of state of wüstite is probably larger than the spread in the curves of Fig. 10.3, but since estimates of the amount of FeO in the mantle range from 10 to 20 mole percent, the effect of this uncertainty is not large. The most important uncertainty still seems to be in the stishovite equation of state. The author's preference is for Case 2, but uncertainties of up to 2% in density and 10% in ϕ within the pressure range of the mantle have to be acknowledged.

Since Birch's (1952) suggestion that the lower mantle resembles a mixture of dense oxides, a number of silicate

phases have been proposed as having the property that their density is very close to that of the isochemical mixture of component oxides (e.g., Ringwood, 1969, 1970). Thus, although a single phase rather than a mixture might exist in the mantle, the idea of representing mantle properties as a combination of those of oxides would still be valid. On the other hand, it has been suggested (e.g., Ringwood, 1969, 1970) that silicate phases slightly denser than the isochemical mixture of their component oxides might also exist in the mantle. The properties of these phases should also be estimated.

The density of a mixture is calculated here by taking the molar average of the molar volumes of the components. Various schemes for estimating the compressibility of a mixture have been proposed. For instance, Al'tshuler et al. (1972a) take weight averages of $1/\rho K_S$, while Anderson (1969) proposed that the compressibility of many silicates and oxides is given approximately by taking the molar average of ϕ of their component oxides. Since the differences between such schemes are probably less than the uncertainty in the component properties in the present case, the simple scheme of Anderson (1969) will be used here.

The effect of a phase change on compressibility can be estimated from empirical trends. Birch (1961) demonstrated that the compressional elastic velocities, V_p, of many silicates and oxides depend primarily on their density and mean

atomic weight, $\bar{M}$, and only secondarily on the specific composition and crystal structure. Similar relationships have since been pointed out for ϕ (Anderson, 1967a, 1969) and the bulk sound speed, $C = \phi^{\frac{1}{2}}$ (McQueen et al., 1964; Wang, 1968). In Fig. 4, ϕ and ρ are plotted for a number of oxides and silicates. The examples of the α-quartz-coesite-stishovite and α-fayalite-γ-fayalite sequences suggest a trend followed by substances undergoing phase changes. A series of points are also shown in Fig. 4 corresponding to mixtures of periclase, stishovite and wüstite of olivine, pyroxene and garnet stoichiometries. It can be seen that the slopes of the lines joining these to their observed low-pressure forms agree fairly well with the slopes of lines joining observed polymorphs. The value of ϕ of phases denser than the oxides mixtures are therefore estimated here by constructing a line of the appropriate slope through the calculated mixed oxides point and reading off the value of ϕ at the density predicted for the denser phase. By applying these methods at various pressures, the properties of these phases can be estimated as functions of pressure.

10.3 Constitution of the Lower Mantle

In Fig. 10.5 the calculated pressure (or depth) dependence of ϕ and ρ of stishovite and periclase at 2,000°K are compared to the pressure dependence of ϕ and ρ of several

earth models deduced from seismic observations. Note that the temperature of the latter curves are unknown. The density models BII (Birch, 1964) and HB (Haddon and Bullen, 1969) were derived with the aid of some physical assumptions, although the latter were adjusted to fit some data on the free earth oscillations. In the Jordan models (Jordan, 1972), on the other hand, the only constraints other than seismological data concern the smoothness of the distributions within each region.

In Figs. 10.6 to 10.8, ϕ and ρ of the earth are compared with ϕ and ρ estimated for various hypothetical phase assemblages at pressures of 0, 0.5 and 1.0 megabars. These Figures require some explanation before their interpretation is discussed.

The ϕ-ρ points of periclase and stishovite are plotted for a "base" temperature: in Fig. 10.6 (zero pressure) this is 300°K, and in Figs. 10.7 and 10.8 it is 2,000°K. The effect of a temperature increase on these points is shown by the short-dashed arrows. In Fig. 10.6, the temperature increase is from 300°K to 2,000°K; in Figs. 10.7 and 10.8, it is from 2,000°K to 3,000°K. Properties of oxides mixtures at the base temperatures, calculated according to the last section, are joined by the solid lines. Compositions corresponding to olivine stoichiometry, i.e., $(Mg, Fe)_2SiO_4$, and pyroxene stoichiometry, i.e., $(Mg, Fe)SiO_3$, are shown. Iron

molar ratios X = Fe/(Fe + Mg) ranging from X = 0 to X = .5 are spanned by these lines. The "olivine" lines could correspond to oxides mixtures or to a single phase having the strontium plumbate structure (Ringwood, 1969, 1970). The "pyroxene" lines could correspond to an oxides mixture or to a mixture of "olivine" and stishovite. No single phase of the mixed oxides density has been proposed for this stoichiometry. The dashed lines parallel to the solid lines are estimates of the properties of slightly denser phases of corresponding stoichiometries. The dense "olivine" lines could represent a single phase having the K_2NiF_4 structure, or possibly the calcium ferrite structure, with densities 4% to 7% denser than the oxides mixtures (Ringwood, 1969, 1970). The dense "pyroxene" line could represent a phase having the perovskite structure, up to 7% denser than the oxides mixtures. The dense "olivine" lines could also represent a mixture of this phase with (Mg, Fe)O in the rock-salt structure (i.e., a solid solution of periclase and wüstite; Ringwood, 1969, 1970). The existence of these phases is still hypothetical, and probably depends partly on the presence of other constituents, such as calcium, aluminum and ferric iron. Their estimated densities are also somewhat uncertain (Ringwood, 1969, 1970). Nevertheless, the examples given here will serve to illustrate the effects to be expected from the presence of such phases, and perhaps to

indicate the likelihood of such phases existing in the mantle.

The ϕ-ρ points of selected earth models are plotted in Figs. 10.6 to 10.8. The effect of a temperature decrease on the mantle points was estimated from the effects of the temperature increase (by the same amount) shown for periclase and stishovite. The upward short-dashed arrows thus indicate the effect of a temperature correction of the mantle to the base temperature of the Figures. In Figs. 10.7 and 10.8, Jordan's (1972) model B1 and Haddon and Bullen's (1969) model are shown. In Fig. 10.6, however, extrapolation to zero pressure of the lower mantle properties is required. Such extrapolations were given by Anderson and Jordan (1970) for the BII model, which is close to Jordan's model B1, and the model of Bullen and Haddon (1967), which is close to the model HB of Haddon and Bullen (1969). These extrapolations are shown in Fig. 10.6.

We can now proceed with the interpretation of Figs. 10.6 to 10.8. Note, firstly, that, in accordance with Birch's (1961) basic observation, the estimated trajectories due to temperature correction, phase change and change in the Mg/Si ratio all have roughly similar slopes. A trade-off of these factors is thus possible. The iron content, on the other hand, is not very dependent on the other factors.

If, for example, one fixes the composition and phase assemblage, then the other factors can be determined. Thus,

if it is assumed that the mantle is an oxides mixture of pyroxene stoichiometry, then the required mantle temperature ranges from about 2,000°K to 3,000°K, and the molar ratio X = Fe/(Mg + Fe) is about 0.17 to 0.20. By assuming the mantle to be hotter, it can be represented as having olivine stoichiometry in the K_2NiF_4 (or similar) structure, with $X \approx 0.10$, or a pyroxene stoichiometry in the perovskite structure, with $X \approx 0.15$. The required temperatures, deduced from Figs. 10.6 to 10.8, are plotted in Fig. 10.9. The corresponding compositions are given in different ways in Table 10.1.

Even apart from the trade-off between temperature, composition and phase assemblage, the temperatures determined in this way are clearly highly uncertain, mainly because of the uncertainty of ϕ for stishovite. A 10% uncertainty in ϕ of stishovite would cause roughly a 1,000°K uncertainty in temperature. The iron content, expressed as the molar ratio Y = Fe/(Mg + Fe + Si) is fairly independent of all of these factors, although it depends somewhat on the assumed phase (see Table 10.1). It is also uncertain because of the uncertainty in the density of the mantle. An uncertainty of 1% in mantle density would imply an uncertainty of about 0.02 in Y.

If it is assumed, for the moment, that the equations of state and assumptions used here are substantially correct,

some models of the mantle appear more likely than others. For instance, a mixture of oxides of olivine stoichiometry would imply temperatures from 1,000°K to about 2,000°K, a range which is unacceptably low on the basis of more reliable estimates of temperature in the upper mantle. For example, Anderson's (1967b) and Graham's (1970) estimates of temperatures in the transition zone, and Clark and Ringwood's (1964) oceanic geotherm are shown in Fig. 10.9. The temperatures obtained for the other three models mentioned above are more reasonable, the "pyroxene-perovskite phase" temperatures possibly being a little high. Upper bounds on the mantle temperature are difficult to obtain. Suitable bounds would be the melting temperature of appropriate silicates or the melting temperature of iron at the center of the earth, but these are very uncertain. Uffen (1952) estimated the melting temperature of the mantle to be about 5,000°K at the core-mantle boundary. Higgins and Kennedy (1971) have estimated the melting temperature of iron as a function of pressure. Their values at the core-mantle boundary and the center of the earth are, respectively, 3,700°K and 4,300°K, and are shown in Fig. 10.9.

Also shown, for comparison, are the temperature profiles assumed by Reynolds and Sumners (1969), and subsequently by Al'tshuler et al. (1972b), and that deduced by Wang (1972). Wang's (1972) determination is based on a comparison of the

shock-wave equations of state of Twin Sisters and Hortonalite dunites (McQueen et al., 1967; Wang, 1968) and the lower mantle. He thus assumes that an olivine stoichiometry is appropriate and that the phase achieved in the dynamic shock compression is the same as that existing under the static conditions of the lower mantle. The uncertainties arising from the latter factors have been demonstrated here, and should be added to his stated uncertainties of $\pm 800^{\circ}K$. He also assumed that the temperature gradient should be adiabatic.

The temperature profiles deduced in the present study tend to have super-adiabatic gradients. We may note that a temperature profile very similar to that of Reynolds and Sumners (1969) would be obtained for a pyrolite composition in the phases denser than the oxides mixture (Ringwood, 1969, 1970).

10.4 Conclusion

The trade-off demonstrated here between composition, temperature and phase assemblage of the lower mantle means that none of these can be determined very well. The iron content is better determined: the molar ratio Fe/(Mg + Fe + Si) is found to be about 0.05-0.10 in this study, depending mainly on the assumed phase assemblage. The ratio Mg/Si can range between that for olivine or pyroxene stoichiometries, or even more silica rich, according to this study. The phase

assemblage would appear to be at least as dense as the isochemical oxides mixture, with possibly an assemblage a few percent denser than this being favored. The temperature is very indeterminate, being very sensitive both to the trade-off with the other factors and to the uncertainties in the value of ϕ of stishovite at high pressure. At this stage it would appear to be more useful to try to find other bounds on the temperature, so as to limit the other factors, rather than to try to determine temperature by the methods used here.

Recent determinations of the iron content of the lower mantle have been discussed by Al'tshuler et al. (1972b). They note a trend converging towards 13-15% by weight, in agreement with their own determination, especially in the work of Al'tshuler et al. (1965), Wang (1968) and Reynolds and Sumner (1969). The present study suggests that these determinations may be dependent on the assumed phase assemblage. Thus the assumption of mixed oxides yields 12-14% by weight, while the assumption of denser phases yields 7-12% by weight. The difference between these determinations depends on the relative effect of the relevant phase changes on density and ϕ, but since these are unknown, this additional source of uncertainty in the iron content of the lower mantle must be acknowledged.

Anderson (1970), Anderson and Jordan (1970) and Anderson et al. (1971) deduced iron contents of the lower mantle in

the range 12-18 mole%. These higher values apparently resulted partly from the use of density models which extrapolate to fairly high densities (especially model CIT 200204), and partly from the use of the Hugoniot data of Twin Sisters and Hortonalite dunites (see below). Phases denser than mixtures of the dunites and stishovite were not considered.

The Hugoniot data of the dunites (McQueen et al., 1967) are important additional constraints on the equations of state of high pressure phases in this range of compositions. Their compatibility with present predictions and the effect of using them as a base reference instead of the oxides have been estimated as follows. Previous studies (e.g., Ahrens et al., 1969; Davies and Anderson, 1971) have suggested that they were in a phase comparable to mixtures of oxides. Accordingly, the mixed oxide zero pressure densities were assumed. Grüneisen parameters, which are unknown, were assumed to have values of about 1.0 and 1.5, with $d \ln \gamma / d \ln V \approx 1.0$. The Hugoniot data were then used to determine the bulk modulus and its pressure derivative. The complete sets of equation of state parameters are given in Table 10.2. Isotherms calculated from these cases were used to plot ϕ-ρ points in Figs. 10.6 to 10.8. At zero pressure, Fig. 10.6, ϕ tends to be higher than predicted for Twin Sisters dunite, which has the approximate formula $(Mg_{.88}Fe_{.12})_2SiO_4$, while it agrees quite well with the prediction for the Hortonalite dunite,

$(Mg_{.45}Fe_{.55})_2SiO_4$. At high pressures, Figs. 10.7 and 10.8, both ϕ and ρ tend to be lower than predicted, although ϕ is somewhat uncertain because of the uncertainty in γ. If the dunites are used as a base to estimate mantle compositions, then at high pressure larger proportions of both SiO_2 and FeO are obtained (assuming that the dunites are indeed in a phase corresponding to oxides mixtures). In particular, the value of X would be increased by about .05, corresponding to an increase of about 5% by weight of FeO to values closer to those of Anderson et al.

The estimates of iron content determined here from the oxide equations of state are lower than those of Anderson et al., and slightly lower than that of Al'tshuler et al. (1972b), especially if the dense phase assemblage is assumed, as suggested by Ringwood (1969, 1970). In fact, the iron contents in the latter case are quite close to those of Ringwood's (1970) pyrolite (8.5% FeO + Fe_2O_3 by weight) and Graham's (1970) determination of the upper mantle iron content (12% FeO by weight). A uniform iron content throughout the mantle would thus be permitted by this study. It has already been noted that a silica content comparable to that of a pyrolite (about 40 mole%) and a phase assemblage a few percent denser than the oxides mixture would imply a quite reasonable temperature distribution.

It has been suggested (Strens, 1969; Davies and Anderson,

1971; Gaffney and Anderson, 1972) that iron might undergo an electronic spin transition in the lower mantle, reducing the radius of the ion, increasing the density of the material, and possibly requiring a new crystal structure. An octahedral coordination of the iron is probably required to produce spin transition, and not all candidates for dense phases have any or all iron in octahedral sites (Gaffney and Anderson, 1972). An extreme case is probably obtained by assuming that the iron occurs as FeO in the rocksalt (wüstite) structure, in which it is all octahedrally coordinated. According to the discussion of Gaffney and Anderson (1972), the effect of a spin transition would be to increase the density of the FeO from about 5.9 g/cm^3 to about 7.5 g/cm^3, while the value of ϕ would not be greatly increased. The only significant effect from this is that the estimates of iron content are reduced by about half. As noted, this is an extreme estimate, so a probable range of iron contents would be 9-10% by weight for the oxides mixtures and 6-8% by weight for the denser phase assemblages. These bracket the iron content of pyrolite (Ringwood, 1969, 1970).

10.5 References

AHRENS T. J., ANDERSON DON L. and RINGWOOD A. E., Rev. Geophys. 7, 667 (1969).

AL'TSHULER L. V., TRUNIN R. F. and SIMAKOV G. V., Bull. (Izv.) Acad. Sci. USSR, Earth Physics, No. 10 (1965).

AL'TSHULER L. V. and SHARIPDZHANOV I. I., Bull. (Izv.) Acad. Sci. USSR, Earth Physics, No. 3, 11 (1971). English translation, 167 (1972a).

AL'TSHULER L. V. and SHARIPDZHANOV L. D., Bull. (Izv.) Acad. Sci. USSR, Earth Physics, No. 4, 3 (1971). English translation, 231 (1972b).

ANDERSON DON L., Geophys. J. R. astr. Soc. 13, 9 (1967a).

ANDERSON DON L., Science 157, 1165 (1967b).

ANDERSON DON L., J. Geophys. Res. 74, 3857 (1969).

ANDERSON DON L., Mineral. Soc. Amer. Spec. Pap. 3, 85 (1970).

ANDERSON DON L. and JORDAN T., Phys. Earth Planet. Interiors 3, 23 (1970).

** ANDERSON DON L., SAMMIS C. and JORDAN T., Science 171, 1103 (1971).

BIRCH F., J. Geophys. Res. 57, 227 (1952).

BIRCH F., Geophys. J. R. astr. Soc. 4, 295 (1961).

BIRCH F., J. Geophys. Res. 69, 4377 (1964).

BULLEN K. E. and HADDON R. A., Proc. Nat. Acad. Sci. 58, (1967).

CLARK S. P. and RINGWOOD A. E., Rev. Geophys. 2, 35 (1964).

DAVIES G. F. and ANDERSON DON L., J. Geophys. Res. 76, 2617 (1971).

GAFFNEY E. S. and ANDERSON DON L., unpublished manuscript, 1972.

GRAHAM E. K., Geophys. J. R. astr. Soc. 20, 285 (1970).

HADDON R. A. and BULLEN K. E., Phys. Earth and Planet. Interiors 2, 35 (1969).

HIGGINS G. and KENNEDY G. C., J. Geophys. Res. 76, 1870 (1971).

JORDAN T. H., Ph. D. Thesis, California Institute of Technology, Pasadena (1972).

McQUEEN R. G., FRITZ J. N. and MARSH S. P., J. Geophys. Res. 69, 2947 (1964).

MIZUTANI H., HAMANO Y., AKIMOTO S. and NISHIZAWA O., Trans. Am. Geophys. Union 53, 527 (1972).

REYNOLDS R. T. and SUMNERS A. L., J. Geophys. Res. 74, 2494 (1969).

RINGWOOD A. E., Earth Planet. Sci. Lett. 5, 401 (1969).

RINGWOOD A. E., Phys. Earth Planet. Interiors 3, 109 (1970).

STRENS R. G. J., in The Application of Modern Physics to the Earth and Planetary Interiors (Edited by S. K. Runcorn), Wiley-Interscience, New York (1969).

Uffen, Trans Am. Geophys. Un. 33, 893 (1952).

WANG C., J. Geophys. Res. 73, 6459 (1968).

WANG C., J. Geophys. Res. 75, 3264 (1970).

WANG C., Geophys. J. R. astr. Soc. 27, 29 (1972).

** ANDERSON DON L. and JULIAN B. R., J. Geophys. Res. 74, 3281 (1969).

TABLE 10.1

Compositions of Lower Mantle Model Mineral Assemblages

Phase assemblage	Stoichiometric formula	X	FeO content Mole fraction	Weight fraction
Olivine, mixed oxides	$(Mg_{1-x}Fe_x)_2SiO_4$	.12-.15	.08-.10	.12-.14
Olivine, "K_2NiF_4" phase	$(Mg_{1-x}Fe_x)_2SiO_4$	.08-.11	.06-.08	.08-.12
Pyroxene, mixed oxides	$(Mg_{1-x}Fe_x)SiO_3$	.17-.20	.08-.10	.12-.14
Pyroxene, "perovskite" phase	$(Mg_{1-x}Fe_x)SiO_3$	.10-.15	.05-.08	.07-.12

TABLE 10.2

Dunite Equation of State Parameters

Rock	Case no.	ρ_0 (g/cm^3)	K_0 (Mb)	ϕ_0 $(Km/sec)^2$	K_0'	γ_0	$\frac{d \ln \gamma}{d \ln V}$
Twin Sisters	1	4.04	2.67	66.2	3.23	0.91	1.1
	2	4.04	2.60	64.4	2.95	1.48	1.2
Hortonalite	1	4.64	2.64	57.0	2.81	0.94	0.9
	2	4.64	2.50	53.8	2.61	1.47	0.7

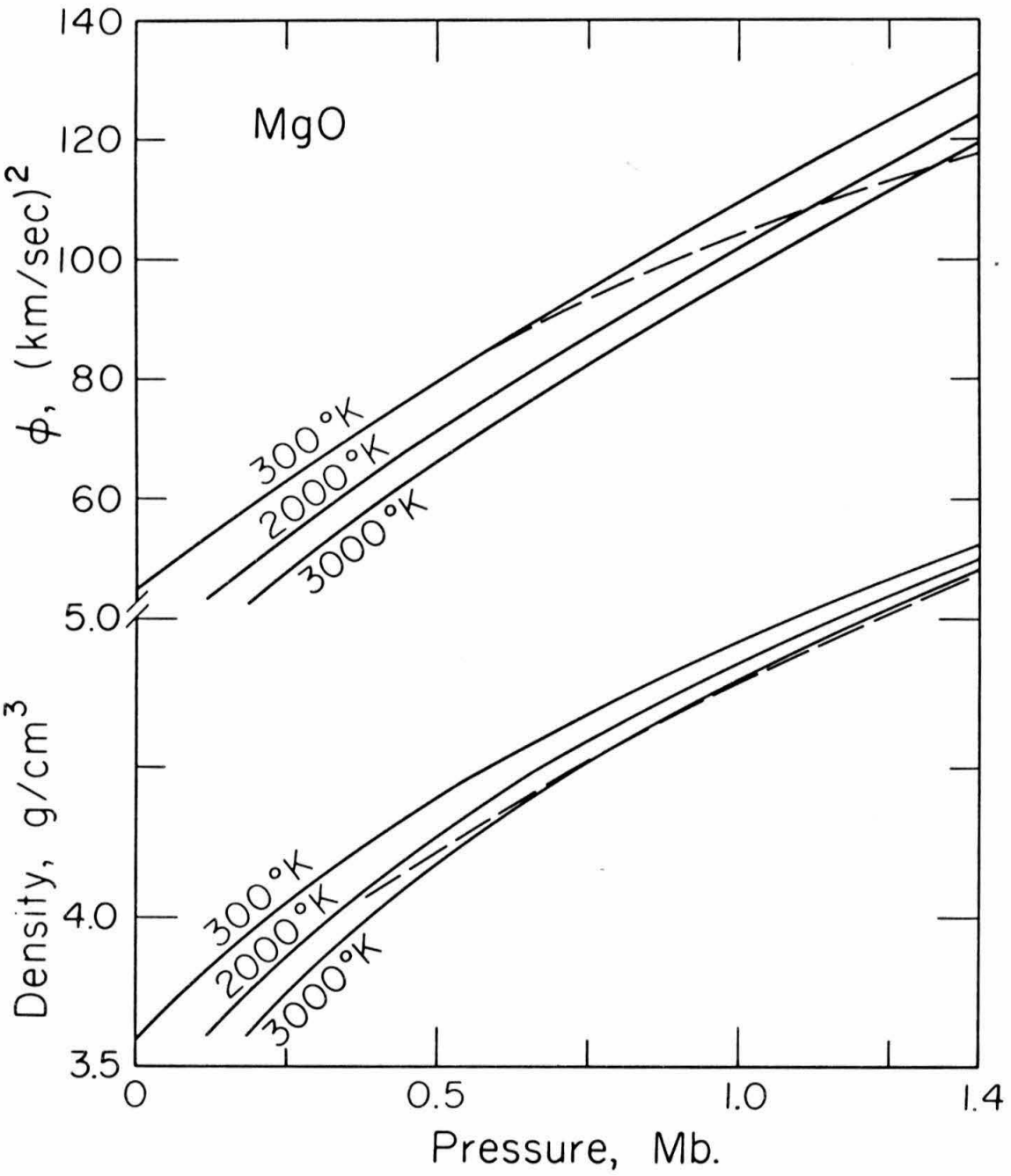

Fig. 10.1. Calculated isothermal densities and seismic parameters, ϕ, of MgO. Dashed curves are 2,000°K values from Al'tshuler et al. (1972).

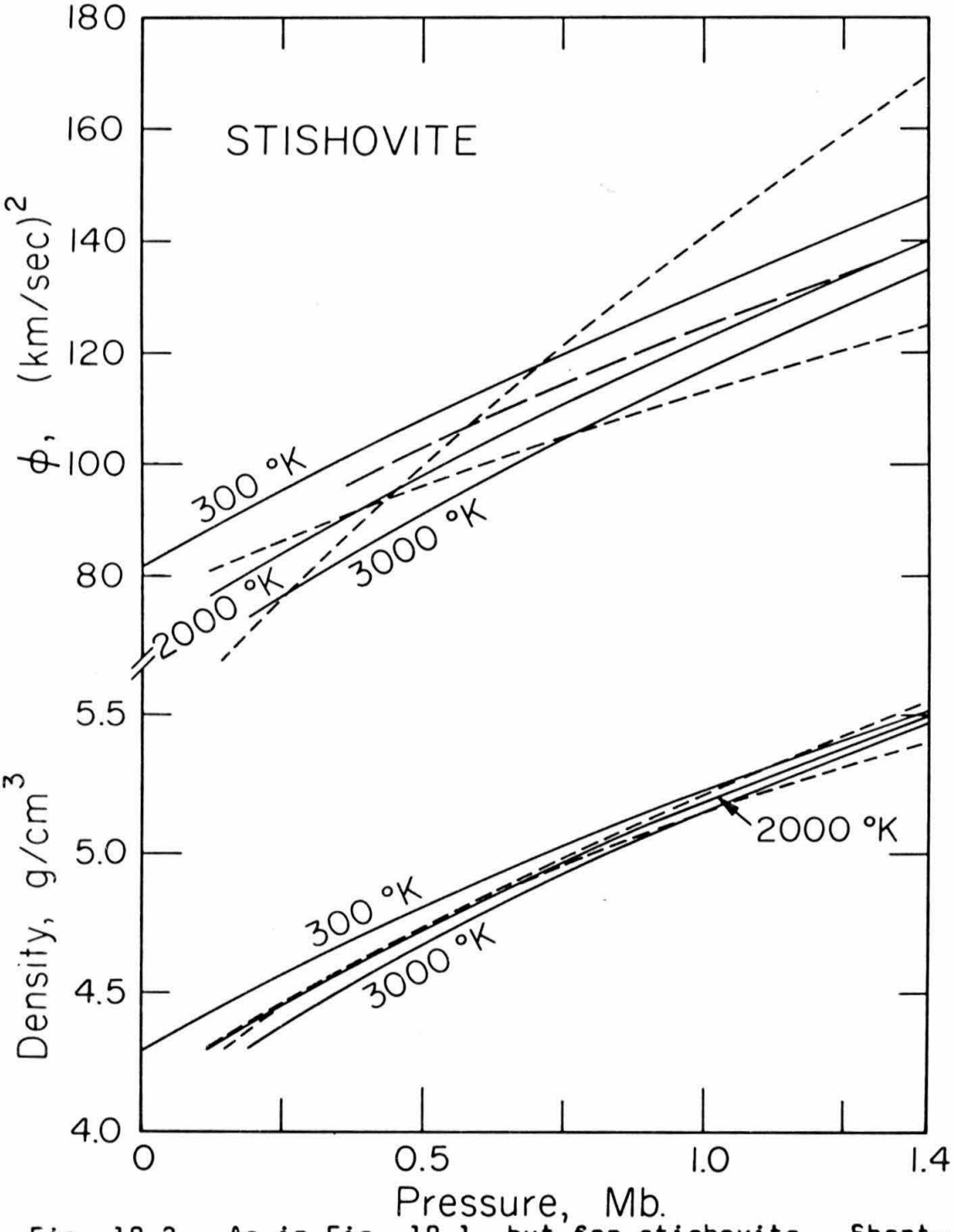

Fig. 10.2. As in Fig. 10.1, but for stishovite. Short-dashed curves are 2,000°K values from Cases 1 and 3 of Chapter 7.

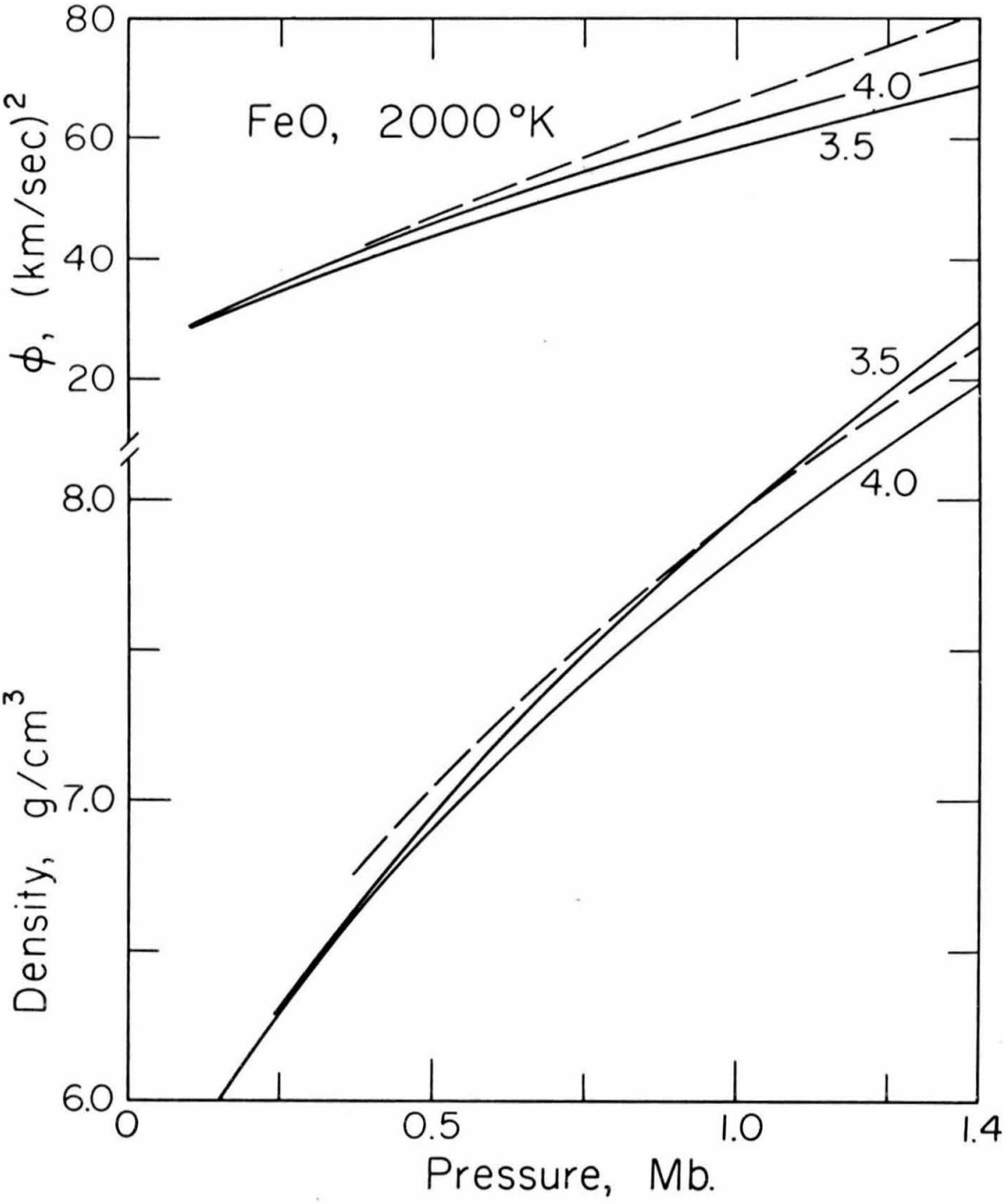

Fig. 10.3. Estimated 2,000°K values of density and ϕ for FeO using dK/dP values of 3.5 and 4.0. Dashed curves are 2,000°K values of Al'tshuler et al. (1972).

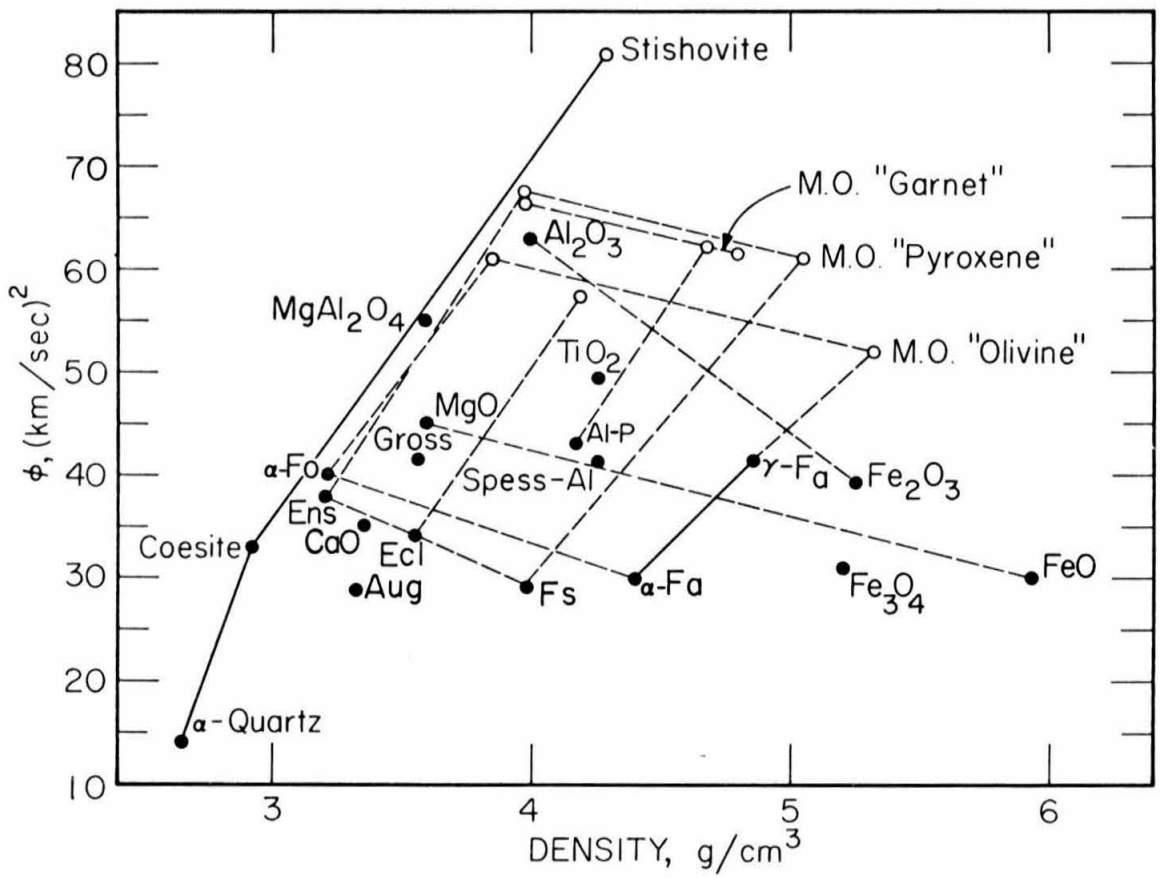

Fig. 10.4. Zero-pressure values of density and ϕ of various oxides and silicates (solid circles). Open circles are estimated values for mixtures of MgO, FeO and SiO_2 (stishovite) of olivine, pyroxene and garnet stoichiometries. Solid and dashed lines of positive slope join real or hypothetical polymorphs. Dashed lines of negative slope join isomorphs formed by iron substitution. (After Davies, 1972, unpublished manuscript.)

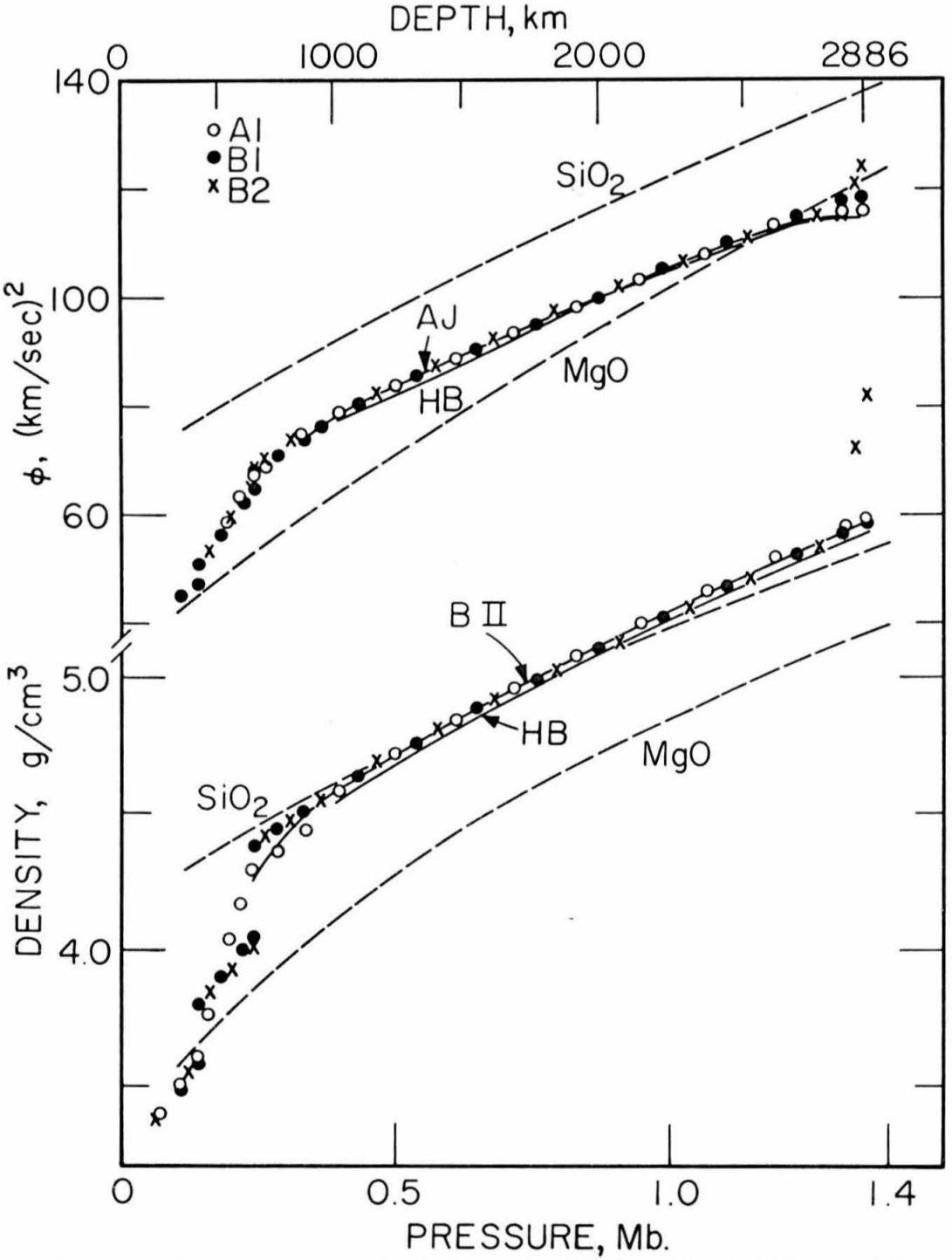

Fig. 10.5. Comparison of MgO and stishovite with mantle models - A1, B1, B2, Jordan (1972); AJ, Anderson and Julian (1969); HB, Haddon and Bullen (1969); BII, Birch (1964).

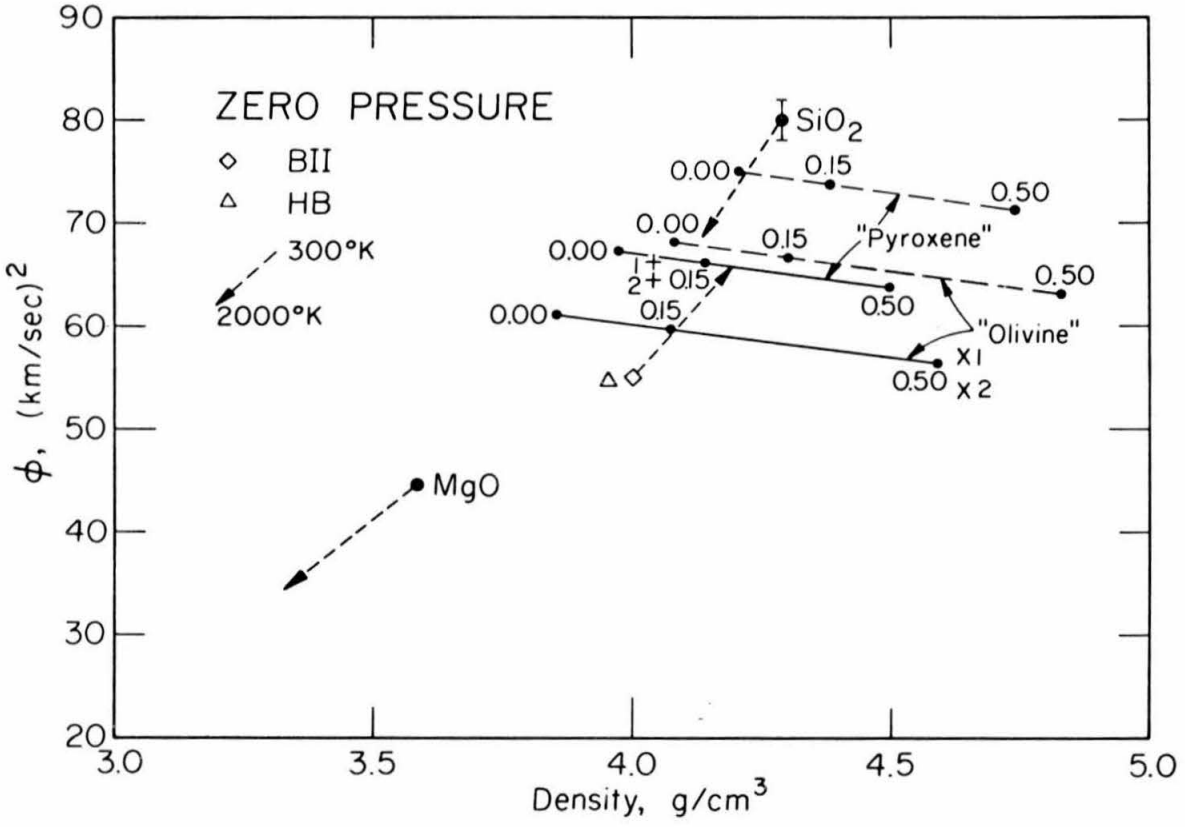

Fig. 10.6. Zero-pressure density and ϕ of models BII and HB compared with 300°K values for MgO, stishovite, mixed oxides (solid lines) and post-mixed-oxides (dashed) of olivine and pyroxene stoichiometries. Numbers give the molar ratio Fe/(Mg + Fe). Also shown are derived values for Twin Sisters dunite (plusses) and Hortonalite dunite (crosses) Cases 1 and 2 (Table 10.2). Dashed arrows indicate calculated effect of temperature change indicated in legend.

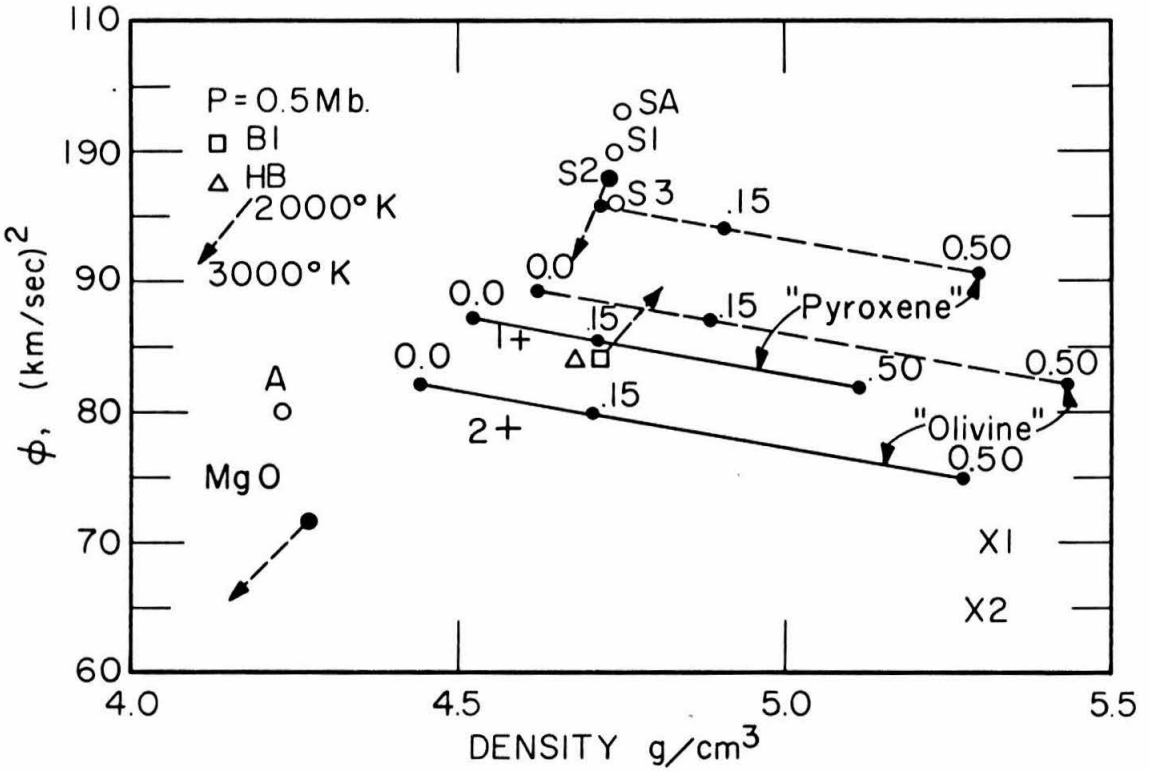

Fig. 10.7. As in Fig. 10.6, but at 0.5 Mb pressure and 2,000°K, and with models B1 and HB. Different stishovite cases are labelled S1, S2 and S3. Al'tshuler et al.'s (1972) stishovite and MgO points are labelled SA and A, respectively.

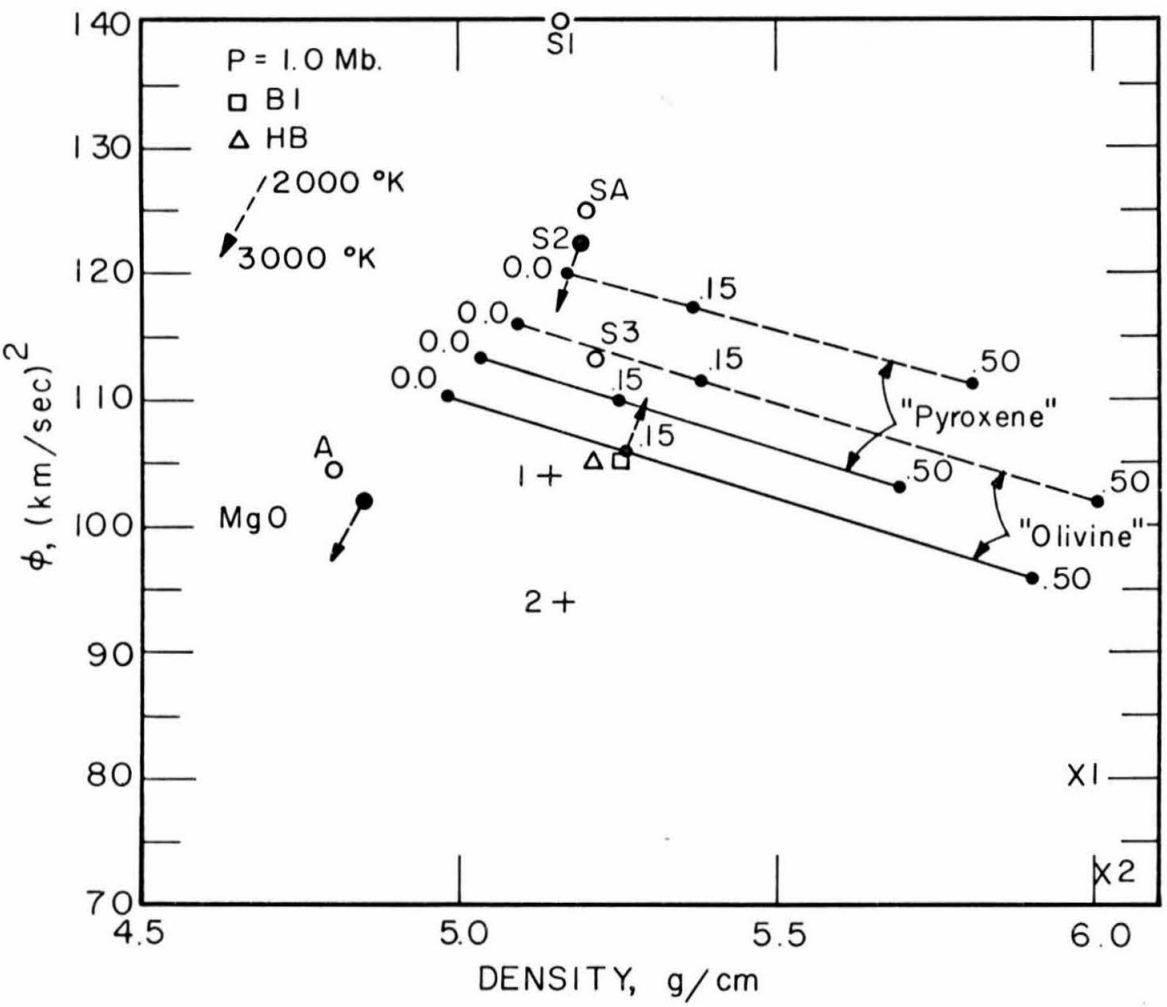

Fig. 10.8. As in Fig. 10.7, but at 1 Mb pressure and 2,000°K.

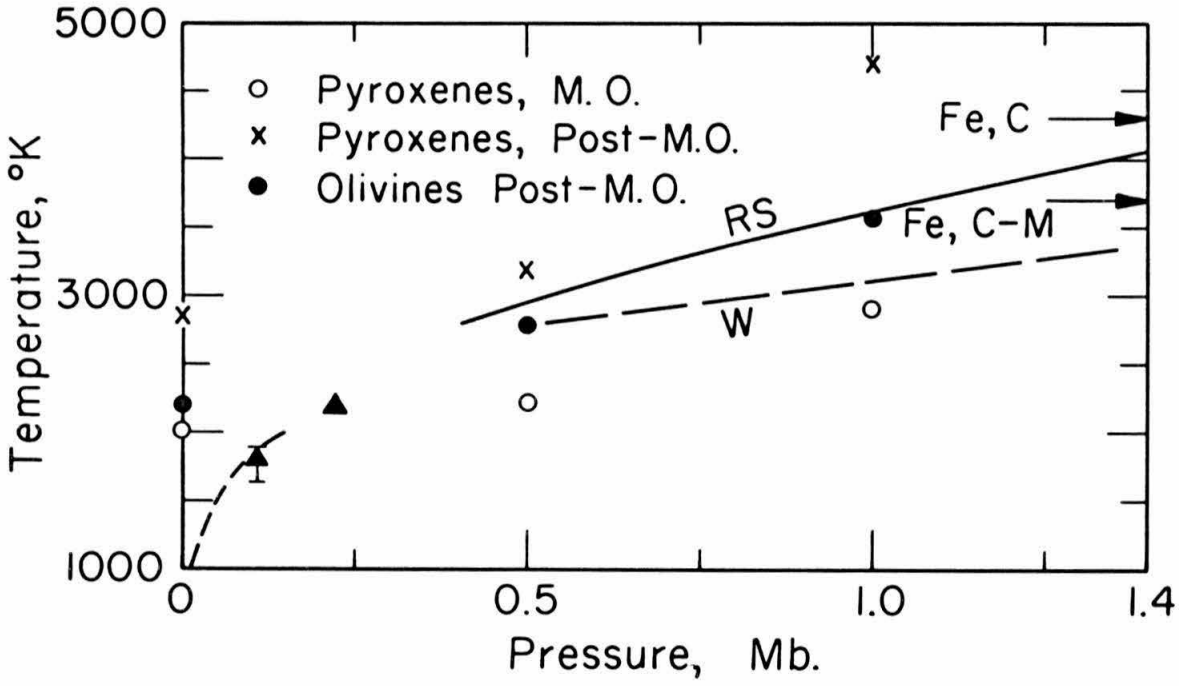

Fig. 10.9. Temperatures inferred for different composition and phase combinations compared with other estimates of mantle temperatures - triangles: Anderson (1967b); error flag: Graham (1970); W: Wang (1972); RS: Reynolds and Sumners (1969); arrows: estimates of melting temperature of iron at the inner-outer core boundary (C) and the core-mantle boundary (C-M) by Higgins and Kennedy (1971).